LIGNINAREN ERALDAKETA BALIO ERANTSIKO PRODUKTUEN LORPENERAKO

Universidad del País Vasco
Euskal Herriko Unibertsitatea

Amaia Morales Matías

2022ko Urtarrila

Ligninaren eraldaketa balio erantsiko produktuen lorpenerako

Amaia Morales Matías-ek aurkeztua

Euskal Herriko Unibertsitateak

Material Berriztagarrien Ingeniaritzako programan

Doktore Titulua lortzeko bete beharreko baldintzak betez

Tesi zuzendariak:

Jalel Labidi eta Patricia Gullón doktoreak

Ingeniaritza Kimikoa eta Ingurumenaren Ingeniaritza Saila

DONOSTIA – SAN SEBASTIÁN

2022

 *“Science is magic that works.”*

Kurt Vonnegut

Esker onak

Zaila egiten zait laborategia lehen aldiz zapaldu nuenetik 5 urte igaro direla pentsatzea. Egia esan, Master Amaierako Lana egiten hasi nintzenera arte doktoretza egitearen ideia ez zen nire buruan agertu. Astelehenetan lanerako gogo eta ilusioz jaikitze hutsak bide honen alde apustu egitea eragin zidan, eta orain, igoera nahiz jaitsiera, barre eta negar, momentu on eta ez horren onez beteriko urte hauen ostean, helmugara iritsi naiz. Horregatik, nire bizitzan hain garrantzitsua izan den etapa honetan nire alboan egondako guztiei eskerrak eman nahiko nizkieke.

En primer lugar, me gustaría agradecer a mi director, el Dr. Jalel Labidi, por haberme animado y haber confiado en mí al blindarme la oportunidad de realizar esta tesis. Quisiera agradecer también a la Universidad del País Vasco/Euskal Herriko Unibertsitatea por concederme esta oportunidad mediante su ayuda a la Formación de Personal Investigador.

En segundo lugar, agradecer a la Prof. Margit Schulze por haberme dado la oportunidad de unirme a su grupo de investigación en Bonn, aunque solo fuese por dos semanas. Igualmente, quisiera darle las gracias a la Prof. Ebru Toksoy, por aparecer en un momento clave de mi tesis y poder colaborar con su grupo de investigación para así poder ponerle el broche final a mi trabajo. Muchísimas gracias a la Dra. Merve Erginer y a la doctoranda Selay Tornaci por haber dedicado su tiempo a mis experimentos.

Quisiera agradecer a todos los compañeros del grupo BioRP por su ayuda y apoyo, y también a Loli, tanto por su apoyo tanto científico como moral durante estos años. Gracias también a compañeros de otros grupos como Joseba, Mireia e Iratxe, que han hecho que el día a día sea más llevadero.

Me gustaría agradecer a mis *Morenitos* por haber sido uno de mis pilares más importantes durante este tiempo, por haberme ayudado a construir la base de esta torre que, como buena arquitecta frustrada, estoy a punto de terminar. Gracias en especial a Julen por su apoyo en mis momentos de crisis científicas y

personales, por rescatar a esta *drama queen* de sus momentos de ahogo en un vaso de agua. Y gracias también a Fabio, que aunque nos costó caernos bien, hemos sido fieles compañeros de viaje y nos hemos apoyado mutuamente cuando más lo hemos necesitado. Porque al mal tiempo, buena cara, y a un mal día (martes normalmente), un buen café.

Me gustaría, como no, dar las gracias a mis queridísimos *Rebujitos*, que me acogieron con los brazos abiertos en este loco mundo y me han ayudado a crecer tanto personal como científicamente. Gracias a Fabio, Rut, Leyre, Izas, Xabi y Jonatan por todos los momentos de locuras, por las risas, por hacerme descubrir mi pasión por las *escape rooms*, por hacer de los congresos viajes inolvidables, por hacer que los *Skypotes* sean ya una nueva tradición y por mimarme tanto por ser la más jovencita (aunque ya no tanto, pero lo seguiré siendo siempre). Que aunque nos vayamos desperdigando, siempre es un placer volver a juntarnos y seguir haciendo maldades y locuras. Nada hubiera sido lo mismo sin vosotros.

Quisiera también dar las gracias a mi cuadrilla, a esas personas que *finde* tras *finde*, han estado ahí escuchando mis aventuras de las no-estancias, las que han intentado entender qué hago en mi día a día, para qué sirven esos *bichos* que se hinchan, etc. Sé que no os lo digo mucho, pero gracias de corazón.

Gracias también a mis compañeros de *Amets Bide*, que han hecho de cada ensayo una vía de escape. Eskerrik asko en especial a Enara y a Beñat por aguantarme tanto, y también por aportar aire fresco de creatividad a esta tesis.

Me gustaría agradecer a mis padres por su apoyo incondicional, por escucharme y aconsejarme, por dejarme elegir mi camino en todo momento sin separarse ni un segundo de mi lado. Gracias a mi familia, en especial a mis abuelos, a los que tanto admiro y se preocupan siempre tanto por mí.

Quisiera agradecer a mi codirectora, la Dra. Patricia Gullón, por su infinita paciencia y su tiempo dedicado a mi trabajo. Gracias a Patri, por estar ahí siempre, por ser una amiga, por confiar en mí, por su profesionalidad. Todo lo

que he conseguido desde el primer día que pisé el laboratorio ha sido en gran parte gracias ella, y esta tesis es un claro reflejo de ello.

Por último, quisiera agradecer a Ander, que en todo este tiempo me ha ayudado a levantarme cada vez que me he tropezado, que me ha dado un abrazo cuando más lo he necesitado, que me ha aguantado día tras día, que me ha escuchado y apoyado siempre. Por poner un poco de cordura a mi locura y por seguir consiguiendo más retos personales y profesionales juntos. "*Questions of science, science and progress do not speak as loud as my heart*". Eskerrik asko, bihotzez.

A todos los que de alguna manera habéis dejado huella en esta tesis,

Mila esker!

Laburpena

Produktu polimerikoek gure eguneroko bizitza irauli dute eta ia sektore guztietan ezinbesteko material bihurtu dira eskaintzen dituzten abantaila ugariei esker. Hala ere, material horiek baliabide fosiletan izan ohi dute euren jatorria, eta ez dira mugagabeak; horregatik, material horiek agortzea eta euren prezioen gorabeherak kezka bihurtu dira egungo gizartearentzat. Gainera, plastiko edo material polimerikoek ez dute biodegradagarritasunik izaten, eta, ondorioz, horiek behar bezala ez eliminatzea eta gaizki kudeatzea kaltegarria da ingurumenarentzat, eta arriskutsua espezie bizidunentzat, gizakia barne.

Testuinguru horretan, aipatutako kezka guzti hauek ordezko baliabide jasangarriak eta ekologikoagoak bilatzeko premia sustatu dute (biopolimeroak, esaterako). Zentzu horretan, biofindegiak irtenbide potentzial gisa agertu dira, biomasa biopolimero eta oinarri biologikoko hainbat produktu merkaturagarrietan bihurtzeko gai baitira. Biomasa lignozelulosikoak arreta handia irabazi du azkenaldian, bere osagai nagusiak (zelulosa, hemizelulosak eta lignina) isolatu ondoren eskaintzen dituzten aplikazio ugarien ondorioz. Horien artean, badirudi lignina etorkizun handiko hautagaia dela karbonoan oinarritutako konposatuak (hala nola, produktu kimikoak eta materialak) fabrikatzeko erabiltzen diren baliabide fosilak ordezkatzeko. Hala ere, badirudi biopolimero hau gutxi ustiatuta dagoela, ziurrenik bere portaera egonkor eta egitura kimiko konplexuagatik. Edonola ere, ligninan oinarrituriko balio erantsiko produktuen ekoizpena funtsezkoa da bio-findegi plantak ekonomikoki lehiakorrak izan daitezen.

Ildo horretan, tesi honen ardatz nagusia ligninari balio erantsi bat ematea da, hidrogelak bezalako balio erantsi handiko konposatu bihurtuz. Tesi honek 5 kapitulu ditu: 1. Sarrera, 2. Helburuak eta erronkak, 3. Metodologia, 4. Emaitzak eta eztabaida eta 5. Ondorioak eta etorkizuneko lanak. 4. kapitulua 4

ataletan banatu da: lehenengoan, tesi honetan erabilitako ligninen karakterizazioa deskribatzen da; bigarrenean, hidrogelen sintesiaren optimizazioa garatzen da, polibinil alkohola eta lignina alkalino komertziala erabiliz; hirugarrenean, hidrogelen propietateetan eragina duten faktore desberdinak eztabaidatzen dira, eta laugarrenean, material anitzen aplikagarritasunerako emaitzak azaltzen dira.

Emaitzek lignina ingurumena errespetatzen duen polimero matrize batekin nahastuz (polibinil alkoholarekin (PVA), hain zuzen), fisikoki saretutako lignina-hidrogelak arrakastaz lor daitezkeela erakutsi dute, eta material horien ezaugarriak zenbait sintesi- eta formulazio-parametro aldatuz egokitu egin daitezkeela. Gainera, lignina hidrogelak hainbat aplikazio eremutan erabiltzeko material moldaerrazak direla frogatu da, hala nola, kutsatutako uren tratamenduan, bilgarrietan edota biomedikuntzan.

Atxikitako argitalpenen zerrenda

I. Artikulua: A. Morales, J. Labidi, P. Gullón, G. Astray, *Synthesis of advanced biobased green materials from renewable biopolymers*, Curr. Opin. Green Sustain. Chem. 29 (2021) 100436. DOI: 10.1016/j.cogsc.2020.100436.

II. Artikulua: A. Morales, J. Labidi, P. Gullón, *Assessment of green approaches for the synthesis of physically crosslinked lignin hydrogels*, J. Ind. Eng. Chem. 81 (2020) 475-487. DOI: 10.1016/j.jiec.2019.09.037.

III. Artikulua: A. Morales, J. Labidi, P. Gullón, *Effect of the formulation parameters on the absorption capacity of smart lignin-hydrogels*, Eur. Polym. J. 129 (2020) 109631. DOI: 10.1016/j.eurpolymj.2020.109631.

IV. Artikulua: A. Morales, J. Labidi, P. Gullón, *Impact of the lignin type and source on the characteristics of physical lignin hydrogels*, Sustain. Mater. Technol. 31 (2021) e00369. DOI: 10.1016/j.susmat.2021.e00369.

V. Artikulua: A. Morales, J. Labidi, P. Gullón, *Influence of lignin modifications on physically crosslinked lignin hydrogels for drug delivery applications*, Ind. Crops. Prod. (under review).

Tesian sartu gabeko ekarpenak

🕮 A. Morales, F. Hernández-Ramos, L. Sillero, R. Fernández-Marín, I. Dávila, P. Gullón, X. Erdocia, J. Labidi, *Multiproduct biorefinery based on almond shells: Impact of the delignification stage on the manufacture of valuable products*, Bioresour. Technol. 315 (2020). DOI: 10.1016/j.biortech.2020.123896.

🕮 A. Morales, J. Labidi, P. Gullón, *Hydrothermal treatments of walnut shells: A potential pretreatment for subsequent product obtaining*, Sci. Total Environ. 764 (2021) 142800. DOI: 10.1016/j.scitotenv.2020.142800.

🕮 L. Sillero, A. Morales, R. Fernández-Marín, F. Hernández-Ramos, I. Dávila, X. Erdocia, J. Labidi, *Life Cycle Assessment of various biorefinery approaches for the valorisation of almond shells*, Sustain. Prod. Consum. 28 (2021) 749–759. DOI: 10.1016/j.spc.2021.07.004.

🕮 A. Morales, J. Labidi, P. Gullón, *Integral valorisation of walnut shells based on a three-step sequential delignification*, J. Environ. Manage. (under review).

Kongresuetarako ekarpenak

✍ BIOPOL 2019 (Ekainaren 17-19, Stockholm - Suedia): A. Morales, J. Labidi, P. Gullón; *Influence of the molecular weight of poly (vinyl alcohol) in physically crosslinked lignin-based green hydrogels* (Ahozko aurkezpena)

✍ BIORESTEC 2021 (Maiatzaren 17-19, Garda - Italia): A. Morales, P. Gullón, J. Labidi; *Effect of differently extracted shell lignins on the synthesis of smart materials* (Posterra)

✍ MZT 2021 (Azaroaren 29-30, Bilbo – Espainia): A. Morales, P. Gullón, J. Labidi; *Fruitu lehorren azaletatik isolaturiko lignina eraldatuek hidrogelen ezaugarrietan duten eragina* (Ahozko aurkezpena)

Nomenklatura

Laburdura	Deskribapena
AS	Almendra azalak
ASL	Azidotan disolbagarria den lignina
ATR-FTIR	Islapen Total Indargetua-Fourierren transformatuaren bidezko espektroskopia infragorria
CQE	Kertzetina komertziala
DMSO	Dimetilsulfoxidoa
DSC	Ekorketa diferentzialeko kalorimetria
FGI	Hazkunde fungikoaren inhibizioa
G units	Ligninaren guaiazilo unitateak
GAE	Azido galikoaren baliokideak
GI	Hazkundearen inhibizioa
H units	Ligninaren 4-hidroxi fenilo unitateak
H/M/LM$_w$	Pisu molekular altua/ertaina/baxua
HPLC	Bereizmen handiko kromatografia likidoa
HPSEC	Tamainaren araberako bereizmen handiko kromatografia
LSR	Disolbatzaile-solido ratioa
MAE	Mikrouhin bidezko erauzketa
MB	Metileno-urdina
M_n	Batez besteko pisu molekularra kopuruan
M_w	Batez besteko pisu molekularra pisuan
M_w/M_n	Polidispertsitate indizea
PBS	Gatz fosfatozko disoluzio indargetzailea
^{31}P NMR	Fosforozko Erresonantzia Magnetiko Nuklearra
PDA	Patata eta dextrosazko agarra
PVA	Polibinil alkohola
Py-GC/MS	Pirolisia-Gasen kromatografia/Masen Espektrometria
QAH	Hidrolisi azido kuantitatiboa
QE	Kertzetina estraktua
RSM	Erantzun-gainazalen metodologia
S units	Ligninaren siringilo unitateak
S/G ratio	Siringilo-guaiazilo ratioa
SEM	Ekorketazko mikroskopia elektronikoa
TFC	Flavonoideen eduki totala
T_g	Beira trantsizio tenperatura

TGA	Analisi termograbimetrikoa
TPC	Konposatu fenolikoen eduki totala
UV-Vis	Argi ultramore-ikusgarrirako espektroskopia
WNS	Intxaur azalak
XL	Gurutzatzea
XRD	X-izpien difrakzioa

Aurkibidea

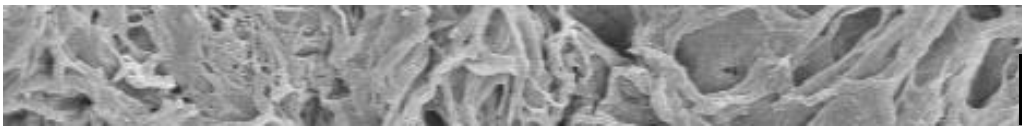

1 Sarrera

1.1 Ingurumen-krisi globala

Antzinatik, gizakiak bere energia-beharrak asetzeko lehen mailako baliabideak etengabe aldatu behar izan ditu. Industria-iraultzak ikatza lehen mailako baliabide gisa erabiltzea bultzatu zuen bezala, XX. mendeak gizarteak petrolioarekiko mendekotasun handia izatea ekarri zuen [1]. Hala ere, baliabide fosilak mugagabeak ez direnez, hauen agortzea, prezioen gorabeherarekin batera, kezka nagusi bihurtu da egungo gizartearentzat. Baliabide horien amaierari buruzko iragarpenak ugariak izan arren, euren kontsumo globala oso handia da oraindik (98.272 mila upel egunean) [2], eta 2030. urterako eskaera horrek gora egiten jarraituko duela uste da [1]. Horrez gain, baliabide fosilen ustiapenak eta kontsumoak ingurumenean eragiten duen kaltea izugarria da, batez ere berotegi-efektuko gasen isurketei dagokienez [1]. 2019an, petrolioa, gasa eta ikatza erretzeko jarduerekin lotutako 34.169 milioi tona (Mt) karbono dioxido isuri ziren [3].

Energiaren ekoizpenaz gain, XX. mendearen erdialdetik polimeroen industria ere petroliotik eratorritako kimika, findegi eta ingeniaritza prozesuen mende egon da erabat [4]. Produktu polimerikoek gure eguneroko bizitza astindu dute eta ia sektore guztietan ezinbesteko material bihurtu dira, urtean 350 milioi tona inguruko mundu mailako ekoizpena izatera iritsiz [5]. Abantaila ugari erakutsi arren, plastikoak edo material polimerikoak ez dira biodegradagarriak izaten. Hori dela eta, hauen kudeaketa desegokiaren ondorioz, hondakin plastiko ugari topa daiteke ingurumenean, batez ere estuario eta itsaso inguruneetan [6,7]. Izan ere, hondakin plastikoek itsasoko zaborraren ia %90a osatzen dute, eta hauen artean elikagaien eta edarien ontzi, zigarro-punta eta poltsen gisako materialak dira ohikoenak [8]. Honek esan nahi du urtean 8 Mt plastiko isurtzen direla ozeanoetan, minuturo betetako kamioi baten karga isurtzearen parekoa izango litzatekeena [8]. Gainera, arrisku hau areagotu

egiten da material hauek partikula txikiagoetan deskonposatzen direnean, "mikro eta nanoplastikoak" deitutakoak sortuz. Izan ere, arrain edo animaliek elikagai moduan irentsi ditzakete partikula hauek, horrela kate trofikoetan eta, ondorioz, giza gorputzean sartuz [5]. Horrez gain, partikula iraunkor hauek haizeak garraia ditzake eta arnastearen ondorioz gizakien biriketaraino hel daitezke [9].

Honela, aipatutako energia-eskari aseezinak eta plastikoen kutsadurak eragindako ondorio larriek ingurumenarekiko errespetu handiagoa duten eta jasangarriagoak diren ordezko baliabideak bilatzeko premia bultzatu dute. Jasangarritasuna egungo eta etorkizuneko gizakien ongizatearen orekarako beharrezkoa da [1]. Horrez gain, ekonomia zirkularra jasangarritasun kontzeptu bezala uler daiteke, ohiko “hartu, egin eta bota” ekonomia modeloa “baliabide, berreskurapen eta birziklapen” ekonomiaz ordezkatzeko helburua duena [10], 1.1 Irudian adierazten den bezala.

1.1 Irudia. Ekonomia lineal eta zirkularraren deskribapen grafikoa.

Testuinguru honetan, baliabide berriztagarriak energia, kimiko eta materialak sortzeko etorkizun handiko ordezko gisa nabarmendu dira azkenaldian, baliabide fosiletan oinarritutako ekonomia baztertu eta bio-baliabideetan oinarrituko den batera bideratzeko [11]. Energia iturri berriztagarriak eolikoa, eguzki-energia, hidraulikoa, geotermikoa, mareomotrizea eta biomasa izan daitezke, esate baterako [1,12]. Horien artean, biomasak arreta handia erakarri du azken urteotan, bere jasangarritasuna dela eta bereziki [4]. Biomasa mineralizazio-prozesurik jasan ez duen edozein material biologiko gisa defini daiteke [1]. Honen barnean landare-jatorriko materia organikoa eta bere eraldaketa natural edo artifizialaren ondoriozko materialak (hondakinak eta azpiproduktuak) sartzen dira [1]. Antzinatik zuzeneko errekuntzarako erabilia izanagatik energia-iturririk zaharrena izan arren, gaur egun ez da ohikoa biomasa produktu kimikoak edota erregaiak lortzeko erabiltzea [4].

Bio-findegiak biomasaren erabilera maximizatu eta hondakinak eta emisioak minimizatzeko garatu dira, biomasa modu jasangarrian produktu espektro zabal bat eta energia bihurtuz [10,13]. Bio-findegiek, beraz, gizateriaren egungo eta etorkizuneko behar energetiko eta materialak ase ahal izateko ikuspuntu iraultzaile bat eskaintzen dute.

1.2 Bio-findegiak eta biomasa

Energiaren Nazioarteko Agentziaren (IEA) arabera, bio-findegia honela defini daiteke: "Merkaturatu daitezkeen oinarri biologikoko produktuak (elikagai eta pentsuetarako osagaiak, produktu kimikoak, materialak, erregaiak, energia, mineralak eta CO_2) eta bioenergia (erregaiak, energia eta beroa) lortzea baimentzen duen biomasaren prozesamendu jasangarria" [14]. Bestela esanda, bio-findegiak hainbat bihurketa-prozesu konbinatzen dituzten industria-instalazioak dira, non oinarri biologiko produktu jasangarriak eskuratzen diren prozesu termokimiko, biologiko, fisiko eta kimikoen bidez [10,15]. Biomasa, beraz, bio-findegien lehengaia da, petrolioa findegiena den bezala.

1.2.1 Bio-findegi motak

Bio-findegiak biomasa mota desberdin ugari eraldatzeko gai direnez, kasu bakoitzean erabili nahi diren lehengaiek eta lortu nahi diren produktuek mugatzen dituzte aplikatu beharreko prozesuak [16]. Ondorioz, lehengai eta produktuen konbinaketen aukera zabala dela eta, zaila da bio-findegiak era bakar batean sailkatzea. IEA-k, esaterako, teknologia-mailaren, biomasa motaren eta gailentzen den eraldaketa prozesuaren arabera sailkatzen ditu [16]. Edonola ere, sortutako produktuen arabera ere sailka daitezke. Hauek energia edo produktuek bultzatutako bio-findegiak izan daitezke, lehenen helburua erregai, gas, bero edota elektrizitatea sortzea izanik eta bigarrenena produktu kimiko edo materialak lortzea [14].

Teknologia-mailaren arabera, lau bio-findegi belaunaldi daudela esan ohi da (1.2 Irudia) [17].

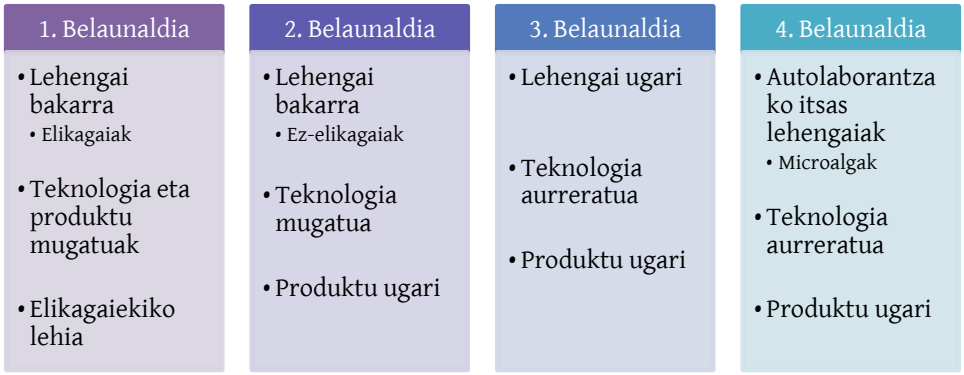

1.2 Irudia. Teknologia-mailaren araberako bio-findegi motak [17].

1.2 Irudian erakusten den bezala, lehen belaunaldiko bio-findegiek lehengai bakarra erabiltzen dute, eta teknologia mugatua dutenez, produktu mugatuak lortzeko gai dira. Bio-findegi hauetan azukre edo olio eduki altua duten lehengaiak, artaburuak edota ekilorea erabili ohi dira, eta bio-erregaien ekoizpenerako erabilgarriak izan arren, erabili beharreko lehengai kopurua oso handia da. Ondorioz, honek elikagaien prezioarekiko lehia sor dezake, eta

hau saihestu beharreko zerbait da. Bigarren belaunaldiko bio-findegiek ere lehengai bakarra erabiltzen dute, baina kasu honetan biomasa lignozelulosikoa erabiltzen dutenez, produktu ugari ekoizteko gai dira, elikagaiekiko lehia ekidinez. Hirugarren belaunaldiko bio-findegiek, aurretik azaldutako biekin alderatuz, abantaila nagusi bat dute: erabilitako teknologia aurreratuari esker, lehengai ugari erabiliz produktu anitz sor ditzakete. Belaunaldi honen helburua, gainera, biomasaren osagai guztien erabilera maximizatzea da, ekoizpen errendimendua hobetuz eta ingurumenaren gaineko eragina gutxituz. Horrez gain, bio-findegi hauek balio erantsiko produktuak ekoizten saiatzen dira. Hirugarren belaunaldikoetan oinarrituz, laugarren belaunaldiko bio-findegiak eskala handiko mikroalgen hazkuntzan zentratzen dira, horretarako prozesuaren kostu ekonomikoa gutxitzen eta ingurumen-onura handitzen saiatuz.

1.2.2 **Biomasa motak**

Aipatu bezala, bio-findegietan lehengai moduan biomasa mota desberdin asko erabil daiteke, likido, solido nahiz gasa izan. Hauen artean, labore eta nekazaritzako hondakinak, industria-hondakinak, udal-hondakinak, uretako organismoak, zurezko hondakinak eta belarrak aipa daitezke, adibidez [17].

- Labore eta nekazaritzako hondakinak: belar- edo egur-espezieak, nekazaritza-lurretan hazteko, uzta biltzeko eta uztatutako lehengaiak prozesatzeko jardueren bidez sortuak [16]. Biomasa honen adibide dira te, tabako eta tomate haziak, laboreen hondakinak, arroz-lastoa, egur-ezpalak eta fruta-hondakinak [16]. Algak ere talde honetan sar daitezke.
- Industria-hondakinak: nekazaritza, basogintza eta elikagaigintza industrietan sortutako azpiproduktuak eta hondakinak. Horien artean daude oliba-olioaren ekoizpenean, zitrikoen prozesatzean, ardogintzan eta garagardogintzan sortutako hondakinak, baita baso-industrien

hondakinak ere (enbor azalak, zerrategi eta arotzeri hondakinak, etab.), zelulosaren industriako azpiproduktuak (likore beltzak) eta material lignozelulosikoak (paletak, eraikuntza-materialak, altzari zaharrak, etab.) berreskuratzearen hondakinak [16].

- ♣ Udal-hondakinak: eguneroko bizitzan sortutako hiri-hondakinen frakzio biodegradagarria. Kategoria honetan sartzen dira araztegiko lokatzak, hondakin-urak eta elikagai hondakinak [16].
- ♣ Uretako organismoak: batez ere makro eta mikroalgak hartzen dituzte, balio-erantsiko elikagai eta produktu bihur daitezkeen bio-konposatuen iturri jasangarriak direnak [10].
- ♣ Zurezko hondakinak eta belarrak: baso-jardueretan sortzen dira. Biomasarik ugariena dira, honen guztizko kopuruaren %89,3 inguru eta mundu osoan urtero ekoizten den biomasaren %42,9 hartzen baitute [15].

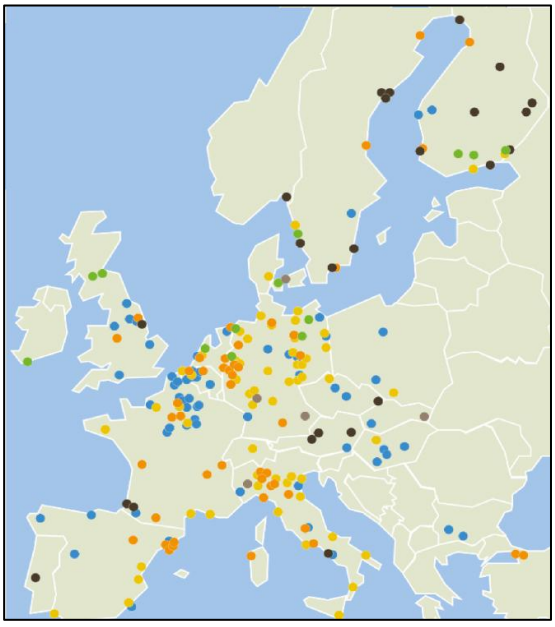

1.3 Irudia. 2017an Europan zeuden bio-findegien mapa, erabilitako lehengaien arabera sailkatuta: bio-hondakinetan oinarrituak (berdea), biomasa lignozelulosikoan oinarrituak (marroi argia), olio/gantzetan oinarrituak biodieselaren ekoizpenerako (horia), olio/gantzetan oinarrituak oleokimikarako (laranja), azukre/almidoian oinarrituak (urdina) eta egurrean oinarrituak (marroi iluna) ([18]-tik moldatua).

1.3 Irudiak 2017an Europan zeuden bio-findegi mota desberdinak erakusten ditu, erabilitako biomasaren arabera sailkatuta. Guztira 234 instalazio zenbatu ziren urte hartan, eta ziurrenik kopuru horrek gora egin du ordutik.

1.3 Biomasa lignozelulosikoa

Biomasa lignozelulosikoa edo begetala bioenergia eta konposatu biokimikoen iturri erakargarri bihurtu da azkenaldian [19]. Planetako biomasa berriztagarririk ugariena da, urtean 200.000 milioi tona ekoizten baitira [20]. Honen barnean zurezko landareak (hau da, egur bigunak eta gogorrak), zerrautsa (zurezko itsasontzi, obra-leku eta zerrategietatik eratorriak) eta azalen bakantze-hondakinak, eta egurrezkoak ez diren landareak, hala nola belar-landaredia, nekazaritza-hondakinak eta elikadurarako nahiz elikadurarako ez diren laboreak [21]. Biomasa lignozelulosikoa oso ugaria izateaz gain, oso erabilgarri dagoen, kabonoan neutroa den eta jangarria ez den bio-baliabide bat da, landareen horma zelularretatik datorrena [21,22].

Material lignozelulosikoa material konposatu natural konplexua da, hiru egitura-osagai nagusi izateaz gain (zelulosa, hemizelulosak eta lignina) egituraren parte ez diren beste batzuez ere (pektina, proteina, estraktu eta errautsez, adibidez) osatzen dena. 1.1 Taulan adierazten den bezala, biomasa mota honen konposizioa lehengaiaren iturri nahiz hazte baldintzen araberakoa da [23].

1.1 Taula. Biomasa lignozelulosikoaren osaera argigarria ([24]-tik moldatua).

Lehengaia	Zelulosa (%)	Hemizelulosak (%)	Lignina (%)
Zur biguna	45–50	25–35	25–35
Zur gogorra	45–55	24–40	18–25
Belarra	25–40	25–50	10–30

Lehengai lignozelulosikoen artean, fruitu lehorren azalak munduan urtero kopuru izugarrian ekoizten dira. 1.4 Irudian 2019 urtean eman zen fruitu lehor batzuen munduko ekoizpena aurkezten da.

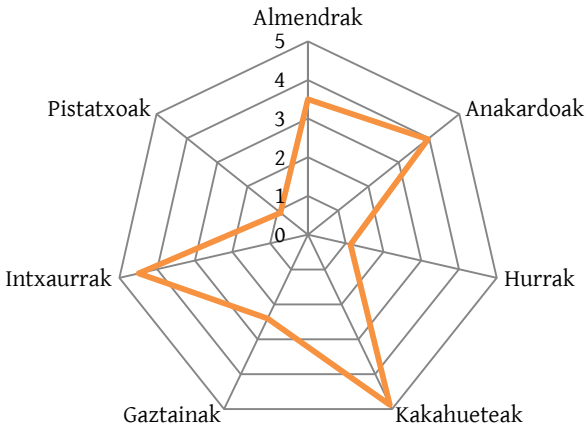

1.4 Irudia. 2019ko fruitu lehor batzuen ekoizpen globala (milioi tonatan, Mt) [25].

Datu hauen arabera, urte horretan 3,5 eta 4,5 miloi tona almendra eta intxaur inguru ekoiztu ziren munduan. Hala ere, fruitu lehor horietan jangarria den ehuneko txikia dela eta, balio-erantsi baxuko industria- edo merkataritza-aplikazioetarako erabiltzen diren azal kopuru handia ekoizten da. Baina oskol horiek biomasa lignozelulosikoari dagozkionez, bio-findegi estrategia baten bidez, balio-erantsi altuko materialak ekoizteko lehengai gisa erabili litezke.

1.3.1 Elementu ez-estrukturalak

Elementu ez-estrukturalak pisu molekular baxuko konposatuak izan ohi dira eta biomasa lignozelulosikoaren %5-10 osatzen dute gehienez. Landareen horma zelularraren egituraren parte ez izan arren, elementu hauek beharrezko propietate fisiologikoak ematen dizkiote landareari, elastikotasuna, iragazkortasuna edota onddo nahiz intsektuen erasoen aurkako babesa, esate baterako. Konposatu hauen artean konposatu fenolikoak, gantz-azidoak, terpenoak, lignanoak, flabonoideak, taninoak eta argizariak topa daitezke. Horietako batzuk bio-aktiboak dira, hau da, osasunarekin loturiko aplikazioetarako balio izateaz gain, elikagaien babeserako ere erabil daitezke, adibidez [23].

1.3.2 Zelulosa

Zelulosa landareen horma zelularraren osagai nagusia da eta erresistentzia mekanikoa eta egonkortasun kimikoa ematen dio [22,26]. Lurreko biopolimerorik ugariena da eta landare, bakteria, alga eta beste biomasa batzuetan ere aurki daiteke [26]. Zelulosa polisakarido lineala da, β–1,4 loturez konektatutako D-glukosazko unitatez osatua [27]. Hidrogeno eta Van der Waals lotura sendoei esker, zelulosazko zuntzak osatzen dira, euren orientazioaren arabera kristalinitate maila desberdinak eragiten dituztenak [21]. Zelulosazko mikrozuntzak beste egitura-elementuekin elkartu eta makrozuntzak osatzen dituzte, era berean horma zelularrak eraikiz (1.5 Irudia). Biopolimero honen ezaugarri fisiko-kimikoak, biodegradagarritasuna, biobateragarritasuna eta berriztagarritasuna direla eta, hainbat aplikaziotarako erabili da, eta gero eta interes handiagoa du tratamendu eta gainazaleko eraldaketa egokien ondoren erakutsitako propietateengatik [21].

1.3.3 Hemizelulosak

Zelulosaren kasuan ez bezala, hemizelulosak kate motzeko heteropolimero adarkatuagoak, amorfoak eta ausazkoak dira [21]. β–1,4 lotura glikosidikoz konektatutako bost eta sei karbonoko azukrez daude osatuta (pentosa eta hexosaz, hurrenez hurren) [20]. Xilosa eta arabinosa bezalako pentosak, glukosa, galaktosa eta manosa bezalako hexosak eta beste sakarido batzuk (ramnosa eta fruktosa, adibidez) konbinatu ohi dira hemizelulosak osatzeko, nahiz eta batzuetan azido uronikoak eta azetil taldeak ere aurkitzea posible izan [21]. Hemizelulosei esker zelulosa zuntzak mikrozuntzetan pilatzen dira, hidrogeno eta Van der Waals loturak osatuz eta ligninarekin ere gurutzatuz [21]. Ondorioz, heteropolimero honek zurruntasuna ematen dio biomasa lignozelulosikoaren matrizeari [20].

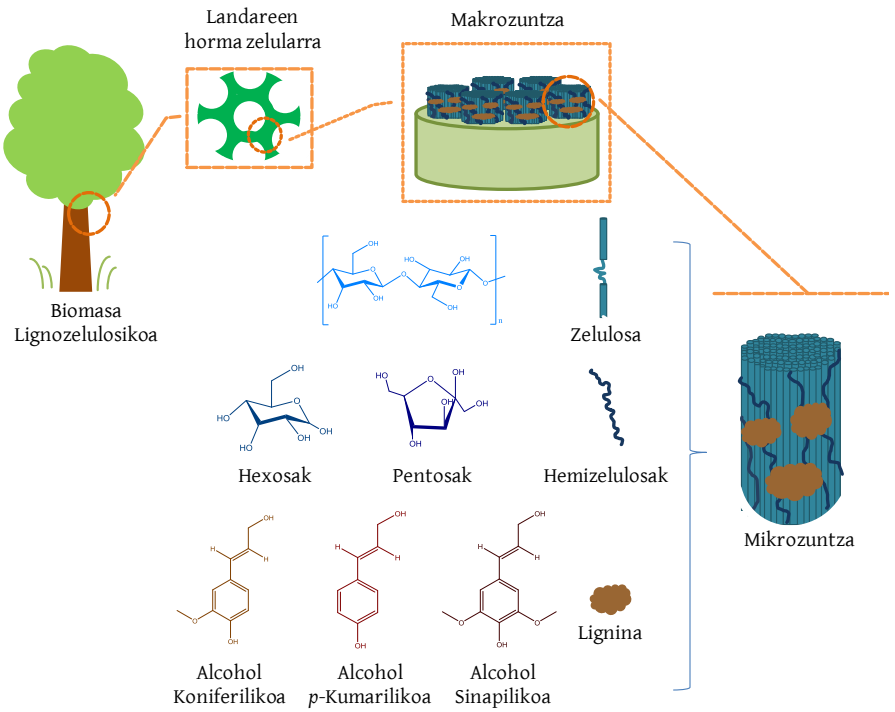

1.5 Irudia. Landare-horma zelularra osatzen duten osagai nagusiak eta horien unitateen egitura kimikoak.

1.3.4 **Lignina**

Lignina Lurreko biopolimero fenolikorik ugariena da. Zur biomasaren %40ra arte osa dezake [26,28,29] eta landareen egiturari zurruntasuna eta hidrofobotasuna ematen dio. Elementu honek mikrobio eta onddoen erasoen, izpi ultramoreen eta suaren aurkako babesa ematen die landareei [24,28]. Urtero 100.000 milioi tona inguru lignina birsortzen direla estimatzen da, horietatik 1,5-1,8 mila milioik industria-ekoizpenarekin zerikusia izanik [30]. Kopuru honetatik 70 milioi tonak egur eta paper industrian dute jatorria, instalazio beraren energia-berreskurapenerako erabili ohi direnak [30]. Edonola ere, biopolimero hau gutxi ustiatuta dagoela uste da, karbonoan oinarritutako hainbat produkturen (kimikoak eta materialak) ekoizpenean baliabide fosilak ordezkatzeko hautagai garrantzitsua izan baitaiteke [30].

Ligninak egitura oso adarkatua du, fenilpropanozko hiru unitateren konbinaketaz osatzen dena: alkohol sinapilikoa (siringilo, S unitatea), alkohol koniferilikoa (guaiazilo, G unitatea) eta alkohol *p*-kumarilikoa (4-hidroxi fenil, H-unitatea) [26,28,29]. Unitate hauek talde funtzional polar ugari dituzte eta ausaz lotzen dira eter loturen bidez, hiru dimentsioko egitura amorfo bat sortuz. Karbono–karbono (C–C) eta karbono–oxigeno (C–O) loturak dira lignina monomeroen arteko lotura ohikoenak [28]. Hala ere, β–O–4 lotura, H unitate baten eta propenil talde baten β-amaieraren arteko C–O lotura, da errepikakorrena [28]. Era berean lotura hau guztietan hauskorrena da eta ligninaren erauzketa prozesuetan erraz hautsi ohi da [31]. 1.6 Irudian ligninarentzat proposatutako egitura kimikoa bat erakusten da.

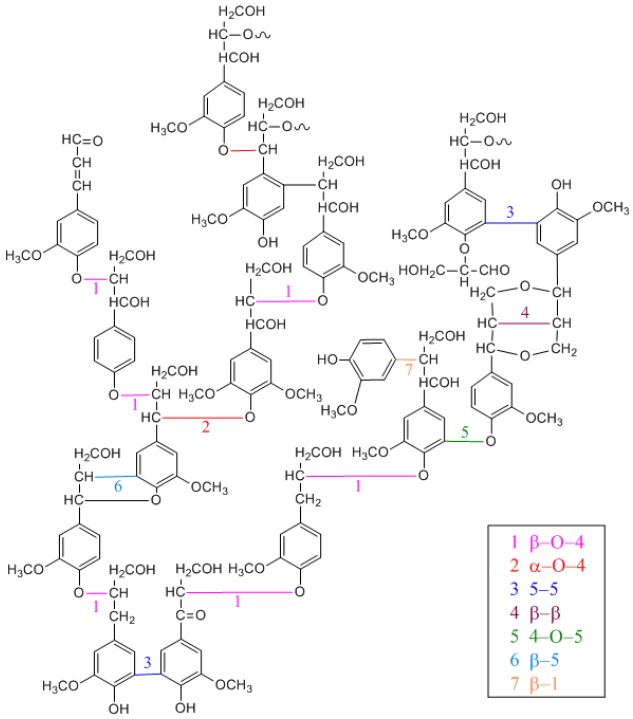

1.6 Irudia. Ligninarentzat proposatutako egitura kimikoa ([32]-tik moldatua).

Ligninaren konposizioa G, S eta H unitateen kopuruaren arabera aldatzen da landaretik landarera [24]. Horrez gain, literaturan 1.000 eta 20.000 g/mol

arteko pisu molekularrak topa daitezkeen arren, ligninaren berezko polimerizazio-maila ezagutzea oso zaila da, izan ere, erauzketa prozesuan zatikatu egiten baita [28]. Zur bigunetan G unitateak dira nagusi, zur gogorretan, ordea, S eta G unitateak nagusitzen dira. Belarren kasuan, H unitateak izan ohi dira ugariagoak [28]. Unitate hauek, beste talde funtzionalen presentzia eta euren arteko β–O–4 loturekin batera, ligninaren despolimerizazio kimiko eta biokimikoen aurkako izaera egonkorraren erantzule dira [33]. Ligninaren portaera honek, bere egitura konplexuak eta degradatutako lignina zatiek jasa ditzaketen kondentsazio-erreakzioek biopolimero hau balioztatzea erronka bat bihurtzen dute. Edonola ere, lignina balio-erantsiko produktu bilakatzea bio-findegien lehiakortasun ekonomikoa bermatzeko erabat beharrezkoa dela uste da [34].

1.3.4.1 Ligninaren erauzketarako metodoak

Aurretik aipatu bezala, erabilitako erauzketa prozesuaren arabera, ligninaren zenbait ezaugarrik aldaketak paira ditzakete. Izan ere, prozesu hauek ligninaren konposizioan, egitura molekularrean, pisu molekularrean eta disolbagarritasuna edota hidrofobotasuna bezalako propietate fisikoengan eragin dezakete [35], ondorengo balio-erantsiko produktuen ekoizpena mugatuz [36].

Ligninaren erauzketa eraginkor batek errendimendu eta purutasun handiko ligninaren isolamendua baimendu beharko luke, ahalik eta β-O-4 lotura gehien mantenduz ondorengo balioztatze prozesuetan mesedegarri izateko [34]. Gaur egun, deslignifikazio metodo ugari aurki daitezke, 1.7 Irudian ikus daitekeen bezala. Euren arteko desberdintasun nagusienak inplikatutako erreaktiboetan, aplikatutako tenperaturetan eta erabilitako denboretan aurki daitezke besteak beste. Hemizelulosekin osatzen dituen lotura kobalenteen eraginez, lignina-karbohidrato konplexuak sortzen dira [30,34]. Deslignifikazio prozesuetan

lotura hauek hautsi egin behar dira [30], eta ligninaren despolimerizazio partziala ere saihestezina izan ohi da biomasatik isolatu ahal izateko [34].

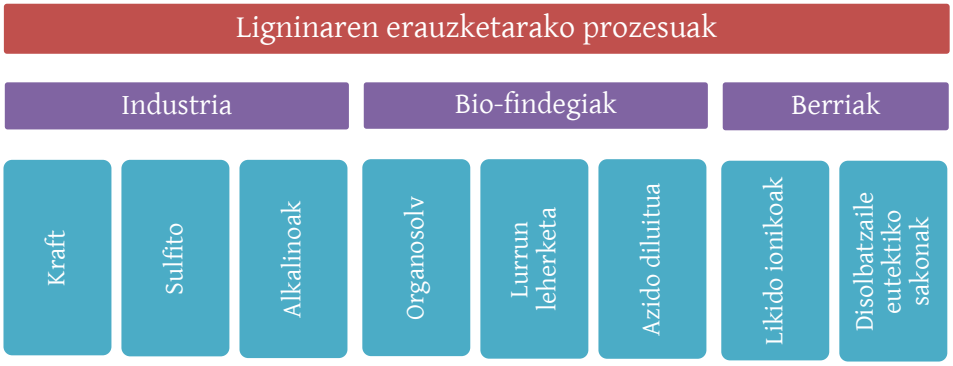

1.7 Irudia. Ligninaren erauzketarako prozesu ezagunenen laburpena.

1.7 Irudian aurkezten diren metodoetatik batzuk aspalditik erabiltzen diren prozesuak dira, besteak beste, Kraft eta sulfito prozesuak XIX. mende amaieratik aurrera mundu osoan erabili izan dira egur eta papergintza industrian. Edonola ere, prozesu hauetan zelulosaren lorpena izan da helburu, lignina azpiproduktu gisa lortu den bitartean. Hala ere, azken urteetan, lignina produktu gisa duten bio-findegi prozesu alternatiboek arreta handia bereganatu dute. Hala eta guztiz ere, metodo horiek guztiek zenbait arazo dakartzate: konplexutasuna, disolbatzaileen eta produktu kimikoen kontsumo handia, prozesatze-denbora luzeak, etab. Horrez gain, energia-eskariari dagokionez, baldintza gogorrak eskatzen direnez, eskari handikoak izan daitezke. Testuinguru horretan, metodo berriak sortu dira erauzketa-eraginkortasun handiagoa lortzeko eta eskala handiagotzea sustatzeko [37].

1.3.4.2 Ligninaren eraldaketarako metodoak

Nahiz eta ligninaren egitura oso adarkatua izan eta bere erreaktibotasunean zuzenean eragiten duten talde funtzional ugari izan [30,38], aplikazio batzuetarako, ligninaren erreaktibotasuna ez da behar bezain altua izaten. Hau bere pisu molekular altuari, oztopo esterikoari eta bere egiturako toki

erreaktibo urriei egotz dakieke [13,39]. Beraz, batzuetan bere erreaktibotasuna hobetuko duen egituraren aldaketa kimiko bat egitea beharrezkoa izaten da [40]. Horretarako, lau bide nagusi daude (1.8 Irudia): lehenak despolimerizazioa edo zatikatzea dakar, bigarrenak kimikoki aktiboak diren leku berrien sintesia du ardatz, hirugarrenak egiturako hidroxilo taldeen funtzionalizazioarekin du zerikusia, eta azkena txertaketazko edo *grafting* kopolimeroen bidez izango litzateke [41]. Eraldaketa horiek, neurri handi batean, erabiltzen ari den ligninaren talde funtzionalen erreaktibotasunaren eta egituraren araberakoak izan ohi dira.

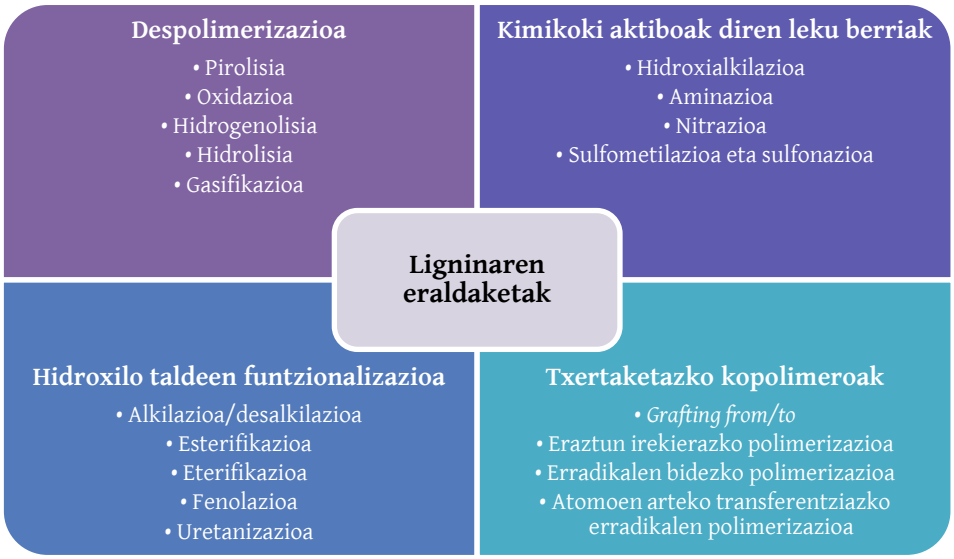

1.8 Irudia. Ligninaren eraldaketa kimiko nagusiak ([41]-tik moldatua).

1.4 Hidrogelak

1.4.1 Definizioa eta propietate orokorrak

Hidrogelak ura xurgatzeko ahalmen handia duten hiru dimentsioko egitura polimerikoak dira. Propietate hau bere sare egiturarekin lotuta dago, non fisikoki edo kimikoki gurutzatutako kate polimerikoen arteko hutsuneek fluido urtsuak edota beste fluido biologiko batzuk bereganatzea ahalbidetzen duten [42,43]. Euren ur edukia %90etik gorakoa izatera hel daiteke, eta horri eta

euren propietate elastikoei esker, hidrogelek giza ehunen antz handia hartzen dute. Propietate hauek zaurien zainketa eta beste hainbat aplikazio biomedikoetarako egokiak bihurtzen dituzte [44,45], hala nola, zelulen kapsularatzean [44], bio-sentsoreetan, hezur-ehunen ingeniaritzan [43], muskulu artifizialen diseinuan, ukipen-lenteetan, eta abar. Aplikazio hauez gain, elikagaien industrian, farmazian, botiken askapen kontrolatuan eta material super-xurgatzaileetan ere erabili izan dira [46]. Funtzio horietako asko material horiek kanpoko estimuluei erantzuteko duten gaitasunari esker lortzen dira, hala nola tenperatura, pH-a, kontzentrazio ionikoa eta eremu magnetiko eta elektrikoen aurkako estimuluei. Hidrogel hauek *smart* edo sistema adimendun bezala ezagutzen dira eta aplikazio teknologiko aurreratuetarako material interesgarri bihurtu dira [47].

1.4.2 Sintesia eta sailkapena

Hidrogelen sintesirako, oro har, hiru elementu nagusi behar izaten dira: monomero bat, abiarazle bat eta erretikulatzaile edo *crosslinker* bat. Ura edo ur-soluzioak erreakzioaren beroa eta ondoriozko materialen propietateak kontrolatzeko ere baliagarriak izan daitezke [48]. Hala ere, materialen ezaugarriak prestatzeko tekniken mende daude erabat.

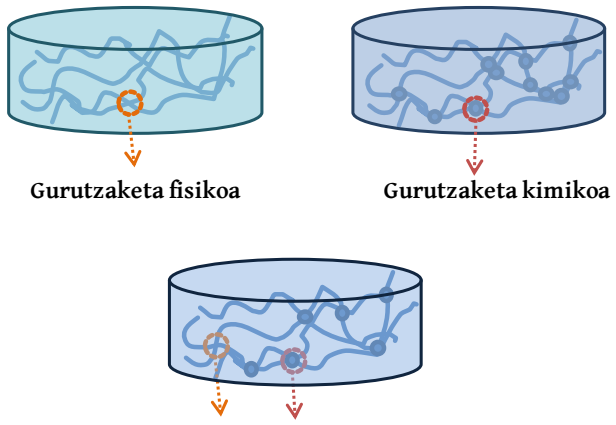

1.9 Irudia. Gurutzaketa fisikoa, kimikoa eta duala duten hidrogelen adierazpen eskematikoa.

Hidrogelak hainbat irizpideren arabera sailka daitezkeen arren, ohikoena saretze motan oinarritzen da. Saretzea kate polimerikoen arteko interakzioen bitartez lortzen da. Lotura hauek fisiko edota kimikoak izan daitezke, eta hidrogelen prestaketa-metodo desberdinak aplikatuz lor daitezke. Gurutzaketa fisikoa lortzeko, adibidez, izozte-desizoztea, irradiazioa, *solvent-casting* edota faseen bereizketa erabil daitezke, eta horrela, interakzio ionikoak, hidrogeno-loturak, hidrofobikoak edota *host-guest* interakzioak eragiten dira. Gurutzaketa kimikoaren kasuan, aldiz, beste metodo batzuk erabil daitezke, adibidez, disoluzio bidezko polimerizazioa edo irradiazioa, erradikal askeen polimerizazioa, kondentsazio eta gehitze erreakzioak [46]. Batzuetan, hidrogelek bi gurutzaketa motak izan ditzakete aldi berean, gurutzaketa edo saretze dual bezala ezagutzen dena (1.9 irudia), eta gurutzaketa kimiko edo fisiko soilak dituzten hidrogelekin alderatuz, propietate desberdinak dituzte [49].

1.4.3 **Hidrogel sintetikoetatik biopolimeroetan oinarritutakoetara**

1960. urtean, Wichterle eta Lim aitzindariak izan ziren giza ehunekin bateragarriak ziren hidrogelen sintesian, eta, ordutik, hidrogelen gaineko arreta esponentzialki handitu da, aurretik aipaturiko "hidrogel adimendunak" deiturikoen garapenerako interesagatik, batez ere [47].

Hidrogelen historia hiru aldi nagusitan banatzen da [47]. Lehen belaunaldian, gurutzaketa-metodo ugari sortu ziren, ur xurgapen gaitasun handiko, propietate mekaniko oneko eta oinarri teoriko errazeko materialak ekoiztuz [47]. Bigarren belaunaldia, 70eko hamarkadan hasi zena, kanpoko estimulu espezifikoei (adibidez, tenperatura, pH-a, etab.) erantzuteko gai ziren materialak lortzean oinarritu zen. Hirugarren belaunaldian, berriz, material estereo konplexuak eta beste interakzio fisiko batzuen bidez sareztatutako hidrogelak ikertu eta garatu ziren [47].

1980ko hamarkadaren amaieran, polimero naturalak, kolagenoa eta marrazo kartilagoak kasu, hidrogeletan erabiltzen hasi ziren [47]. Ordutik, biopolimeroetan oinarritutako hidrogelak oso ezagunak egin dira elikaduraren, kosmetikoen, produktu farmazeutikoen eta inplante biomedikoen arloetan duten aplikagarritasunagatik, besteak beste [50]. Petrolio-erreserba mugatuek, material mota horren degradazioan sortutako konposatu toxikoek eragindako ingurumen-arazoek eta hidrogelen merkatuaren hedapenak ingurumena errespetatu eta seguruak diren material berriztagarrietan oinarritutako hidrogel alternatiboak garatzeko premia eragin dute. Era berean, horien garapenak biomasaren berrerabilpena eta birziklapena bultzatu eta bio-ekonomia zirkularra sustatuko lukete (1.10 Irudia) [11].

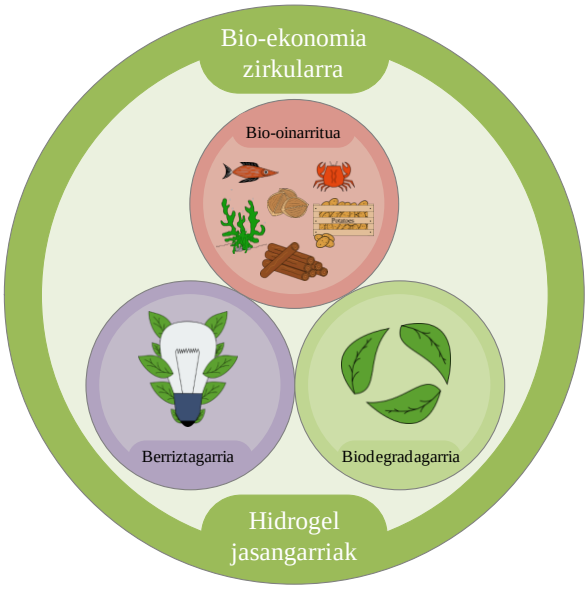

1.10 Irudia. Hidrogel jasangarrien definizio grafikoa.

1.4.4 Ligninan oinarrituriko hidrogelak

Erabilgarri eta ugariak diren biopolimeroen artean, lignina da aromatikoa den bakarra, hidrogel funtzionaletan aplikatzeko interesgarri egiten duena [50]. Ikerketa askok berriki frogatu dute ligninatik eratorritako konposatuak

arrakastaz erabil daitezkeela ehunen zainketa eta botiken askapenerako edota UV izpien xurgatzaile gisa erabiliko diren materialen sintesirako [51]. Ondorioz, azken urteotan ligninari eta bere aplikazioei buruzko argitalpenen goranzko joera garbia ikusi da [30,52,53]. Lignina beste polimero biosintetiko edo sintetiko batzuekin konbinatu ohi da bere kabuz saretzeko gai ez delako. Horregatik, hainbat sare polimerikotan gehitu da, hidrogelen eraketa sustatzen duten interakzio fisiko edota erreakzio kimikoen bidez [54].

1.4.5 Ligninan oinarrituriko hidrogelen aplikazioak

Orain arte ligninan oinarrituriko hidrogelen ehuneko handi bat ur disoluzioetan dauden metal astunak eta konposatu kationikoak xurgatzeko erabili da [55]. Hala ere, material hauek biomedikuntzan (botiken askapenerako, adibidez) edota ehunen ingeniaritzan ere erabiliak izan dira [55].

Uraren askapen kontrolatua nekazaritzan erabiltzen den termino bat da. Euria urria den klimetan, zoruak maiz ureztatu behar izaten dira. Hala ere, lurrak hidrogel txiki eta adimendunez hornitzeak, hala nola ligninaz egindako hidrogelez hornitzeak, ur kantitate esanguratsuak xurgatu eta gordetzen dituela frogatu da, laboreek behar duten arte [50]. Hidrogelen ur-edukia aldatu egin daiteke haien saretze-mailaren arabera, eta parametro hau euren sintesian kontrola daiteke.

Ligninaren talde funtzionalek (fenol eta alkoholetako hidroxiloak, metoxi eta karboxiloak) adsortzio-leku gisa jardun dezakete tindagaien molekula eta metal astunentzat [56]. Egitura horiek molekula positiboak erakartzeko gai dira, negatiboki kargatutako talde funtzionalei esker, eta konposatu organiko-aromatikoak erakartzeko gai π-π erreakzioen bidez [50]. Horregatik, ioi inorganikoak eta konposatu organikoak lurzoru eta uretatik ezabatzeko erabili izan dira [50]. 1.2 Taulak aplikazio eremu horretako lan batzuk laburbiltzen ditu.

1.2 Taula. Hidrogelak kutsatzaileen xurgatzaile gisa erabili dituzten lanen berrikuspen bibliografikoa.

Erabilitako lignina mota	Kutsatzailea	Ingurua	Xurgapena	Erreferentzia
Sodio lignosulfonatoa	Kadmio ioiak (Cd^{2+})	Lurra	< 61,77 ± 1,09 mg/g	[57]
Lignina	Metileno-urdina (MB) eta berun ioiak (Pb^{2+})	Ura	201,7 mg/g MB eta 753,5 mg/g Pb^{2+}	[58]
Kraft lignina, organosolv lignina eta alkalinoa	Toluenoa	Ura	164 –170 mg/g	[59]
Lignina alkalino aminatua	Metal astunezko ioiak (Pb^{2+}, Hg^{2+} eta Ni^{2+}) eta tindagaiak (Metileno-urdina, metil-laranja eta anilina berdea)	Ura	2,1–55 mg/g metal astunezko ioientzat eta 2–155 mg/g tindagaientzat	[60]
Kraft lignina, hidrolisi entzimatikotik eratorritakoa eta alkalinoa	6G Rodamina, anilina morea, metileno-urdina eta metil-laranja	Ura	10–196 mg/g	[56]
Kraft lignina, organosolv lignina eta alkalinoa	Metileno-urdina	Ura	69–629 mg/g	[61]
Pinutik isolaturiko Kraft ligninan oinarrituriko AT indulina	Prednisolona botika eta 3,4-dikloroanilina	Ura	1,35 mg/g prednisolona eta 4 mg/g 3,4-dikloroanilina	[62]
Lignina alkalinoa	Kromoa, Cr (VI)	Ura	599,9 mg/g	[63]
Azidoz aurretrataturiko lignina alkalinoa	Pb^{2+}, Cu^{2+} eta Cd^{2+} ioiak	Ura	1,076 mmol/g Pb^{2+}, 0,323 mmol/g Cu^{2+} eta 0,059 mmol/g Cd^{2+}	[64]

Hidrogelak elikagaiak ontziratzeko sistemetan aplikatzeko aukera interesgarri bat ere izan daitezke, hala nola, plaka xurgatzaileetan [65]. Ura xurgatzeko gai izateaz gain, material hauek biltegiratutako elikagaien bizitza erabilgarria handitu behar dute eta elikagaien gainazalean mikrobio-hazkundea saihestu [65]. Beraz, hidrogelen sarea osatzen duten polimeroen mikrobioen aurkako portaera oso garrantzitsua da. Testuinguru horretan, ligninak eta haren deribatuek eta lignina-hidrogelezko estaldurek portaera antimikrobianoa dutela erakutsi dute [66–68]; beraz, elikagaiak ontziratzeko erabil daitezkeela esan daiteke.

Mikrobio nahiz oxidazioaren aurkako ezaugarriak eta zitotoxikotasun baxua izatea ere garrantzitsuak dira material bio-bateragarrien sintesirako. Zentzu horretan, hidrogelek zaurietan desiragarriak ez diren metabolitoak modu eraginkorrean ezabatu ditzakete euren xurgapen gaitasuna dela eta, eta ligninak zauria aurrerago sor daitezkeen arazoetatik babesten lagun dezake, hala nola lesio edo kutsadura berrietatik, bere propietate mekaniko onei esker [53]. Hori dela eta, ligninak zaurien zainketan [69] eta ehunen ingeniaritzan [70] garrantzia hartu du.

Lignina hidrogelak eremu biomedikoaren beste zati garrantzitsu batean ere erabilgarriak dira: botika hidrofobikoak [67] eta hidrofilikoak modu kontrolatuan askatzeko, esaterako. Lignina eta beste (bio)polimero batzuk konbinatuz, estimuluekiko sentikorrak diren hidrogelak sor daitezke. Hidrogel horiek oso interesgarriak dira botikak garraiatu eta askatzeko, haien bolumena alda baitezakete ingurumen-estimuluei erantzunez [71], pH-a, tenperatura edo argiaren eraginez, adibidez [54].

Ligninan oinarritutako materialak energia alorreko gailuetan ere erabilgarri direla ikusi da [72]. Beste aplikazio batzuen artean, material hauek super-kondentsadoreentzako elektrodo bezala erabil daitezke, euren gainazal zabal eta egonkortasun kimikoari esker, baina baita euren eroankortasun elektriko altuarengatik ere [72,73].

Aurreko guztia kontuan hartuta, iraganean gutxi erabili den arren, ligninak abantaila ugari eta erabilera eremu zabala dituela ondoriozta daiteke, bai ekonomiaren ikuspegitik (erabilgarritasun handia eta kostu txikia) eta baita ingurumenaren (berriztagarria eta biodegradagarria) eta teknologia (ezaugarri fisiko-kimiko bikainak) ikuspegietatik ere. Guzti horregatik, aplikazio askotarako erabilgarria izan daitekeen material garrantzitsu bat bilakatzen ari da.

1.5 Hutsune zientifikoa

Azken urteotan lignina hidrogelekiko ikerketa-interesak gora egin duen arren, aztertutako sistema gehienek gurutzaketa kimikodun egiturak dituzte, eta askotan oso toxikoak diren erreaktiboak erabiltzen dira hauek lortzeko. Gainera, polimero matrizeetan gehitutako lignina kopuruak oso txikiak izan ohi dira, eta horrek biopolimero horren balorizazioa mugatu egiten du. Horrez gain, ikerketa askotan lignina mota bakar batek sintetizaturiko hidrogelen propietateetan duen eragina aztertzen da, eta horrek beste lignina-mota batzuk erabili behar direnean estrapolazioa zailtzen du.

Aurrekoa kontuan hartuta, lan honen ardatza ligninan oinarritutako hidrogelen sintesia optimizatu eta karakterizazioa burutzea da, lignina alkalino komertzial eta polibinil alkoholezko matrizearen arteko konbinaziotik abiatuta. Baldintza optimoak nekazaritzako elikagaien hainbat hondakin lignozelulosikoetatik (almendra eta intxaur-oskolak) isolatutako eta eraldatutako ligninetan oinarritutako hidrogelen sintesirako erabiliko dira. Ekoiztutako materialak karakterizatu eta aplikazio aurreratu batzuetarako ebaluatuko dira, hala nola, kutsatutako uren arazketarako, ontziratze aktiborako eta botiken askapenerako, era berean ligninari balio erantsi bat emanez.

2 Helburuak eta erronkak

Tesi honen helburu nagusia lignina mota desberdinei hidrogel aurreratuak lortzeko erabiliz balio-erantsia ematea izan da, hidrogel horiek karakterizatuz euren aplikazio egokienak definitzeko asmoz. Helburu hau lortzeko, lehenik, hidrogelen sintesiko hainbat parametro optimizatu dira eta, jarraian, estimaturiko baldintza optimoak lignina desberdinetan oinarritutako hidrogel gehiago lortzeko erabili dira.

2.1 Helburu espezifikoak

Helburu nagusia betetzeko, eta literatura azterketa sakon baten ondoren **(I. Artikulua)**, ondoko helburu espezifiko hauek proposatu dira:

- **1. Helburua (II. Artikulua):** Ligninan oinarritutako hidrogelen sintesia optimizatzea diseinu esperimentalen bidez, ur xurgatze-ahalmena maximizatuz eta lignina galera minimizatuz.
- **2. Helburua (III. Artikulua):** Matrize polimerikoaren pisu molekularrak lignina-hidrogelen propietateetan duen eragina aztertzea, hidrogelak aurretik ondorioztatutako baldintza optimoetatik abiatuta sintetizatuz.
- **3. Helburua (IV. Artikulua):** Hainbat prozesu eta material lignozelulosikotatik abiatuz ligninak erauztea eta karakterizatzea, eta hauek hidrogelen sintesirako erabiltzea.
- **4. Helburua (V. Artikulua):** Lignina komertzial eta erauzitako ligninen eraldaketa kimikoa eta karakterizazioa burutu ondoren, hobetutako propietateak dituzten hidrogelen sintesirako erabiltzea.
- **5. Helburua (III, IV eta V. Artikuluak):** Sintetizaturiko hidrogelek hainbat aplikaziotarako duten baliagarritasuna ikertzea: kutsatutako uren tratamendurako (kutsatzaileak xurgatzeko), ontzi aktiboetarako (material antifungikoen moduan, esaterako) eta biomedikuntzarako (botiken askapena eta biobateragarritasuna).

2.2 Erronka nagusiak

Tesi honen erronka nagusiak ligninaren egitura ezezagunaren eta bere jatorri eta erauzketa metodoaren araberako aldakortasunaren ondorio dira. Gainera, bere pisu molekular handia eta eragozpen esterikoa direla eta, biopolimero honekin lan egitea neketsua eta erronkaria da. Bestalde, jakina da materialen sintesian kanpoko parametro askoren eragina izan ohi dela, batzuetan kontrolaezinak direnak, baina eragin handia izan dezaketenak produktuen lorpenean eta ezaugarrietan. Beraz, parametro horien eragina identifikatzea eta hautematea ere erronka handia da.

Aurrekoa kontuan hartuta, material berrien sintesia are zailagoa da lignina erabiltzen denean. Beraz, tesi hau zuloz betetako bide bat bezala aurkezten da, arreta eta kontu handiz gurutzatu beharko dena.

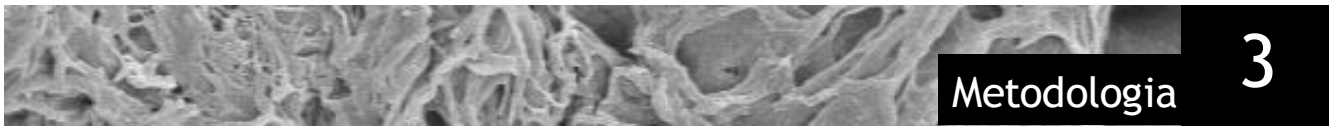

3 Metodologia

Argitalpen guztietarako erreaktibo komertzialak hornitu bezala erabili ziren. Informazio zehatzagoa **Atxikitako Argitalpenetan** irakur daiteke.

3.1 Lehengaiak

IV eta V. Artikuluetan erabilitako almendra azalak (AS) (Marcona motakoak) bertako baserritarrek emanak izan ziren eta intxaur azalak (WNS), berriz, Olagi sagardotegiak (Altzaga, Gipuzkoa) emandakoak.

3.2 Lehengaien karakterizazioa

Azalen konposizioa aurrez deskribatutako metodoen bidez aztertu zen [74]. Hezetasun, errauts eta etanol-tolueno erauzgarrien kopurua zehazteko TAPPI arauak erabili ziren (TAPPI T264-om-88, TAPPI T211-om-02 eta TAPPI T204-cm-97, hurrenez hurren). Klason lignina eta karbohidrato edukia National Renewable Energy Laboratory-k (NREL) deskribatutako TP-510-42618 protokoloaren bidez zehaztu ziren. Protokolo hau bi etapako hidrolisi azido kuantitatiboaz (QAH) osatzen da: lehena, solidoa pisuan %72ko purutasuna duen H_2SO_4-arekin ordubetez 30 ºC-ra mantenduz, eta bigarrena, pisuan %4ko purutasuna duen H_2SO_4-arekin ordubetez 121 ºC-ra mantenduz. QAHren ondoren berreskuratu zen fase solidoa grabimetrikoki neurtu zen eta Klason ligninatzat hartu zen, fase likidoa, berriz, azukreak (glukosa, xilosa eta arabinosa), azido galakturonikoa eta azido azetikoa kuantifikatzeko, bereizmen handiko kromatografia likidoaren bidez (HPLC) aztertu zen. Azidotan disolbagarria den lignina (ASL) espektrofotometrikoki zehaztu zen (TAPPI UM250-um-83). Analisi guztiak hiru aldiz errepikatu ziren.

3.3 Ligninaren erauzketa eta eraldaketarako prozedurak

Tesi honetako **Atxikitako Argitalpen** bakoitzean erabilitako ligninak eskema honetan deskribatzen dira:

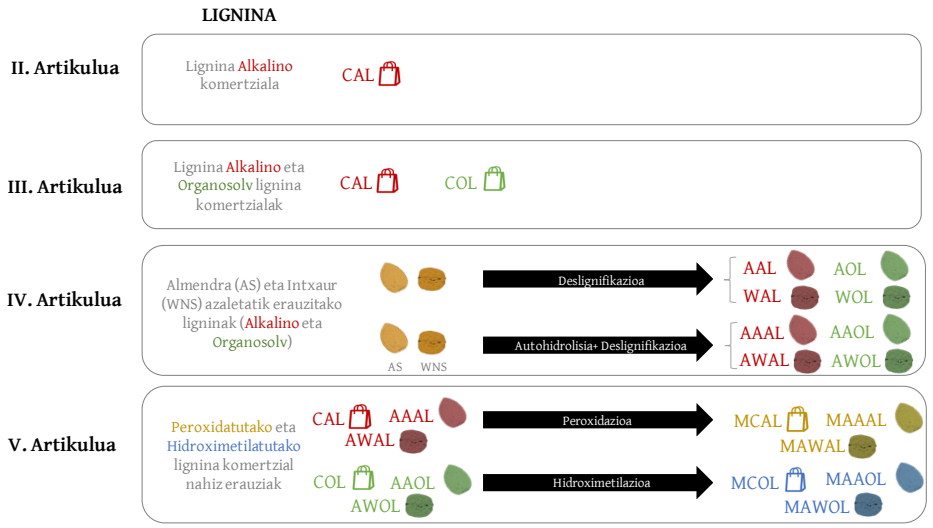

3.1 Irudia. Tesi honetan erabilitako lignina lagin guztien laburpen eskematikoa.

3.3.1 Almendra eta intxaur azaletatik eratorritako ligninen erauzketa

IV eta V. Artikuluetan ikus daitekeen bezala, almendra eta intxaur azalak ehotu eta bahetu egin ziren 2 eta 1 mm arteko partikula tamaina lortu arte. Ondoren, 3.2 Irudian ikus daitekeen bezala, azal mota bakoitzak bi prozesu ezberdin jasan zituzten: batetik, deslignifikazio hutsez osatutako prozesua, eta, bestetik, aurretratamendu etapa batek (autohidrolisia) eta ondorengo deslignifikazio etapa batek osatutakoa.

Bi lehengaien autohidrolisia aurrez egindako ikerketen arabera egin zen [74,75]. Almendra azalak 8 g H_2O/g AS lehorreko disolbatzaile-solido ratioa (LSR) mantenduz 179 ºC-ra berotu ziren 4848 Parr kontrolatzailedun 1,5 L-ko altzairu herdoilgaitzeko erreaktore batean, 23 minutuz aipaturiko tenperaturan mantenduz. Intxaur azalak, berriz, LSR berdina mantenduz, 200 ºC-ra berotu ziren erregimen ez-isotermoan, hau da, tenperatura honetara

iritsi bezain laster hoztuz. Tratamenduen ondoren, solidoak urarekin garbitu ziren eta 50 ºC-ra lehortu ziren.

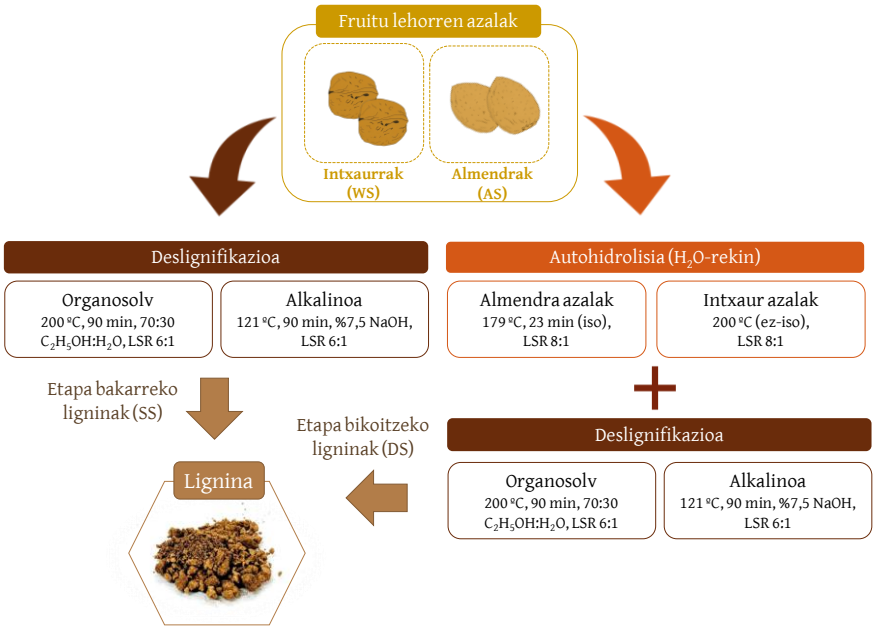

3.2 Irudia. Fruitu lehorren azaletatik eratorritako ligninak erauzteko prozeduraren eskema.

Lehengaien deslignifikazioa ere aurrez egindako ikerketen arabera egin zen. Almendra eta intxaur azalei tratamendu alkalino nahiz organosolv tratamenduak aplikatu zitzaizkien. Tratamendu alkalinoa aurrez tratatutako nahiz tratatu gabeko azalak pisuan %7,5 NaOH disoluzio batekin nahasi ziren 6 g/g LSR ratioa mantenduz. Ondoren, 121 ºC-ra berotu ziren autoklabe batean 90 minutuz. Organosolv tratamenduak LSR eta denbora berdina mantenduz egin ziren, baina kasu honetan azalak bolumenean %70eko etanol/H_2O disoluzio bat erabiliz eta aurretik deskribatutako erreaktorean 200 ºC-ra berotuz.

Deslignifikazio prozesuen ondoren, nahasketak iragazi egin ziren eta likore beltzeko ligninak hauspeatu egin ziren. Tratamendu alkalinoen kasuan, %96ko purutasuna duen H_2SO_4-a gehitu zitzaion likoreari honek pH=2 izan arte, eta organosolv tratamenduaren kasuan, aldiz, azidifikaturiko uraren (pH=2)

bolumen bikoitza erabiliz (likorearen bolumena kontuan izanik). Hauspeakina iragazi eta ur distilatuaz garbitu zen pH neutrora arte. Azkenik, ligninak 50 ºC-ra lehortu ziren 24-48 orduz.

3.3.2 Isolaturiko ligninen eraldaketa

V. Artikulurako, IV. Artikuluan lortutako ligninak eta lignina komertzialak erabili ziren. Konkretuki bi etapaz osaturiko prozesuetatik erauzitako lignina organosolv eta alkalinoak erabili ziren. Lignina alkalinoek mikrouhinen (flexiWAVE, Milestone Srl) bidezko peroxidazio prozesu bat jasan zuten hidrogeno peroxidoa erabiliz (H_2O_2), Infante *et al.* (2007)-ek deskribatu bezala [76]. Labur esanda, lignina eta H_2O_2-a presio altuko ontzi batean sartu ziren 10 ml H_2O_2/lignina g-ko LSR-a mantenduz. Ontzia ongi itxi ondoren, 1100 W-ko 10 segundoko iraupeneko hiru irradiazio zikloren eraginpean jarri zen, irradiazioen artean 30 segundoko tartea utziz. Azkenik, ontzia ur destilatuaz garbitu zen eta berreskuratutako nahasketa lehortzen utzi zen berogailu baten gainean.

Organosolv ligninei hidroximetilazio erreakzioa aplikatu zitzaien formaldehidoa erabiliz Chen *et al.* (2020)-ek aipatu bezala [39]. Laburbilduz, 0,6 g lignina NaOH-zko disoluzio baten 140 mL-tan disolbatu ziren. Gero, formaldehidozko 0,495 mL gehitu zitzaizkion disoluzioari eta hau 80 ºC-ra berotu eta 3,5 orduz erreakzionatzen utzi zen irabiaketa magnetikoa eta kondentsadorea erabiliz. Ondoren, eraldatutako lignina %2ko azido klorhidrikozko disoluzio bat erabiliz hauspeatu, iragazi, neutralizatu eta lehortu egin zen.

3.4 Hidrogelen sintesia

Hidrogel guztien sintesiko lehen pausua berdina izan zen (3.3 Irudia). Lehenik, pisuan %2 NaOH duen disoluzio batean kasu bakoitzari zegokion polibinil alkohola (PVA) gehitu zitzaion, 80–90 ºC-ra berotu eta magnetikoki irabiatuz

polimeroa guztiz disolbatu arte. Ondoren, kasu bakoitzari zegokion lignina kopurua gehitu zitzaion aurreko disoluzioari, hau ere magnetikoki irabiatuz lignina guztiz disolbatu arte. Nahasketa hauek silikonazko moldeetara isuri ziren kopuru jakinetan, disoluzioan harrapatutako burbuilak moldeak ultrasoinuen bainu batean sartuz eta, azalean gelditutakoak, berriz, eskuz orratz batekin zulatuz.

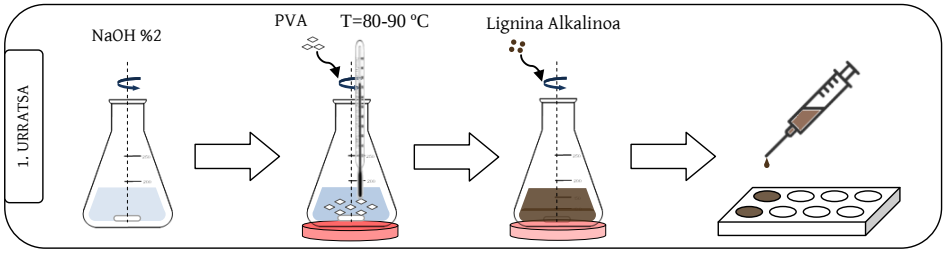

3.3 Irudia. Hidrogelen sintesiko 1. urratsaren adierazpen grafikoa.

Sintesiaren bigarren zatia (3.4 Irudia) **II. Artikuluan** adierazi bezala optimizatu zen, eta baldintza optimoak hurrengo argitalpenetan erabili ziren. Gurutzaketa fasearen ondoren, hidrogel lagin bakoitza ur destilatuzko 50 mL-tan garbitu zen 27–48 orduz, ur hau denbora tarte jakin batzuen ondoren berrituz, erreakzionatu gabeko lignina eta NaOH hondakinak kanporatzeko asmoz.

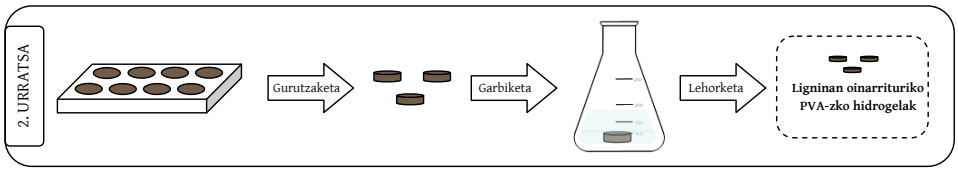

3.4 Irudia. Hidrogelen sintesiko 2. urratsaren adierazpen grafikoa.

III. Artikuluan, **II. Artikulutik** ondorioztatutako gurutzaketa optimoa jarraitu zen, izozte eta desizozte zikloen konbinaketaz osatutakoa. Edonola ere, kasu honetan zikloen denbora murriztea erabaki zen, eta prozedura hau hurrengo argitalpenetan (**IV.** eta **V. Artikuluak**) ere erabili zen.

IV. Artikuluan, hidrogelen sintesirako erabilitako ligninak fruitu lehorren azaletatik erauzi ziren 3.3.1 Atalean eta 3.5 Irudian azaldu bezala. Kasu honetan, aurreko paragrafoan azaldutako zikloen iraupenaren murrizketa aplikatzeaz gain, azken desizozte prozesuaren eragina aztertu zen, honen iraupena 24 ordura luzatuz.

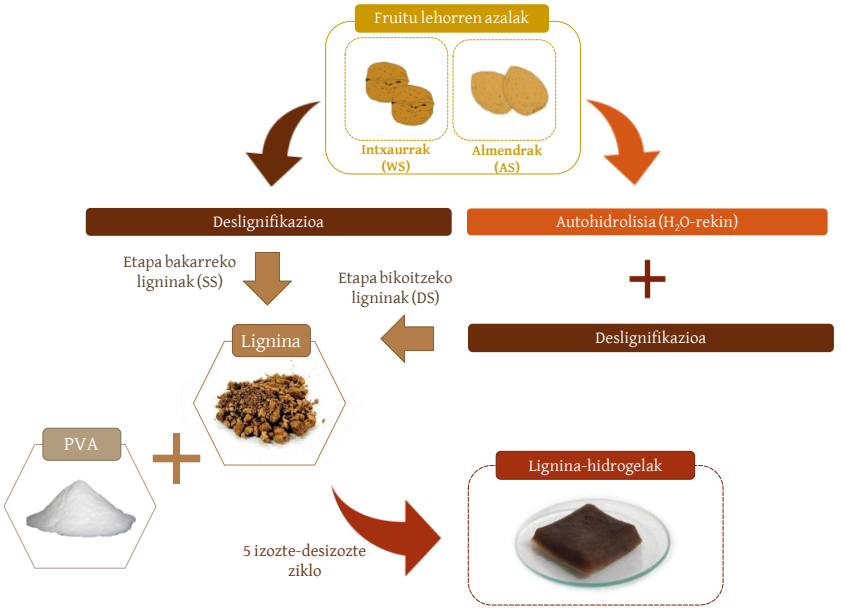

3.5 Irudia. IV. Artikuluko prozedura esperimentalaren azalpen eskematikoa.

V. Artikuluan, erabilitako ligninak 3.3.2 atalean deskribatu bezala eraldatutakoak izan ziren. Horrez gain, sintesiaren bigarren zatia gurutzaketa ziklo motzen bidezkoa izan zen, **III.** eta **IV. Artikuluetan** egindakoaren antzera.

3.5 Karakterizazio metodoak

3.1 Taula. Artikulu bakoitzean erabilitako karakterizazio metodoak.

Analisia	Argitalpena			
	II	III	IV	V
Purutasuna	-	-	L	L
Azidotan disolbagarria den lignina (ASL)	-	-	L	L
Konposizioa (Py-GC/MS)	-	-	L	-
Batez besteko pisu molekularra (HPSEC)	-	-	L	L
Konposatu fenolikoen eduki totala (TPC)	-	-	L	L
Degradazio termikoa (TGA)	HG, L	HG	L	L
Kristalinitatea (XRD)	HG, L	HG	L	L
Egitura kimikoa (ATR-FTIR)	HG, L	HG	L	L
Lignina galera	HG	HG	HG	HG
Ur-xurgatze gaitasuna	HG	HG	HG	HG
Morfologia (SEM)	HG	HG	HG	HG
Propietate termikoak (DSC)	HG, L	HG	HG	HG
Konpresio saiakuntzak	HG	HG	HG	HG

L: Lignina; HG: Hidrogelak

3.5.1 Ligninaren karakterizaziorako metodo orokorrak

3.5.1.1 Purutasuna

Erauzitako ligninen purutasuna Dávila *et al.* (2017)-ek deskribatu bezala zehaztu zen [77], Klason lignina eta azidotan disolbagarria den lignina aintzat hartuz. Ligninei bi urratseko hidrolisi azido kuantitatibo (QAH) bat aplikatu zitzaien, lehenik pisuan %72ko purutasuna duen H_2SO_4-arekin ordubetez 30 ºC-ra mantenduz, eta ondoren, pisuan %12ko purutasuna duen H_2SO_4-arekin ordubetez 121 ºC-ra mantenduz. Jarraian, laginak iragazi ziren eta berreskuraturiko fase solidoa Klason ligninatzat hartu zen. Fase likidoak HPLC teknikaren bidez aztertu ziren monosakarido (glukosa, xilosa eta arabinosa), azido galakturoniko, azido azetiko eta degradazio produktuen (hidroximetil furfurala eta furfurala) zehaztapenerako.

ASL edukia, aurretik aipatu bezala, espektrofotometriaren bidez zehaztu zen, Jasco UV-Vis 730 espektrofotometro bat erabiliz. QAH-an bereizitako fase likidoak 1 M H_2SO_4-rekin diluitu ziren, 205 nm-tan neurtutako absorbantzia 0,1 eta 0,8 artean kokatu arte (TAPPI UM250 um-83). Kalkuluak egiteko, 3.1 Ekuazioa erabili zen, non Abs_{250nm} laginaren absorbantzia den 205 nm-tan (1 M H_2SO_4-aren absorbantzia 205 nm-tan erreferentziatzat hartuz), DF diluzio faktorea den, VF iragazitakoaren bolumena den, ε ligninaren extintzio koefizientea den 205 nm-tan (110 L·cm/g) eta DM_i laginaren pisua den QAH-a baino lehen (g lehorretan).

$$ASL\ (\%) = \frac{Abs_{250nm} \cdot DF \cdot VF}{\varepsilon \cdot DM_i} \cdot 100 \qquad \text{(3.1 Ekuazioa)}$$

3.5.1.2 Pisu molekularra

Ligninen batez besteko pisu molekularra pisuan (M_w) eta kopuruan (M_n), eta polidispertsitate indizeak tamainaren araberako bereizmen handiko kromatografiaren (HPSEC) bidez zehaztu ziren. Horretarako, Jasco LC Net

II/ADC kromatografo bat erabili zen, errefrakzio-indizearen detektagailuduna eta Varian Polymer Laboratories-en bi PolarGel-M zutabe seriean dituena (300 mm × 7,5 mm). Ligninak litio bromurodun (%0,1) dimetilformamidazko fase mugikorrean disolbatu ziren analisietarako. Funtzionamendu-baldintzak hauek izan ziren: 20 µL-ko injekzio bolumena, 0,7 mL/min-ko fluxua eta 40 °C. Kalibraketa zuzena pisu molekular ezberdineko poliestirenozko patroiak (62.500–266 g/mol, Sigma Aldrich) erabiliz eraiki zen.

3.5.1.3 Konposizio analisiak

Pirolisi-Gasen kromatografia/Masen Espektrometria (Py-GC/MS) teknika erabili zen ligninen konposizio analisietarako. Honetarako, Pyroprobe 5150 (CDS Analytical Inc.) pirolizatzaile bat erabili zen, Agilent 6890 gas kromatografo batekin eta aldi berean Agilent 5973 (Agilent Technologies Inc.) masa espektrometro batekin konektatuta zegoena, Dávila *et al.* (2017)-ek adierazi bezala [77]. Gas kromatografoak 30 m × 0.25 mm × 0.25 µm-ko lodieradun HP-5MS ((%5 fenil)-metilpolisiloxano)-zko zutabe bat zuen eta helioa erabili zen gas garraiatzaile moduan. Pirolisia 600 °C-tan (15 s) egin zen 20 °C/ms-ko abiadurarekin eta interfazea 260 ºC-ra mantenduz. Gas kromatografoaren berogailua 50 ºC-tik (2 min) 120 ºC-ra (5 min), gero 280 ºC-ra (8 min) eta azkenik 300 ºC-ra (10 min) 10 ºC/min-ko abiaduraz berotzeko programatu zen. Konposatuak euren masa espektroak National Institute of Standards Library-ren (NIST) eta literaturan aurkitutako konposatuenekin alderatuz identifikatu ziren.

3.5.1.4 Konposatu fenolikoen eduki totala (TPC)

Lignina laginak dimetil sulfoxidoan (DMSO) disolbatu ziren TPC analisietarako. Hauek Folin-Ciocalteau metodo espektrofotometrikoaren bidez zehaztu ziren [75]. Labur esanda, lehenik, kalibraketa zuzen bat eraiki zen, absorbantzia neurriak eta konposatu fenolikoen edukiaren arteko erlazionatzeko balio duena. Edukia azido galikoaren baliokideetan eman ohi da (C_{GAE}, mg/L). Beraz,

kalibraketa zuzena azido galikozko kontzentrazio jakinezko (0-200 ppm) disoluzioak erabiliz eraiki zen. Neurketetarako, saio-hodi batean lagin edo azido galikozko disoluzioen 300 µL sartu ziren eta ondoren, bolumenean 1/10-eko Folin-Ciocalteau disoluzio baten 2,5 mL gehitu ziren. Ondo nahasi ondoren, pisuan %7,5eko sodio karbonatozko (Na_2CO_3) disoluzio baten 2 mL gehitu ziren, berriro ere ondo nahasiz 50 ºC-ra 5 minutuz inkubatu aurretik. Azkenik, saio-hodiak giro tenperaturaraino epeltzen utzi ziren eta euren absorbantzia neurtu zen 760 nm-ra Jasco UV-Vis 730 espektrofotometro bat erabiliz.

3.5.1.5 Fosforozko Erresonantzia Magnetiko Nuklearra (^{31}P NMR)

V. Artikuluan burututako organosolv ligninen hidroximetilazio erreakzioa egiaztatzeko, ^{31}P NMR teknika erabili zen, Chen *et al.* (2020) eta Meng *et al.* (2020)-ek aipatutakoaren arabera [38,39]. Horretarako, kloroformo deuteratu ($CDCl_3$) eta piridina anhidridozko disoluzio bat prestatu zen bolumenean 1:1,6-ko erlazioa mantenduz. Ondoren, patroia prestatu zen kromo (III) azetilazetonatoa ($Cr(acac)_3$) 5 mg/mL-ko kontzentrazioan aurreko disoluzioari gehituz. Gero, N-hidroxi-5-norborneno-2, 3-azido dikarboxiliko imida (NHND) gehitu zitzaion $Cr(acac)_3$ disoluzioari 18 mg/mL-ko kontzentrazioan.

Laginen 30 mg inguru disolbatu ziren 0,5 mL $CDCl_3$/piridina disoluziotan. Honi 0,1 mL patroi disoluzio gehitu zitzaizkion, eta azkenik, 2-kloro-4,4,5,5-tetrametil-1,3,2-dioxafosfolanozko (TMDP) 0,1 mL gehitu zitzaizkion hidroxilo taldeekin erreakzionatzeko. Laginak nahastu egin ziren eta NMR hodietan sartu ziren analisietarako.

3.5.2 **Hidrogelen karakterizazioa**

3.5.2.1 Lignina galera

Hidrogelen garbiketa prozesuan galdutako lignina kuantifikatzeko asmoz, periodikoki aldatutako uraren laginak gorde ziren. Lagin hauetako lignina kontzentrazioa zehazteko, kalibraketa kurba bat eraiki zen lehenik, pisuan

NaOH %2ko disoluzioa erabiliz, kontzentrazio jakineko lignina disoluzioak prestatuz. Ondoren, disoluzio hauen absorbantzia neurtu zen Jasco UV-Vis 730 espektrofotometro baten bidez, kasu bakoitzean aurretik zehaztutako absorbantzia maximodun uhin luzeran. Honela, absorbantzia balio bakoitza zegokion disoluzioaren kontzentrazioarekin erlazionatu zen, kalibraketa zuzena osatuz. Gero, laginen absorbantzia neurtu zen, kasu bakoitzean erabili beharreko diluzioak eginez. Neurketen emaitzak eta kalibraketa zuzena erabiliz, laginen lignina kontzentrazioa kalkulatu zen, eta garbiketa uraren bolumena kontuan hartuz (50 mL), lignina galera kalkulatu zen.

3.5.2.2 Ur-xurgatze gaitasuna

Hasteko, hidrogelak egoera lehorrean pisatu ziren eta 40 mL ur distilatutan sartu ziren 48 orduz. Ur-xurgatze zinetikarako, hidrogelak denbora tarte jakin batzuen ondoren pisatu ziren, aurretik gainazaleko ura lehortuz. Ur-xurgapena edo *swelling*-a 3.2 Ekuazioaren bitartez kalkulatu zen:

$$Swelling\ (\%) = \frac{m_{swollen} - m_{dry}}{m_{dry}} \cdot 100 \qquad \text{(3.2 Ekuazioa)}$$

non $m_{swollen}$ eta m_{dry} hidrogelen pisua den ura xurgatu ostean eta aurretik, hurrenez hurren.

3.5.2.3 Ekorketazko mikroskopia elektronikoa (SEM)

SEM analisiak hidrogelen morfologia aztertzeko egin ziren. Laginak ur distilatutan 48 orduz murgilduta egon ondoren, -20 ºC-tan izoztu ziren. Jarraian Alpha 1–4 LD gailu batean liofilizatu ziren. Bigarren mailako elektroien irudiak MEB JEOL 7000-F batekin hartu ziren, eta lan baldintzak 5 kV eta 0,1 nA-ko intentsitatea izan ziren. Laginak kobrez estali ziren analisia egin ahal izateko.

3.5.2.4 Konpresio saiakuntzak

Hidrogelei norabide bakarreko konpresio-saiakuntzak egin zitzaizkien euren erresistentzia mekanikoa ebaluatzeko. Horretarako, Instron 5967 makina batean konpresio-osagarri bat ezarri zen, 500 N-ko karga-zelula bat erabiliz eta 2 mm/min-ko zapaltze-abiadurarekin. Ur distilatutan 48 orduz murgildutako hidrogelak 5 x 5 mm-ko lagin karratuetan moztu ziren eta hauek euren hasierako lodieraren %80raino konprimitu ziren. Deformazio ehuneko hau beste lan batzuetan oinarrituz eta konpresio-saiakuntzako aparailuaren mugen arabera hautatu zen. Lagin bakoitzaren konpresio-modulua, G_e, automatikoki kalkulatu zen 3.3 Ekuazioa erabiliz.

$$\sigma = \frac{F}{A} = G_e \cdot \left(\lambda - \frac{1}{\lambda^2}\right) \qquad \text{(3.3 Ekuazioa)}$$

non F aplikatutako indarra den, A laginaren hasierako zeharkako azalera den eta $\lambda = L/L_0$ non L_0 eta L laginaren lodierak diren konpresio saiakuntzaren aurretik eta ondoren, hurrenez hurren.

3.5.3 Metodo orokorrak

3.5.3.1 Islapen total indargetua - Fourierren transformatuaren bidezko espektroskopia infragorria (ATR-FTIR)

Laginen egitura kimikoa ikertzeko, diamantezko leiardun Islapen total indargetua neurtzeko Universal Attenuated Total Reflectance (ATR) osagaidun PerkinElmer Spectrum Two FTIR espektrometro bat erabili zen. Neurketak 600 eta 4000 cm^{-1} artean egin ziren, lagin bakoitzerako guztira 20 ekorketa eginez 8 cm^{-1}-ko bereizmenarekin [78].

3.5.3.2 X izpien difrakzioa (XRD)

X izpien hauts difrakzio-saiakuntzak Phillips X'Pert PRO difraktometro automatiko batekin egin ziren, 40 kV eta 40 mA-tan theta-theta konfigurazioarekin lan eginez. Cu-Kα erradiazio monokromatikoa erabili zen

(λ = 1,5418 Å), baita PIXcel egoera solidoko detektagailu bat ere (luzera aktiboa 2θ 3,347 º-tan). Bildutako datuak giro-tenperaturan 5 eta 80 º arteko 2θ balioetatik hartu ziren, θ laginarekiko X-izpiaren elektroi-sortaren eraso-angelua izanik. Laginak egoera lehor eta birrinduan aztertu ziren. Kristalen gutxi gorabeherako tamaina (*D*) Scherrer ekuazioa (3.4 Ekuazioa) erabiliz kalkulatu zen:

$$D = \frac{k \cdot \lambda}{\beta \cdot cos\ \theta} \qquad \text{(3.4 Ekuazioa)}$$

non *D* eremu ordenatuen tamaina den (nm), *k* Scherrer-en konstantea den (0,9), λ X izpien uhin luzera den (0,154 nm) eta β dagokion Bragg-en angelutik islapenaren erdian dagoen gehieneko zabalera den (ingelesez FWHM), 2θ-n neurtuta [78].

3.5.3.3 Ekorketa diferentzialeko kalorimetria (DSC)

DSC analisiak Mettler Toledo DSC 822 ekipamendu batean egin ziren. Aurrez aluminio kapsuletan pisatutako 3 eta 5 mg arteko laginak -25 ºC-tik 225 ºC-ra berotu ziren 10 ºC/min-eko abiaduraz nitrogenozko ingurune batean oxidazio erreakzioak ekiditeko. Lehenengo beroketa prozesu baten ondoren, hozte prozesu bat eta bigarren berotze prozesu bat ere burutu ziren. Bigarren berotze kurbako bero espezifikoaren aldaketaren inflexio puntua beira trantsizio tenperaturatzat hartu zen (T_g). Gailuaren kalibraketa indiozko patroiaz egin zen.

Hidrogelen kasuan, kristalinitate gradua (χ_c) kristalizazio prozesuko entalpia eta 3.5 ekuazioaren bitartez kalkulatu zen:

$$\chi_c = \frac{\Delta H}{\Delta H_0 \cdot (1 - m_{filler})} \cdot 100 \qquad \text{(3.5 Ekuazioa)}$$

non ΔH kristalizazio edo fusio entalpia den, ΔH_0 %100 kristalinoa den PVA-ren fusio entalpia den (bataz besteko balioa: 161.6 J/g) eta $(1 - m_{filler})$ hidrogelen PVA-zko masaren ehunekoa den [78].

3.5.3.4 Analisi termograbimetrikoa (TGA)

TGA analisietarako TGA/SDTA RSI analyzer 851 Mettler Toledo ekipamendu bat erabili zen. Aluminiozko kapsuletan 3 eta 5 mg arteko laginak pisatu ziren eta 25 °C-tik 800 °C-ra berotu ziren nitrogenozko ingurune batean 10 °C/min-ko abiaduran.

3.6 Hidrogelen aplikazioak aztertzeko metodo espezifikoak

3.6.1 Metileno-urdina xurgatzeko ahalmena

III eta **IV. Artikuluetan** hidrogelek metileno-urdina (MB) xurgatzeko duten ahalmena ikertu zen [79]. Horretarako, 1 mg/L-ko MB disoluzio bat prestatu zen eta hydrogel lehor zatiak (0.5 g inguru) disoluzio honen 15 mL-tan murgildu ziren. Esperimentu hauek era estatikoan burutu ziren giro-tenperaturan 24-48 orduz. Ondoren, kalibraketa zuzen bat diseinatu zen kontzentrazio jakineko zenbait MB disoluzio erabiliz (0.25–5 mg/L) eta euren absorbantzia Jasco UV-Vis 630/730 espektrofotometro baten bitartez neurtuz 665 nm-tan. Honela, absorbantzien emaitzak disoluzioen kontzentrazioekin erlazionatuz kalibraketa zuzena eraiki zen. Laginen MB xurgatze saiakuntzen ostean, hasierako eta amaierako disoluzioen absorbantziak neurtu ziren, eta kalibraketa zuzenaren bitartez euren kontzentrazioak ere bai. Azkenik, xurgatze-errendimendua kalkulatu zen 3.6 Ekuazioa erabiliz:

$$Q_e \left(\frac{mg_{MB}}{g_{HG}}\right) = \frac{C_0 - C_{eq}}{m \cdot V} \qquad \text{(3.6 Ekuazioa)}$$

non C_0 hasierako MB disoluzioaren kontzentrazioa den, C_{eq} MB disoluzioaren amaierako kontzentrazioa den, V lagin bakoitza murgiltzeko erabili den disoluzioaren bolumena den eta m hidrogel lehorraren pisua den.

Xurgatutako MB-aren ehunekoa 3.7 Ekuazioaren bidez kalkulatu zen:

$$P(\%) = \frac{C_0 - C_{eq}}{C_0} \cdot 100 \qquad \text{(3.7 Ekuazioa)}$$

non P xurgatutako MB disoluzioaren ehunekoa den eta gainontzeko aldagaiak 3.6 Ekuazioarentzat definitutakoen berdinak diren.

3.6.2 Gaitasun antifungikoa neurtzeko saiakuntza

IV. Artikuluan, laginen gaitasun antifungikoa aztertu zen Salaberria *et al.* (2017) eta da Silva *et al.* (2018)-ek adierazitako protokoloetan oinarrituz [80,81]. Labur esanda, *Aspergillus niger* (CBS 554.65) onddoa 7 egunez patata eta dextrosazko agarrez (PDA) estalitako Petri ontzietan hazi ondoren (25 ºC ± 1,5 ºC-tan), espora batzuk gatz fosfatozko disoluzio indargetzaile (PBS) batean diluitu ziren eta espora kopurua 1,21x10^6 espora/ml-ko kontzentraziora doitu zen, zelulen kontaketarako Cellometer® Mini aparailua erabiliz. Ondoren, prozedura laginaren arabera moldatu zen.

Lignina laginen kasuan, laginak DMSO-n disolbatu ziren (75–100 mg/mL-ko kontzentrazioan) eta ondoren, lagin bakoitzeko 40 µL igaro zen PDA-z estalitako Petri ontzi batera, tantaren ingurua, spray baten bidez, onddoaren disoluzioaz inokulatuz. *Kontrola* edo *zuria* deritzoguna, DMSO purua erabiliz egin zen [81]. Hidrogel laginen kasuan, berriz, 1 cm x 1 cm inguruko laukitxoak ezarri ziren Petri ontzien PDA-ren gainean, behin PDA onddoaren disoluzioaz inokulatu ostean. *Kontrola* edo *zuria* PVA hutsezko hydrogel bat erabiliz egin zen. Analisi bakoitza bitan errepikatu zen.

7 egunez 25 ºC ± 1,5 ºC-ra inkubatu ondoren, lignina laginen kasuan onddoaren hazkundearen inhibizioa (GI) bisualki ebaluatu zen ISO 846-ko eskala numerikoaren arabera (3.2 Taula) [81]. Hidrogelen kasuan aldiz, laginak agar gainetik kendu eta 1 mL PBS-rekin garbitu ziren, honekin bildutako esporak Eppendorf batean jasoz.

3.2 Taula. Onddoaren GI-aren ebaluaketa bisualerako eskala ISO 846-aren arabera.

GI	Ebaluaketa
0	Ez dago ageriko nahiz handipeneko hazkunderik
1	Ez dago ageriko hazkunderik baina handipenaren bidez ikus daiteke
2	Azaleraren %25erainoko hazkunde ikusgarria
3	Azaleraren %50erainoko hazkunde ikusgarria
4	Azaleraren %75erainoko hazkunde ikusgarria
5	Azaleraren %75a baino gehiago hartzen duen hazkunde bizia

Ondoren, Eppendorfetan jasotako disoluzioak tripano urdinaren 5 µL erabiliz urdinez tindatu eta ongi nahastu ondoren, espora kontzentrazioa neurtu zen aurretik aipatutako gailuaz [80]. Laginen hazkunde fungikoaren inhibizioa (FGI) 3.8 Ekuazioaren bidez kalkulatu zen [80]:

$$FGI(\%) = \frac{C_g - T_g}{C_g} \cdot 100 \qquad \text{(3.8 Ekuazioa)}$$

non C_g *kontrol* laginen bataz besteko espora kontzentrazioa den eta T_g aztertutako laginen bataz besteko espora kontzentrazioa den, biak espora/mL-tan adierazita.

3.6.3 Kertzetinaren erauzketa eta karakterizazioa

3.6 Irudia. Tipula gorrien azalak.

V. Artikuluan adierazitako kertzetinaren erauzketarako George *et al.* (2019) eta Jin *et al.* (2011)-ek aipatutako metodoak konbinatu ziren [82,83]. Lehenik eta behin, etxe-hondakinetatik ateratako tipula gorrien azalak uretan garbitu, 50 ºC-tan lehortu eta xehatu egin ziren. Gero,

kertzetina eta beste konposatu batzuk erauzi ziren mikrouhinen bidez (flexiWAVE, Milestone Srl) aurretik egindako esperimentu batzuen emaitzetan oinarrituta (azaldu gabeko datuak), Jin *et al.* (2011)-ek adierazitako mikrouhinen potentzia aldatuz. Erauzketa bolumenean %70eko etanol disoluzio bat erabiliz eta 40:1-eko LSR-a mantenduz egin zen. Erradiazio-denbora 10 segundokoa izan zen eta potentzia 375 W-etan finkatu zen. Erreakzioaren iraupena 2 minutukoa izan zen, erradiazio eta erradiazio artean 20 segundoko tartea utziz. Erreakzioaren ostean, fase solidoa iragazi egin zen eta fase likidoa kontzentratu egin zen, etanola biraketa-lurrungailuaz kenduz. Matrazean gelditutako disoluzio akuosoa kertzetina estraktu bezala izendatu zen (QE).

Kertzetina estraktuaren kontzentrazioa Jasco UV-Vis espektrofotometro baten bidez zehaztu zen. Horretarako, kalibraketa zuzen bat eraiki zen kertzetina komertzialezko (CQE) kontzentrazio jakineko zenbait disoluzio erabiliz eta hauen absorbantzia 375 nm-ra neurtuz [83]. QE liofilizatu egin zen eta ATR-FTIR teknikaren bidez lortutako espektroa CQE-aren espektroarekin alderatu zen. Erauzketa-errendimendua QE-aren solido edukiaren (konposatu ez-hegazkorrak) bidez kalkulatu zen. Honetarako, estraktuaren 2 mL pisatu ziren ontzi lehorretan eta 24 orduz lehortu ziren 105 ºC-tan. Ondoren, ontziak epeldu eta berriro ere pisatu ziren, solido edukia 3.9 Ekuazioaren bidez kalkulatuz:

$$Yield(\%) = \frac{m_f - m_r}{m_i - m_r} \cdot 100 \qquad \text{(3.9 Ekuazioa)}$$

non m_r ontzi lehorraren masa den, m_i ontziaren masa den estraktuaren 2 mL gehitu ondoren eta m_f ontziaren pisua den 24 orduz estraktua lehortzen utzi ondoren, aldagai guztiak gramotan adieraziz.

QE-aren karakterizazio sakonago bat egin zen honen flabonoide eta konposatu fenolikoen eduki totala neurtuz (TFC eta TPC, hurrenez hurren). TPC-a 3.5.1.4

Atalean ligninarentzat deskribatu bezala egin zen, baina kasu honetan DMSO-a metanolez ordezkatu zen Sillero *et al.* (2019)-ek azaldu bezala [23]. TFC-aren kasuan aluminio kloruroaren ($AlCl_3$) kolorimetria saiakuntza burutu zen, kertzetina komertziala patroitzat erabiliz [82,84] eta Sillero *et al.* (2019)-ek deskribatutako metodoa jarraituz [23]. Laburbilduz, aurrez diluitutako estraktuaren 2 mL pisuan $NaNO_2$ %5eko disoluzio baten 0,3 mL-rekin nahastu zen. 5 minuturen ostean, pisuan $AlCl_3$ %10eko disoluzio baten 0,3 mL gehitu zitzaizkion eta beste 6 minuturen ondoren, NaOH 1N disoluzio baten 2 mL gehitu zitzaizkion nahasketa neutralizatzeko. 5 minuturen ostean, nahasketaren absorbantzia neurtu zen Jasco UV-Vis espektrofotometro batean 415 nm-ko uhin luzeran. Emaitzak estraktu lehorraren gramo bakoitzeko dauden kertzetina baliokideen miligramotan eman ziren (kertzetina baliokideen mg/estraktu lehor g).

3.6.4 Kertzetinaren xurgapen eta askapen saiakuntzak

V. Artikulurako, hidrogelak kertzetinaz hornitu ziren gero honen askapenaren zinetika aztertzeko. Horretarako, hidrogel lagin lehorrak (≈ 0,5 g) QE diluituzko (1 mL QE/250 mL ur distilatu) disoluzioan murgildu ziren 24 orduz. Denbora honetan xurgatutako QE kopurua hasiera eta amaierako disoluzioen kontzentrazioak konparatuz kalkulatu zen [82]. Hidrogelak lehortu ondoren, pisatu egin ziren eta PBS-zko disoluzio batean murgildu ziren ondoren 37 ºC-tan (*in vitro* baldintzak simulatuz) 24 orduz. QE askapen zinetikarako denbora tarte jakin batzuen ondoren disoluzioaren absorbantzia (eta ondorioz, QE kontzentrazioa) neurtuz estimatu zen. Esperimentu guztiak hirutan errepikatu ziren. Emaitzak zerogarren maila, lehen maila, Korsmeyer–Peppas eta Higuchi (3.10-3.13 Ekuazioak) eredu zinetikoetan aplikatu ziren, hidrogelek QE-a askatzeko jarraitzen duten mekanismoa ulertzeko asmoz [82,85,86].

$$F = k_0 \cdot t \qquad \text{(3.10 Ekuazioa)}$$

$$\ln(1 - F) = -k_1 \cdot t \qquad \text{(3.11 Ekuazioa)}$$

$$\frac{M_t}{M_\infty} = k_{kp} \cdot t^n \qquad \text{(3.12 Ekuazioa)}$$

$$F = k_h \cdot t^{1/2} \qquad \text{(3.13 Ekuazioa)}$$

non *F,* t denbora jakin batera askatutako QE den, k_0, k_1, k_{kp} and k_h zerogarren maila, lehen maila, Korsmeyer-Peppas eta Higuchi ereduetako erreakzio abiadura-konstanteak diren, hurrenez hurren, eta *n* difusio berretzailea den.

3.6.5 *In-Vitro* Biobateragarritasun saiakuntzak

Hidrogelen *in vitro* biobateragarritasun probak Marmarako Unibertsitateko Industria Bioteknologiaren eta Sistemen Biologiaren Ikerketa Taldeko Laborategian egin ziren, Bioingeniaritza Sailean. Esperimentuen etapa guztiak ahalik eta esterilitate baldintza handienetan egin ziren bitarteko eta ekipo esterilekin, onddo, bakterio edo legamiek eragindako edozein kutsadura saihesteko.

3.6.5.1 Laginen esterilizazioa

Hidrogelak PBS-zko disoluziotan utzi ziren 48 orduz (hau xurgatuz), eta ondoren, bolumenean %70 den etanola eta UV izpiekin ordu batez, eta %2an Penizilina-Estreptomizina zuen PBS disoluzio batez 2 orduz esterilizatu ziren. Gero, PBS soilezko disoluzioaz garbitu ziren eta DMEM-z (Dulbecco's Modified Eagle Medium) saturatu ziren esperimentuak hasi aurretik.

3.6.5.2 Zelulen ereite eta ugaltze saiakuntza

Zelula-ugalketaren probetarako giza fibroblasto dermikoen zelulak erabili ziren (PCS-201-012). Labur esanda, izoztutako zelulak berehala desizoztu ziren, eta DMEM inguruarekin batera (%10eko behi-fetu-seruma (FBS) eta %1eko penizilina-estreptomizina zuena) zentrifugatu zen. Sedimentu zelularra

hazkuntza zelularreko T25 matraze batean erein zen, inkubagailu batean zelulen finkapena eta hazkundea ahalbidetzeko, %5eko CO_2 baldintzetan eta 37 ºC-tan. Zelulen bateratzea gertatu ostean, azpi-kultiboko protokolo bat aplikatu zen. Horretarako, hazkuntza-ingurunea xurgatu eta zelulak PBS-z bi aldiz garbitu ziren. Tripsina-EDTA erreaktiboaren 1 mL gehitu zitzaien zelulei eta inkubagailu batean pare bat minutuz inkubatu ziren. Atxikimendu zelularra hautsi ondoren, matrazeetan DMEM ingurua gehitu zen, eta zelulen suspentsioa 2000 rpm-ra zentrifugatu zen 5 minutuz. Ondoren, sedimentu zelularra berreseki zen eta T75 (TPP) kultibo zelularreko matrazeetara igaro zen hazkunde zelularrerako. Zelula kopuru egokia lortu zenean, lehen deskribatu bezala askatu ziren, eta zelula horiek zelula zenbaketarako tripan urdinez tindatu ondoren mikroskopio baten laguntzaz zenbatu ziren.

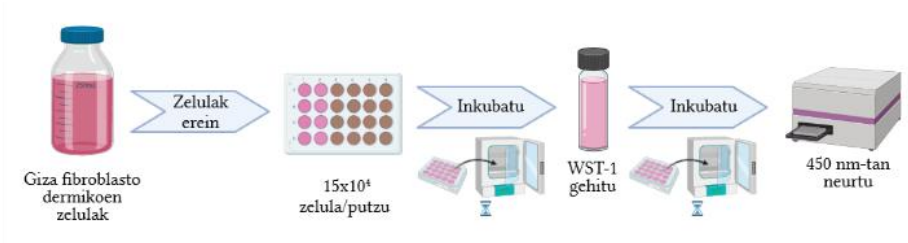

3.7 Irudia. Zelulen ereite eta ugaltze saiakuntzaren azalpen eskematikoa.

Ondoren, 3.7 Irudian adierazten den bezala, aurretik esterilizatu eta zelulen hazkuntza-inguruz asetako hidrogeletan erein ziren 96 putzuko plakan, $15x10^4$ zelula/putzuko dentsitatean, eta 24, 48 eta 72 orduz inkubatu ziren. Inkubazio denboraren amaieran, zelulei WST-1 disoluzioa gehitu zitzaien ((4-[3-(4-iodofenil)-2-(4-nitrofenil)-2H-5-tetrazolio]-1,3-benzenedisulfonatoa) (1:10 v/v), eta beste 2 orduz inkubatu zen, ondoren, absorbantzia Biotek Cytation 3 mikroplaka-irakurgailu baten bidez neurtu zen 450 nm-tan.

3.6.5.3 Zelulen bideragarritasunen kalkuluak

Laginen bideragarritasunak ondorengo prozedura jarraituz kalkulatu ziren:

a. Lagin guztien absorbantziak irakurri ondoren, bideragarritasun-ehuneko bihurtu ziren, kontrol-zelulen putzuaren xurgapena erreferentziatzat hartuta (%100eko bideragarritasuna).
b. Balio atipikoak Grubbs-en probaren bidez detektatu ziren (3.14 Ekuazioa), datu-serie bakoitzaren batez besteko balioa eta desbiderapen estandarra kontuan hartuz.

$$Z = \frac{|x_{mean} - x|}{SD} \qquad \text{(3.14 Ekuazioa)}$$

non x_{mean} datu-seriearen batezbesteko balioa den, x balio susmagarria den eta SD datu-seriearen desbideratze estandarra den. Kalkulatutako Z-ren balioa aztertutako datu kopuruarentzako taulatutako balio kritikoa baino handiagoa bada, aukeratutako balioa atipikoa dela kontsideratzen da. Handiagoa ez bada, aldiz, balio hori kalkuluetarako aintzat hartu beharko da.

c. 48 eta 72 ordu ondoren egindako esperimentuetarako ere bideragarritasunak 24 ordu ondorengo kontrol-laginaren absorbantzia erreferentziatzat hartuta kalkulatu ziren.
d. Esperimentuak 24 orduz baino gehiagoz egin ziren kasuetan, laginen bideragarritasunen bigarren hurbilketa bat egin zen, lagin zurien absorbantziak (PVA hutsezko hidrogelenak, B1 eta B2 laginak) kontrol gisa hartuz.

Emaitzak eta eztabaida

4

4 Emaitzak eta eztabaida

Tesi honetan, ligninan oinarrituriko hidrogelak sintetizatu dira material eta formulazio desberdinak konbinatuz. Lehenik eta behin, sintesi-prozedura optimizatu zen sei sintesi-ibilbide desberdinetarako diseinu esperimental bat eta erantzun-gainazalaren metodologia (RSM) erabiliz. Hemendik ondorioztaturiko baldintza optimoak hidrogel berrien sintesirako erabili ziren. Kasu honetan pisu molekular desberdineko matrize polimerikoak (PVA) erabili ziren, hidrogelen propietateengan parametro honek zuen eragina aztertzeko. Gero, baldintza berberak aplikatu ziren fruitu lehorren azaletatik erauzitako ligninan oinarrituriko hidrogelen garapenerako, eta baita kimikoki eraldatutako ligninetan oinarriturikoenak ere. Emaitza horiek guztiak artikulu desberdinetan argitaratu badira ere, aurkikuntza nagusien laburpena atal hauetan antolatu da:

4.1 Ligninen karakterizazioa

4.2 Ligninan oinarrituriko hidrogelen sintesiaren optimizazioa

4.3 Formulazio parametro desberdinek hidrogelen propietateengan duten eragina

- 4.3.1 Lehortze mota
- 4.3.2 PVA-ren pisu molekularra eta izozte-desizozte ziklo kopurua
- 4.3.3 Lignina mota
- 4.3.4 Izozte-desizozte zikloen iraupena
- 4.3.5 Ligninaren eraldaketa mota

4.4 Sintetizaturiko lignina-hidrogelen aplikazioak

- 4.4.1 Tindagaien xurgapena
- 4.4.2. Propietate antifungikoak
- 4.4.3 Botiken askapena
- 4.4.4 Biobateragarritasuna

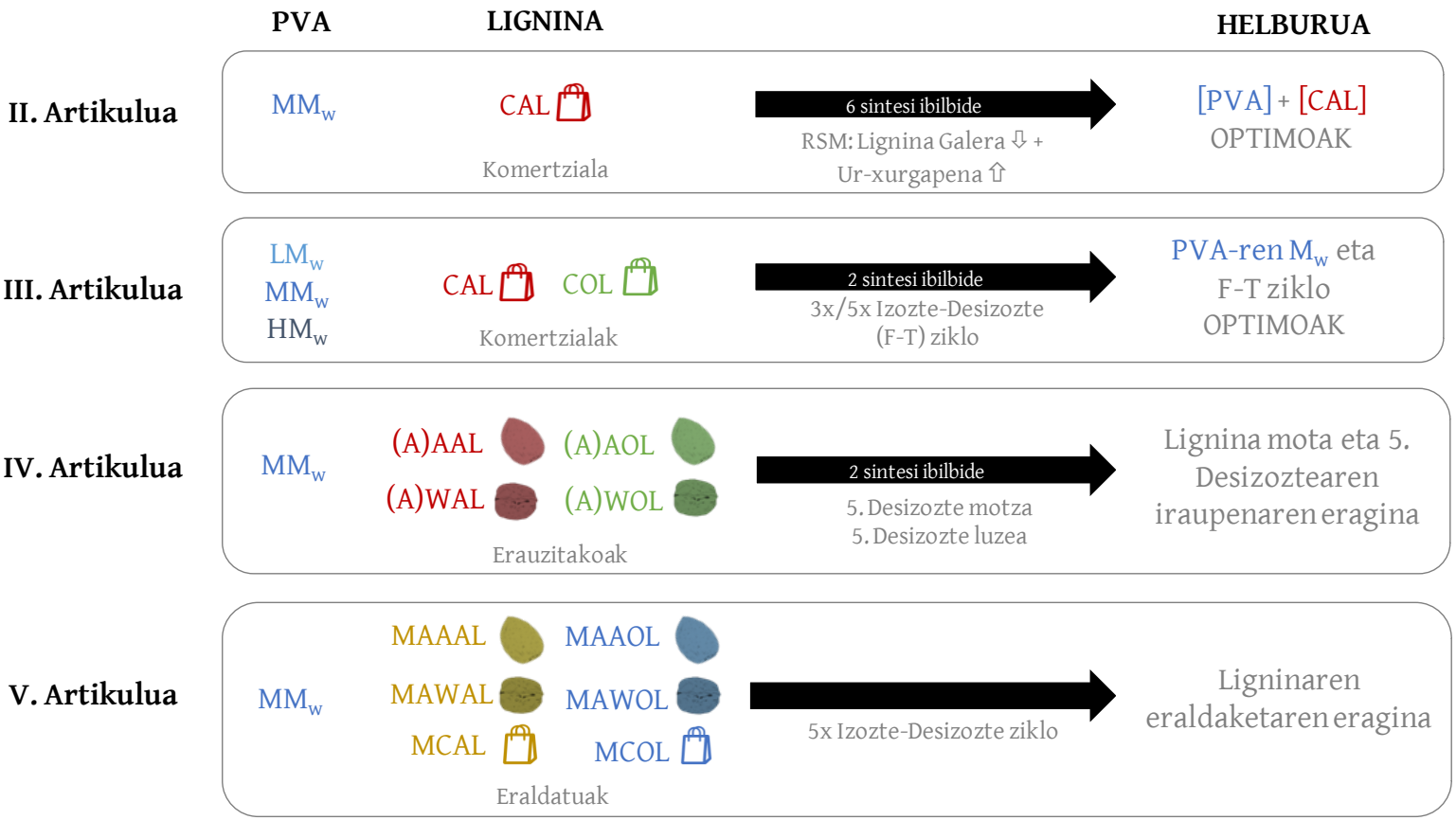

4.1 Irudia. Artikulu desberdinetan egindako esperimentuen laburpen eskematikoa.

4.1 Ligninen karakterizazioa

4.1.1 Lignina komertzialak eta erauzitako ligninak

4.1.1.1 Purutasuna

4.1 Taulan ikusten den bezala, purutasun-emaitzak, oro har, handiagoak izan ziren organosolv ligninen kasuan alkalinoen kasuan baino; izan ere, organosolv erauzketen selektibitatea handiagoa izan ohi da [87]. Lignina komertzialek %92 inguruko purutasunak izan zituzten. Autohidrolisirik gabeko organosolv ligninek (AOL eta WOL laginek) ere %90etik gorako purutasuna izan zuten, eta alkalinoek, berriz, %59 baino gutxiagokoa. Hala ere, lehengaiaren autohidrolisia egin ondoren, lignina alkalinoen purutasunak %88-95era igo ziren; organosolv-en kasuan, berriz, igoera hori %3-5ekoa baino ez zen izan. Beraz, esan daiteke autohidrolisiak lignina alkalinoen purutasuna hobetzen duela bereziki [77].

4.1.1.2 Pisu molekularra

HPSEC azterketetatik lignina alkalino komertziala organosolv-a baino askoz homogeneoagoa zela ikusi zen, azken horrek oso pisu molekular (M_w) altua baitzuen, ez ohikoa organosolv ligninetan (4.1 Taula). Autohidrolisirik gabeko fruitu lehor azaletako organosolv ligninek ere alkalinoek baino M_w altuagoa izan zuten. Etapa bikoitzeko prozesutik zetozen ligninen kasuan (autohidrolisidunak), aldiz, aurkako portaera ikusi zen. Antzeko joera hauteman zen polidispertsitate indizeetan. Gainera, autohidrolisi tratamenduak batez besteko pisu molekularrak areagotzen zituela ikusi zen, bai kopuruan eta baita pisuan ere. Aipatzekoa da organosolv lignina guztien M_W-a oso antzekoa izan zela, eta lignina alkalinoen kasuan, berriz, izugarrizko aldea zegoela. Hala ere, purutasun-ehunekoak eta aurreko lanak kontuan hartuta [88], baliteke emaitza horiek, AAL eta WAL laginetan aztertutako lignina-frakzioetarako, lignina-lagin guztiaren adierazgarri ez izatea.

4.1 Taula. Ligninen purutasun, HPSEC, TPC eta TGA azterketen emaitzen laburpena.

Lagina	Deskribapena	Purutasuna (%)	M_w [a] (g/mol)	M_n [b] (g/mol)	M_w/M_n [c]	TPC (% GAE[d])	T_{max} [e] (ºC)
CAL	Lignina alkalino komertziala	91,5	9333	1365	6,8	20,3	379
COL	Organosolv lignina komertziala	92,5	32933	1123	29,3	19,3	343
AAL	AS lignina alkalinoa	58,2	4770	1109	4,3	13,8	307
AOL	AS organosolv lignina	90,4	8301	1072	7,8	15,6	389
WAL	WNS lignina alkalinoa	49,4	4761	1054	4,5	10,6	295
WOL	WNS organosolv lignina	92,7	6371	1246	5,1	16,5	388
AAAL	Autohidrolizaturiko AS lignina alkalinoa	88,2	12793	1528	8,4	33,1	355
AAOL	Autohidrolizaturiko AS organosolv lignina	95,2	9020	1520	5,9	26,2	357
AWAL	Autohidrolizaturiko WNS lignina alkalinoa	95,7	16670	1604	10,4	33,8	354
AWOL	Autohidrolizaturiko WNS organosolv lignina	95,2	7644	1359	5,6	27,2	365
MCAL	Eraldatutako CAL	91,9	12141	1718	7,1	25,8	396
MCOL	Eraldatutako COL	96,5	32997	968	34,07	21,5	390
MAAAL	Eraldatutako MAAAL	85,2	17675	1348	13,1	25,3	384
MAAOL	Eraldatutako MAAOL	92,3	9557	1636	5,8	20,4	383
MAWAL	Eraldatutako AWAL	84,0	19939	1369	14,6	27,6	384
MAWOL	Eraldatutako AWOL	83,6	8187	1420	5,8	23,6	383

[a] M_w: batez besteko pisu molekularra pisuan; [b] M_n: batez besteko pisu molekularra kopuruan; [c] M_w/M_n: polidispertsitate indizea; [d] % GAE: azido galikoaren baliokideen ehunekoa; [e] T_{max}: TG/DTGA kurbetatik lorturiko gehieneko degradazio-tenperatura.

4.1.1.3 Konposatu fenolikoen eduki totala (TPC)

Konposatu fenolikoen eduki totalaren emaitzei dagokienez (4.1 Taula), fruitu lehorren azalak zuzenean deslignifikatzearen ondorioz lortutako lignina (AAL, AOL, WAL eta WOL) laginen balioak bi urratseko prozesutik eratorritakoenak (AAAL, AAOL, AWAL eta AWOL) edota lignina komertzialenak baino askoz baxuagoak izan zirela ikusi zen. Fenomeno hau euren purutasunarekin lotuta egon daiteke [89]. Dávila *et al.* (2019)-ek iradoki bezala, aurretratamendu hidrotermiko bat erabakigarria izan daiteke ligninan eduki fenoliko handiak lortzeko [89].

4.1.1.4 Analisi termograbimetrikoa (TGA)

Ligninen degradazio termikoko kurbetatik (4.2 Irudia) 4.1 Taulan azaltzen diren gehieneko degradazio-tenperaturak detektatu ahal izan ziren. Lagin guztiek 100 ºC-tik beherako degradazio etapa bat zuten hasieran, hezetasuna lurruntzeari zegokiona. Honen ondoren, lignina alkalino komertzialak bigarren degradazio-urrats jasan zuen, degradazio handieneko etapa izan zena, 379 ºC inguruan. Degradazio hori erauzitako laginetan ere ikusi zen, baina etapa bakarreko prozesuen bidez lortutako lignina alkalinoek (AAL eta WAL) gehieneko degradazio-tenperatura 300 ºC ingurukoa izan zuten bitartean, organosolv ligninena nabarmen handiagoa izan zen (390 ºC). Hala ere, organosolv lignina komertzialak degradazio-fase bat izan zuen degradazio handieneko etapa baino lehen, eta azken hau 343 ºC inguruan detektatu zen, erauzitako organosolv laginek erakutsitakoa baino txikiagoa. Egonkortasun termikoaren murrizketa ezpurutasun kopuru handiari egotzi ohi zaio, baita pisu molekular txikiko frakzioei ere [77,90]. Etapa bikoitzeko prozesuetatik eratorritako ligninek antzeko degradazio-tenperatura maximoak izan zituzten (354-365 ºC), etapa bakarreko prozesuko ligninenen artean zeudenak eta aurreko emaitzekin bat zetozenak [75]. Tenperatura tarte honetan, β–O–4 eter loturen zatiketa gertatzen da, eta ondoren, C-C loturen eta eraztun aromatikoen zatiketa eman ohi da [90]. Hirugarren degradazio-etapa bat ikusi

zen, 420 ºC inguruan, baina tenperatura hori berriz ere txikiagoa izan zen AAL eta WAL laginentzat (390 ºC) eta handiagoa AOL eta WOL laginentzat (470 ºC). Azken hauek pisu galera konstantea izan zuten gero, hasierako pisuaren %37ra iristeraino. Gainerako laginek laugarren degradazio-etapa bat izan zuten, 700 ºC inguruan, eta hasierako pisuaren %20 eta %29 arteko hondakin bat sortu zen, *biochar* deiturikoa. Azken etapa hau ligninaren produktu lurrunkorren demetoxilazio edo kondentsazio erreakzioekin lotuta egon liteke [90], eta utzitako *biochar* kopuruak aurretik aipatutakoen antzekoak izan ziren [75].

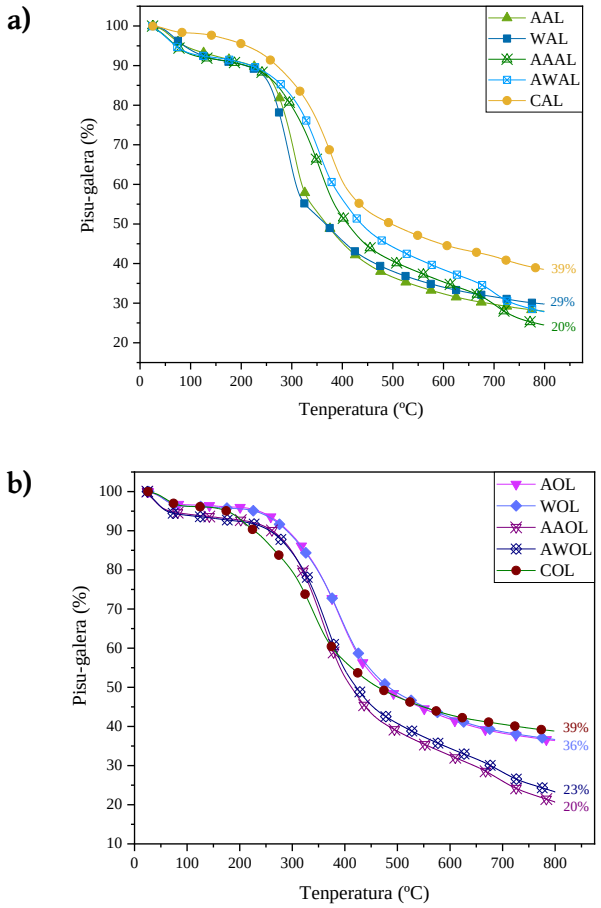

4.2 Irudia. Tesi honetan erabilitako jatorrizko a) lignina alkalinoen eta b)organosolv ligninen TGA kurbak.

4.1.1.5 Islapen total indargetua - Fourierren transformatuaren bidezko espektroskopia infragorria (ATR-FTIR)

Erabilitako ligninen talde funtzional nagusiak ATR-FTIR teknikaren bidez zehaztu ziren (4.3 eta 4.4 Irudiak). Erregistratutako espektro guztiek ligninen ohiko bandak aurkeztu zituzten arren (4.2 Taula) [74,89,91–94], horietako batzuen intentsitateak lagin batetik bestera aldatu ziren.

4.2 Taula. Ligninaren ATR-FTIR espektroaren banda bereizgarrienak.

Uhin zenbakia (cm^{-1})	Esleipena
3460-3215	-OH taldeen luzatze-bibrazioa
2998-2947	Alkilo taldeen bibrazio asimetrikoa
2913-2827	C-H aromatikoen luzatze-bibrazioa
1710	Konjugatu gabeko C=O taldeen luzatze-bibrazioa
1679-1650	C=O ester lotura
1597	C=C taldeen luzatze-bibrazioa
1513	C=C aromatikoen bibrazioa
1456	Metilo taldeen C-H lotura
1429	Egitura aromatikoen bibrazioa
1325-1269	G and S unitateen arnasketa + ez-purutasunak
1215	Metil eter aromatikoak
1100	C–C loturak
1157-1030	C-O loturen luzatze-bibrazioa + ez-purutasunak
975	Planoz kanpoko –HC=CH bibrazioa
910-896	C–H loturen deformazio-bibrazioa
865	C-C loturen luzatze-bibrazioa
832-317	-CH aromatikoen planoz kanpoko bibrazioa + β-glukosidiko loturak

Lignina komertzialen artean, desberdintasun nagusienak 1330, 1265 eta 840 cm^{-1} inguruko bandetan aurkitu ziren, S eta G unitateen aldakuntzari eta ezpurutasunei egotz dakiekeena. Erauzitako ligninen artean, 2827-2998 cm^{-1} tartean aldaketa nabarmenak ikusi ziren, ligninaren eta polisakaridoen C-H luzatze-bibrazioari dagozkionak [91], eta nabarmenagoak izan ziren lignina alkalinozko laginentzat, ziur asko azukre-unitate gehiago zutelako. 1650 cm^{-1}-ean, etapa bakarreko ligninentzat C=O konjugatuen luzatze-bibrazioari dagokion banda bat detektatu zen [91], baina autohidrolisidun laginetan desagertu egin zen. Nahiz eta autore batzuek aurretik banda hau prozesu

alkalinoekin lotu [95], AAL, WAL, AOL eta WOL ligninetan ezpurutasunak egoteari egotz dakiokeela uste da.

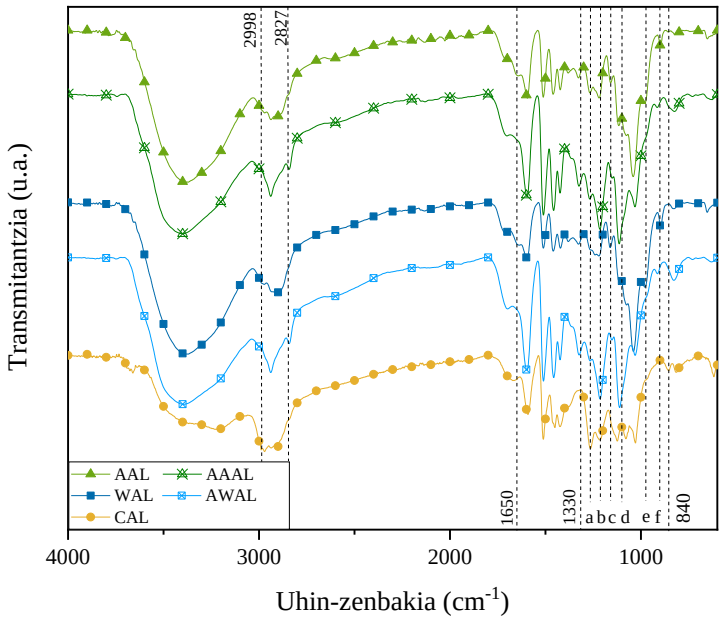

4.3 Irudia. Tesi honetan erabilitako jatorrizko lignina alkalinoen ATR-FTIR espektroak.

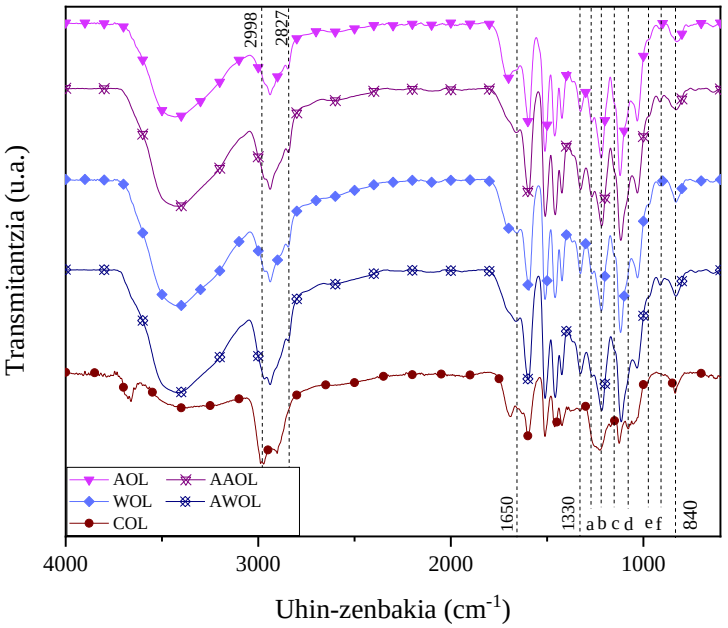

4.4 Irudia. Tesi honetan erabilitako jatorrizko organosolv ligninen ATR-FTIR espektroak.

Fingerprint edo hatz-marka eremuan (1500-600 cm^{-1}) banden intentsitatearen aldaketa nagusiak ikusi ziren. AAL eta WAL laginetan, adibidez, kondentsaturiko siringilo edo guaiazilo unitateen arnasketari esleitutako banden intentsitatea nabarmen murriztu zen (1325 cm^{-1}) [92,96] eta baita ligninaren metil eter aromatikoena ere (1215 cm^{-1}) [91]. 1157, 1080, 975 eta 896 cm^{-1}-ra kokatutako banden intentsitatea, aldiz, areagotu egin zen. Seinale hauek, ester taldeen C–O luzatze-bibrazioari [92,96], bigarren mailako alkoholen eta eter alifatikoen C–O deformazioari, planoz kanpoko –HC=CH eta C – H deformazio bibrazioei dagozkie, hurrenez hurren [92].

4.1.1.6 Konposizio analisiak (Py-GC/MS)

Py-GC/MS analisietatik abiatuta zehaztu ziren konposatuak 4.3 Taulan azaltzen dira. Erauzitako ligninen pirogramek hasierako minutuetan (3-7 min) erakutsitako seinaleak ezpurutasunetatik eratorritako degradazio-konposatuei zegozkien (furfurala, adibidez) [75], purutasun baxuko lignina-laginetan (AAL eta WAL) bereziki ikus zitezkeenak. Hala, 7-23 minutuko tartean identifikatutako konposatuak egitura aromatikoaren jatorriaren arabera (*p*-hidroxifenilo (H), guaiakol (G) eta siringol (S)) multzokatu ziren [74,75,92,94].

Identifikatutako konposatuen artean, guaiakola, 4-metilguaiakola, siringola eta 4-metilsiringola izan ziren ugarienak lignina lagin guztietan, bereziki CAL laginean, non guaiakola izan zen konposatu nagusia. 4-etilguaiakola eta 4-binilguaiakola lagin guztietan topatu ziren kopuru handitan. *p*-hidroxifenilo unitatetik zetozen konposatuak, fenola, *p*-cresola eta *p*-etilfenola kasu, intxaur azaletatik (WNS) isolaturiko ligninetan ugariagoak zirela antzeman zen. Beste konposatu batzuk, banillina esaterako, organosolv ligninetan baino ez ziren topatu, eta 4-propilguaiakola lignina hauetan eta CAL laginean agertu zen. S unitatetik eratorritako konposatu batzuk, 4-metilsiringola, 4-etilsiringola eta 4-binilsiringola barne, erauzitako ligninetan bakarrik detektatu ziren, erauzketa prozesuarekin nolabaiteko lotura izan dezakeela iradokiz.

4.3 Taula. Jatorrizko ligninentzat Py-GC/MS bidez hautemandako konposatuen identifikazioa eta ugaritasuna (azalera erlatiboa, %).

Denbora (min)	Konposatua	Jatorria	Lignina Lagina									
			CAL	COL	AAL	AOL	WAL	WOL	AAAL	AAOL	AWAL	AWOL
7,5-7,7	Fenola	H	1,80	3,85	1,62	0,98	6,56	3,29	1,16	-	4,26	2,95
8,7-8,9	*o*-Kresola	H	1,60	0,79	1,53	1,04	2,42	1,22	1,80	1,14	1,66	1,21
9,0-9,2	*p*-Kresol	H	1,55	1,71	1,82	1,62	5,22	5,31	1,39	0,92	4,58	4,12
9,3-9,5	Guaiakola	G	38,40	9,65	13,62	11,80	9,30	8,91	17,14	7,40	11,72	7,56
10,4	2,6-Dimetil fenola	H	-	-	1,68	1,38	1,45	1,53	1,95	1,77	1,44	1,52
10,7-10,8	*p*-Etilfenola	H	-	-	0,74	-	2,40	1,66	0,54	-	1,71	1,43
11,0-11,1	3-Metilguaiakola	G	1,85	0,63	2,08	1,35	0,94	1,29	3,90	1,17	2,28	1,24
11,7-11,9	Katekola	S	2,70	1,27	0,64	-	0,35	-	-	-	0,40	-
11,4-11,6	4-Metilguaiakola	G	5,07	3,87	9,75	12,74	5,23	10,86	15,19	8,08	10,07	7,73
13,3-13,5	3-Metoxikatekola	S	-	3,06	0,19	3,29	0,95	4,22	2,56	3,67	4,39	4,33
13,8-14,0	4-Etilguaiakola	G	4,02	4,58	7,78	5,67	3,80	5,15	8,82	3,63	7,09	3,79
15,0-15,2	4-Binilguaiakola	G	8,15	18,74	6,94	7,16	3,76	5,77	4,52	3,00	3,51	3,10
16,1-16,2	Siringola	S	1,98	8,07	7,45	9,69	3,96	10,57	8,13	5,42	16,52	7,18
16,3	3,4-Dimetoxifenola	S	-	0,90	1,69	1,87	0,64	2,55	1,82	0,88		2,13
16,3-16,4	4-Propilguaiakola	G	0,86	0,52	-	1,48	-	1,34	-	0,88	-	0,94
17,1-17,3	Banillina	G	-	0,86	-	0,82	-	0,80	-	0,71	-	0,63
17,4	cis-Isoeugenola	G	4,83	1,18	1,12	1,70	0,34	1,60	1,19	0,85	1,35	0,84
18,3	4-Metilsiringola	S	-	-	4,75	12,03	2,69	13,66	5,94	6,80	9,23	7,54
18,8-19,0	Azetobanillona	G	4,22	-	-	0,85	-	1,23	0,26	0,97	0,49	-
19,6	4-Etilsiringola	S	-	-	1,02	1,28	0,78	1,95	1,16	0,82	2,47	0,90
20,2-20,8	4-Binilsiringola	S	-	-	0,23	1,92	0,24	1,72	0,62	0,73	0,87	0,96
21,6	Siringaldehidoa	S	0,70	-	-	1,20	0,47	0,62	0,40	1,65	0,16	2,56
22,1	4-Allilsiringola	S	0,93	2,27	0,51	2,09	0,83	2,11	0,50	0,40	0,51	1,56
22,5	Acetosiringona	S	1,82	-	0,13	2,03	0,87	0,86	0,34	1,45	0,17	2,44
23	Azido homosiringikoa	S	0,89	-	-	1,07	-	0,42	0,15	0,64	-	1,30
	S totala		9,03	15,57	16,60	36,48	11,78	38,67	21,62	22,47	34,72	30,90
	G totala		67,40	40,02	41,29	43,59	23,37	36,96	51,04	26,70	36,51	25,83
	S/G ratioa		0,13	0,39	0,40	0,84	0,50	1,05	0,42	0,84	0,95	1,20

Zenbatetsitako S/G erlazioei dagokienez, lagin guztiek G unitate gehiago izan zituztela esan daiteke, WOL eta AWOL laginek izan ezik. Horrela, S/G erlazio ia guztiak 1 baino txikiagokoak izan ziren. Lignina komertzialek erakutsi zituzten S/G baliorik txikienak, eta ondoren, almendra azaletatik (AS) eratorritako lignina alkalinoek. Hala ere, erlazio hori areagotu egin zen etapa bakarreko prozesuko ligninetatik bi etapako prozesukoetara pasatzerakoan, eta gertaera hau sakonago aztertuko da azalpen zentzudun bat aurkitzeko. Edonola ere, balio horiek aurretik lortutakoekin alderatuz [74,75], nahiko desberdinak direla esan daiteke, lehengaien osaerarekin edota erauzketa-prozesuko edozein aldaketarekin zuzenki lotuta egon litekeena.

4.1.2 Eraldatutako ligninak

4.1.2.1 Purutasuna

4.1 Taulan ikus daitekeen bezala, eraldatutako ligninen purutasunak (komertzial nahiz erauzitakoena), eraldaketa-metodoa edozein izanik, behera egin zuen, erauzitako ligninetan bereziki. Gertaera hau erabilitako erreaktiboen ondorio izan liteke.

4.1.2.2 Pisu molekularra

Jatorrizko ligninekin alderatuta, eraldatutako ligninen batez besteko pisu molekularrek gora egin zuten kasu guztietan, batez ere lignina alkalinoetan. Eraldatutako lignina alkalino erauzien eta organosolv lignina komertzialaren kasuan, kopuruan batez besteko pisu molekularrak (M_n) murriztu egin ziren eta horrek polidispertsitate indizea handitzea ekarri zuen. Organosolv lignina komertzialari dagokionez, bere bertsio eraldatua (MCOL) lignina eraldaturik heterogeneoena izan zen berriro ere, erauzitako jatorrizko eta eraldatutako organosolv ligninak (AAOL, AWOL, MAAOL eta MAWOL) homogeneoenak izan ziren bitartean.

Peroxidazio erreakzioak lignina zatikatzen duela suposatzen den arren, kateen ehuneko handi batek, dirudienez, birkondentsazio erreakzioak jasan zituen,

honen ondorioz, eraldatutako lignina alkalinoen batez besteko pisu molekular totalak handitu zirelarik.

Bestalde, hidroximetilaturiko ligninen pisu molekularren banaketek (**V. Artikuluko** datu osagarriak) eta estimatutako batez besteko pisu molekularrek eraldaketa arrakastaz gertatu zela iradoki zuten [97]. Nahiz eta ligninen polidispertsitate indizeen aldaketak ez izan lignina homogeneoagoak lortu izanaren adierazgarri, pisu molekularren banaketek pisu molekular handieneko frakzioak pisu molekular txikiagokoetara homogeneizatzeko joera erakutsi zuten. Portaera hau beste autore batzuek ere ikusi zuten [98]. Horrez gain, MAAOL eta MAWOL laginetan pisu eta kopuruan batez besteko pisu molekularraren igoera ikusi zen, eta hori ere autore berek aurretik antzemandakoa da belar ligninentzat [98].

4.1.2.3 Konposatu fenolikoen eduki totala (TPC)

Lignina alkalino peroxidatuen kasuan, eduki fenoliko totalaren aldaketak ligninaren eraztun aromatikoen degradazioa iradoki zuen [76,99]. Hala ere, MCAL laginak kontrako joera aurkeztu zuen, eta horrek hasierako pH desberdintasunekin izan lezake zerikusia. Xinping *et al.* (2010)-en emaitzen arabera [99], erreakzioak baldintza alkalinoetan degradazio-konposatu gehiago sor litzake [41], baina Infante *et al.* (2007)-ek katalizatzailerik gabe ere efektu berdina ere lor zitekeela erakutsi zuten, eta erreakzio hau azken autore hauen arabera burutu zen [76].

Lignina hidroximetilatuen kasuan, lignina komertzialean izan ezik, TPC-an jaitsiera txiki bat ikusi zen, eraztun aromatikoen oxidazioari egotz dakiokeena.

4.1.2.4 Analisi termograbimetrikoa (TGA)

Eraldatutako lagin guztien egonkortasun termikoa aldatu egin zen eraldaketa-erreakzioen ondorioz (4.5 Irudia). Izan ere, gehieneko degradazio-tenperatura handiagotu egin zen kasu guztietan. Hala ere, lignina alkalinoen kasuan, beste degradazio-fase bat agertu zen hezetasunaren lurrunketari dagokion etaparen

(< 100 ºC) eta degradazio handieneko etaparen artean. Etapa hori 300 ºC inguruan detektatu zen, eta eraldaketa-erreakzioren ondorioz sortutako ligninaren pisu molekular txikieneko frakzioei egotzi zitzaien [77,90].

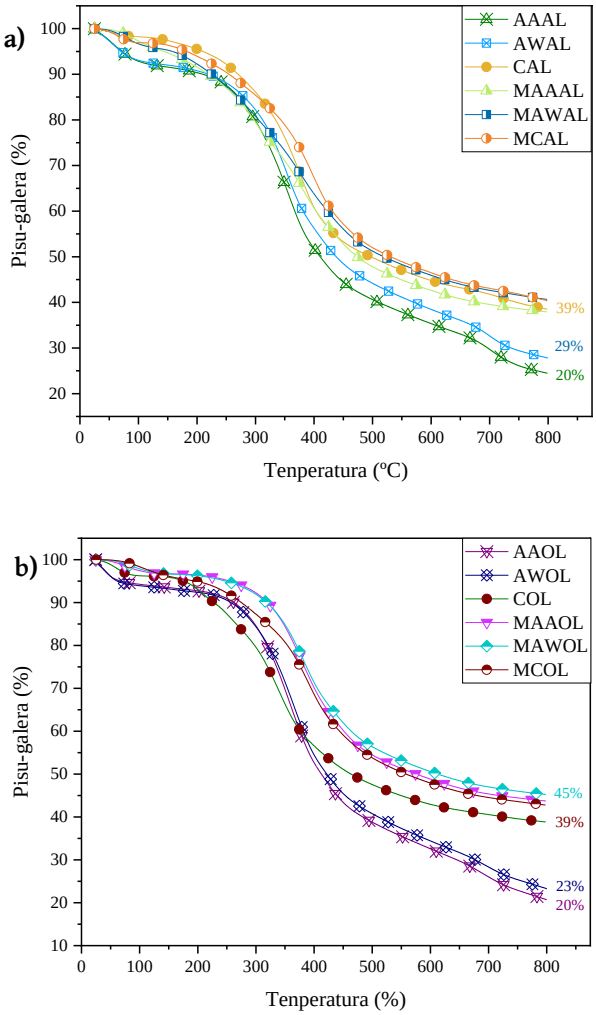

4.5. Irudia. Eraldatutako a) lignina alkalinoen eta b) organosolv ligninen TGA kurbak.

Gainera, organosolv ligninak termikoki egonkorragoak zirela ikusi zen, hau da, lignina alkalinoak baino tenperatura altuagoetara hasi zirela pisua galtzen, nahiz eta euren degradazio-tenperatura maximoak apur bat baxuagoak izan. Jatorrizko ligninekin alderatuta, eraldatutako organosolv ligninek

egonkortasun termiko handiagoa eta amaierako hondakin handiagoa izan zuten, beste egile batzuek ere ikusi bezala [39]. Gainera, sortutako *biochar* guztiak laginaren hasierako pisuaren %40 inguru izan arren, eraldatutako organosolv ligninek alkalinoek baino hondakin handiagoak utzi zituzten, jatorrizko ligninekin gertatu ez bezala, eta hori ligninaren eraldaketa- eta prezipitazio-etapei egotz dakieke.

4.1.2.5 *Islapen total indargetua - Fourierren transformatuaren bidezko espektroskopia infragorria (ATR-FTIR)*

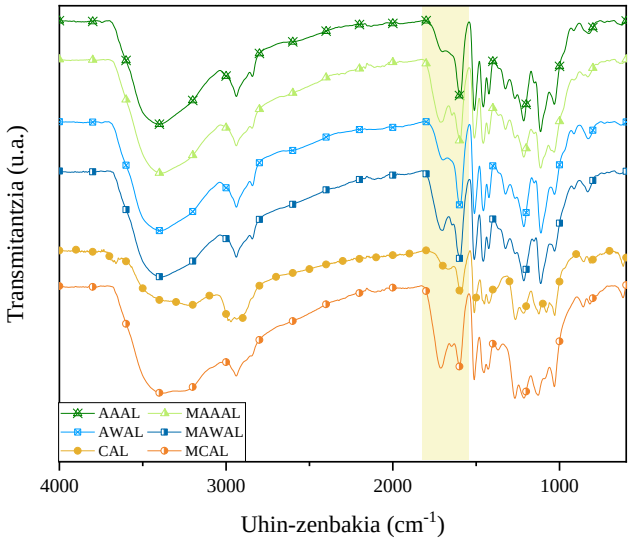

4.6 Irudia. Eraldatutako lignina alkalinoen ATR-FTIR espektroak.

Eraldatutako ligninen ATR-FTIR espektroetan, euren egituran aldaketaren bat iradokitzen zuten seinale batzuk agertu ziren. Lignina peroxidatuen kasuan, espektroen 1600-1730 cm^{-1} arteko diferentziek erreakzioa baieztatu zuten (4.6 Irudia). Izan ere, 1710 cm^{-1} inguruko banda uhin zenbaki altuagoetara mugitu zen kasu guztietan, alboko kateen -OH oxidazioari egotzi zitzaiona, 1599 cm^{-1}-ko seinalea ahultzearekin batera, C=C aromatikoaren luzatze-bibrazioari dagokiona. Gainera, Infante *et al.* (2010)-ek aipatu bezala, 1640 cm^{-1} inguruko

bandaren agerpena eraztun aromatikoen degradazioaren adierazgarri izan zen [76].

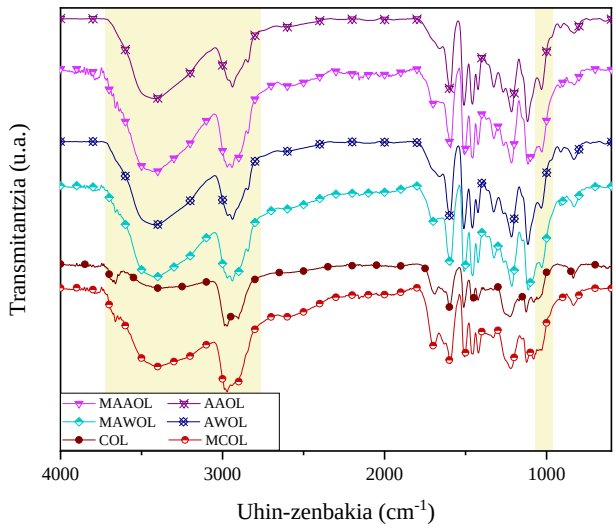

4.7 Irudia. Eraldatutako organosolv ligninen ATR-FTIR espektroak.

Bestalde, 4.7 Irudian ikusten den bezala, lignina hidroximetilatuen kasuan, -OH bandaren areagotzeak (3400 cm^{-1}), C-H loturari dagokionak (2930 cm^{-1} inguruan), metoxilo eta hidroximetilo taldeei dagokienak (2850 cm^{-1} inguruan) eta C-OH alifatikoen C-O eta C-OH alifatikoen C-O loturaren luzatze-bibrazioarekin lotutakoak (1030 cm^{-1} inguruan) erreakzioari esker hidroximetilo taldeak gehitu izanaren seinale garbiak izan ziren [39,97]. Horrez gain, 3660 cm^{-1}-eko banda leunaren agerpenak lignina eraldatuen egituraren barruan -OH talde askeak egotea iradoki zuen [100]. Ondorioz, espektroek erreakzioaren arrakasta baieztatu zuten. Emaitza horiek bat datoz ^{31}P RMN analisietan lortutakoekin. Analisi horietan, erreakzioaren ostean, lagin guztietan hidroxilo alifatikoen 150 eta 145,4 ppm arteko seinalea handitu zela ikusi zen [39] (**V. Argitalpeneko** datu osagarriak).

4.1.3 Ondorioak

Atal honetan tesi guztian zehar erabilitako organosolv nahiz alkalinoak diren lignina komertzialak, erauziak eta eraldatuak karakterizatu dira. Erauzitako ligninak almendra eta intxaur oskoletatik isolatu ziren bi bio-findegi-estrategia desberdinen bidez: deslignifikazio-prozesu bakar baten bidez eta urrats bikoitzeko prozesu baten bidez, autohidrolisi-etapa batek eta deslignifikazio-etapa baten konbinaketaz osatua. Ligninen karakterizazioak desberdintasun nabarmenak erakutsi zituen laginen artean, batez ere konposizioan, batezbesteko pisu molekularretan eta eduki fenoliko totaletan. Espero bezala, autohidrolisiak ligninen purutasuna hobetu zuen, bereziki alkalinoen kasuan, eta pisu molekular altuagoak zituzten ligninak ateratzea ere sustatu zuen. Ligninen eraldaketak erabilitako karakterizazio tekniken bidez berretsi ziren. Hauek batez besteko pisu molekular altuagoak eragin zituzten, eta, beraz, baita termikoki egonkorragoak ziren ligninak ere.

4.2 Ligninan oinarrituriko hidrogelen sintesiaren optimizazioa

II. Artikuluan erakusten den bezala, ligninan oinarritutako hidrogelen sintesia optimizatzeko, lignina alkalino komertziala (CAL) eta polibinil alkohola (PVA, M_w = 83000- 124000 g/mol, %99+ hidrolizatua) nahastu ziren hiru mailatako eta bi faktoreko diseinu esperimental batek adierazitako kontzentrazioetan, erdiguneko puntuaren hiru errepikapenarekin. Ondoren, erantzun-gainazalaren metodologia (RSM) erabili zen lignina-hidrogelen sintesiaren baldintzak modelizatzeko eta optimizatzeko.

Hidrogel guztiak 3.4 Atalean deskribatu bezala prestatu ziren, eta nahasketei hiru gurutzaketa-metodo (XL) desberdin aplikatu zitzaizkien: 3 eta 5 izozte-desizozte ziklo (16 h 20 ºC-tan eta 8 h 28 ºC-tan) eta 37 ºC-ko huts-kanpai baten barruan (60 cm Hg) astebetez. Gurutzaketa-etaparen ondoren, hidrogelak bereizita garbitu ziren, eta, ondoren, erdiak giro-tenperaturan lehortzen utzi ziren, eta beste erdiak hutsean lehortu ziren (60 cm Hg) 27 ºC-tan. Konposizio optimoak zituzten hidrogelak aurrekoen antzera prestatu ziren, zegozkien lignina eta PVA kantitate optimoak erabiliz. 4.8 Irudian ondorengo sei sintesi-ibilbideak irudikatzen dira:

(1) Hutseko XL + Giro-lehorketa (Vac–Air)
(2) Hutseko XL + Hutseko lehorketa (Vac–Vac)
(3) 5 Izozte-desizozte ziklozko XL + Giro-lehorketa (F–T x5–Air)
(4) 5 Izozte-desizozte ziklozko XL + Hutseko lehorketa (F–T x5–Vac)
(5) 3 Izozte-desizozte ziklozko XL + Giro-lehorketa (F–T x3–Air)
(6) 3 Izozte-desizozte ziklozko XL + Hutseko lehorketa (F–T x3–Vac)

Aipatu den bezala, hautatutako aldagai askeak lignina alkalinoa (x_1) eta PVA-ren kontzentrazioak (x_2) izan ziren, %5-25 (p/p) eta %5-11 (p/p) artekoak, hurrenez hurren. Aitzitik, erantzun-aldagaiak hidrogelen ur-xurgatze ahalmena (%, y_1) eta garbiketa-etapako lignina-galera (%, y_2) izan ziren. Hamaika esperimentu diseinatu ziren bide bakoitzerako, hautatutako

parametroen balioak eta erdiko puntua hirukoiztuta kontuan hartuta; beraz, guztira hirurogeita sei esperimentu egin ziren. Optimizazioaren helburua lignina galera minimoa eta ur-xurgatze ahalmen handiena zuten hidrogelak lortzea zen. Ereduak baliozkotzeko, esperimentuak baldintza optimoak erabiliz egin ziren, eta esperimentuetan lortutako emaitzak teorikoki aurreikusitako datuekin alderatu ziren.

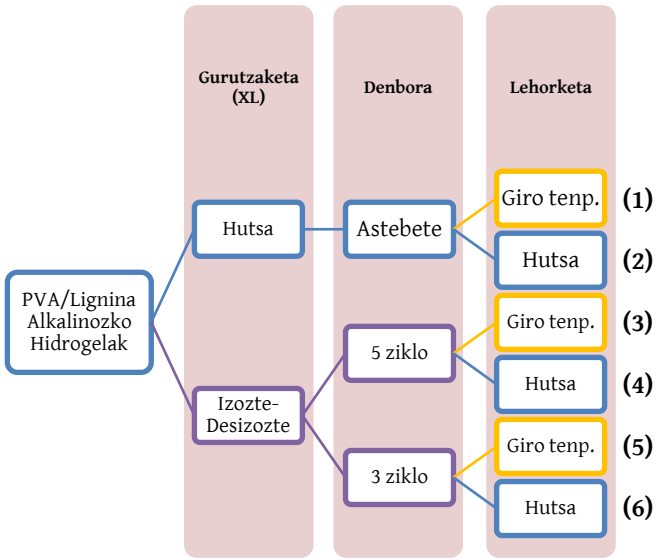

4.8 Irudia. Hidrogelak sintetizatzeko sei bideen eskema.

4.2.1 Hidrogelen konposizioa modelizatzea eta optimizatzea

Hidrogel sintetizatuen ur-xurgatze gaitasuna eta lignina-galera neurtu ondoren, Statgraphics Centurion XV softwarearen bidez sei kontzentrazio optimoak kalkulatu ziren. Horiek 4.4 Taulan erakusten dira, erantzun-aldagaien aurreikusitako balioekin batera. Sei bideetarako kalkulatutako baldintza optimoak hidrogelak hirukoiztuta sintetizatuz balioztatu ziren. 4.5 Taulak eredu bakoitzerako lortutako erregresio-koefizienteak erakusten ditu, bigarren mailako ekuazio polinomiko baten arabera, bere esangura estatistikoa (Student-en *t* proban oinarritua), ereduen korrelazioa (R^2) eta esangura estatistikoa (Fisher-en *F* proba) neurtzen dituzten parametroak.

4.5 Taulan erakusten den bezala, aldagai gehienetarako zehaztutako R^2-a 0,86 baino handiagoa izan zen, eta horrek eredua hautatutako aldagaien arteko erlazio errealak irudikatzeko egokia izan zela adierazten du [101], baina beste kasu batzuetan balio hori 0,82 baino txikiagoa izan zen. Gainera, zenbatetsitako esanahi-mailek datuen doikuntza berresten dute. Ekuazioaren termino bakoitzaren balioak beren interakzio linealaren ekarpena eta aldagai independenteen efektu koadratikoak ebaluatzeko kalkulatu ziren. %90eko konfiantza-mailan kalkulatutako erregresio-koefiziente esanguratsuak erabiliz, erregresio koadratikoko bi ekuazio ezarri ziren, bat irteera-aldagai bakoitzarentzat (y_1-Ur-xurgatze gaitasuna eta y_2-Lignina galera), sei modeloentzat. Horrela, hamabi ekuazio lortu ziren guztira, **II. Artikuluan** deskribatzen direnak.

4.2.2 Aldagai askeek ur-xurgatze gaitasunarekiko duten eragina

Ur-xurgatze gaitasunak %314 eta %1647 artekoak ziren, (1) eta (2) ibilbideetako 4. esperimentuei zegokienak, hurrenez hurren. Erregresio-koefizienteen arabera (4.5 Taula), bi sarrera-aldagaiek ur-xurgatze ahalmenean eragina izan zutela ikusi zen. Zehazki, x_2-k eragin esanguratsua izan zuen irteera-aldagai horretan, baita x_1-ren efektu koadratikoak ere (x_1^2). Sarrerako bi aldagaien arteko elkarrekintza ere garrantzitsua izan zen (5) eta (6) ibilbideen kasuan. x_2-ren efektu koadratikoak (x_2^2) eragin handia izan zuen (4) ibilbidean. Ciolacu *et al.* (2018) eta Yang *et al.* (2018)-ek ere ur-xurgatze ahalmena hidrogelen konposizioaren araberakoa dela jakinarazi zuten [68,102].

(1), (2) eta (3) sintesi-ibilbideetarako gainazalen grafikoen arabera (4.9-a, b eta c Irudiak) (4.2), PVA-ren kontzentrazio finko baterako, lignina-edukia handitu ahala hidrogelen ur-xurgatze ahalmena handitu egiten zela erakusten da. Hala ere, lignina kontzentrazio jakin batetik aurrera (> %15), ur-xurgatze ahalmena murriztu egin zen, muturreko lignina kontzentrazioen artean puntu gorena finkatuz.

4.4 Taula. Erantzun-aldagaietarako baldintza optimo eta balio teorikoak eta esperimentalak.

Sintesi Ibilbidea	Lignina Alkalinoa (%, p/p)	PVA (%, p/p)	Aurreikusitako Balioa		Batez besteko balio esperimentala		Errorea (%)	
			Ur-xurgatze gaitasuna (%)	Lignina Galera (%)	Ur-xurgatze gaitasuna (%)	Lignina Galera (%)	Ur-xurgatze gaitasuna (%)	Lignina Galera (%)
(1)	23,02	5	710,29	69,17	345,30	81,16	51,39	-17,34
(2)	22,26	5	1083,59	70,88	199,26	82,75	81,61	-16,74
(3)	9,12	9,87	770,14	58,11	789,89	51,94	-2,57	10,63
(4)	5	10,39	587,82	49,09	567,06	41,06	3,53	16,35
(5)	25	11	719,77	46,71	659,67	45,77	8,35	2,02
(6)	25	11	729,51	46,71	547,93	44,12	24,90	5,55

4.5 Taula. Erregresio-koefizienteak eta ereduen korrelazioa eta esanahia neurtzen dituzten parametro estatistikoak.

	(1) Vac-Air		(2) Vac-Vac		(3) F-T x5-Air		(4) F-T x5-Vac		(5) F-T x3-Air		(6) F-T x3-Vac	
	y_1	y_2	y_1	y_2	y_1	y_2	y_1	y_2	y_1	y_2	y_1	y_2
β_0	778,78	80,99	1144,76	80,99	902,17	69,08	468,74	69,08	552,83	68,70	557,40	68,70
β_1	40,67[b]	-0,93	46,89	-0,93	-56,45	-1,83	-47,17	-1,83	-37,92	-0,87	-66,98	-0,87
β_2	-64,45[a]	-3,34	-146,12	-3,34	-98,37[b]	-10,58[a]	60,89[c]	-10,58[a]	-112,85[b]	-7,15[c]	-0,96	-7,15[c]
β_{11}	-344,30[a]	-10,18[a]	-686,08[a]	-10,18[a]	-241,29[a]	-14,26[a]	95,02[c]	-14,26[a]	55,44	-18,08[b]	105,88	-18,08[b]
β_{22}	42,65	-2,91	100,40	-2,91	-49,67	0,03	-105,90[c]	0,03	43,03	1,91	-52,12	1,91
β_{12}	-16,27	6,19[b]	-26,17	6,19[b]	4,41	1,49	5,72	1,49	219,24[a]	2,20	186,30[b]	2,20
R^2	0,98	0,92	0,86	0,92	0,93	0,90	0,76	0,90	0,89	0,82	0,77	0,82
F-exp	50,93	11,12	5,96	11,12	13,53	9,22	3,24	9,22	8,467	4,44	3,32	4,44
S.L.* (%)	99,97	99,03	96,39	99,03	99,37	98,54	88,87	98,54	98,24	93,61	89,29	93,61

[a] **%99ko konfiantza-mailarako koefiziente esanguratsuak.**
[b] **%95eko konfiantza-mailarako koefiziente esanguratsuak.**
[c] **%90eko konfiantza-mailarako koefiziente esanguratsuak.**
*** Esangura maila (ingelesetik, *Significance Level*)**

Aipatzekoa da, halaber, ur-xurgatze ahalmena handiagoa izan zela PVA-ren kontzentrazio txikiagoetarako, baina lignina-edukiak PVA-renak baino eragin nabarmen handiagoa izan zuen erantzun-aldagai honekiko. Portaera hau ligninaren gai koadratikoak ur-xurgatze-ekuazioetan duen eragin handiaren ondorio bezala azal daiteke [101].

(4), (5) eta (6) sintesi-ibilbideetarako gainazal-grafikoek, PVA-ren kontzentrazio finko baterako, hidrogelen ur-xurgatze ahalmena lignina-edukia handitu ahala murriztu egiten zela erakutsi zuten (4.9-d, e eta f Irudiak). Hala ere, lignina kontzentrazio jakin batetik aurrera (> %15), ur-xurgapen ahalmena berriz ere handitzen hasi zen. Beraz, azalerek minimo bat izan zuten ligninaren muturreko edukien artean, eta puzteko gaitasun handienak goiko eta beheko kontzentrazio-mugetan aurkitu ziren. Edonola ere, hiru azalera horietan ez zen aldagai nagusi argirik ikusi, gai koadratikoek ez baitzuten hain esangura-maila handirik.

Sintesi-ibilbide bakoitzerako balio optimoak 4.4 Taulan ageri dira. Argi ikusi zen lignina gehitzeak, kasu guztietan, ur-xurgatzean efektu positiboa izan zuela. Fenomeno hau, hidrogel zurien sintesi eta karakterizazioari esker baieztatu zen, hau da, %5, 8 eta 11ko PVA kontzentrazioak dituzten PVA puruko hidrogelak aurretik aipatutako sintesi-bide berdinak jarraituz. Material horien ur-xurgapena ez zen %350etik gorakoa izan. Beraz, lignina-hidrogelen ur-xurgatze gaitasun handiak lignina-molekulen tamainari egotz dakioke, pisu molekular handiko kateak baitira eta poro handiagoak sor baitaitezke, ur-molekulak errazago sartzea eta mugitzea ahalbidetuz [102,103]. Ciolacu *et al.* (2018)-ek kimikoki gurutzatutako PVA-lignina hidrogelek ere jokabide bera izan zutela jakinarazi zuten [102]. Yang *et al.* (2018)-ek ere baieztatu zuten ligninak kitosano eta PVA-zko hidrogelen ur-xurgapen ahalmena hobetzen zuela [68].

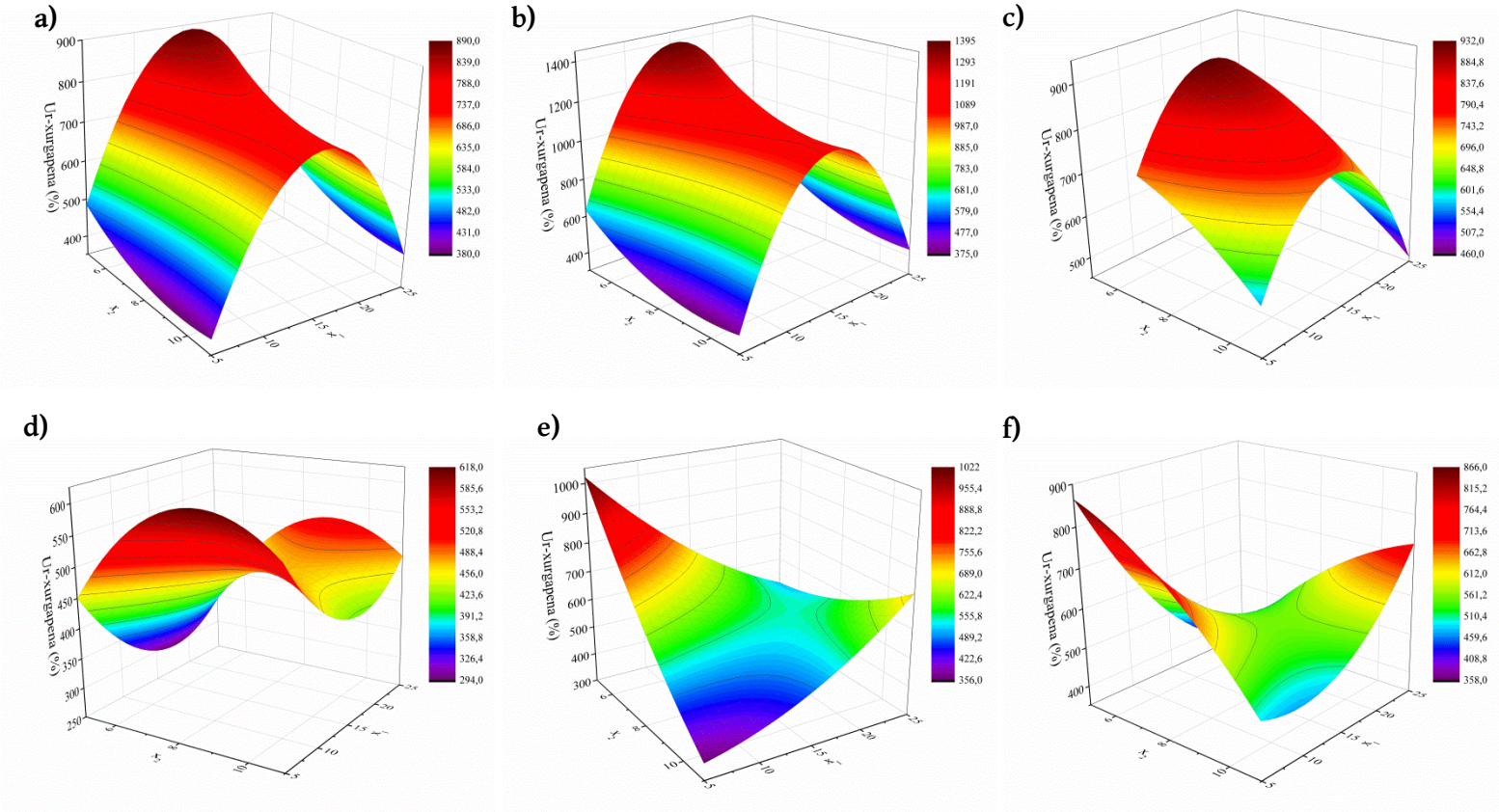

4.9 Irudia. 1 – 6 sintesi ibilbideetako hidrogelen ur-xurgapenerako lorturiko erantzun-gainazalak (a – f, hurrenez hurren).

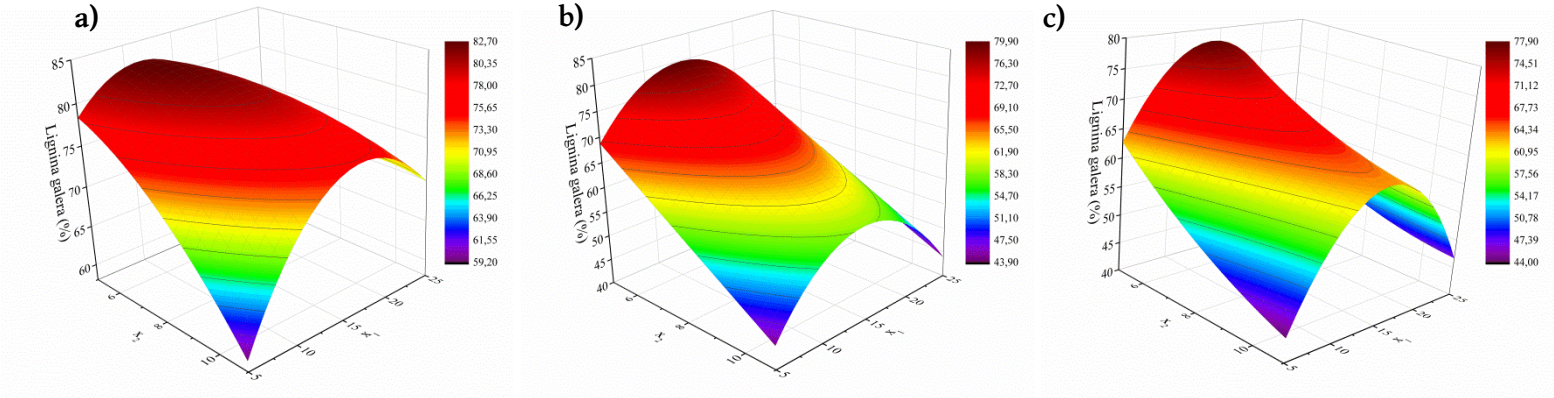

4.10 Irudia. a) 1eta 2, b) 3 eta 4, c) 5 eta 6 sintesi ibilbideetako hidrogelen lignina-galeretarako lorturiko erantzun-gainazalak.

4.2.3 Aldagai askeek lignina-galerarekiko duten eragina

Sei ibilbideetatik sintetizatutako hidrogelen lignina-galera %44,5 eta %85 artekoa zen, (5) eta (6) ibilbideetako 3. Esperimentuari eta (1) eta (2) ibilbideetako 5. esperimentuari zegokiena, hurrenez hurren. Ikusi zenez, hutseko gurutzaketarekin alderatuz, izozte-desizozteko metodoari esker, lignina gehiago atxiki ahal izan zen matrizearen barruan.

(1) eta (2) ibilbideetan, lignina-galeran eragin handiena izan zuten erregresio-koefizienteak x_1-ren efektu koadratikoa (x_1^2) eta bi sarrera-aldagaien arteko x_1x_2 interakzioa izan ziren. Beste lau sintesi-bideetan, erregresio-koefiziente esanguratsuenak x_1-ren efektu koadratikoa (x_1^2) eta x_2 bera izan ziren. Beraz, ondoriozta daiteke PVA-ren edukiak eragin zuzena duela lignina-galerarengan. Dakigunez, bibliografian ez da garbiketa-etapako lignina-galerari buruzko daturik jaso hidrogelak karakterizatzeko garaian. Beraz, baieztapen hori ezin da beste lanekin alderatu.

Sintesi-ibilbide guztietako gainazal-grafikoek (4.10 Irudia), PVA-ren kontzentrazio finko baterako, lignina-edukia handitu ahala lignina-galerak gora egiteko joera zutela erakutsi zuten. Portaera hori gune erreaktiboak gehitzearekin eta bi osagaien arteko gurutzaketa-maila handiagoarekin lotuta egon liteke. Lignina kontzentrazio jakin batetik aurrera, ordea, lignina-galera gutxitu egin zen. Sei ibilbideetarako, gutxieneko lignina-galerarako kontzentrazio optimoak 4.4 Taulan adierazten dira.

4.2.4 Sintesirako baldintzen optimizatzea eta ereduaren baliozkotzea

Optimizazioaren helburua sintesi-ibilbide bakoitzerako aldi berean ur-xurgatze gaitasun handiena eta lignina-galera baxuena emango luketen formulazioak zehaztea izan zen. Horretarako, erantzun-aldagaien balioak desiragarritasun-funtzio baten bidez bihurtu ziren. Funtzio honek, ur-xurgatze ahalmena maximizatu eta aldi berean lignina-galera minimizatzen zituzten sintesi-aldagaien konbinazioa baimendu zuen. Baldintza optimoekin sintetizaturiko hidrogelen erantzun-aldagaietarako aurreikusitako emaitzak

eta emaitza esperimentalak 4.4 Taulan azaltzen dira. RSM ereduek iragarpen kuantitatiboetarako zuten egokitasuna sei sintesi-ibilbideetako aurreikusitako balioak eta balio esperimentalak bat etortzearekin egiaztatu zen. Ur-xurgatze gaitasun aldagaiaren erroreak %4tik gorakoak izan ziren kasu guztietan, (3) eta (4) ibilbideetan izan ezik. Bestalde, lignina-galeraren errore txikienak (5) eta (6) ibilbideetan ikusi ziren. Hala ere, ur-xurgapen gaitasunaren zehaztasuna lignina-galerarena baino garrantzitsuagotzat jo zenez, eta optimizazioaren helburuetako bat sintesi-ibilbiderik onena lortzea zenez, (3) eta (4) ibilbideak hautatu ziren bide optimo gisa.

4.2.5 Ondorioak

Atal honetan, ligninan oinarrituriko PVA-zko hidrogelen sintesi-baldintzak arrakastaz optimizatu ziren, hiru maila eta bi faktoreko diseinua erabiliz. Analisi estatistikoak PVA eta lignina kontzentrazioek hidrogelen garbiketa-etapako lignina-galeran eta hauen ur-xurgatze ahalmenean eragin handia zutela frogatu zuen. Hautatutako sintesi-ibilbide optimoak 5 izozte-desizozte ziklotan oinarritutakoak izan ziren eta hauek fisikoki gurutzatutako hidrogelak lortzea ahalbidetu zuten, %800era arteko ur-xurgapen gaitasuna eta %40-50 arteko lignina-galera erakutsi zutenak.

4.3 Formulazio parametro desberdinek hidrogelen propietateengan duten eragina

Atal honetan, zenbait formulazio-parametrok sintetizaturiko hidrogelen propietateengan duten eragina aztertu da. Horretarako, hainbat artikulutan lortutako emaitzak konbinatu dira. Aztertutako parametroak eta atal bakoitzean eztabaidatutako argitalpenak ondorengo taulan laburtzen dira:

4.6 Taula. Aztertutako parametroen eta eztabaida-atal bakoitzean inplikatutako argitalpenen laburpena.

Parametroa	Artikulua			
	II	III	IV	V
Lehortze mota	✓			
PVA-ren M_w/Izozte-desizozte ziklo kopurua		✓		
Lignina mota		✓	✓	
Izozte-desizozte zikloen iraupena	✓	✓	✓	
Ligninaren eraldaketa mota			✓	✓

4.3.1 Lehortze mota

II. Artikuluan ibilbide optimoetatik (4.2 Atala) lortutako laginak (hots, 3 eta 4 laginak) sakonki karakterizatu ziren, PVA soilezko euren lagin bikiekin batera (3.0 eta 4.0 laginak, hurrenez hurren), lehortze motak izandako eragina ikertzeko asmoz.

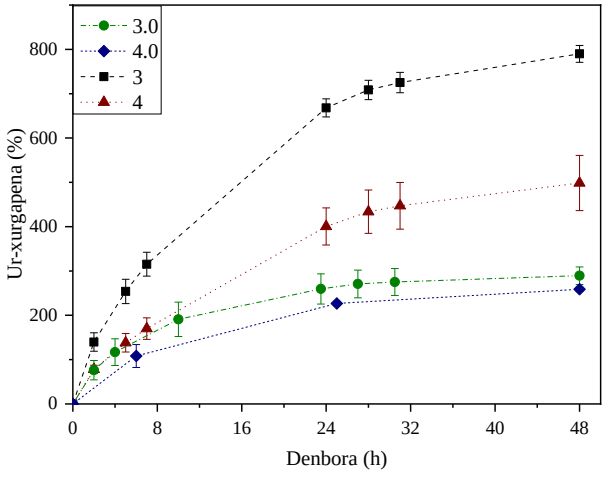

4.11 Irudia. Hidrogelen ur-xurgapena lehen 48 orduetan.

Lau lagin hauen ur-xurgatze zinetika 4.11 Irudian ikus daiteke. Gainontzeko laginekin alderatuz, 3. Ibilbidea jarraituz lortutako hidrogelak ur-xurgatze gaitasun nabarmen handiagoa izan zuela ikusi zen. Izan ere, 4. Ibilbidea jarraituz lortutako laginak 3 izeneko laginaren xurgatze gaitasunaren ia erdia erakutsi zuen.

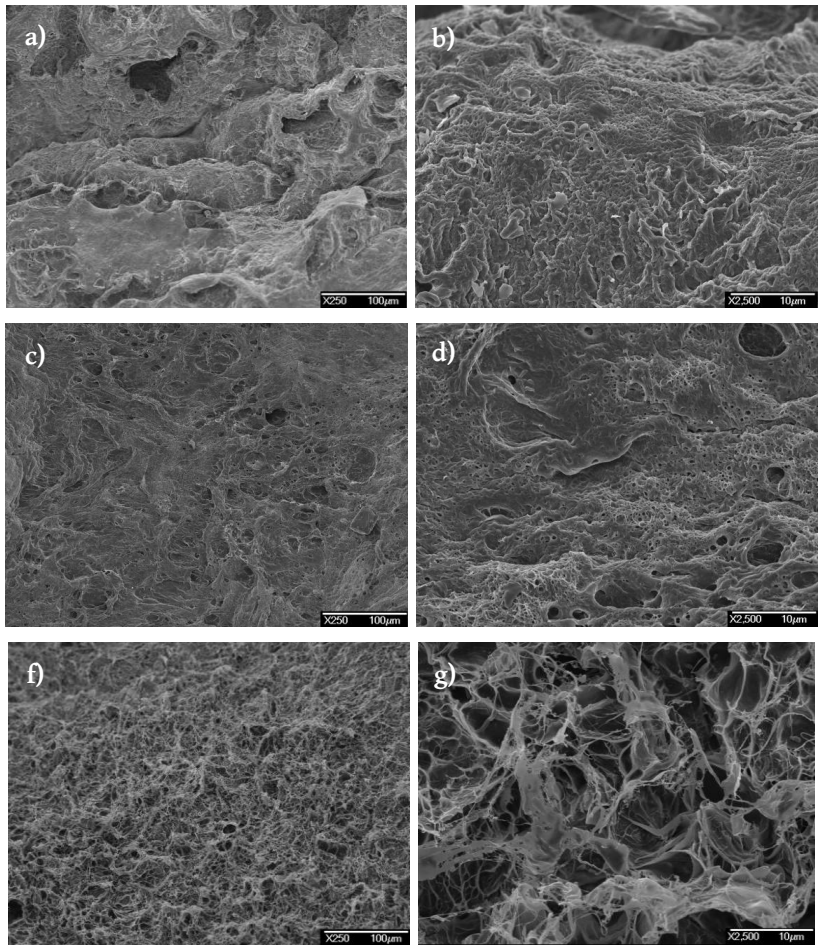

4.12 Irudia. 3.0, 4.0 eta 4 laginen SEM mikrografiak 250x (a, c eta e) eta 2500x (b, d eta f) handipenetara.

4.12 Irudian, PVA puruzko eta PVA eta ligninazko hidrogel liofilizatuen SEM mikrografiak erakusten dira, bi handipenetan (250x eta 2500x). Aztertutako lagin guztietan poro handiko egiturak eta poroen tamainaren banaketa desberdinak ikusi ziren. Hala ere, PVA hutseko hidrogelentzat (4.12- a-d

Irudiak) lignina-hidrogelarentzat baino (4.12- e eta f Irudiak) morfologia homogeneoagoa ikusi zen. Gainera, poro handi samar batzuk ere agertu ziren hutsean lehorturiko lignina gabeko laginean (4.0 lagina, 4.12-c eta d Irudiak), eta horrek gurutzaketa-metodoaz gain, lehortze-metodoak morfologiari ere eragin ziola adierazten du [104]. Makroporoek sare polimerikoan ura erraz sartzeko aukera ematen duten arren, hasieran azkar puzteko ahalmena eraginez [103], hemen ez zen hori gertatu; izan ere, lignina-hidrogelek ura puzteko gaitasun handiagoa izan zuten kasu guztietan. Gainera, PVA soilezko hidrogelek aurkeztutako poro gehienak 1 μm-tik beherakoak ziren, eta lignina-hidrogelek aurkeztutakoak, berriz, handiagoak. Gertaera horrek ligninaren pisu molekular handiagatik sortutako poroen tamaina eta honek ur-xurgatze ahalmenean duen eraginari buruzko aurreko baieztapena berretsiko luke [102]. Horrez gain, SEM irudietan ez zen lignina aglomeraturik topatu, eta horrek osagaien arteko nahaskortasun ona berretsi zuen [105].

Laginen TG eta DTG kurbetatik lortutako hasierako eta degradazioko handieneko tenperaturak eta proba-amaierako hondakina 4.7 Taulan laburbiltzen dira. PVA hutseko hidrogelentzako (3.0 eta 4.0), lau pisu-galera etapa ikusi ziren: 150, 250, 375 eta 440 ºC inguruan, barneko uraren lurruntzeari, polimeroaren hasierako degradazioari, polimeroaren unitate azetilatuen eta desazetilatuen despolimerizazioari eta PVA-ren azpiproduktu batzuen degradazio termikoari zegozkienak, hurrenez hurren [68], 375 ºC-koa gehieneko degradazioari zegokiona izanik. Lignina alkalino komertzialak pisu galera konstantea izan zuen; hala ere, degradazio maximoaren tenperatura 380 ºC-an erregistratu zen, eta azken hondakina ia %40an geratu zen. Hidrogelei lignina gehitzean, laginek hiru pisu-galera etapa nagusi izan zituzten (120, 280 eta 430 ºC-tan), baina bigarrenean bi etapa gainjarri zirela ondorioztatu zen. Degradazio-etapa nagusia 330 ºC inguruan agertu zen, baina 280 ºC-koarekin gainjarri zen. Galera hori, PVA puruarenarekin alderatuta, tenperatura altuagoetara mugitu zen, egonkortasun termikoa hobetu baitzen, PVA kateetan ligninaren egitura aromatikoak sartzearen ondorioz [106]. PVA

puruaren hidrogeletarako gehieneko degradazio-tenperaturan aldaketa nabarmenik egon ez zen arren, lignina-hidrogelen kasuan 15 ºC inguruko aldaketa egon zen lehortze-metodoa aldatzean.

4.7 Taula. Laginen hasierako eta degradazioko handieneko tenperaturak, TGA-ren amaierako hondakina eta konpresio modulua.

Lagina	T_{onset} (ºC)	T_{max} (ºC)	Hondakina (%)	Konpresio-modulua (MPa)
CAL	172,0	380,0	39,0	-
3.0	225,0	372,5	2,7	77,57 ± 8,40
4.0	230,5	374,0	2,6	41,64 ± 3,42
3	217,0	323,0	19,5	18,75 ± 0,53
4	223,0	334,5	14,7	29,21 ± 6,18

Laginen konpresio-saiakuntzen emaitzak 4.7 Taulan adierazten dira. Deformazio maximoa jasan ondoren, lagin guztiek osotasuna eta forma berreskuratzeko gaitasun bikaina erakutsi zuten. Horren arrazoia kate polimerikoen berrantolaketak eragindako tentsioaren egokitzapena eta honen ondorioz garatutako indar elastiko erretraktilak izan litezke [107].

3.0 eta 4.0 hidrogel zurietarako zenbatetsitako konpresio-moduluak 77,6 eta 41,7 MPa ingurukoak izan ziren, hurrenez hurren. Laginei lignina gehitu zitzaienean, moduluak 18,8 eta 29,2 MPa ingurura jaitsi ziren 3 eta 4 laginetarako, hurrenez hurren. Beraz, lignina gehitzean, hidrogelen moduluak murriztu egin ziren, eta horrek laginen poroen tamainarekin zerikusia izan lezake, xurgatze-ahalmenerako ondorioztatutakoa berretsiz; hau da, lignina eta PVA nahastean, poro handiagoak sortu ziren, PVA-ren barruko interakzioak gutxitzearen ondorioz, zeinak, aldi berean, uraren xurgapena areagotu zuen, hidrogelaren trinkotasuna eta zurruntasuna murriztuz [68]. Gainera, lehen aipatu bezala, lehortze-metodoak laginen morfologia aldatu zuen eta, ondorioz, konpresio-moduluak aldatu ziren. Hala ere, PVA-lignina laginetarako lortutako moduluak lurzoru-geruzen pisua jasateko bezain altuak izango lirateke, nekazaritzan aplikatu nahi balira, adibidez.

II. Artikuluan adierazten den bezala, gainontzeko karakterizazio teknikek (FTIR, XRD eta DSC), ez zuten informazio garrantzitsu gehiago lortzeko balio izan.

4.3.2 PVA-ren pisu molekularra eta izozte/desizozte zikloen kopurua

PVA-ren pisu molekularrak hidrogel sintetizatuen propietateetan duen eragina aztertzeko, lignina alkalino komertziala eta 3 polibinil alkohol desberdin nahastu ziren (PVA, M_w = 13000-23000 g/mol, %87-89 hidrolizatua; M_w = 83000-124000 g/mol, +%99 hidrolizatua eta M_w = 130000 g/mol, +%99 hidrolizatua). Hidrogelak **II. Artikuluan** aztertutako bide optimoaren (3. ibilbidea) eta 5. ibilbidearen arabera sintetizatu ziren.

Hautatutako erreaktiboen kontzentrazioei esker, pisu molekular ertaineko (MM_w PVA) eta altuko (HM_w PVA) PVA eta lignina alkalinoaren arteko gurutzaketa era arrakastatsuan egin ahal izan zen, 3 eta 5 izozte-desizozte zikloren bidez. Pisu molekular txikiko PVA (LM_w PVA) zuten laginak, ordea, ez ziren gurutzaketa egokirik eragiteko gai izan. Baliteke pisu molekular horretako PVA-k lignina kantitate horrentzako gune erreaktibo gutxiegi izatea [56] edo, baita PVA-ren hidrolisi-mailarengatik ere. Azken hau PVA-ren molekulako azetato taldeen kopuruarekin lotuta dago, PVA aurrepolimerizatuko polibinilo azetatoaren hidrolisitik abiatuz sintetizatzen baita [68,108]. Horrek hidrolisi maila altuko PVA-n azetato talde gutxiago egongo direla esan nahi du, talde horiek eragina izan baitezakete PVA-ren propietate kimikoetan, disolbagarritasunean eta kristalizatzeko gaitasunean [108]. Gainera, azetato taldeen presentziak hurbileko hidroxilo taldeen arteko molekulen barneko nahiz arteko hidrogeno-loturak ahultzen ditu. Soluzioan, hidrolisi-maila handitu ahala, PVA-kateen arteko banaketa-distantzia murriztu egiten da [108]. Beraz, gurutzaketa ez arrakastatsua LM_w PVA-k (%87-89) MM_w eta HM_w PVA-rekin alderatuta (+%99) zuen hidrolisi maila txikiagoari egotz dakioke. Hori kontuan izanik, LM_w PVA-zko laginak baztertuak izan ziren ondorengo azterketetarako. 4.13 Irudian, hidrogelaren matrizearen barne-interakzioen eskema posible bat proposatzen da.

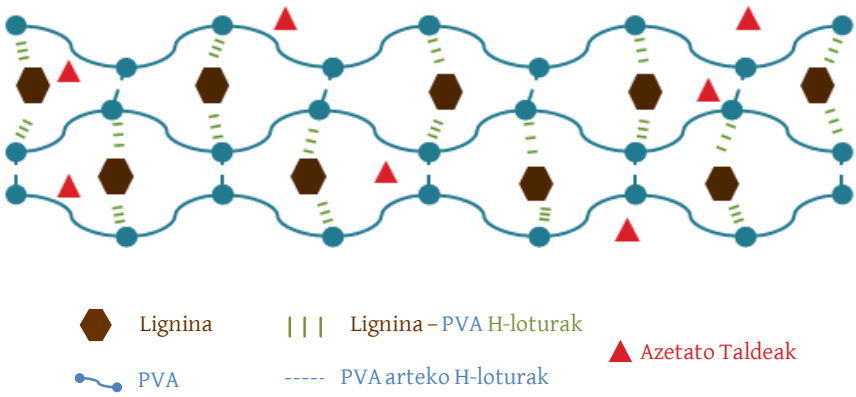

4.13 Irudia. PVA eta ligninaren arteko gurutzaketa posiblearen eskema.

HM_w PVA zuten laginen lignina galera (%69,5 eta %49,5, 3HL eta 5HL laginetarako, hurrenez hurren), MM_w PVA zuten laginena baino txikiagoa izan zen (%77,8 eta %57, 3ML eta 5ML laginetarako, hurrenez hurren). Hau PVA-ren gune erreaktiboen kopuruarekin lotuta egon liteke, hau da, posible litzateke polimero-kate luzeenek ligninarekin lotura handiagoa izatea. Hennink *et al.* (2012)-ek PVA-ren pisu molekularrak sortutako *gel*aren propietateengan eragiten duela aipatu zuten [109]. Gainera, ziklo kopuruak lignina galerari ere eragin zion; izan ere, 3 izozketa-desizozte zikloren bidez sortutako hidrogelek 5 zikloren ondoren sortutakoek baino lignina galera handiagoa izan zuten. Horrek zikloen kopurua handitzerakoan elementuen arteko loturak areagotu egin zirela esan nahiko luke [46,109].

4.14 Irudian ikus daitekeen bezala, 5 izozte-desizozte zikloren bidez lortutako hidrogeletan (%890 eta %790 HM_w eta MM_w PVA laginetarako, hurrenez hurren) 3 zikloren bidez sintetizatutakoetan baino (%380 eta %360 HM_w eta MM_w PVA laginetarako, hurrenez hurren) ur-xurgatze ahalmen nabarmen handiagoa izan zen. Gainera, pisu molekular handieneko PVA zuten hidrogelen kasuan, puzteko ahalmena ere handiena izan zen (≈ %900). Horrek erabilitako PVA-ren pisu molekularra eta ziklo kopurua bezalako parametroen eraginari buruzko aurreko baieztapena indartuko luke [109]. Ziklo kopurua eta PVA-ren pisu molekularra handitu ahala, ligninarekiko interakzioak gehitu eta poro gehiago eta handiagoak sortzea ahalbidetuko luke, eta, beraz, baita ura

xurgatzeko ahalmen handiagoa ere. Wu *et al.* (2019)-ek aipatu zuten lignina kopuru optimo batek PVA-zko sarea erlaxatuago mantenduko lukeela, eta horrek ur-xurgapen handiagoa eragingo lukeela [56]. Era berean, esan beharra dago PVA puruzko hidrogelek ur-xurgatze ahalmen oso txikia zutela (%200-300ekoa), eta ligninak poroen tamaina handitzen duenez, ura sarearen barruan mantentzea ahalbidetzen duela baieztatuko luke [56,102,103].

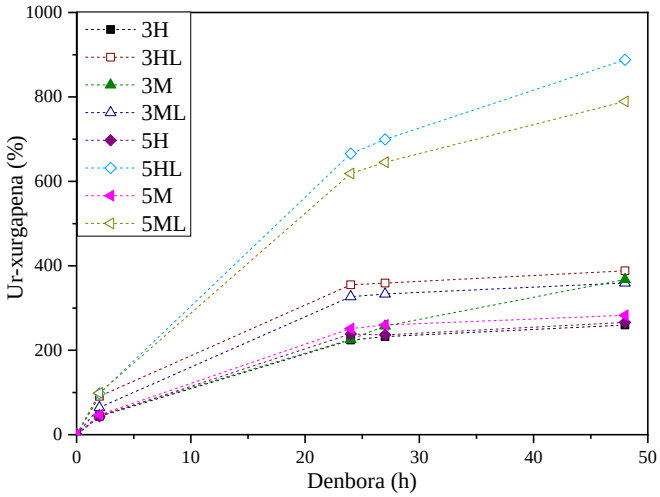

4.14 Irudia. M_w desberdineko PVA-zko hidrogelen ur-xurgapena lehen 48 orduetan.

4.15 Irudian, SEM teknikaren bidez lortutako irudiak aurkezten dira, 2500x handipenarekin. Hidrogelen mikroegiturek hiru dimentsiotan elkarri konektatutako sare porotsuak erakutsi zituzten. Izozte- eta desizozte-prozesua da egitura porotsu horien arduradun nagusia; izan ere, desizozte-etapan, izoztean hidrogelen barruan sortutako izotz-kristalak urtu egiten dira, laginetan egitura porotsua eta gurutzaketa-maila altua utziz [110]. PVA puruzko laginek egitura porotsu homogeneoagoa erakutsi zuten, polimeroaren pisu molekularra handiagoa eta ziklo kopurua txikiagoa zen heinean poroak handiagoak izanik. Lignina gehitzean, poroen tamainaren banaketa heterogeneoagoa izan zen, eta makroporo asko sortu ziren, ligninak nukleazio-eragile [68] edota bereizgailu gisa funtzionatzen duela uste baita [111].

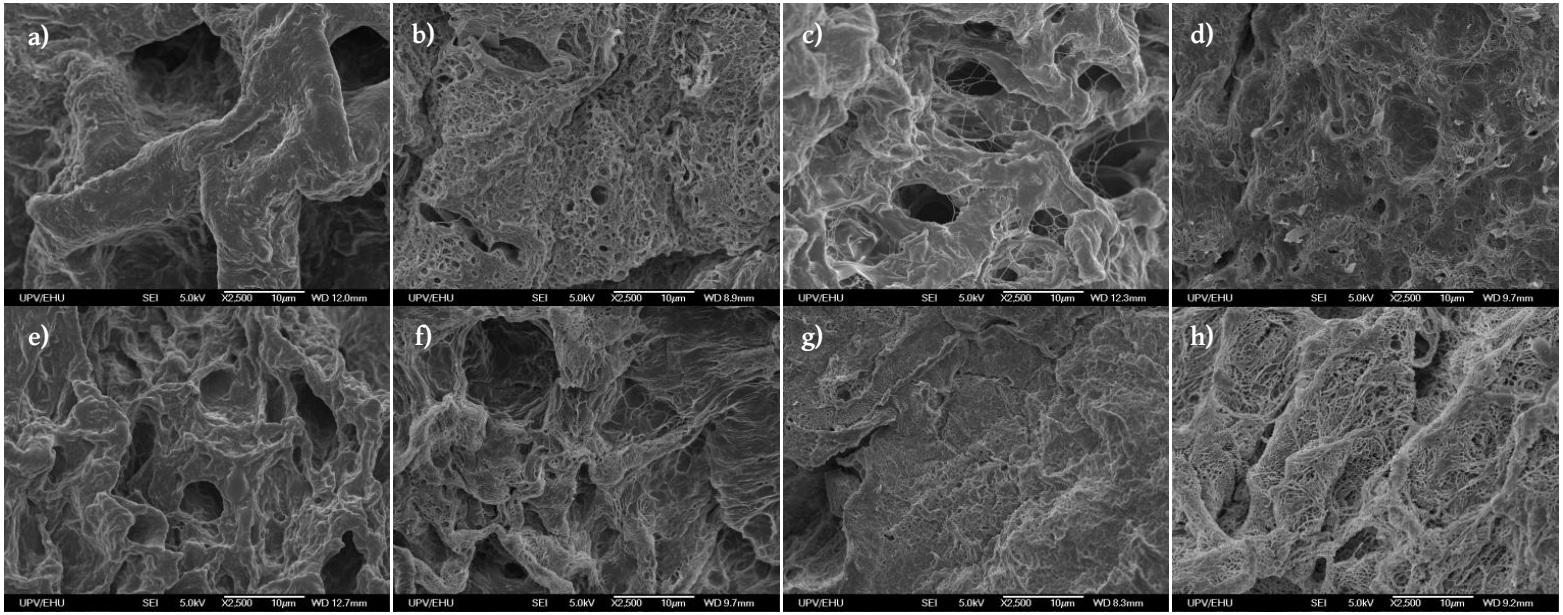

4.15 Irudia. 3H, 3HL, 3M, 3ML, 5H, 5HL, 5M and 5ML (a–h) laginen SEM irudiak 2500x handipenarekin.

Bereizgailu gisa txertatutako ligninaren portaerak mikrohutsen artean horma finagoak sortu izana azal lezake. Horiek hidrogelen ura atxikitzeko ahalmenari nabarmen lagundu zioten honekin kontaktuan zegoen azalera handiagoa izanik eta, ondorioz, honen difusioari ere lagunduz [103,111].

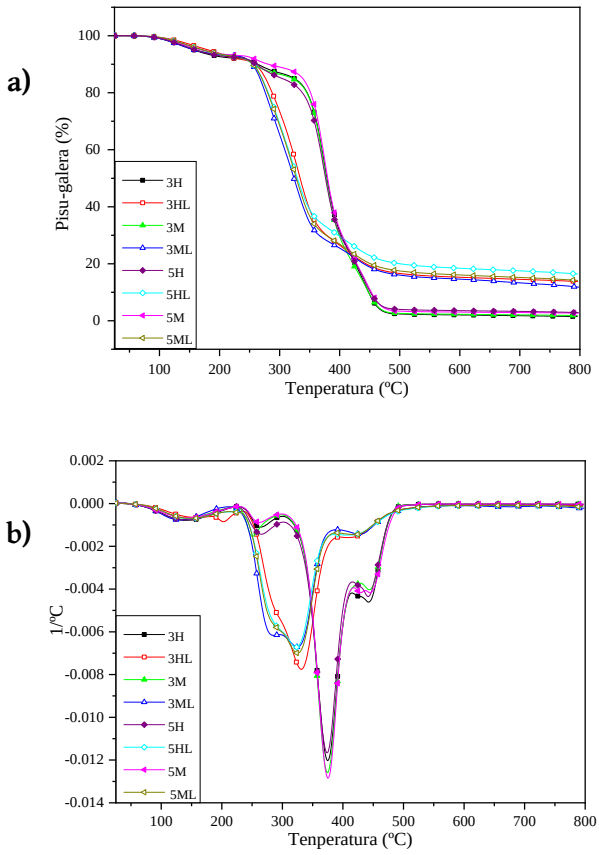

4.16 Irudia. M_w desberdineko PVA-zko hidrogelen a) TG and b) DTG kurbak.

II. Artikuluan gertatu bezala, TG eta DTG emaitzek antzeko degradazio-profilak erakutsi zituzten PVA puruaren laginetarako (4.16 Irudia). Aurreko kasuan bezala, pisu-galerako lau etapa nagusi ikusi ziren 150, 250, 375 eta 440 °C-tan, eta %3tik beherako hondakina ikusi zen lagin guztietan. Lignina gehitu zenean ere, lau degradazio-etapa nagusi ikusi ziren. Lehenengoa, 150 ° C ingurukoa, hezetasunaren lurruntzeari egotzi zitzaion, eta, PVA puruaren hidrogelen kasuan bezala, ez zen inolako aldaketarik ikusi matrize

polimerikoaren pisu molekularra aldatzean. Bigarrena 280 °C ingurukoa izan zen MM_w PVA zuten laginentzat, eta 290 °C ingurukoa HM_w PVA zutenentzat, eta hori PVA puruzko laginena baino handiagoa izan zen, ligninaren egonkortasun termikoa dela eta, ziurrenik [112]. Hirugarren urratsa, degradazio-urrats nagusia, 330 °C-ra aurkitu zen, eta laugarrena 425 °C-ra; horietan ez zen aldaketa argirik antzeman PVA-ren pisu molekularra aldatzean. Hala ere, lignina gehitzean, amaieran utzitako hondakina nabarmen handitu zen, eta pisu molekular handieneko eta ziklo kopuru handieneko lagina izan zen (5HL) hondakin handiena utzi zuena (%17) eta pisu molekular txikiena eta ziklo gutxien (3ML) izan zituena hondakin txikiena utzi zuena (%12,5). Beraz, lignina gehitzeak eta erabilitako polimero matrizearen ziklo kopurua eta pisu molekularra handitzeak azken hondakin handiagoa eragin zuten.

4.8 Taula. M_w desberdineko PVA-zko hidrogelen konpresio-saiakuntzetako emaitzak.

Lagina	Konpresio-modulua (MPa)
3M	18,13 ± 4,23
3ML	8,77 ± 2,27
3H	28,13 ± 4,4
5M	19,85 ± 2,53
5ML	9,64 ± 4,56
5H	22,06 ± 3,29
5HL	10,32 ± 3,05

Laginen konpresio-saiakuntzek lagin guztiek berreskuratzeko gaitasun ona zutela erakutsi zuten, horietako bat ere ez baitzen hautsi eta osotasun osoa mantendu baitzuten. Kalkulatutako datuak 4.8 Taulan agertzen dira. Ligninarik gabeko laginetarako, konpresio-moduluak 18 eta 28 MPa artekoak izan ziren, eta horietatik baliorik txikienak MM_w PVA (18,13 eta 19,85 MPa 3 eta 5 ziklotako laginentzako, hurrenez hurren) eta HM_w PVA (28,13 eta 22,06 MPa 3 eta 5 ziklotarako, hurrenez hurren). 3 eta 5 ziklo artean, HM_w PVA-zko hidrogelen moduluak jaitsi zirela ikusi zen, baina MM_w PVA-ren kasuan kontrako portaera ikusi zen.

4.3.1 Atalean aipatu bezala, lignina gehitzean, moduluek nabarmen egin zuten behera kasu guztietan (> %50), eta horrek lotura zuzena izan zuen ura

xurgatzeko gaitasun handiarekin. Gainera, moduluen gorakada txiki bat ikusi zen zikloen kopurua handitu zenean, eta hori bat dator MM_w PVA hutseko hidrogeletarako ikusitako joerarekin. Beste autore batzuek ere antzeko portaerak erregistratu dituzte [56,113].

4.3.3 Lignina mota

Atal honetan **III.** eta **IV. Artikuluetan** sintetizatutako hidrogelak hartu dira kontuan. **IV. Artikuluko** hidrogelak erauzitako ligninen bidez sintetizatu ziren, eta horiek AS eta WNS-tik isolatu ziren, 3.3.1 Atalean deskribatzen den bezala. Ondoren, lignina hidrogelak **III. Artikuluaren** arabera sintetizatu ziren, nahasketen kontzentrazioak eta izozte-desizozte zikloen iraupen bera mantenduz.

4.9 Taula. Fruitu lehorren azaletatik eratorritako ligninadun hidrogelen lignina galera.

Lagina	Lignina galera (%)
AA	66,5 ± 2,9
AO	56,2 ± 2,4
WA	68,5 ± 0,7
WO	60,0 ± 1,8
AAA	59,6 ± 2,8
AAO	71,1 ± 3,0
AWA	44,2 ± 1,6
AWO	59,9 ± 4,0

Lignina-galeraren emaitzak 4.9 Taulan ageri dira. Lignina alkalinoz egindako laginen kasuan, urrats bakarreko prozesuetatik eratorritako ligninak (AA eta WA) zituztenek lignina-galera handiagoak izan zituzten bi urratseko prozesuetatik zetozenak (AAA eta AWA) zituztenek baino. Antzeko joera hauteman zen WNS-tik zetozen organosolv ligninen (WO eta AWO) kasuan; aldiz, AS-tik zetozen (AO eta AAO) ligninadun laginen portaera kontrakoa izan zen. Gainera, urrats bakarreko ligninen kasuan, AS ligninetarako WNS-etakoetarako baino galera txikiagoak ikusi ziren (%56,2-66,5 vs. %60,0-68,5), eta urrats bikoitzeko ligninen kasuan, berriz, kontrakoa (%44,2-59,9 vs. %59,6-71,1). Era berean, azpimarratu behar da urrats bakarreko prozesuko ligninak

zituzten laginen artean lignina alkalinoa zutenek organosolv lignina zutenek baino galera handiagoa izan zutela; aldiz, urrats bikoitzeko ligninak zituzten laginek alderantzizko joera erakutsi zuten.

Sintetizatutako hidrogelen ur-xurgatze ahalmena 4.17 Irudian azaltzen da. Laginek %336 eta %505 arteko puzte-balioak izan zituzten, eta AWO eta WA laginei zegozkien, hurrenez hurren. Gainera, lignina alkalinoa zuten laginek ura xurgatzeko gaitasun handiagoa erakutsi zuten kasu guztietan, aurretik emandako datuekin bat etorriz [79].

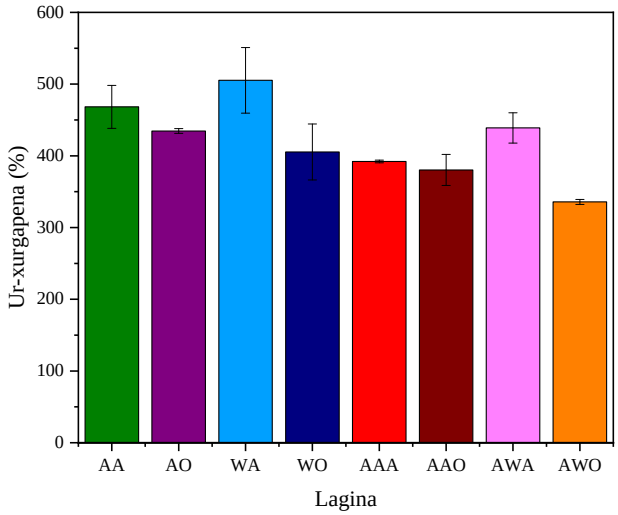

4.17 Irudia. Fruitu lehorren azaletatik eratorritako ligninadun hidrogelen ur-xurgatze gaitasuna.

Aipatzekoa da urrats bakarreko prozesuetatik zetozen ligninak zituzten laginek urrats bikoitzeko prozesuetatik zetozenak zituztenek baino ura xurgatzeko gaitasun handiagoa erakutsi zutela, ziurrenik haien ezpurutasun eta matrize polimerikoaren artean sortutako interakzioengatik. Wu *et al.* (2019)-ek ur-xurgatze propietateak talde hidroxilo fenolikoen edukiarekin eta erabilitako ligninen pisu molekularrarekin lotu zituzten arren, haien hipotesiak ez luke hidrogelek kasu honetan izandako portaera azalduko [56]. Izan ere, eduki fenoliko total txikiagoa eta batez besteko pisu molekular txikiagoa zuten ligninadun (AA eta WA) laginek ur-xurgatze gaitasun

handiagoa erakutsi zuten. Hala ere, horrek lignina horietarako zehaztutako batez besteko pisu molekularrei buruzko aurreko baieztapena berretsi lezake, baita ezpurutasunen interakzioei buruzkoa ere, lagin horiek lignina-galera handiak izan baitzituzten.

4.18 Irudian hidrogel sintetizatuen morfologia ikus daiteke, SEM bidez aztertua. Lehen begiratuan, lagin guztiek egitura porotsuak zituzten arren, banaketa, tamaina eta dentsitatea desberdinak zirela ikusi zen. Izan ere, urrats bakarreko prozesuetatik eratorritako ligninak zituzten hidrogelei zegozkien lagin guztiak nahiko antzekoak izan ziren, eta abaraska itxurako egitura oso porotsua zuten, ligninadun PVA hidrogeletarako espero zen bezala [79,114–116]. Poroen tamaina eta banaketek nahiko homogeneoak ziruditen, baina mikro-hutsuneen arteko hormak leunagoak eta hauskorragoak ziruditen AA eta WA laginen kasuan, AO eta WO laginetan baino, azken hauek horma lodiagoak erakutsi baitzituzten. Egitura horiek izan ziren xurgatzeko gaitasun handien arduradunak [78].

Urrats bikoitzeko prozesuetatik eratorritako ligninak erabili zirenean, hidrogelek egitura askoz trinkoagoak eta jarraituagoak erakutsi zituzten, ia antzemanezinak ziren poroekin, eta horrek lignina horiekin gurutzaketa-dentsitate altuagoa lortu izanarekin izan lezake lotura, hidroxilo fenoliko talde gehiago erakutsi baitzituzten [56]. Rachip *et al.* (2013) ere hidrogelen morfologia aldakorrei buruz mintzatu ziren, ligninaren -OH eta -COOH taldeen arabera alda zitekeena [117]. Mikroegitura horiek azalduko lukete lagin hauen ur-xurgatze ahalmenaren beherakada, aurrez aipatutakoekin alderatuta.

Konpresio-saiakuntzetako tentsio-deformazio diagrametatik abiatuta, konpresio-moduluak kalkulatu ziren, 4.10 Taulan ikus daitekeen bezala. Proben amaieran, entseatutako hidrogel gehienak osorik mantendu ziren (urrats bakarreko prozesuetako lignina alkalinoa zutenek izan ezik), eta guztiek berreskuragarritasun bikaina erakutsi zuten.

Lagina	Etapa bakarreko Alk.	Etapa bakarreko Org.	Etapa bikoitzeko Alk.	Etapa bikoitzeko Org.
AS (500x)	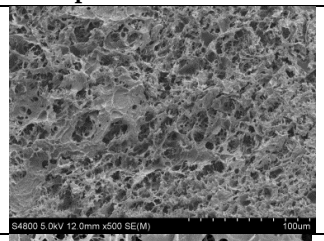	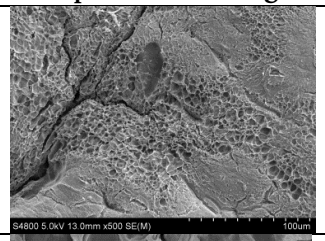	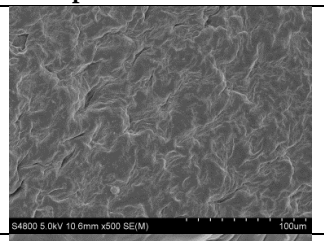	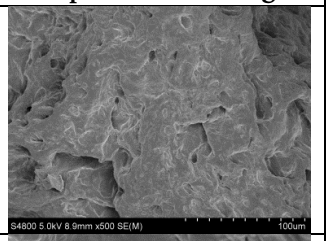
AS (5000x)	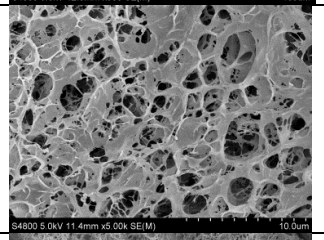	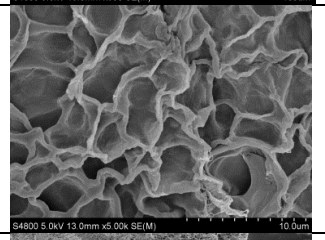	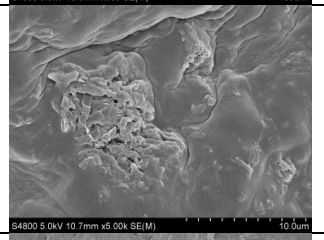	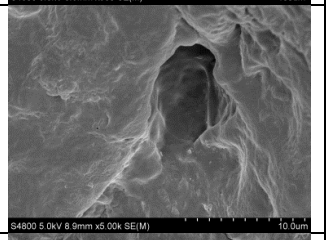
WNS (500x)	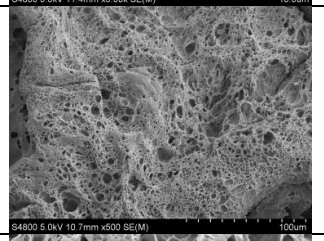	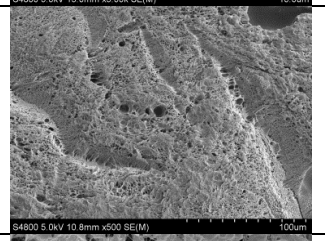	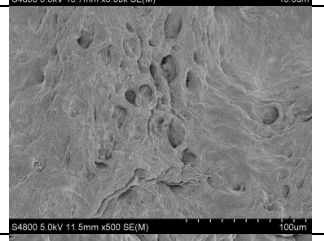	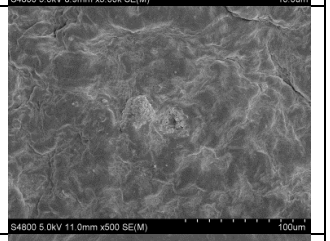
WNS (5000x)	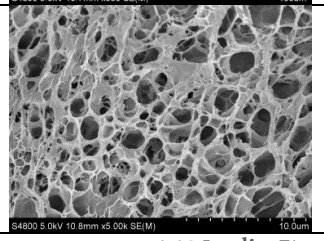	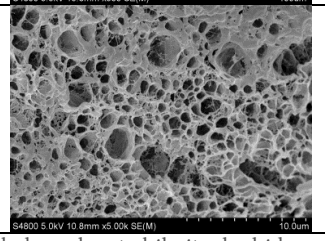	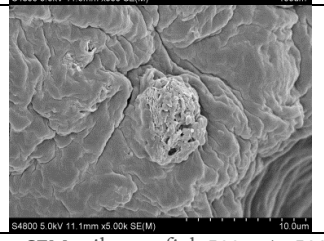	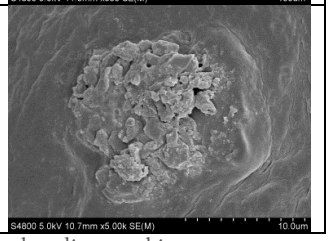

4.18 Irudia. Etapa bakarreko eta bikoitzeko hidrogelen SEM mikrografiak 500x eta 5000x handipenarekin.

Aipatutako lagin hauek (AA eta WA) izan ziren konpresio-modulu handienak aurkeztu zituztenak (14,8 eta 16,3 MPa, hurrenez hurren), baina baita ur-xurgatze gaitasun handiena izan zutenak ere, eta horrek matrizeak lignina eta haren ez-purutasunekin izandako interakzioengatik sortutako abaraska-egiturekin izan lezake lotura, SEM mikrografietan ikusi bezala. Antzeko morfologia izan arren, urrats bakarreko organosolv ligninak zituzten laginek (AO eta WO) aurrekoek baino konpresio-modulu askoz ere baxuagoak izan zituzten (4,95 eta 6,01 MPa, hurrenez hurren). Antzeko portaera izan zuten urrats bikoitzeko ligninaz osatutako laginek: lignina alkalinoa zutenek konpresio-modulu altuagoak izan zituzten (6,63-13,07 MPa) organosolv ligninak zituztenek baino (2,05-5,4 MPa). Zenbatetsitako modulu guztiak bat zetozen aurreko emaitzekin [79], eta beste autore batzuek lignina-hidrogeletarako emandakoak baino handiagoak izan ziren [113,118].

4.10 Taula. Fruitu lehorren azaletatik eratorritako ligninadun hidrogelen konpresio-moduluak.

Lagina	Konpresio-modulua (MPa)
AA	16,3 ± 1,8
AO	5,0 ± 1,9
WA	14,9 ± 1,9
WO	6,0 ± 1,0
AAA	13,1 ± 0,8
AAO	2,1 ± 1,0
AWA	6,6 ± 2,9
AWO	5,4 ± 2,8

Emaitza horiek **III. Artikulukoekin** konparatzean, alde handiak ikusi ziren, bereziki hidrogelen ur-xurgatze gaitasunean. Hala ere, sintesi-prozedura antzera egin zenez, bazirudien desberdintasun horiek ez zetozela bat espero ziren emaitzekin. Horrela, **III. Artikuluko** 5ML hidrogelak errepikatu ziren, organosolv lignina eta lignina alkalino komertzialetatik abiatuz. Emaitzak, kasu honetan, azken atal honetan aipatutakoenen antzekoagoak izan ziren. Izan ere, lignina alkalinoa zuten hidrogelek %450eko ur-xurgatze ahalmena izan zuten, eta organosolv lignina zutenek, berriz, %360koa. **III. Artikuluan** ere eman zen horren berri, eta lignina motari egotzi zitzaion. Datu horien

ondorioz, aurreko hidrogelen sintesian zerbait arbuiatu zela pentsatu zen. Jarraitutako prozedura sakon aztertzean, azken desizozte-zikloaren iraupenean aurkitu zen erantzuna: hidrogel batzuk 28 ºC-ra utzi ziren ia 24 orduz, logistika-kontuengatik. Horrela, **IV. Artikuluko** hidrogelak desizozteko azken urratsa luzatuz errepikatu ziren, eta emaitzak hurrengo atalean aurkezten dira.

4.3.4 Izozte-desizozte zikloen iraupena

III. eta **IV. Artikuluetan**, 3.4 atalean azaldu bezala, **II. Artikuluan** jasotako sintesi-prozesuko izozte- eta desizozte-zikloen iraupena murriztu zen. Murrizketa horren eragina **III. Artikuluan** antzeman zen, hidrogel horiek ur-xurgatze balio txikiagoak izan baitzituzten (%970 vs. %890-790, II. eta III. Artikuluetako laginentzat, hurrenez hurren). Hala ere, SEM mikrografietan aldaketa esanguratsurik antzeman ez zen arren, konpresio-moduluetan eragin handia ikusi zen, %50eraino jaitsi baitziren. Ur-xurgapenaren egiaztapena egin zenean, askoz ere nabarmenagoa izan zen izozte- eta desizozte-zikloen iraupenaren murrizketaren eragina.

4.11 Taula. 5. Desizozte luzedun (LC) hidrogelen lignina galera.

Lagina	Lignina galera (%)
AA	48,5 ± 3,0
AO	53,9 ± 3,4
WA	26,0 ± 6,4
WO	53,9 ± 2,1
AAA	36,3 ± 2,0
AAO	48,1 ± 3,3
AWA	74,3 ± 3,7
AWO	51,7 ± 2,2

Arestian aipatu bezala, aurreko esperimentuetan oinarrituta, desizoztearen azken etaparen iraupenak sintetizatutako hidrogelen ezaugarriak alda zitzakeela pentsatu zen. Beraz, **IV. Artikuluan** bosgarren desizozte etapa luzeagoa zuten hidrogelak prestatu ziren (24 ordu berogailuaren barruan, 28 ºC-ra). Lagin horiek LC lagin gisa etiketatu ziren (“long cycle” edo ziklo luzea),

eta, oro har, desizozte laburreko bosgarren etapa duten hidrogelak baino lignina-galera baxuagoak aurkeztu zituzten (4.11 Taula). Horrek azken zikloaren luzapenak PVA eta ligninaren arteko interakzioak areagotu zituela iradokitzen du. Gainera, urrats bakarreko WNS lignina alkalinoa (WA) zuten laginetan nabarmen murriztu zen lignina-galera. Aitzitik, urrats bikoitzeko WNS lignina alkalinoa (AWA) zuten laginek lehenago jakinarazitakoak baino askoz ere lignina-galera handiagoak izan zituzten. Era berean, AWA laginak izan ezik, lignina alkalinoa zuten hidrogel guztiek organosolv lignina zutenek baino lignina gutxiago galdu zutela esan daiteke.

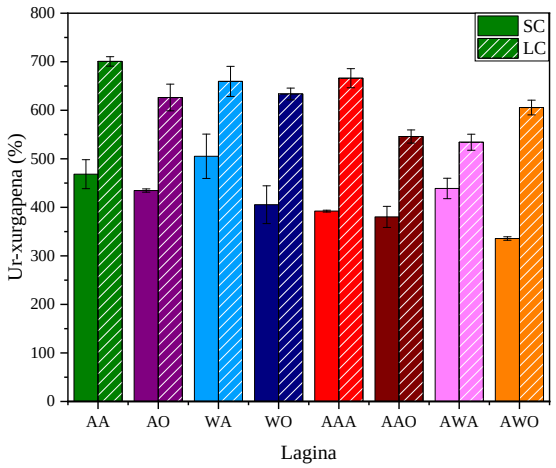

4.19 Irudia. 5. Desizozte motz (SC) eta luzedun (LC) laginen ur-xurgatze gaitasuna.

Lagin horiek (LC) desizozte laburreko (SC) azken etapa dutenekin alderatuz gero, argi eta garbi ikus daiteke ur-xurgatze ahalmena izugarri hobetu zela (4.19 Irudia). Hobekuntzarik nabarmenena (aurreko ur-xurgatze ahalmenarekin alderatuta, %80 gehiago) AWO laginean ikusi zen, lagin horrek izan baitzuen aurretik puzteko gaitasun txikiena. Aitzitik, hobekuntzarik txikiena izan zuen lagina AWA izan zen, %22 baino ez baitzen hobetu. Agudelo *et al.* (2018)-en arabera, desizozte zikloen gehiegizko luzapenak izoztean sortutako kristalen disoluzioa dakar, eta honek haien kopurua eta tamaina murrizten ditu, eta, beraz, baita gurutzaketa dentsitatea eta hidrogelaren ur-xurgatze ahalmena ere [119]. Hala ere, atal honetan desizozte luzeko urratsa

Lagina	Etapa bakarreko Alk.	Etapa bakarreko Org.	Etapa bikoitzeko Alk.	Etapa bikoitzeko Org.
AS (500x)	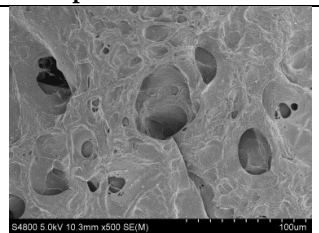	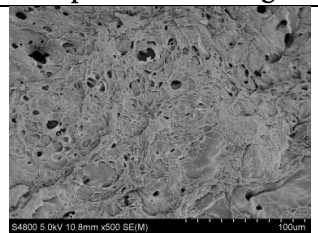	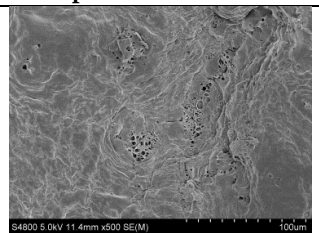	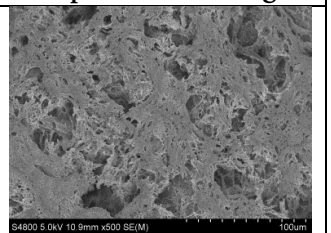
AS (5000x)	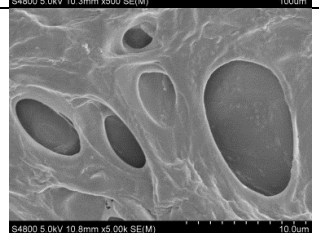	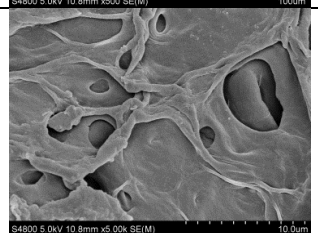	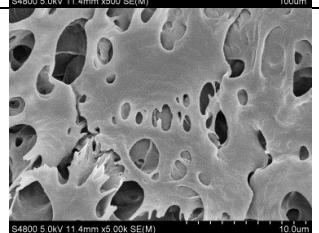	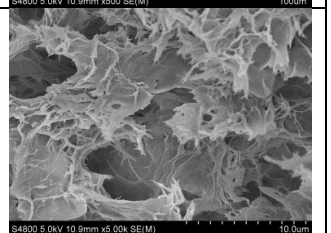
WNS (500x)	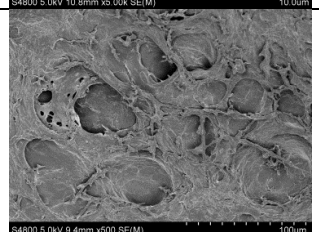	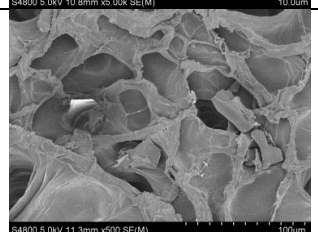	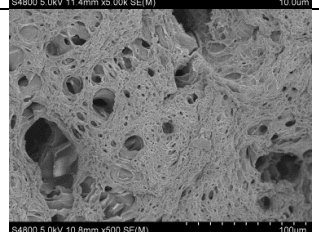	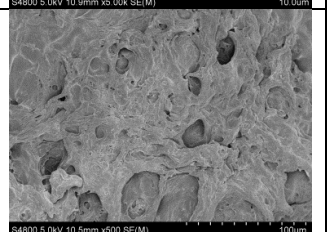
WNS (5000x)	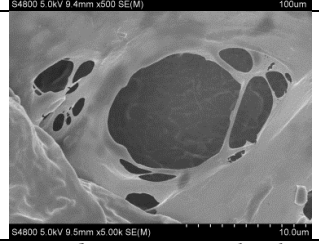	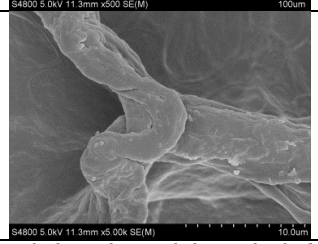	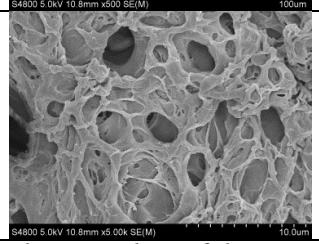	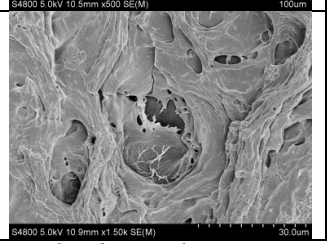

4.20 Irudia. 5. Desizozte luzeko etapa bakarreko eta bikoitzeko hidrogelen SEM mikrografiak 500x eta 5000x handipenarekin.

azkena izan zenez, litekeena da urtutako kristalak lurrundu izana eta horrek laginen ura xurgatzeko gaitasuna hobetu izana.

Emaitza horiek bat zetozen, neurri handi batean, 4.20 Irudian erakutsitako SEM irudiekin. Azken desizozte urratsa luzatzean, kasu guztietan makroporoak sortu zirela antzeman zen. Esan bezala, sintesiaren azken urratsean urtutako kristalak lurruntzeari egotzi dakioke hori, egitura horiek sortzea ahalbidetu baitzuen eta hidrogel guztien ur-xurgapen errendimendua hobetu baitzuen, haien ligninen jatorria edo erauzketa-mota edozein izanda ere.

4.12 Taula. 5. Desizozte motz (SC) eta luzedun (LC) laginen konpresio-moduluak.

Lagina	Konpresio-modulua (MPa)	
	SC	LC
AA	16,3 ± 1,8	10,8 ± 3,2
AO	5,0 ± 1,9	2,1 ± 0,7
WA	14,9 ± 1,9	13,6 ± 0,8
WO	6,0 ± 1,0	2,0 ± 0,8
AAA	13,1 ± 0,8	7,5 ± 2,7
AAO	2,1 ± 1,0	2,0 ± 0,8
AWA	6,6 ± 2,9	6,4 ± 1,3
AWO	5,4 ± 2,8	2,88 ± 1,2

4.12 Taulan ikus daitekeen bezala, lagin guztien konpresio-moduluek beherakada txiki bat izan zuten desizoztearen azken urratsaren iraupena luzatzean, ziurrenik makroporoak sortu zirelako, lehen aipatu bezala. Joera hori **IV. Artikuluan** laginen DSC analisietatik ondorioztatutako T_g balioetarako ikusitakoarekin ere bat zetorren, eta horrek lortutako egitura ez zela hain trinkoa izan iradoki zuen. Hala ere, zenbatetsitako modulu guztiak bat zetozen aurreko emaitzekin [79].

4.3.5 Lignina eraldaketa mota

V. Artikuluan eraldatutako lignina alkalino eta organosolv erauzi nahiz komertzialetatik hidrogelak sintetizatu ziren. Lignina horiek 4.1 Atalean zehaztu bezala karakterizatu ziren. Ondoren, hidrogelak egin ziren **IV.**

Artikuluan deskribatutako sintesi-bideari jarraituz, desizozte laburreko bosgarren etapa batekin.

Lignina eraldatua zuten hidrogelek aurreko laginek baino lignina-galera baxuagoa izatea espero zen, aldatutako ligninek erreaktibotasun handiagoa izatea espero zelako. Hala ere, emaitzek hipotesi hau zuzena ez zela frogatu zuten, lagin guztietarako zehaztutako lignina-galerak aurretik jakinarazitakoak baino handiagoak izan baitziren. Emaitza horiek guztiak 4.13 Taulan agertzen dira. Aldaketa hori nabarmen handiagoa izan zen MCAL eta MCOL zuten laginetan, hasierako lignina kopuruaren ia %89 eta %97 galdu baitzuten, hurrenez hurren. MAWA laginek ere gorakada handia erakutsi zuten euren lignina-galeran. Gainerako laginetan lignina-galeraren gehikuntza txikiagoa izan zen, %12 eta %14 artekoa, hain zuzen.

4.13 Taula. Jatorrizko lignina eta lignina eraldatudun hidrogelen lignina-galera.

Lagina	Jatorrizkoa (%)	Eraldatua (%)
AAA	59,6 ± 2,8	73,5 ± 0,5
AAO	71,1 ± 3,0	83,4 ± 4,6
AWA	44,2 ± 1,6	71,6 ± 0,5
AWO	59,9 ± 4,0	74,0 ± 4,8
CA	67,8 ± 2,0	88,7 ± 3,4
CO	77,4 ± 1,7	96,5 ± 0,3

Ikusitako lignina-galerak hain ustekabekoak izan zirenez, lignina hauek hauspeatzea erabaki zen beren pisu molekularrak aztertu ahal izateko. Emaitza horietatik abiatuta, kasu guztietan galdutako ligninek hasierakoek baino batezbesteko pisu molekular txikiagoa zutela ikusi zen, eta, gainera, homogeneoagoak zirela. Horrek matrize polimerikoak pisu molekular handieneko frakzioekin erreakzionatu zezakeela iradoki zuen.

Ligninen eraldaketek sintetizaturiko hidrogelen propietateengan izandako eragina zehazteko asmoz, lagin hauen ur-xurgatze ahalmena aztertu zen. Emaitzak 4.21 Irudian adierazten dira. Aurreko emaitzekin alderatuta, eraldatutako lignina alkalinoa zuten laginen kasuan, ur-xurgatze ahalmena

nabarmen murriztu zela ikusi zen. Emaitza horiek ur-xurgatze gaitasun handiko hidrogelak lortzeko peroxidazio bidezko eraldaketa ez zela egokiena iradokitzen dute. Aitzitik, organosolv lignina eraldatuak erabili zirenean, haien ur-xurgatze gaitasuna handitu egin zen, batez ere MCOL zuten laginen kasuan (%450), baina lignina-galera handiena ere aurkeztu zutenak ere badira. Gainera, MAAO laginak izan ziren bigarren ur-xurgatze gaitasun handiena izan zutenak (%410), eta hori ere bat zetorren bigarren lignina-galera handienarekin. Era berean, MAWO laginek propietate honen hobekuntza txikiena erakutsi zuten, eta lignina-galera txikiena ere erakutsi zuten eraldatutako organosolv ligninak zituzten laginen artean. Beraz, ondoriozta liteke hidroximetilazioa metodo egokia izan litekeela organosolv ligninaz egindako hidrogelen ur-xurgatze ahalmena hobetzeko.

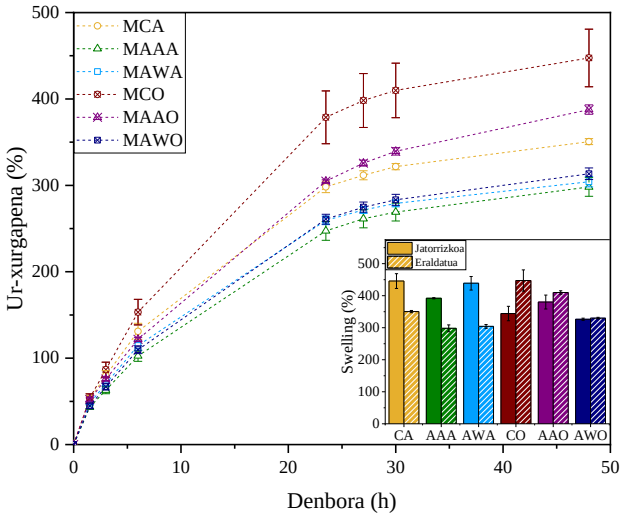

4.21 Irudia. Lignina eraldatudun hidrogelen ur-xurgapena lehen 48 orduetan eta jatorrizko ligninadun hidrogelenarekiko konparaketa.

Emaitza hauei erreparatuz eta aurrekoekin alderatuz, aipatzekoa da hidroximetilazioak lignina-hidrogelen ur-xurgatze ahalmena hobetzeko eraginkorra zela frogatu bazuen ere, sintesi-prozesuan izandako beste aldaketa batzuek (desizoztearen azken urratsaren luzapena, adibidez) hobekuntza

handiagoak ekarri zituztela propietate horrengan, jatorrizko ligninak eraldatzeko beharrik gabe.

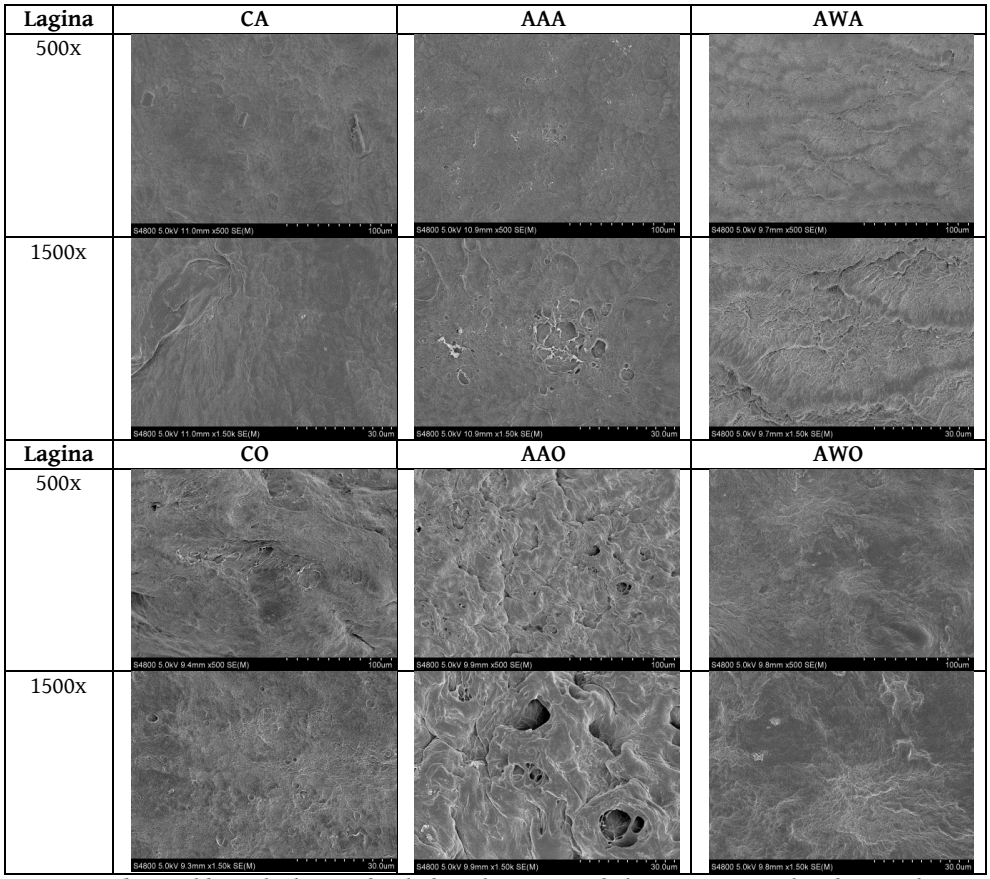

4.22 Irudia. Eraldatutako ligninadun hidrogelen SEM irudiak 500x eta 1500x handipenarekin.

SEM teknikaren bidez lortutako irudiek (4.22 Irudia) ez zituzten oso egitura porotsuak erakutsi; izan ere, morfologia nahiko trinkoak eta jarraituak erakutsi zituzten, ia ikusi ezin ziren hutsuneekin. Joera hau nabarmenagoa izan zen lignina alkalinoak zituzten laginetan, eta hori erretikulazio-dentsitate handiagoari egotz dakioke, ur-xurgatze ahalmenaren murriztea ere argituko lukeena. Organosolv ligninak zituzten laginetan, batez ere MAAO laginetan, sortutako hutsuneak nabariagoak ziren, eta horrek eragin zuen, ziurrenik, ura xurgatzeko gaitasunaren handitzea. Edonola ere, xurgapen saiakuntza aurretik erabilitako baldintza beretan egin zenez, posible da sortutako egiturek matrize

barreneko uraren difusioa oztopatu izatea, eta ondorioz, uretan denbora gehiago murgilduta egon ondoren, baliteke euren ur-xurgapena handitzea.

Propietate termikoei dagokienez, zehaztutako T_g balio guztiak 77-103 ºC-ko tartean zeuden. Balio horiek aurretik jakinarazitakoak baino handiagoak izan ziren, eta horrek ligninaren eraldaketek egitura trinkoagoak eragin zituztela iradoki zuen, egitura horietako kate polimeriko amorfoen mugimendua zailduz, eta SEM mikrografiekin ere bat etorriz.

Laginen konpresio-saiakuntzetan entseatutako hidrogel guztiak, euren portaera elastikoari esker, osotasun osoa eta berreskuragarritasun ona izateko gai izan zirela erakutsi zuten beste behin. 4.14 Taulako emaitzetatik lignina alkalinoak zituzten hidrogelek organosolv ligninak zituztenek baino konpresio-modulu handiagoak zituztela ondorioztatu zen. Hau bat zetorren analisi termikoan lortutako emaitzekin. Izan ere, lignina alkalinodun laginen konpresio-moduluaren balio guztiak 10-12 MPa tartean zeuden, organosolv lignina zuten hidrogelenak bikoiztuz (4,5 eta 6 MPa artean). Aurreko emaitzekin alderatuta, lignina alkalinodun laginetarako konpresio-modulua handitu egin zela ikusi zen, batez ere, MCA laginerako, eta organosolv ligninak zituzten laginetarako moduluaren balioa murriztu egin zen, nahiz eta MAAO laginarena pixka bat handiagoa izan.

4.14 Taula. Jatorrizko ligninak eta eraldatudun hidrogelen konpresio-modulua.

Lagina	**Konpresio-modulua (MPa)**	
	Jatorrizkoa	Eraldatua
CA	2,3 ± 0,8	12,0 ± 3,6
AAA	13,1 ± 0,8	11,4 ± 3,7
AWA	6,6 ± 2,9	10,1 ± 2,5
CO	8,1 ± 0,7	5,9 ± 3,9
AAO	2,1 ± 1,0	4,5 ± 1,8
AWO	5,4 ± 2,8	5,0 ± 0,8

4.3.6 **Ondorioak**

Atal honetan sintesi-parametro desberdinek lignina-hidrogelen propietateengan izandako eragina aztertu zen. Aztertutako parametro guztiek eragin handia izan zuten hidrogelen morfologian, eta horrek ur-xurgatze gaitasunak eta propietate mekanikoak aldatzea ekarri zuen. Giro-tenperaturan lehortzeko metodoari esker, puzteko ahalmen handiagoa zuten hidrogelak lortu ahal izan ziren, eta HM_w PVA erabiltzeak eta izozte- eta desizozte-zikloen kopurua eta horien iraupena handitzeak antzeko joerak eragin zituzten. Lignina desberdinak erabili zirenean, lignina mota beraren artean, ikusitako aldeak ez ziren hain esanguratsuak izan. Hala ere, lignina alkalinoak zituzten laginetatik organosolv ligninak zituzten laginetara propietateak asko aldatu ziren, eta ligninen purutasunak ezaugarri hauetan eragin handia zuela ikusi zen. Era berean, aukeratutako ligninaren eraldaketa-erreakzioaren arabera, hidrogelen propietateak asko alda daitezkeela ondorioztatu zen. Izan ere, hidroximetilazio erreakzioak jatorrizko ligninak zituzten hidrogelen ur-xurgatze ahalmena handiagotzea eragin zuen, peroxidazioak propietate honen murrizketa eragin zuen bitartean. Hala ere, portaera hau uraren difusio zailtasunari ere egotz dakioke. Beraz, aurreko guztia kontuan izanik, material horien azken propietateei eragiten dieten parametro ugari daudela ondoriozta daiteke, eta horietako batzuk kontrolaezinak diren arren edo normalean arbuiatzen diren arren, sakonago aztertu beharko liratekeela ikusi da, garrantzitsuak izan baitaitezke.

4.4 Sintetizaturiko lignina-hidrogelen aplikazioak

4.4.1 Tindagaien xurgatzea

Lignina-hidrogelek hainbat karga negatibo dituzte gainazalean azido karboxiliko talde ugarien ondorioz [56], eta hauek sortutako π–π interakzio hidrofobikoei esker, honako hidrogel hauek karga positiboa duten tindagaiak, hau da, koloratzaile kationikoak, erakartzeko gaitasuna dute [56]. Tindagai hauen artean, metileno-urdina (MB) aurki daiteke. Substantzia hau kotoia, zura eta zeta tindatzeko erabiltzen da eta gizaki nahiz animalientzat oso kaltegarria izan daitekeela frogatu da [61]. Horregatik, **III. eta IV. Artikuluetan** sintetizatu ziren hidrogelen MB adsortzioa 24 orduz ebaluatu zen.

Nahiz eta errendimendu-balioak ez izan beste autore batzuek aurrez adierazitakoak bezain handiak [56,61], xurgatze-balioak haiek adierazitakoak baino handiagoak izan ziren. **III. Artikuluko** laginen artean, entseatutako lignina-hidrogelek (5HL eta 3ML) deuseztapen-ehuneko handiak izan zituztela ikusi zen (%71,6 5HL-rako eta %69,1 3ML-rako); hidrogel zuriak (5H), berriz, tindagaiaren %34,8a soilik xurgatzeko gai izan zen.

IV. Artikuluko laginek ere MB-arekiko adsortzio-potentzial handia erakutsi zuten, xurgatze-baliorik txikiena %75ekoa eta handiena kutsatzailearen %93koa izanik (4.23 Irudia), **III. Artikuluan** lortutako emaitzak gaindituz. Oro har, prozesu bikoitzeko ligninak zituzten laginak tindagai kantitate handiagoak erakartzeko gai izan ziren, eta lignina alkalinoa zutenek organosolv lignina zutenek baino MB kantitate txikixeagoak xurgatu zituzten, euren TPC balioen joerarekin ere bat etorriz. Beste autore batzuek ere lignina alkalinodun laginek organosolv ligninadunek baino MB adsortzio-balio baxuagoen berri ere eman zuten [61]. Autore hauek portaera hau ligninetan aurkitutako hidroxilo fenolikoekin taldeen kopuruarekin lotu zuten [61]. Bestalde, desizoztearen azken zikloa luzatu zenean, lignina alkalinoak zituzten

laginen MB-ren adsortzio-ahalmena handitu egin zen, organosolv lignina zuten hidrogelena apur bat murriztu zen bitartean. Horrek, desizoztearen azken zikloak laginen porositatea areagotu zuen arren, gainazalean karga negatiboen eskuragarritasuna aldatu egin zela iradokitzen du; hala ere, baieztapen hau ezin izan da frogatu.

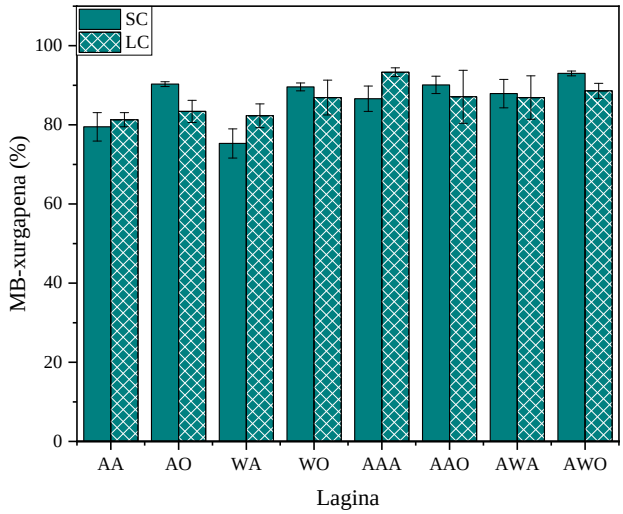

4.23 Irudia. 5. desizozte-urrats laburdun laginen (SC) eta luzedunen (LC) MB-ren xurgatze-ahalmenen arteko konparaketa.

4.4.2 **Propietate antifungikoak**

Elikagaien ontziratze-sektorean, ingurumena errespetatzen duten material berriak bilatzeko beharrak garrantzia handia hartu du azkenaldi honetan. Testuinguru horretan, sistema horientzat oinarri biologikoko hidrogelak balizko xurgatzaile gisa agertu dira [65]. Hala ere, material horiek ontziratutako produktuen iraupena luzatu behar dute, eta horrek mikroorganismoen eta onddoen hazkundea oztopatu behar dutela esan nahi du [65,120]. Horrela, **IV. Artikuluko** ligninen eta lignina-hidrogelen *Aspergillus niger*en (usteldura arrearen onddoa) aurkako propietate antifungikoak aztertu ziren, hau da, elikagaiak hondatzeko onddo ohikoenetako baten aurkako efektua ikertu zen.

Lehenik eta behin, ligninaren gaitasun antifungikoaren ebaluazio bisuala egin zen. Nahiz eta nagusiki usteldura zuriko onddoak lignina despolimerizatzeko gai izan [121], autore batzuek ikusi dute usteldura marroiko onddoak ere lignina degradatzeko gai izan daitezkeela. Hala ere, kasu honetan, entseatutako onddoek ez zuten gaitasun hori izan (4.24 Irudia). Lagin guztien agarraren gainazalean onddoak hazi baziren ere, laginean utzitako lignina-tantak argi eta garbi ikus zitezkeen probaldiaren ondoren. Honek ligninaren gaitasun antifungikoa frogatu zuen, aurretik beste egile batzuek frogatu zuten bezala. Aztertutako laginen artean, lignina alkalinoek hazkuntza fungikoa organosolv ligninek baino eraginkortasun handiagoz inhibitu zuten, eta, ondorioz, 3 indizeko hazkunde-intentsitatea (GI = 3) esleitu zitzaien; gainerako lagin gehienek, berriz, intentsitate handiagoak izan zituzten (GI ≈ 4), ISO 846 arauaren arabera [81].

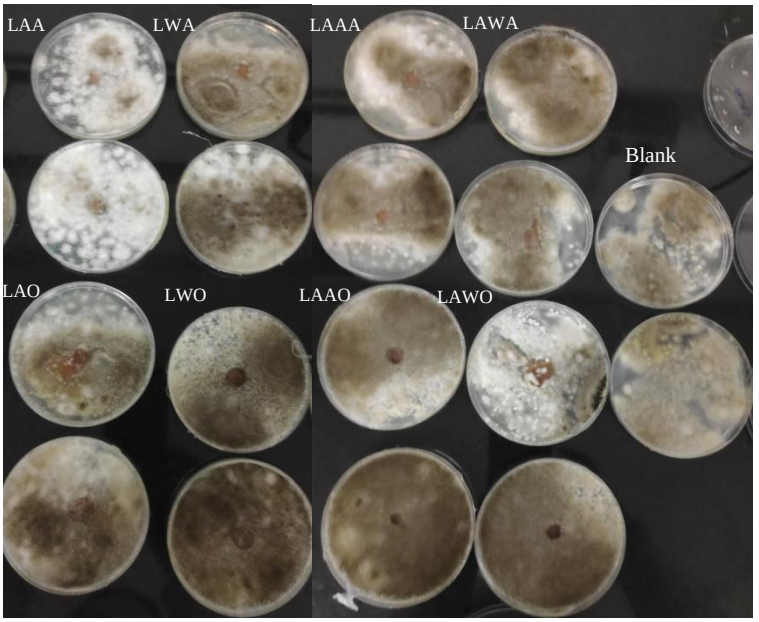

4.24 Irudia. Ligninen saiakuntza antifungikoen irudiak.

Bestalde, hidrogelei proba berdina egin zitzaien (4.25 Irudia). Kasu guztietan, probaren ondoren, entseatutako hidrogel zatia osorik mantendu zela ikusi zen. Lehen begiratuan, WNS lignina alkalinoak (WA eta AWA) zituzten laginek eta

AS organosolv ligninak (AO eta AWO) zituzten laginek beste ligninak zituzten laginek baino gehiago inhibitu zuten garapen fungikoa. Gainera, laginen goiko gainazaleko hazkuntza fungikoa ia antzemanezina izan zen. Kasu honetan, esleitutako hazkundearen intentsitatea 3 eta 4 artean legoke lagin guztientzat [81].

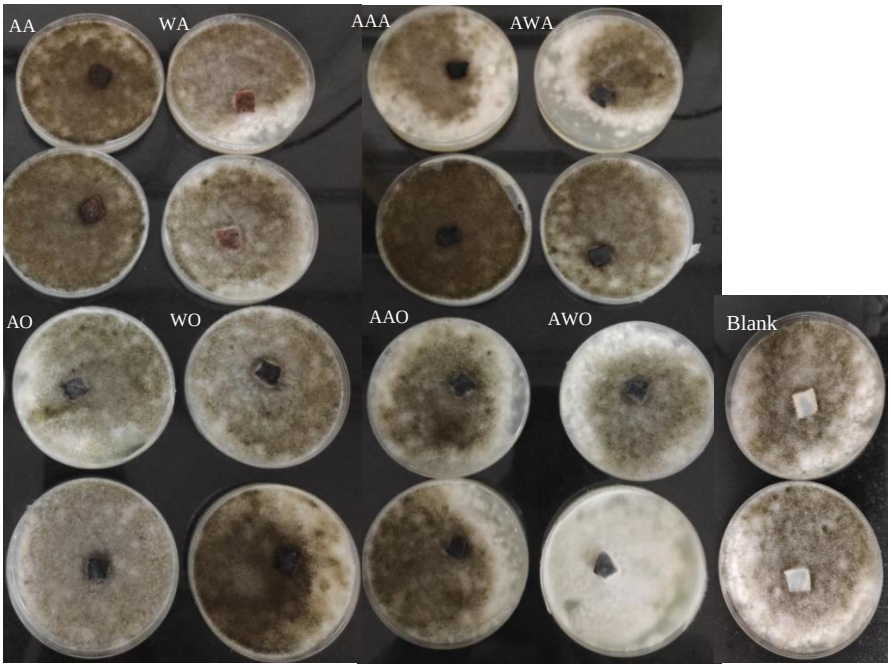

4.25 Irudia. Hidrogelen saiakuntza antifungikoen irudiak.

Laginak PBSz garbitu ondoren, inguruko esporak 3.6.2 atalean aipatu den bezala kuantifikatu ziren. Estimatutako FGI balioetatik abiatuta (4.26 Irudia), aztertutako laginen artean jarduera fungiko txikiena zutenak WO eta AAO (FGI handienarekin) izan zirela ikusi zen, eta hazkunde handiena izan zuena AWA zela, aurretik suposatutakoaren kontra joan arren. Gainera, urrats bakarreko prozesuko AS ligninak zituzten laginek bi urratseko AS ligninak zituztenek baino FGI balio baxuagoak zituztela ikusi zen. Aldiz, urrats bikoitzeko prozesuko WNS ligninak zituzten laginek jarduera antifungiko okerragoa erakutsi zuten urrats bakarreko WNS ligninak zituztenek baino. Estimatutako balioak gutxi gorabeherakoak izan ziren arren, emaitza hauek laginek zituzten

propietate antifungikoen ideia bat egiten lagundu zuten. Aipatzekoa da, halaber, aztertutako laginetako batek ere ez zuela pisurik galdu saiakuntza antifungikoan, eta horrek *A. niger*-en aurkako eraginkortasuna bermatzen du.

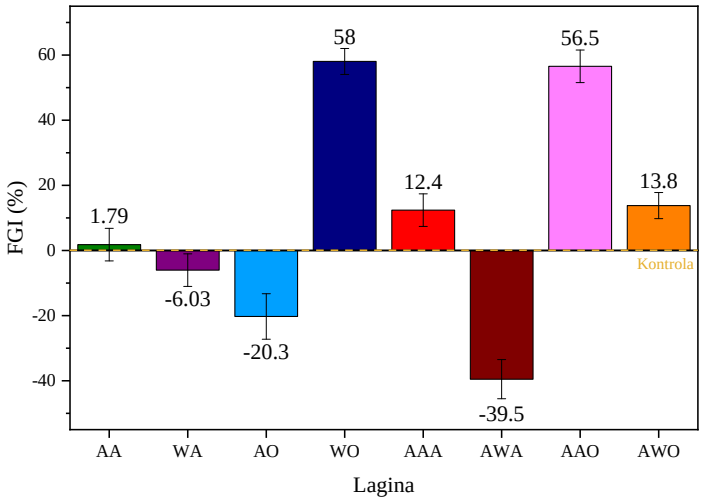

4.26 Irudia. Laginen hazkuntza fungikoaren inhibizioaren (FGI, %) balioak, hidrogel zurienak kontroltzat harturik (y = 0).

Zenbait autorek antzeko FGI balioen berri eman zuten elikagaiak ontziratzeko beste material batzuetarako. Adibidez, Salaberria *et al.* (2017)-ek funtzionalizaturiko kitina nano-kristaldun PLA filmetarako %52 eta 62 arteko inhibizioa topatu zuten [80]. Fernández-Marín *et al.* (2021)-en ikerketan, balio horiek %72 eta %86 artekoak izan ziren haien kitosano/β-kitina nano-zuntz nano-konposatuen kasuan, *Origanum majorana* L. deterpenatuaren olio esentziala gehitzearen ondorioz [122]. Aitzitik, Dey *et al.* (2021)-ek %51 eta %56 arteko balioen berri eman zuten PVA puruko filmen kasuan, zelulosa nano-kristalak eta kitosano nano-partikulak gehitzeak kalte egin baitzien [123]. Beraz, datu horiek kontuan hartuta, ondoriozta daiteke WO eta AAO hidrogeletarako emandako emaitzak guztiz bat datozela beste autore batzuek emandakoekin, eta elikagaiak ontziratzeko erabil litezkeela.

4.4.3 Kertzetina askapena

Kertzetina (QE) fruta eta barazkietan topa daitekeen bioflavonoide bat da, hantura, herdoil, obesitate eta minbiziaren aurkako propietate interesgarriak dituena [82,83,124]. Aipatutako ezaugarriengatik eta sintetizatutako botiken ordez konposatu naturalak hobesteko egungo joeragatik, kertzetinak arreta handia bereganatu du azkenaldian. Horrela, **V. Artikuluan**, konposatu hau mundu osoan hondakin ugaria den tipula gorrien azaletatik prozesu ekologiko baten bidez isolatu zen (mikrouhinen bidezko erauzketaz), hondakin honi balio erantsi bat emanez. Argitalpen berean sintetizatutako hidrogelak QE-rekin kargatu ziren eta botika honen askapen zinetika aztertu zen.

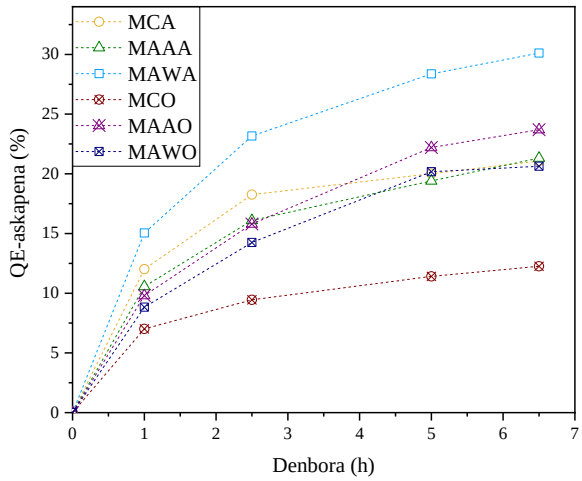

4.27 Irudia. Eraldaturiko ligninadun hidrogelen QE-askapena.

Hidrogelak QE-z hornitu eta lehortu ondoren, **V. Artikuluan** adierazten den bezala, PBS disoluziotan 37 ºC-tan murgildu ziren botika askatzeko, *in vitro* baldintzak simulatuz. Askapen-ingurunearen absorbantzia denbora-tarte jakin batzuen ondoren egin zen entseguaren lehen 6,5 orduetan zehar. Hidrogelek oraindik lignina askea zutenez, eta lignina honek 330 nm-tan xurgatze tontor bat zuenez, kontzentrazio altuetan, tontor honek QE-ri zegokion tontorreko emaitzak 375 nm-tan hondatzen zituen. Horregatik, askapen zinetika lehen 6,5 orduetan egin zen, askatutako lignina antzemanezina zen bitartean.

4.27 Irudian azaldutako askapen-profiletatik abiatuta, lagin guztiak antzeko botika-kopuruekin kargatu ahal izan ziren arren, lagin bakoitzerako askapen-gaitasuna guztiz desberdina izan zela ondorioztatu zen. Izan ere, xurgatutako botika kopuruei dagokienez, askatutako botiken ehunekoak %12 eta %30 artekoak izan ziren. Botikaren askatze-ehuneko handiena MAWA eta MAAA laginek izan zuten. Askatze txikiena, berriz, MCO laginerako ikusi zen, eta horrek, botika xurgatzeko ahalmen handiagoa izan zuen arren, honekin zituen interakzioek botika askatzea zaildu zutela iradokitzen du. Hala ere, kontuan izan behar da profil hauek lehenengo 6,5 orduetarako bakarrik izan zirela, eta ezin direla denbora luzeagotara estrapolatu.

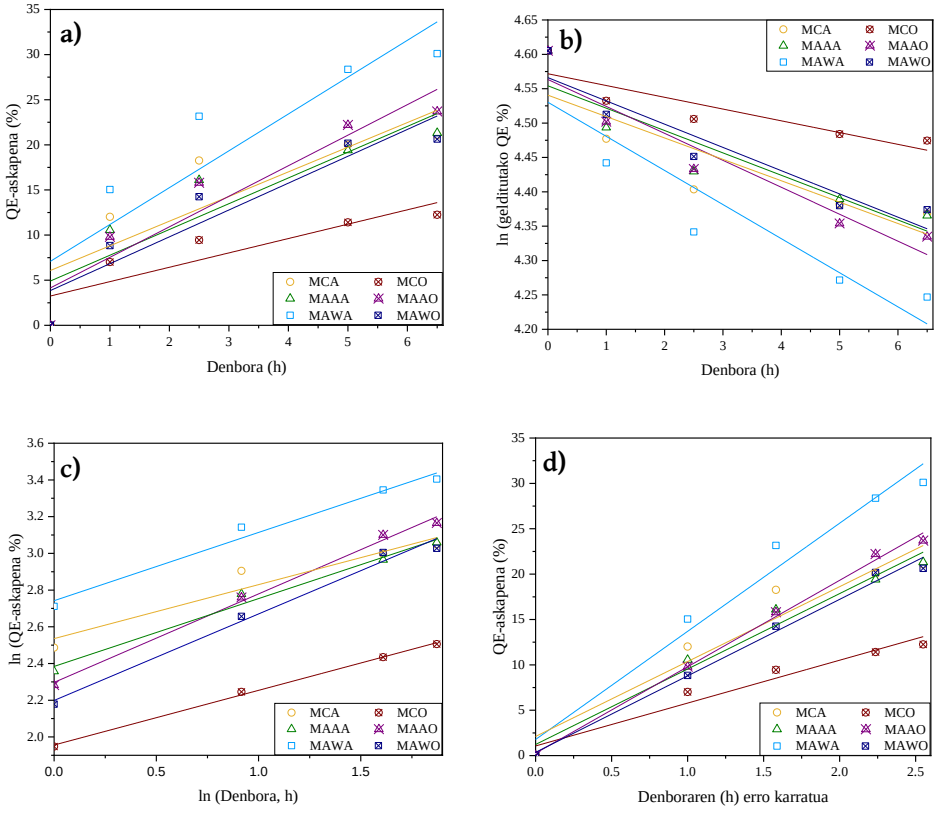

4.28 Irudia. a) Zero maila, b) lehen maila, c) Korsmeyer–Peppas eta d) Higuchi eredu zinetikoetan oinarrituriko QE-askapen profilak.

Askapen-zinetika zehazteko, hainbat eredu aplikatu ziren (hau da, zerogarren maila, lehen maila, Korsmeyer-Peppas eta Higuchi) [82,85,86]. Lau eredu zinetikoen irudikapen grafikoak 4.28 Irudian azaltzen dira, eta horietako bakoitzerako zenbatetsitako parametro zinetikoak 4.15 Taulan. Jatorrizko askatze-profiletik abiatuta, askatze-zinetika zero ordenako eredu batera ez zela behar bezala egokituko ondorioztatu zen, eta hori zehaztapen-koefizienteek (R^2) berretsi zuten. Gainontzeko modeloen artean, Korsmeyer-Peppasena izan zen hoberen doitu zena, MCA laginerako izan ezik, honen doikuntza ere ez baitzen hobetu Higuchiren modeloarekin.

4.15 Taula. QE-askapen eredu zinetikoetatik ondorioztatutako parametro zinetikoak.

	Karga	**Zero maila**	**Lehen maila**	**Korsmeyer–Peppas**			**Higuchi**
Lagina	(%)	R^2	R^2	R^2	n	k_{kp}	R^2
MAAA	29,0	0,8194	0,8438	0,9852	0,37	10,85	0,9764
MAAO	31,8	0,8946	0,9165	0,9947	0,48	9,94	0,9962
MAWA	30,4	0,8134	0,849	0,9809	0,37	15,52	0,9741
MAWO	32,0	0,8781	0,8968	0,9868	0,47	9,01	0,9904
MCA	26,0	0,7248	0,7473	0,9284	0,29	12,63	0,9294
MCO	34,5	0,7725	0,7872	0,9978	0,30	7,07	0,9562

Saidi *et al.* (2020)-ek adierazi bezala [86], datu esperimentalen difusio-berretzaileak (n) eta abiadura-konstanteak (k_{kp}) grafikoen (ln *(QE %)* vs. ln t) maldetatik eta jatorrizko ordenatuetatik zehaztu ziren. 4.15. Taulan ikus daitekeen bezala, n-rako zenbatetsitako balio guztiak 0,5 baino txikiagoak izan ziren. Nahiz eta normalean difusio bat Fickiarra dela esateko n=0,5 izan behar den [82,85], kasu honetan ere esan liteke QE-ren askapenek difusio Fickiar bat jarraitu zutela [82]. Beraz, esan liteke hidrogel sintetizatuak sendagaiak modu kontrolatuan askatzeko sistema gisa erabil litezkeela.

4.4.4 *In-vitro* Biobateragarritasun probak

PCS-201-012 fibroblasto-zelulen bideragarritasun-emaitzak, kontrol-laginetarako, B1 eta B2 lagin zurietarako eta AWA, AAA, AAO eta AWO

laginetarako neurtu ziren 24, 48 eta 72 orduren ondoren. Lehen 24 orduen amaieran, ligninadun laginen bideragarritasun-emaitzak (4.29 Irudian eta 4.16 Taulan ikus daitekeen bezala) %70etik beherakoak izan ziren, PVA puruzko hidrogelen kasuan %80tik gorakoa izan zen bitartean. 48 orduren ondoren, ligninadun laginen bideragarritasunak %66tik beherakoak izan ziren, eta PVAzko lagin bakarrak erakutsi zuen %70etik gorako balioa. Hirugarren egunaren amaieran (72 ordu), lagin guztiek %60tik beherako balioak erakutsi zituzten, PVAzko 2. lagin zuriak izan ezik.

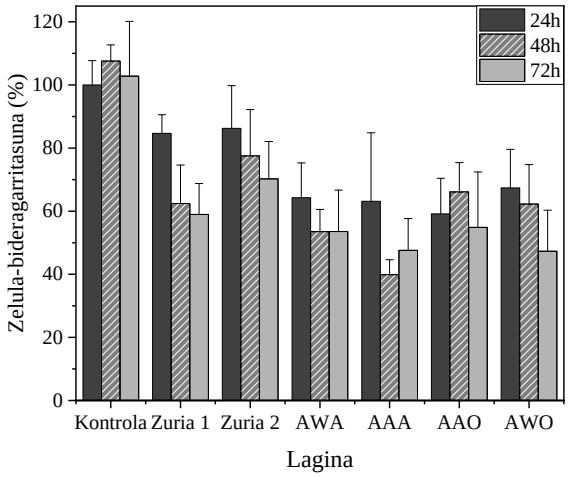

4.29 Irudia. PCS-201-012 zelulekin (giza fibroblasto dermikoen zelulak) kultibaturiko hidrogelen zelula-bideragarritasunen emaitzak 24, 48 eta 72 h ondoren.

4.16 Taula. PCS-201-012 zelulekin kultibaturiko hidrogelen zelula-bideragarritasunen emaitzak 24, 48 eta 72 h ondoren.

Lagina	**Zelula-bideragarritasuna(%)**		
	24 h	48 h	72 h
Kontrola	100±7,7	107,6±5,1	102,8 ± 17,4
Zuria 1	84,7±5,9	62,4±12,2	59,0±9,8
Zuria 2	86,3±13,5	77,5±14,7	70,2±11,9
AWA	64,3±11,0	53,5±7,0	53,5±13,1
AAA	63,2±21,7	39,9±4,7	47,6±10,1
AAO	59,2±11,3	66,1±9,3	54,85±17,6
AWO	67,4±12,2	62,3±12,5	47,3±13,0

Zuria 1 eta Zuria 2 laginak kontrol gisa hartu zirenean (4.30 Irudia), AWA, AAA, AAO eta AWO laginen bideragarritasuna birkalkulatu egin zen, eta emaitza hauek 4.17 eta 4.18 Tauletan agertzen dira. Alde batetik, Zuria 1 lagina kontrol-talde gisa kontuan hartuta bideragarritasun zelularra kalkulatu zenean (4.30-a Irudia), lehen 24 orduen ondoren, laginen bideragarritasuna %70etik gorakoa izan zen kasu guztietan. Inkubazio-denbora 48 ordura luzatu zenean, organosolv lignina zuten laginek soilik erakutsi zuten %70etik gorako bideragarritasuna. 72 orduen amaieran, bideragarritasun-ehunekoak %55 eta %64 artekoak izan ziren ligninadun laginentzat. Aipatzekoa da lagin zuriaren kasuan, bideragarritasunak ere beherakada handia izan zuela lehen 24 orduen ondoren lortutako emaitzarekin alderatuta, %70 baino balio txikiagoa erakutsi baitzuen amaieran.

4.17 Taula. PCS-201-012 zelulekin kultibaturiko hidrogelen zelula-bideragarritasunen emaitzak 24, 48 eta 72 h ondoren, B1 lagina kontroltzat hartuz.

Lagina	**Zelula-bideragarritasuna(%)**		
	24 h	48 h	72 h
Zuria 1	100,0±6,7	72,8±14,2	68,8±11,4
AWA	75,9±13,0	62,4±8,2	62,4±15,3
AAA	74,6±25,6	46,5±5,5	55,5±11,8
AAO	69,9±13,3	77,1±10,9	64,0±20,5
AWO	79,6±14,5	72,7±14,6	55,2±15,2

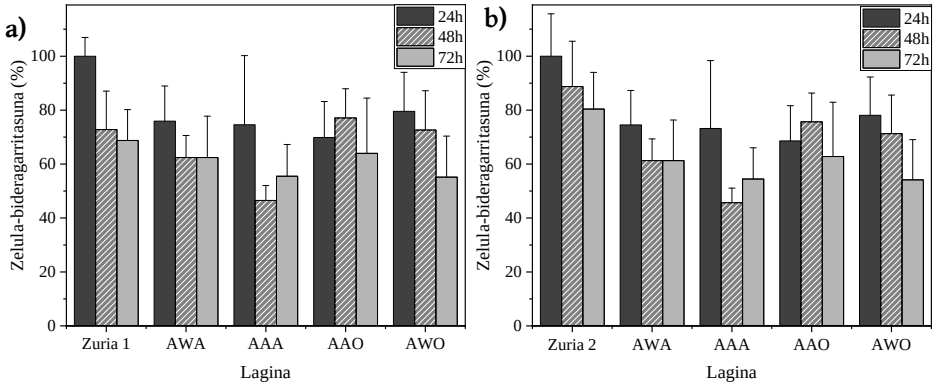

4.30 Irudia. PCS-201-012 zelulekin (giza fibroblasto dermikoen zelulak) kultibaturiko hidrogelen zelula-bideragarritasunen emaitzak 24, 48 eta 72 h ondoren, B1 eta B2 laginak kontroltzat hartuz.

Bestalde, Zuria 2 lagina kontrol gisa hartu zenean (4.30-b Irudia), lehen 24 orduetan, erregistratutako bideragarritasunak %70 gainetik mantendu ziren. Hurrengo 24 orduetarako, balio horiek aldaketa nabarmena jasan zuten, lignina alkalinodun laginen kasuan. Organosolv ligninadun laginen bideragarritasunek %70tik gorakoak izaten jarraitu zuten. 72 orduko inkubazio-aldiaren amaieran, bideragarritasun-emaitzek jaitsiera nabarmena pairatu zuten organosolv ligninadun laginen kasuan, lignina alkalinodunen kasuan igoera bat erakutsi zuten bitartean. Aipatzekoa da, kasu honetan kontrol-laginak izandako bideragarritasunaren beherakada 1. Lagin zuriak jasandakoa baino txikiagoa izan zela.

4.18 Taula. PCS-201-012 zelulekin kultibaturiko hidrogelen zelula-bideragarritasunen emaitzak 24, 48 eta 72 h ondoren, B2 lagina kontroltzat hartuz.

Lagina	**Zelula-bideragarritasuna(%)**		
	24 h	48 h	72 h
Zuria 2	100,0±15,7	88,8±16,8	80,4±13,6
AWA	74,5±12,8	61,3±8,1	61,3±15,0
AAA	73,2±25,2	45,7±5,4	54,5±11,6
AAO	68,6±13,1	75,7±10,7	62,8±20,1
AWO	78,1±14,2	71,3±14,3	54,1±14,9

Lagin guztiak batera ebaluatu zirenean, lehen 24 orduen ondoren, AWA, AAA eta AWO laginak izan ziren bideragarrienak. Hala ere, saiakuntzaren hurrengo 48 orduetan, balio horiek behera egin zuten eta, probaren amaieran, AAO laginak erakutsi zuen bideragarritasun handiena. Bi hidrogel zuriekin alderatzean, hiru egunen ondoren, zelulen ugaritze handiena ere lagin honek erakutsi zuen. Izan ere, lagin hori izan zen 24 ordutik 48 ordura zelulak ugaltzea ahalbidetu zuen bakarra.

ISO 10993-5 arauaren arabera, material ez-zitotoxikoen bideragarritasuna %70etik gorakoa izan behar denez [125,126], esan liteke kasu honetan entseatutako lignina-hidrogel bakar bat ere ez litzatekeela guztiz biobateragarria izango.

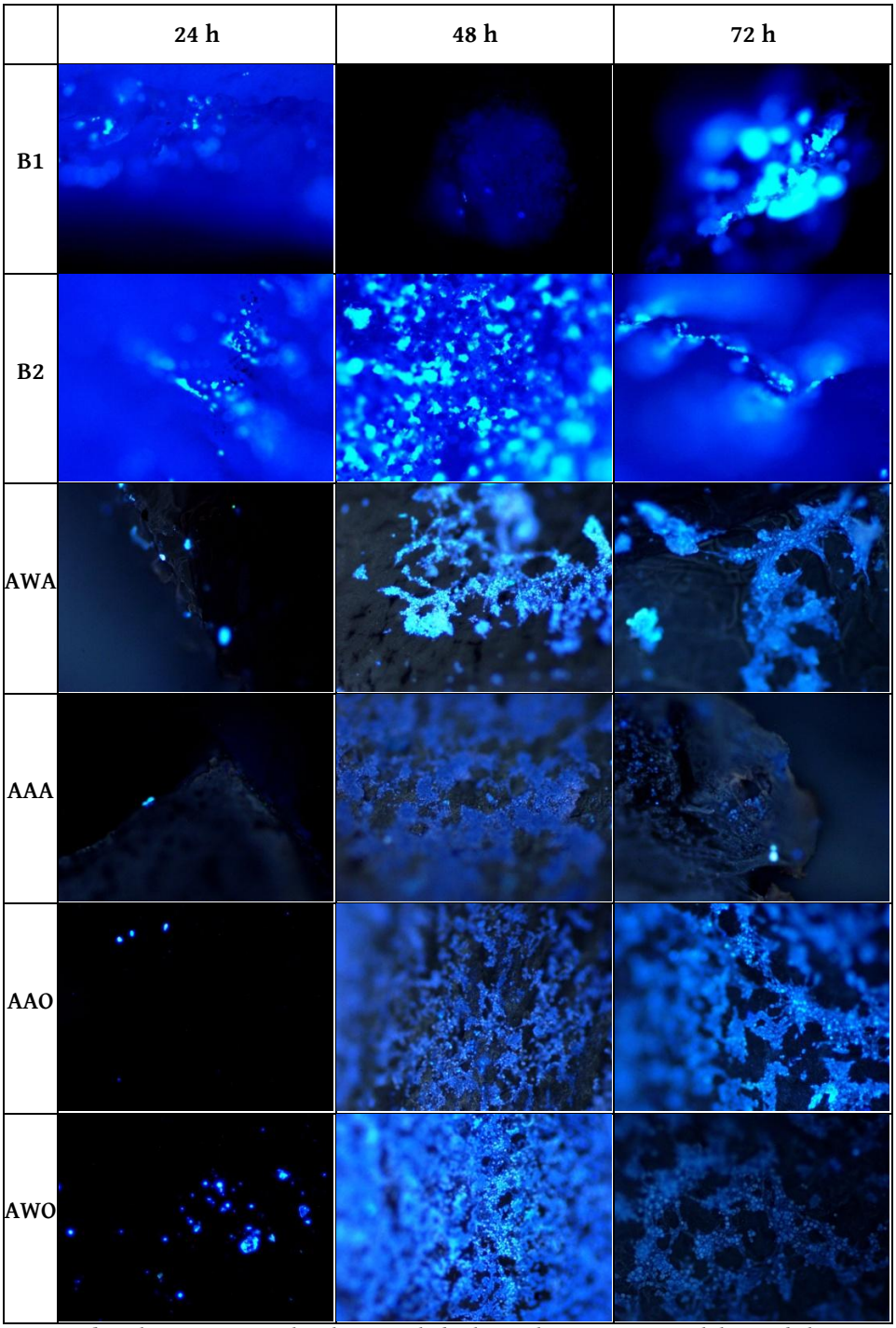

4.31 Irudia. Fluoreszentzia mikroskopiaren bidez lortutako PCS-201-012 zelulen irudiak B1, B2, AWA, AAA, AAO eta AWO laginekin 24, 48 and 72 orduz kultibatu ondoren.

PVA material biobateragarritzat jotzen den arren [125,127], PVA soilezko hidrogelek ere zelulen biobateragarritasuna murriztu zuten proban zehar, eta horrek lignina hidrogelen biobateragarritasunean ere eragin negatiboa izango luke. Aipatutako laginak finkatu egin ziren eta gainazaleko zelulen nukleoak DAPI erreaktiboarekin tindatu ziren, fluoreszentzia-mikroskopioaz aztertu ahal izateko. Laginen gainazalean zelulak aurkitu ziren (4.31 Irudia), baina bideragarritasun balio eskasetatik zelulak gainazalean finkatu bezain laster hil zirela ondorioztatu zen, eta, ondorioz, grafikoetako bideragarritasun-balioak murriztu egin ziren.

Autore batzuek aipatu izan dute entseatutako materialen porotasuna funtsezkoa izan daitekeela zelulen hazkuntzarako [128]. Beraz, aurreko laginen porotasuna kontuan hartuta, bigarren saiakuntza bat egin zen lagin porotsuagoak erabiliz, baita lignina alkalino komertzialetik abiatuta sintetizatu zirenak ere, arazoa erauzitako ligninetan zegoela baztertzeko asmoz. Bigarren saiakuntza horretan, hidrogel laginak PBS bidez garbitu ziren irabiagailu orbital batean 48 orduz, eta, ondoren, lehen aipatutako zelulak esterilizatzeko eta ereiteko prozedura berdina aplikatu zen. Laginen bideragarritasun-emaitzak 24 orduz entseatu ondoren aztertu ziren (4.32 Irudia).

Kontrol-lagin eta CA, AAA, AA, WA eta AWA laginetarako erregistratutako bideragarritasuna %100,0, 16,56, 33,16, 31,46, 44,35 eta 34,58 izan zen, hurrenez hurren. Porotasun handiagoa zuten hidrogeletan (AA eta WA), bideragarritasun zelularraren hobekuntza nabarmenagoa izan zen, bereziki WA laginarena. AA eta AAA laginek antzeko bideragarritasun-emaitzak izan zituzten, baina neurketen desbideratzeak nahiko handiak izan ziren. Lignina alkalino komertziala zuen lagina (CA) izan zen emaitzarik txarrena erakutsi zuena. Gertaera horrek lignina honen FTIR analisien bidez [78] aurrez detektatu zen sufre-edukiarekin lotura izan lezake, zelula bizidunetarako kaltegarria izan baitaiteke.

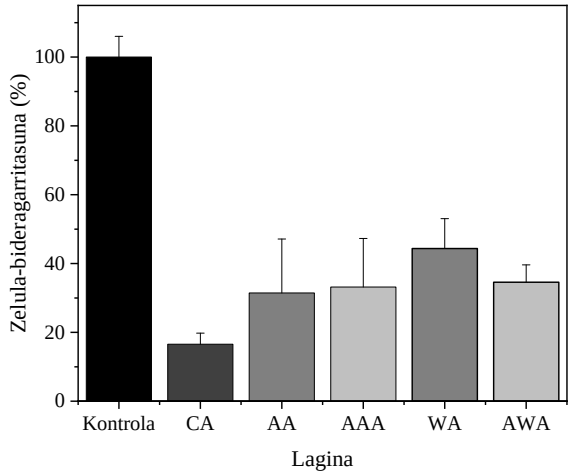

4.32 Irudia. PCS-201-012 zelulekin (giza fibroblasto dermikoen zelulak) kultibaturiko hidrogelen zelula-bideragarritasunen emaitzak 24 h ondoren.

Laginen porotasuna eragin handiko parametroa dela frogatu den arren, hidrogelen ur-xurgatze ahalmenen arteko desberdintasunek zelulen ugaltzeari ere eragin diezaiokete. Izan ere, hidrogel batzuek aldez aurretik xurgatutako ingurune zelularraren zati bat askatu zuten, eta horrek, lignina kantitatearekin batera, zelulen heriotza ekar lezake, hidrogelen bideragarritasuna murriztuz. Autore batzuen arabera, PVA-zko hidrogelei lignina gehitzeak biobateragarritasuna hobetu lezake [129], baina beste egile batzuek, aldiz, ligninen zitotoxikotasuna erabilitako kontzentrazioaren menpekoa izan daitekeela jakinarazi dute [130,131]. Beraz, egoera honetan bi aukera posible aurreikusten dira: lehenengoa, jatorrizko lignina soilen bideragarritasun zelularra aztertzea; eta bigarrena, hidrogelak sintetizatzeko erabilitako lignina-edukia murriztea, hauen biobateragarritasuna hobetzeko asmoz.

4.4.5 **Ondorioak**

Atal honetan tesi honetan sintetizatutako hidrogelen aplikagarritasuna ebaluatu da. Lortutako emaitzetatik material horiek ur-arazketa sistema gisa erabilgarriak izan daitezkeela ondoriozta daiteke, batez ere tindagai

kationikoak xurgatzeko. Gainera, sintetizatutako hidrogeletako batzuk ontzi aktiboetan erabiltzeko aproposak direla frogatu da, portaera antifungikoa baitute. Gainera, material horiek botika natural batekin kargatuak izan eta Fickiar difusio eredu bati jarraituz hau askatzeko gaitasuna erakutsi zuten. Material hauen biobateragarritasuna hobetzeko lanean jarraitu behar bada ere, ekoitzitako hidrogelek diziplina anitzeko aplikazioetarako material potentzialak eta moldakorrak direla erakutsi dute.

5 Ondorioak eta etorkizuneko lanak

5.1 Ondorio orokor eta espezifikoak

Tesi honen ondorio orokor gisa, esan daiteke fisikoki gurutzaturiko lignina-hidrogelak arrakastaz lor daitezkeela lignina ingurumena errespetatzen duen matrize polimeriko batekin nahastuz, polibinil alkoholarekin (PVA), hain zuzen ere. Gainera, frogatu da material horien propietateak hainbat sintesi- eta formulazio-parametro aldatuz egokitu daitezkeela. Horrez gain, lignina-hidrogelak aplikazio-eremu askotan aplikatzeko material potentzialak direla frogatu da, hala nola uraren arazketan, ontziratzean edo botiken askapenean. Material hauen biobateragarritasuna hobetu badaiteke ere, lorturiko emaitzek bio-medikuntza arloan ere etorkizuna izan dezaketela erakutsi dute. Tesi honetatik ateratako ondorio espezifikoak honako hauek dira:

- ✓ Lignina alkalino komertzialaren eta MM_w PVA-ren nahasketaren bidezko hidrogelen sintesia optimizatzearen ondorioz, ur-xurgatze gaitasun handiko materialak lortu ziren, gurutzaketa eta lehortze metodoaren arabera molda zitezkeenak.
- ✓ PVA-ren pisu molekularrak eragin handia izan zuen sintetizatutako hidrogelen gurutzaketan eta lortutako materialen amaierako propietateetan, ur-xurgatze ahalmena handituz matrize polimeroaren pisu molekularra handitu ahala.
- ✓ Fruitu lehorren azaletatik erauzitako ligninen propietateek sintetizatutako hidrogelen ezaugarriengan eragin zuzena dutela erakutsi zuten, eta ligninen purutasuna eragin handiko faktorea dela.
- ✓ Izozte- eta desizozte-zikloen iraupena murrizteak hidrogelen ur-xurgatze ahalmena murriztea ekarri zuen. Aitzitik, desizoztearen azken etaparen iraupena luzatu izanak nabarmen hobetu zuen propietate hori.

- ✓ Erabilitako ligninen eraldaketa kimikoa hidrogelen ezaugarriak aplikazio bakoitzak eskatzen dituen beharretara egokitzeko baliagarria izan daiteke.
- ✓ Sintetizaturiko hidrogelek emaitza oparoak erakutsi zituzten frogatutako aplikazioetarak: ur-inguruneko tindagaien adsortzioan, elikagaiak ontziratzeko material antifungiko moduan eta botiken askapenean.
- ✓ Biobateragarritasun saiakuntzetako emaitzak espero bezain egokiak ez izan arren, material hauek arlo honetan ere etorkizuna izan dezaten jarraitu beharreko bidearen ateak zabaldu dituzte.

5.2 Etorkizuneko lanak

Tesi honetan parametro askoren eragina eta zenbait aplikazio posible aztertu badira ere, oraindik ere lignina-hidrogelei buruzko asko dago ikasteko. Hori dela eta, ondoko alderdi hauek sakonago ikertu beharko lirateke etorkizunean:

- Proposatutako hidrogelen sintesi-prozedura eskala handiago batera eramateko aukera.
- Tesi honetako hidrogelen bizi-zikloaren azterketa (LCA).
- Sintetizatutako hidrogelen biobateragarritasunaren hobekuntza bio-medikuntza eremuan erabili ahal izateko.
- Ingurumena errespetatzen duten beste matrize polimeriko batzuk erabiltzea fisikoki gurutzatutako lignina-hidrogelen garapenerako.
- Jatorri desberdinetako ligninak erabiltzea, hala nola belarra, zur gogorra eta zur biguna.
- Ligninaren eraldaketarako erreakzio desberdinak erabiltzea eta horiek hidrogelen propietateengan duten eragina aztertzea.

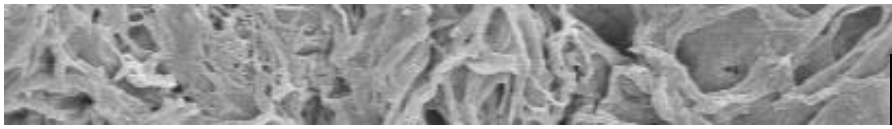

Erreferentziak

[1] D. Londoño-Pulgarin, G. Cardona-montoya, J.C. Restrepo, F. Muñoz-Leiva, Fossil or bioenergy? Global fuel market trends, 143 (2021). doi:10.1016/j.rser.2021.110905.

[2] BP, Statistical Review of World Energy (Oil), (2020).

[3] BP, Statistical Review of World Energy (CO_2), (2020).

[4] H. Nakajima, P. Dijkstra, K. Loos, The recent developments in biobased polymers toward general and engineering applications: Polymers that are upgraded from biodegradable polymers, analogous to petroleum-derived polymers, and newly developed, Polymers (Basel). 9 (2017) 1–26. doi:10.3390/polym9100523.

[5] S. Walker, R. Rothman, Life cycle assessment of bio-based and fossil-based plastic: A review, J. Clean. Prod. 261 (2020) 121158. doi:10.1016/j.jclepro.2020.121158.

[6] J. Soares, I. Miguel, C. Venâncio, I. Lopes, M. Oliveira, Public views on plastic pollution: Knowledge, perceived impacts, and pro-environmental behaviours, 412 (2021) 125227. doi:10.1016/j.jhazmat.2021.125227.

[7] J.R. Jambeck, R. Geyer, C. Wilcox, T.R. Siegler, M. Perryman, A. Andrady, R. Narayan, K.L. Law, Plastic waste inputs from land into the ocean, Science, 347 (2015) 768–771. doi:10.1126/science.1260352.

[8] A. Pellis, M. Malinconico, A. Guarneri, L. Gardossi, Renewable polymers and plastics: Performance beyond the green, N. Biotechnol. 60 (2021) 146–158. doi:10.1016/j.nbt.2020.10.003.

[9] S.N. Akanyange, X. Lyu, X. Zhao, X. Li, Y. Zhang, J.C. Crittenden, C. Anning, T. Chen, T. Jiang, H. Zhao, Does microplastic really represent a threat? A review of the atmospheric contamination sources and potential impacts, Sci. Total Environ. 777 (2021) 146020. doi:10.1016/j.scitotenv.2021.146020.

[10] A.T. Ubando, C.B. Felix, W.H. Chen, Biorefineries in circular bioeconomy: A comprehensive review, Bioresour. Technol. 299 (2020)

122585. doi:10.1016/j.biortech.2019.122585.

[11] A. Morales, J. Labidi, P. Gullón, G. Astray, Synthesis of advanced biobased green materials from renewable biopolymers, Curr. Opin. Green Sustain. Chem. 29 (2021) 100436. doi:10.1016/j.cogsc.2020.100436.

[12] S. Bilgen, Structure and environmental impact of global energy consumption, Renew. Sustain. Energy Rev. 38 (2014) 890–902. doi:10.1016/j.rser.2014.07.004.

[13] G. Dragone, A.A.J. Kerssemakers, J.L.S.P. Driessen, C.K. Yamakawa, L.P. Brumano, S.I. Mussatto, Innovation and strategic orientations for the development of advanced biorefineries, Bioresour. Technol. 302 (2020) 122847. doi:10.1016/j.biortech.2020.122847.

[14] R. van Ree, The Role of Biorefining and Bioenergy in the Circular Economy, (2017).

[15] A.S. Nizami, M. Rehan, M. Waqas, M. Naqvi, O.K.M. Ouda, K. Shahzad, R. Miandad, M.Z. Khan, M. Syamsiro, I.M.I. Ismail, D. Pant, Waste biorefineries: Enabling circular economies in developing countries, Bioresour. Technol. 241 (2017) 1101–1117. doi:10.1016/j.biortech.2017.05.097.

[16] BioPlat., SusChem., Ministerio de Economía., I. y Competitividad, Manual sobre Biorrefinerías en España, Minist. Econ. Ind. Y Compet. (2017) 1–92.

[17] Y. Liu, Y. Lyu, J. Tian, J. Zhao, N. Ye, Y. Zhang, L. Chen, Review of waste biorefinery development towards a circular economy: From the perspective of a life cycle assessment, Renew. Sustain. Energy Rev. 139 (2021) 110716. doi:10.1016/j.rser.2021.110716.

[18] Bio-based Industries Consortium, Nova Institute, Biorefineries in Europe 2017, (2017).

[19] L.A. Zevallos Torres, A. Lorenci Woiciechowski, V.O. de Andrade Tanobe, S.G. Karp, L.C. Guimarães Lorenci, C. Faulds, C.R. Soccol, Lignin as a potential source of high-added value compounds: A review, J. Clean. Prod. 263 (2020) 121499. doi:10.1016/j.jclepro.2020.121499.

[20] A.R. Mankar, A. Pandey, A. Modak, K.K. Pant, Pretreatment of lignocellulosic biomass: A review on recent advances, Bioresour. Technol. 334 (2021) 125235. doi:10.1016/j.biortech.2021.125235.

[21] J.J. Liao, N.H.A. Latif, D. Trache, N. Brosse, M.H. Hussin, Current advancement on the isolation, characterization and application of lignin, Int. J. Biol. Macromol. 162 (2020) 985–1024. doi:10.1016/j.ijbiomac.2020.06.168.

[22] R. Singh, A. Shukla, S. Tiwari, M. Srivastava, A review on delignification of lignocellulosic biomass for enhancement of ethanol production potential, Renew. Sustain. Energy Rev. 32 (2014) 713–728. doi:10.1016/j.rser.2014.01.051.

[23] L. Sillero, R. Prado, M.A. Andrés, J. Labidi, Characterisation of bark of six species from mixed Atlantic forest, Ind. Crops Prod. 137 (2019) 276–284. doi:10.1016/j.indcrop.2019.05.033.

[24] S.L. Mathews, J. Pawlak, A.M. Grunden, Bacterial biodegradation and bioconversion of industrial lignocellulosic streams, Appl. Microbiol. Biotechnol. 99 (2015) 2939–2954. doi:10.1007/s00253-015-6471-y.

[25] FAOSTAT, Crops and livestock products, (2019). https://www.fao.org/faostat/en/#data/QCL (accessed June 30, 2021).

[26] H. Chen, Chemical Composition and Structure of Natural Lignocellulose, in: Biotechnology of Lignocellulose, Springer, 2014: pp. 25–71. doi:10.1007/978-94-007-6898-7.

[27] A. Satlewal, R. Agrawal, S. Bhagia, P. Das, A.J. Ragauskas, Rice straw as a feedstock for biofuels: Availability, recalcitrance, and chemical properties, Biofuels, Bioprod. Biorefining. 12 (2018) 83–107. doi:10.1002/bbb.1818.

[28] W.O.S. Doherty, P. Mousavioun, C.M. Fellows, Value-adding to cellulosic ethanol: Lignin polymers, Ind. Crops Prod. 33 (2011) 259–276. doi:10.1016/j.indcrop.2010.10.022.

[29] C.G. Yoo, X. Meng, Y. Pu, A.J. Ragauskas, The critical role of lignin in lignocellulosic biomass conversion and recent pretreatment strategies: A comprehensive review, Bioresour. Technol. 301 (2020) 122784. doi:10.1016/j.biortech.2020.122784.

[30] A. Tribot, G. Amer, M. Abdou Alio, H. de Baynast, C. Delattre, A. Pons, J.D. Mathias, J.M. Callois, C. Vial, P. Michaud, C.G. Dussap, Wood-lignin: Supply, extraction processes and use as bio-based material, Eur. Polym. J. 112 (2019) 228–240. doi:10.1016/j.eurpolymj.2019.01.007.

[31] S. Constant, H.L.J. Wienk, A.E. Frissen, P. de Peinder, R. Boelens, D.S. van Es, R.J.H. Grisel, B.M. Weckhuysen, W.J.J. Huijgen, R.J.A. Gosselink, P.C.A. Bruijnincx, New insights into the structure and composition of technical lignins: a comparative characterisation study, Green Chem. 18 (2016) 2651–2665. doi:10.1039/C5GC03043A.

[32] V. Hemmilä, S. Adamopoulos, O. Karlsson, A. Kumar, Development of sustainable bio-adhesives for engineered wood panels-A Review, RSC Adv. 7 (2017) 38604–38630. doi:10.1039/c7ra06598a.

[33] V.K. Ponnusamy, D.D. Nguyen, J. Dharmaraja, S. Shobana, J.R. Banu, R.G. Saratale, S.W. Chang, G. Kumar, A review on lignin structure, pretreatments, fermentation reactions and biorefinery potential, Bioresour. Technol. 271 (2019) 462–472. doi:10.1016/j.biortech.2018.09.070.

[34] H. Wang, Y. Pu, A. Ragauskas, B. Yang, From lignin to valuable products–strategies, challenges, and prospects, Bioresour. Technol. 271 (2019) 449–461. doi:10.1016/j.biortech.2018.09.072.

[35] A. Kumar, Anushree, J. Kumar, T. Bhaskar, Utilization of lignin: A sustainable and eco-friendly approach, J. Energy Inst. 93 (2020) 235–271. doi:10.1016/j.joei.2019.03.005.

[36] E. Paone, T. Tabanelli, F. Mauriello, The rise of lignin biorefinery, Curr. Opin. Green Sustain. Chem. 24 (2020) 1–6. doi:10.1016/j.cogsc.2019.11.004.

[37] X. Erdocia, F. Hernández-ramos, A. Morales, N. Izaguirre, P.L. De Hoyos-martínez, J. Labidi, Lignin extraction and isolation methods, in: H. Santos, P. Figueiredo (Eds.), Lignin-Based Mater. Biomed. Appl., Elsevier Inc., 2021: pp. 61–104. doi:10.1016/c2019-0-01345-3.

[38] X. Meng, C. Crestini, H. Ben, N. Hao, Y. Pu, A.J. Ragauskas, D.S. Argyropoulos, Determination of hydroxyl groups in biorefinery resources via quantitative 31P NMR spectroscopy, Nat. Protoc. 14 (2019) 2627–2647. doi:10.1038/s41596-019-0191-1.

[39] Y. Chen, H. Zhang, Z. Zhu, S. Fu, High-value utilization of hydroxymethylated lignin in polyurethane adhesives, Int. J. Biol. Macromol. 152 (2020) 775–785. doi:10.1016/j.ijbiomac.2020.02.321.

[40] M. Goliszek, D. Kołodyńska, I. V. Pylypchuk, O. Sevastyanova, B. Podkościelna, Synthesis of lignin-containing polymer hydrogels with tunable properties and their application in sorption of nickel(II) ions, Ind. Crops Prod. 164 (2021) 20–31. doi:10.1016/j.indcrop.2021.113354.

[41] P. Figueiredo, K. Lintinen, J.T. Hirvonen, M.A. Kostiainen, H.A. Santos, Properties and chemical modifications of lignin: Towards lignin-based nanomaterials for biomedical applications, Prog. Mater. Sci. 93 (2018) 233–269. doi:10.1016/j.pmatsci.2017.12.001.

[42] V. Maharana, D. Gaur, S.K. Nayak, V.K. Singh, S. Chakraborty, I. Banerjee, S.S. Ray, A. Anis, K. Pal, Reinforcing the inner phase of the filled hydrogels with CNTs alters drug release properties and human keratinocyte morphology: A study on the gelatin- tamarind gum filled hydrogels, J. Mech. Behav. Biomed. Mater. 75 (2017) 538–548. doi:10.1016/j.jmbbm.2017.08.026.

[43] K. Lavanya, S.V. Chandran, K. Balagangadharan, N. Selvamurugan, Temperature- and pH-responsive chitosan-based injectable hydrogels for bone tissue engineering, Mater. Sci. Eng. C. 111 (2020) 110862. doi:10.1016/j.msec.2020.110862.

[44] C. Echalier, L. Valot, J. Martinez, A. Mehdi, G. Subra, Chemical cross-linking methods for cell encapsulation in hydrogels, Mater. Today Commun. 20 (2019) 100536. doi:10.1016/j.mtcomm.2019.05.012.

[45] J. Xiang, L. Shen, Y. Hong, Status and future scope of hydrogels in wound healing: Synthesis, materials and evaluation, Eur. Polym. J. 130 (2020) 109609. doi:10.1016/j.eurpolymj.2020.109609.

[46] K. Varaprasad, G.M. Raghavendra, T. Jayaramudu, M.M. Yallapu, R. Sadiku, A mini review on hydrogels classification and recent developments in miscellaneous applications, Mater. Sci. Eng. C. 79 (2017) 958–971. doi:10.1016/j.msec.2017.05.096.

[47] N. Chirani, L. Yahia, L. Gritsch, F.L. Motta, S. Chirani, S. Faré, History and Applications of Hydrogels, J. Biomed. Sci. 04 (2015) 1–23. doi:10.4172/2254-609x.100013.

[48] E.M. Ahmed, Hydrogel: Preparation, characterization, and applications: A review, J. Adv. Res. 6 (2015) 105–121. doi:10.1016/j.jare.2013.07.006.

[49] F. Ullah, M.B.H. Othman, F. Javed, Z. Ahmad, H.M. Akil, Classification, processing and application of hydrogels: A review, Mater. Sci. Eng. C. 57 (2015) 414–433. doi:10.1016/j.msec.2015.07.053.

[50] Y. Meng, J. Lu, Y. Cheng, Q. Li, H. Wang, Lignin-based hydrogels: A review of preparation, properties, and application, Int. J. Biol. Macromol. 135 (2019) 1006–1019. doi:10.1016/j.ijbiomac.2019.05.198.

[51] S. Iravani, R.S. Varma, Greener synthesis of lignin nanoparticles and their applications, Green Chem. 22 (2020) 612–636. doi:10.1039/c9gc02835h.

[52] D. Kun, B. Pukánszky, Polymer/lignin blends: Interactions, properties, applications, Eur. Polym. J. 93 (2017) 618–641. doi:10.1016/j.eurpolymj.2017.04.035.

[53] O. Yu, K.H. Kim, Lignin to materials: A focused review on recent novel lignin applications, Appl. Sci. 10 (2020) 4626. doi:10.3390/app10134626.

[54] D. Rico-García, L. Ruiz-Rubio, L. Pérez-Álvarez, S.L. Hernández-Olmos, G.L. Guerrero-Ramírez, J.L. Vilas-Vilela, Lignin-Based Hydrogels : Synthesis and Applications, Polymers (Basel). 12 (2020) 1–23. doi:10.3390/polym12010081.

[55] R. Mohammadinejad, H. Maleki, E. Larrañeta, A.R. Fajardo, A.B. Nik, A. Shavandi, A. Sheikhi, M. Ghorbanpour, M. Farokhi, P. Govindh, E. Cabane, S. Azizi, A.R. Aref, M. Mozafari, M. Mehrali, S. Thomas, J.F. Mano, Y.K. Mishra, V.K. Thakur, Status and future scope of plant-based green hydrogels in biomedical engineering, Appl. Mater. Today. 16 (2019) 213–246. doi:10.1016/j.apmt.2019.04.010.

[56] L. Wu, S. Huang, J. Zheng, Z. Qiu, X. Lin, Y. Qin, Synthesis and characterization of biomass lignin-based PVA super-absorbent hydrogel, Int. J. Biol. Macromol. 140 (2019) 538–545. doi:10.1016/j.ijbiomac.2019.08.142.

[57] Y. Liu, Y. Huang, C. Zhang, W. Li, C. Chen, Z. Zhang, H. Chen, J. Wang, Y. Li, Y. Zhang, Nano-FeS incorporated into stable lignin hydrogel: A novel strategy for cadmium removal from soil, Environ. Pollut. 264 (2020)

114739. doi:10.1016/j.envpol.2020.114739.

[58] H. Qian, J. Wang, L. Yan, Synthesis of lignin-poly(N-methylaniline)-reduced graphene oxide hydrogel for organic dye and lead ions removal, J. Bioresour. Bioprod. 5 (2020) 204–210. doi:10.1016/j.jobab.2020.07.006.

[59] N. Tahari, P.L. de Hoyos-Martinez, M. Abderrabba, S. Ayadi, J. Labidi, Lignin - montmorillonite hydrogels as toluene adsorbent, Colloids Surfaces A Physicochem. Eng. Asp. 602 (2020) 125108. doi:10.1016/j.colsurfa.2020.125108.

[60] Y. Meng, C. Li, X. Liu, J. Lu, Y. Cheng, L.P. Xiao, H. Wang, Preparation of magnetic hydrogel microspheres of lignin derivate for application in water, Sci. Total Environ. 685 (2019) 847–855. doi:10.1016/j.scitotenv.2019.06.278.

[61] J. Domínguez-Robles, M.S. Peresin, T. Tamminen, A. Rodríguez, E. Larrañeta, A.S. Jääskeläinen, Lignin-based hydrogels with “super-swelling” capacities for dye removal, Int. J. Biol. Macromol. 115 (2018) 1249–1259. doi:10.1016/j.ijbiomac.2018.04.044.

[62] F. Flores-Céspedes, M. Villafranca-Sánchez, M. Fernández-Pérez, Alginate-based hydrogels modified with olive pomace and lignin to removal organic pollutants from aqueous solutions, Int. J. Biol. Macromol. 153 (2020) 883–891. doi:10.1016/j.ijbiomac.2020.03.081.

[63] H. Yuan, J. Peng, T. Ren, Q. Luo, Y. Luo, N. Zhang, Y. Huang, X. Guo, Y. Wu, Novel fluorescent lignin-based hydrogel with cellulose nanofibers and carbon dots for highly efficient adsorption and detection of Cr(VI), Sci. Total Environ. 760 (2021) 143395. doi:10.1016/j.scitotenv.2020.143395.

[64] M. Liu, Y. Liu, J. Shen, S. Zhang, X. Liu, X. Chen, Y. Ma, S. Ren, G. Fang, S. Li, C. Tong Li, T. Sun, Simultaneous removal of Pb2+, Cu2+ and Cd2+ ions from wastewater using hierarchical porous polyacrylic acid grafted with lignin, J. Hazard. Mater. 392 (2020) 122208. doi:10.1016/j.jhazmat.2020.122208.

[65] R.A. Batista, P.J.P. Espitia, J. de S.S. Quintans, M.M. Freitas, M.Â. Cerqueira, J.A. Teixeira, J.C. Cardoso, Hydrogel as an alternative structure for food packaging systems, Carbohydr. Polym. 205 (2019)

106–116. doi:10.1016/j.carbpol.2018.10.006.

[66] I. Spiridon, Biological and pharmaceutical applications of lignin and its derivatives: A mini-review, Cellul. Chem. Technol. 52 (2018) 543–550.

[67] E. Larrañeta, M. Imízcoz, J.X. Toh, N.J. Irwin, A. Ripolin, A. Perminova, J. Domínguez-Robles, A. Rodríguez, R.F. Donnelly, Synthesis and Characterization of Lignin Hydrogels for Potential Applications as Drug Eluting Antimicrobial Coatings for Medical Materials, ACS Sustain. Chem. Eng. 6 (2018) 9037–9046. doi:10.1021/acssuschemeng.8b01371.

[68] W. Yang, E. Fortunati, F. Bertoglio, J.S. Owczarek, G. Bruni, M. Kozanecki, J.M. Kenny, L. Torre, L. Visai, D. Puglia, Polyvinyl alcohol/chitosan hydrogels with enhanced antioxidant and antibacterial properties induced by lignin nanoparticles, Carbohydr. Polym. 181 (2018) 275–284. doi:10.1016/j.carbpol.2017.10.084.

[69] Y. Zhang, B. Yuan, Y. Zhang, Q. Cao, C. Yang, Y. Li, J. Zhou, Biomimetic lignin/poly(ionic liquids) composite hydrogel dressing with excellent mechanical strength, self-healing properties, and reusability, Chem. Eng. J. 400 (2020) 125984. doi:10.1016/j.cej.2020.125984.

[70] L. Musilová, A. Mráček, A. Kovalcik, P. Smolka, A. Minařík, P. Humpolíček, R. Vícha, P. Ponížil, Hyaluronan hydrogels modified by glycinated Kraft lignin: Morphology, swelling, viscoelastic properties and biocompatibility, Carbohydr. Polym. 181 (2018) 394–403. doi:10.1016/j.carbpol.2017.10.048.

[71] W. Farhat, R. Venditti, N. Mignard, M. Taha, F. Becquart, A. Ayoub, Polysaccharides and lignin based hydrogels with potential pharmaceutical use as a drug delivery system produced by a reactive extrusion process, Int. J. Biol. Macromol. 104 (2017) 564–575. doi:10.1016/j.ijbiomac.2017.06.037.

[72] D. Wang, S.H. Lee, J. Kim, C.B. Park, “Waste to Wealth”: Lignin as a Renewable Building Block for Energy Harvesting/Storage and Environmental Remediation, ChemSusChem. 13 (2020) 2807–2827. doi:10.1002/cssc.202000394.

[73] T. Liu, X. Ren, J. Zhang, J. Liu, R. Ou, C. Guo, X. Yu, Q. Wang, Z. Liu, Highly compressible lignin hydrogel electrolytes via double-crosslinked strategy for superior foldable supercapacitors, J. Power Sources. 449

(2020) 227532. doi:10.1016/j.jpowsour.2019.227532.

[74] A. Morales, J. Labidi, P. Gullón, Hydrothermal treatments of walnut shells: A potential pretreatment for subsequent product obtaining, Sci. Total Environ. 764 (2021) 142800. doi:10.1016/j.scitotenv.2020.142800.

[75] A. Morales, F. Hernández-Ramos, L. Sillero, R. Fernández-Marín, I. Dávila, P. Gullón, X. Erdocia, J. Labidi, Multiproduct biorefinery based on almond shells: Impact of the delignification stage on the manufacture of valuable products, Bioresour. Technol. 315 (2020) 123896. doi:10.1016/j.biortech.2020.123896.

[76] M. Infante, F. Ysambertt, M. Hernández, B. Martínez, N. Delgado, B. Bravo, A. Cáceres, G. Chávez, J. Bullón, Microwave assisted oxidative degradation of lignin with hydrogen peroxide and its tensoactive properties, Rev. Tec. La Fac. Ing. Univ. Del Zulia. 30 (2007) 108–117.

[77] I. Dávila, P. Gullón, M.A. Andrés, J. Labidi, Coproduction of lignin and glucose from vine shoots by eco-friendly strategies: Toward the development of an integrated biorefinery, Bioresour. Technol. 244 (2017) 328–337. doi:10.1016/j.biortech.2017.07.104.

[78] A. Morales, J. Labidi, P. Gullón, Assessment of green approaches for the synthesis of physically crosslinked lignin hydrogels, J. Ind. Eng. Chem. 81 (2020) 475–487. doi:10.1016/j.jiec.2019.09.037.

[79] A. Morales, J. Labidi, P. Gullón, Effect of the formulation parameters on the absorption capacity of smart lignin-hydrogels, Eur. Polym. J. 129 (2020) 109631. doi:10.1016/j.eurpolymj.2020.109631.

[80] A.M. Salaberria, R.H. Diaz, M.A. Andrés, S.C.M. Fernandes, J. Labidi, The antifungal activity of functionalized chitin nanocrystals in poly (Lactid Acid) films, Materials (Basel). 10 (2017) 1–16. doi:10.3390/ma10050546.

[81] D.T. Da Silva, R. Herrera, B.M. Heinzmann, J. Calvo, J. Labidi, Nectandra grandiflora by-products obtained by alternative extraction methods as a source of phytochemicals with antioxidant and antifungal properties, Molecules. 23 (2018) 1–16. doi:10.3390/molecules23020372.

[82] D. George, P.U. Maheswari, K.M.M.S. Begum, Synergic formulation of onion peel quercetin loaded chitosan-cellulose hydrogel with green zinc oxide nanoparticles towards controlled release, biocompatibility,

antimicrobial and anticancer activity, Int. J. Biol. Macromol. 132 (2019) 784–794. doi:10.1016/j.ijbiomac.2019.04.008.

[83] E.Y. Jin, S. Lim, S. oh Kim, Y.S. Park, J.K. Jang, M.S. Chung, H. Park, K.S. Shim, Y.J. Choi, Optimization of various extraction methods for quercetin from onion skin using response surface methodology, Food Sci. Biotechnol. 20 (2011) 1727–1733. doi:10.1007/s10068-011-0238-8.

[84] K. Pallab, B. Tapan K, P. Tapas K, K. Ramen, Estimation of Total Flavonoids Content (TFC) and Anti Oxidant Activities of Methanolic Whole Plant Extract of Biophytum Sensitivum Linn, J. Drug Deliv. Ther. 3 (2013) 33–37. doi:10.22270/jddt.v3i4.546.

[85] D. George, K.M.M.S. Begum, P.U. Maheswari, Sugarcane Bagasse (SCB) Based Pristine Cellulose Hydrogel for Delivery of Grape Pomace Polyphenol Drug, Waste and Biomass Valorization. 11 (2020) 851–860. doi:10.1007/s12649-018-0487-3.

[86] M. Saidi, A. Dabbaghi, S. Rahmani, Swelling and drug delivery kinetics of click-synthesized hydrogels based on various combinations of PEG and star-shaped PCL: influence of network parameters on swelling and release behavior, Polym. Bull. 77 (2020) 3989–4010. doi:10.1007/s00289-019-02948-z.

[87] J. Fernández-Rodríguez, X. Erdocia, C. Sánchez, M. González Alriols, J. Labidi, Lignin depolymerization for phenolic monomers production by sustainable processes, J. Energy Chem. 26 (2017) 622–631. doi:10.1016/j.jechem.2017.02.007.

[88] A. Morales, B. Gullón, I. Dávila, G. Eibes, J. Labidi, P. Gullón, Optimization of alkaline pretreatment for the co-production of biopolymer lignin and bioethanol from chestnut shells following a biorefinery approach, Ind. Crops Prod. 124 (2018) 582–592. doi:10.1016/j.indcrop.2018.08.032.

[89] I. Dávila, B. Gullón, J. Labidi, P. Gullón, Multiproduct biorefinery from vine shoots: Bio-ethanol and lignin production, 142 (2019) 612–623.

[90] C. Xu, F. Liu, M.A. Alam, H. Chen, Y. Zhang, C. Liang, H. Xu, S. Huang, J. Xu, Z. Wang, Comparative study on the properties of lignin isolated from different pretreated sugarcane bagasse and its inhibitory effects on enzymatic hydrolysis, Int. J. Biol. Macromol. 146 (2020) 132–140. doi:10.1016/j.ijbiomac.2019.12.270.

[91] J. Li, P. Feng, H. Xiu, J. Li, X. Yang, F. Ma, X. Li, X. Zhang, E. Kozliak, Y. Ji, Morphological changes of lignin during separation of wheat straw components by the hydrothermal-ethanol method, Bioresour. Technol. 294 (2019) 122157. doi:10.1016/j.biortech.2019.122157.

[92] L. Chen, X. Wang, H. Yang, Q. Lu, D. Li, Q. Yang, H. Chen, Study on pyrolysis behaviors of non-woody lignins with TG-FTIR and Py-GC/MS, J. Anal. Appl. Pyrolysis. 113 (2015) 499–507. doi:10.1016/j.jaap.2015.03.018.

[93] S. De, S. Mishra, E. Poonguzhali, M. Rajesh, K. Tamilarasan, Fractionation and characterization of lignin from waste rice straw: Biomass surface chemical composition analysis, Int. J. Biol. Macromol. 145 (2020) 795–803. doi:10.1016/j.ijbiomac.2019.10.068.

[94] A. Sequeiros, J. Labidi, Characterization and determination of the S/G ratio via Py-GC/MS of agricultural and industrial residues, Ind. Crops Prod. 97 (2017) 469–476. doi:10.1016/j.indcrop.2016.12.056.

[95] M. Brahim, N. Boussetta, N. Grimi, E. Vorobiev, I. Zieger-Devin, N. Brosse, Pretreatment optimization from rapeseed straw and lignin characterization, Ind. Crops Prod. 95 (2017) 643–650. doi:10.1016/j.indcrop.2016.11.033.

[96] X. Yang, Y. Zhao, H. Mussana, M. Tessema, L. Liu, Characteristics of cotton fabric modified with chitosan (CS)/cellulose nanocrystal (CNC) nanocomposites, Mater. Lett. 211 (2018) 300–303. doi:10.1016/j.matlet.2017.09.075.

[97] I.A. Gilca, R.E. Ghitescu, A.C. Puitel, V.I. Popa, Preparation of lignin nanoparticles by chemical modification, Iran. Polym. J. 23 (2014) 355–363. doi:10.1007/s13726-014-0232-0.

[98] A.M. Căpraru, E. Ungureanu, L.C. Trincă, Ț. Mălutan, V.I. Popa, Chemical and spectral characteristics of annual plant lignins modified by hydroxymethylation reaction, Cellul. Chem. Technol. 46 (2012) 589–597.

[99] X. Ouyang, Z. Lin, Y. Deng, D. Yang, X. Qiu, Oxidative Degradation of Soda Lignin Assisted by Microwave Irradiation, Chinese J. Chem. Eng. 18 (2010) 695–702. doi:10.1016/S1004-9541(10)60277-7.

[100] D. Zang, F. Liu, M. Zhang, Z. Gao, C. Wang, Novel superhydrophobic and

superoleophilic sawdust as a selective oil sorbent for oil spill cleanup, Chem. Eng. Res. Des. 102 (2015) 34–41. doi:10.1016/j.cherd.2015.06.014.

[101] B. Gullón, P. Gullón, T.A. Lú-Chau, M.T. Moreira, J.M. Lema, G. Eibes, Optimization of solvent extraction of antioxidants from Eucalyptus globulus leaves by response surface methodology: Characterization and assessment of their bioactive properties, Ind. Crops Prod. 108 (2017) 649–659. doi:10.1016/j.indcrop.2017.07.014.

[102] D. Ciolacu, G. Cazacu, New Green Hydrogels Based on Lignin, J. Nanosci. Nanotechnol. 18 (2018) 2811–2822. doi:10.1166/jnn.2018.14290.

[103] N. Thombare, S. Mishra, M.Z. Siddiqui, U. Jha, D. Singh, G.R. Mahajan, Design and development of guar gum based novel, superabsorbent and moisture retaining hydrogels for agricultural applications, Carbohydr. Polym. 185 (2018) 169–178. doi:10.1016/j.carbpol.2018.01.018.

[104] A. Kumar, S.S. Han, PVA-based hydrogels for tissue engineering: A review, Int. J. Polym. Mater. Polym. Biomater. 66 (2017) 159–182. doi:10.1080/00914037.2016.1190930.

[105] K.J. Lee, J. Lee, J.Y. Hong, J. Jang, Influence of amorphous polymer nanoparticles on the crystallization behavior of Poly(vinyl alcohol) nanocomposites, Macromol. Res. 17 (2009) 476–482. doi:10.1007/BF03218895.

[106] X.-Q. Hu, D.-Z. Ye, J.-B. Tang, L.-J. Zhang, X. Zhang, From waste to functional additives: thermal stabilization and toughening of PVA with lignin, RSC Adv. 6 (2016) 13797–13802. doi:10.1039/C5RA26385A.

[107] M.R. Guilherme, F.A. Aouada, A.R. Fajardo, A.F. Martins, A.T. Paulino, M.F.T. Davi, A.F. Rubira, E.C. Muniz, Superabsorbent hydrogels based on polysaccharides for application in agriculture as soil conditioner and nutrient carrier: A review, Eur. Polym. J. 72 (2015) 365–385. doi:10.1016/j.eurpolymj.2015.04.017.

[108] H.S. Mansur, C.M. Sadahira, A.N. Souza, A.A.P. Mansur, FTIR spectroscopy characterization of poly (vinyl alcohol) hydrogel with different hydrolysis degree and chemically crosslinked with glutaraldehyde, Mater. Sci. Eng. C. 28 (2008) 539–548. doi:10.1016/j.msec.2007.10.088.

[109] W.E. Hennink, C.F. van Nostrum, Novel crosslinking methods to design hydrogels, Adv. Drug Deliv. Rev. 64 (2012) 223–236. doi:10.1016/j.addr.2012.09.009.

[110] L.Y. Wang, M.J. Wang, Removal of Heavy Metal Ions by Poly(vinyl alcohol) and Carboxymethyl Cellulose Composite Hydrogels Prepared by a Freeze-Thaw Method, ACS Sustain. Chem. Eng. 4 (2016) 2830–2837. doi:10.1021/acssuschemeng.6b00336.

[111] H. Bian, L. Wei, C. Lin, Q. Ma, H. Dai, J.Y. Zhu, Lignin-Containing Cellulose Nanofibril-Reinforced Polyvinyl Alcohol Hydrogels, ACS Sustain. Chem. Eng. 6 (2018) 4821–4828. doi:10.1021/acssuschemeng.7b04172.

[112] H. Bian, L. Jiao, R. Wang, X. Wang, W. Zhu, H. Dai, Lignin nanoparticles as nano-spacers for tuning the viscoelasticity of cellulose nanofibril reinforced polyvinyl alcohol-borax hydrogel, Eur. Polym. J. 107 (2018) 267–274. doi:10.1016/j.eurpolymj.2018.08.028.

[113] Y. Chen, K. Zheng, L. Niu, Y. Zhang, Y. Liu, C. Wang, F. Chu, Highly mechanical properties nanocomposite hydrogels with biorenewable lignin nanoparticles, Int. J. Biol. Macromol. 128 (2019) 414–420. doi:10.1016/j.ijbiomac.2019.01.099.

[114] X. Han, Z. Lv, F. Ran, L. Dai, C. Li, C. Si, Green and stable piezoresistive pressure sensor based on lignin-silver hybrid nanoparticles/polyvinyl alcohol hydrogel, Int. J. Biol. Macromol. 176 (2021) 78–86. doi:10.1016/j.ijbiomac.2021.02.055.

[115] L. Sun, Z. Mo, Q. Li, D. Zheng, X. Qiu, X. Pan, Facile synthesis and performance of pH/temperature dual-response hydrogel containing lignin-based carbon dots, Int. J. Biol. Macromol. 175 (2021) 516–525. doi:10.1016/j.ijbiomac.2021.02.049.

[116] Q. Wang, J. Guo, X. Lu, X. Ma, S. Cao, X. Pan, Y. Ni, Wearable lignin-based hydrogel electronics: A mini-review, Int. J. Biol. Macromol. 181 (2021) 45–50. doi:10.1016/j.ijbiomac.2021.03.079.

[117] I.E. Raschip, G.E. Hitruc, C. Vasile, M.C. Popescu, Effect of the lignin type on the morphology and thermal properties of the xanthan/lignin hydrogels, Int. J. Biol. Macromol. 54 (2013) 230–237. doi:10.1016/j.ijbiomac.2012.12.036.

[118] R.M. Kalinoski, J. Shi, Hydrogels derived from lignocellulosic compounds: Evaluation of the compositional, structural, mechanical and antimicrobial properties, Ind. Crops Prod. 128 (2019) 323–330. doi:10.1016/j.indcrop.2018.11.002.

[119] J.I. Daza Agudelo, J.M. Badano, I. Rintoul, Kinetics and thermodynamics of swelling and dissolution of PVA gels obtained by freeze-thaw technique, Mater. Chem. Phys. 216 (2018) 14–21. doi:10.1016/j.matchemphys.2018.05.038.

[120] N. Nguyen Van Long, C. Joly, P. Dantigny, Active packaging with antifungal activities, Int. J. Food Microbiol. 220 (2016) 73–90. doi:10.1016/j.ijfoodmicro.2016.01.001.

[121] O.Y. Abdelaziz, D.P. Brink, J. Prothmann, K. Ravi, M. Sun, J. García-Hidalgo, M. Sandahl, C.P. Hulteberg, C. Turner, G. Lidén, M.F. Gorwa-Grauslund, Biological valorization of low molecular weight lignin, Biotechnol. Adv. 34 (2016) 1318–1346. doi:10.1016/j.biotechadv.2016.10.001.

[122] R. Fernández-Marín, M. Mujtaba, D. Cansaran-Duman, G. Ben Salha, M.Á.A. Sánchez, J. Labidi, S.C.M. Fernandes, Effect of deterpenated origanum majorana l. Essential oil on the physicochemical and biological properties of chitosan/β-chitin nanofibers nanocomposite films, Polymers (Basel). 13 (2021) 1507. doi:10.3390/polym13091507.

[123] D. Dey, V. Dharini, S.P. Selvam, E.R. Sadiku, M.M. Kumar, J. Jayaramudu, U.N. Gupta, Physical, antifungal, and biodegradable properties of cellulose nanocrystals and chitosan nanoparticles for food packaging application, Mater. Today Proc. 38 (2021) 860–869. doi:10.1016/j.matpr.2020.04.885.

[124] S.G. Lee, J.S. Parks, H.W. Kang, Quercetin, a functional compound of onion peel, remodels white adipocytes to brown-like adipocytes, J. Nutr. Biochem. 42 (2017) 62–71. doi:10.1016/j.jnutbio.2016.12.018.

[125] M.S. Kim, G.W. Oh, Y.M. Jang, S.C. Ko, W.S. Park, I.W. Choi, Y.M. Kim, W.K. Jung, Antimicrobial hydrogels based on PVA and diphlorethohydroxycarmalol (DPHC) derived from brown alga Ishige okamurae: An in vitro and in vivo study for wound dressing application, Mater. Sci. Eng. C. 107 (2020) 110352. doi:10.1016/j.msec.2019.110352.

[126] T. Demirci, M.E. Hasköylü, M.S. Eroğlu, J. Hemberger, E. Toksoy Öner, Levan-based hydrogels for controlled release of Amphotericin B for dermal local antifungal therapy of Candidiasis, Eur. J. Pharm. Sci. 145 (2020) 105255. doi:10.1016/j.ejps.2020.105255.

[127] C. Luo, A. Guo, Y. Zhao, J. Sun, Z. Li, Facile fabrication of nonswellable and biocompatible hydrogels with cartilage-comparable performances, Mater. Today Commun. 27 (2021) 102375. doi:10.1016/j.mtcomm.2021.102375.

[128] A. Shamloo, Z. Aghababaie, H. Afjoul, M. Jami, M.R. Bidgoli, M. Vossoughi, A. Ramazani, K. Kamyabhesari, Fabrication and evaluation of chitosan/gelatin/PVA hydrogel incorporating honey for wound healing applications: An in vitro, in vivo study, Int. J. Pharm. 592 (2021) 120068. doi:10.1016/j.ijpharm.2020.120068.

[129] Y. Zhang, M. Jiang, Y. Zhang, Q. Cao, X. Wang, Y. Han, Novel lignin – chitosan – PVA composite hydrogel for wound dressing, Mater. Sci. Eng. C. 104 (2019) 110002. https://doi.org/10.1016/j.msec.2019.110002.

[130] O. Gordobil, A. Oberemko, G. Saulis, V. Baublys, J. Labidi, In vitro cytotoxicity studies of industrial Eucalyptus kraft lignins on mouse hepatoma, melanoma and Chinese hamster ovary cells, Int. J. Biol. Macromol. 135 (2019) 353–361. doi:10.1016/j.ijbiomac.2019.05.111.

[131] O. Gordobil, P. Olaizola, J.M. Banales, J. Labidi, Lignins from agroindustrial by-products as natural ingredients for cosmetics: Chemical structure and in vitro sunscreen and cytotoxic activities, Molecules. 25 (2020) 1131. doi:10.3390/molecules25051131.

Atxikitako argitalpenak

A

I. Artikulua

I

Synthesis of advanced biobased green materials from renewable biopolymers

A. Morales, J. Labidi, P. Gullón, G. Astray

http://10.1016/j.cogsc.2020.100436

Curr. Opin. Green Sustain. Chem. 29 (2021) 100436

Available online at www.sciencedirect.com

ScienceDirect

Current Opinion in
Green and Sustainable Chemistry

Synthesis of advanced biobased green materials from renewable biopolymers

Amaia Morales[1], Jalel Labidi[1], Patricia Gullón[2] and Gonzalo Astray[3,4]

Polymeric materials such as hydrogels have become necessary in our daily lives. Hydrogels are three-dimensionally cross-linked polymeric networks that can absorb large amounts of water. Thanks to their properties, hydrogels are very useful in multiple application fields. However, they have usually been obtained from petroleum-derived polymers, contributing to plastic pollution and global warming. In this context, biomass has emerged as an appropriate alternative for production of chemicals, building blocks and biopolymers. Lignin is the second most ample and disposable biopolymer in the world. This biopolymer has been underused until recent decades, but as it has been demonstrated to provide composite materials such as hydrogels with excellent features, its valorization would mean a step forward in sustainability and circular economy. Hence, this review focuses on the state of the art of hydrogels and lignin-based hydrogels, as well as on their current applications.

Addresses
[1] Chemical and Environmental Engineering Department, University of the Basque Country UPV/EHU, Plaza Europa 1, 20018, San Sebastian, Spain
[2] Nutrition and Bromatology Group, Department of Analytical and Food Chemistry, Faculty of Food Science and Technology, University of Vigo, Ourense Campus, 32004, Ourense, Spain
[3] Physical Chemistry Department, Faculty of Sciences, University of Vigo, Ourense Campus, 32004, Ourense, Spain
[4] CITACA, Agri-Food Research and Transfer Cluster, University of Vigo, Campus Auga, 32004, Ourense, Spain

Corresponding author: Gullón, Patricia (patricia.gullon@ehu.es)

Current Opinion in Green and Sustainable Chemistry 2021, **29:**100436

This reviews comes from a themed issue on **Sustainable solutions for renewable wastes**

Edited by **Sara González García** and **Beatriz Gullón**

https://doi.org/10.1016/j.cogsc.2020.100436

Introduction

Currently, synthetic polymer–based materials such as hydrogels have become indispensable for our everyday lives. These materials are usually obtained by polymerizing low-molecular-weight organic compounds that derive from fossil resources. Hydrogels are considered three-dimensionally cross-linked polymeric networks that contain many hydrophilic groups that allow huge absorption of water molecules within their porous structure without being dissolved [1]. Apart from their excellent swelling properties, these materials stand out for their morphology and for their resistance to compression [2]. Different properties (control diffusion process, response to different factors — ionic strength changes, pH and/or temperature — and capacity to trap chemical species) [2] have made that hydrogels grow in popularity in the last decades. Owing to their outstanding features and the wide variety of substrates and forms they can be presented in, hydrogels have been applied in multiple fields such as personal hygiene, agriculture (water retention), environmental remediation (CO_2 capture) and biomedicine (drug delivery, among others) [1]. In fact, their global market represented in 2016 a total of $15.6 billion, and the market should total $22.3 billion in 2022 [3]. However, the high cost related to the complex production process of hydrogels, coupled with environmental hazards from disposable synthetic hydrogel products, is some of the major drawbacks restraining the growth of the market globally.

Since the middle years of the 20th century, the petroleum-derived chemistry, refinery and engineering processes have been the basis of the polymer industry [4]. The first decades of the 21st century have led to a big economic growth together with an irrecoverable environmental concern in which plastic pollution has been remarked as a global crisis. The latest involves plastic's whole life cycle, that is, from its production to its disposal and incineration. In this context, the development of biodegradable polymers has become one of the most suitable alternatives in this industry to face ecological problems [4], contributing at the same time both to sustainability and circular economy [5]. Therefore, the urgent transition from a petroleum-based to a biobased economy has marked the beginning of the current century, shifting the type of carbon resources from fossil to natural and renewable ones [6].

In the search of an appropriate solution to the exposed problem, biomass has resulted to be an alternative to petrochemicals for the production of chemicals, sugars and biopolymers [6]. Biopolymers are classified as natural polymers produced by plants, animals and microorganisms, which present biodegradability [4] as their main advantage. More specifically, lignocellulosic feedstock has emerged as a promising, renewable and vast

source for chemicals. This biomass is mainly constituted by carbohydrate polymers (cellulose and hemicelluloses) and by aromatic polymers (lignin and tannins), which can be isolated and used to form hydrogels without competing with other biopolymers with food applications such as starch. Although biopolymer-based hydrogels can sometimes exhibit poorer mechanical properties than synthetic ones, many strategies have recently been explored to overcome this drawback [7], and for this reason, renewable polymers are showing the tremendous potential to replace traditional polymers owing to their capacity for reducing energy consumption and pollution.

Among the aforementioned biopolymers, lignin, just after cellulose, is the second most plenty and fascinating terrestrial biopolymer [8]. In fact, about 150 billion tons of lignin is annually synthesized by Earth plants [9]. This intricate aromatic macromolecule is mostly constituted by three different types of phenyl propane monomers (p-coumaryl, coniferyl and sinapyl alcohols) that are cross-linked through different stable bondage types [8]. Lignin can be obtained by several isolation methods using different raw materials such as agricultural residues, dedicated crops or wood [8]. Owing to this, it is widely available as an important by-product from different industries, such as pulp and paper industry, among others, and it can be specifically produced in treatments of the new biorefinery schemes.

Figure 1

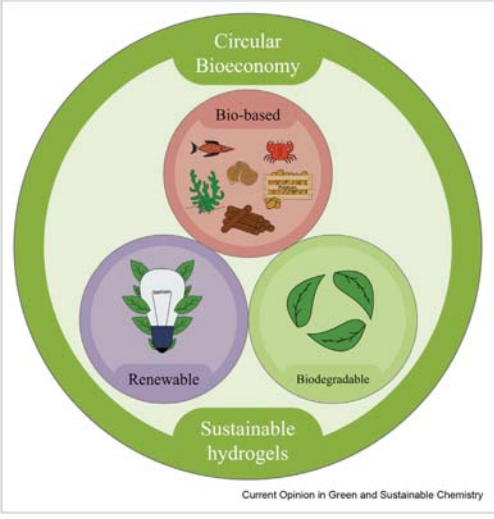

Graphical definition of sustainable hydrogels.

In the last ten years, the development of biorefinery approaches for biomass revalorization has increased the academic and industrial research about lignins. In this sense, renewable lignin as a new feedstock for biomaterial synthesis is being investigated for its positive effect on the thermal behaviour, hydrophilicity, biocompatibility and biodegradability of these systems [10]. Furthermore, its three-dimensional structure makes lignin suitable as a new potential cross-linking component for the development of hydrogels. Thus, the formulation of these materials has experimented a rapid shift from synthetic polymers to biopolymers [11].

Because less than 2% of the total amount of lignin generated by year in pulp and paper industry has an added value [8], the development of new green materials from lignin has attracted great attention from an environmental and economic point of view. Limited oil reserves, the environmental problems caused by the toxic compounds from the degradation of this type of materials and the expanding hydrogel market generate an urgent need for the development of environmentally friendly and safe alternative hydrogels from renewable materials, which would also expand the life cycle opportunities for reuse and recycling of lignocellulosic biomass and contribute to circular bioeconomy (see Figure 1). Hence, the novelty and potentiality of this review are focused on the use of this biopolymer for the synthesis of hydrogels and their applications in several fields to promote sustainable development.

Hydrogels and lignin

Over the last few years, studies on biopolymer-based hydrogels have become very popular owing to their applicability in the fields of food, cosmetics, pharmaceuticals and biomedical implants [12]. Besides, the integration of biopolymers together with other molecules can improve the functionality of the resultant hydrogels, making possible to formulate hydrogels capable of imitating the interrelated nature of human tissue [13]. Among these biopolymers, lignin is the only aromatic one, which makes it interesting for its application on functional hydrogels [12]. Although there is no defined structure for lignin [2], many studies have recently demonstrated that it can be successfully used for the formulation of lignin-derived composites used for tissue scaffolding and drug release or as UV absorbents [14]. Thus, if adequate routes for improving handling of lignin and development of technologies to process it were further investigated, this natural polymer would undoubtedly play an important role in the synthesis of new materials [15]. A clear increasing trend of the publications about lignin and lignin applications in the last years has been reported [9,15,16].

The lignin extraction method determines the type and features of the resultant lignin, which can be more or

less reactive depending on the used technique. The typical types of lignin used for hydrogel synthesis are kraft, lignosulfonate, alkaline and organosolv [2,12]. In any case, there are usually two pathways to valorize this biopolymer: the first one uses lignin as a macropolymer (to obtain valuable materials), whereas the second one implicates lignin depolymerization (to obtain low-molecular-weight monomers) [16]. In case of hydrogels, lignin is usually combined with other biosynthetic or synthetic polymers owing to the lack of self–gel-forming properties. For this reason, it has been included in different polymeric networks through physical interactions or chemical reactions that promote hydrogel structure [2].

Applications of lignin-based hydrogels

A big part of the synthesized lignin-based hydrogels has been used to remove heavy metal and cationic compounds present in aqueous solutions [17]. Nonetheless, Mohammadinejad et al. [17] also report their use in fields such as biomedicine for drug delivery and tissue engineering. Some hydrogel applications studied to date are described in the following paragraphs.

The controlled release of water is a commonly used term in agriculture. In climates wherein rain is scarce, soils need to be irrigated frequently. Nevertheless, equipping soils with small and smart hydrogels, such as lignin-based hydrogels, has proven to absorb significant amounts of water and retain it until the crops require it [12]. The water content of hydrogels can vary based on their degree of cross-linking, which can be controlled during their synthesis. Mazloom et al. [18,19], for instance, synthesized a lignin-based hydrogel (lignin alkali polymers–poly(ethylene glycol) diglycidyl ether) and then tested them as controlled water releasers in agricultural soils, which resulted in promising findings. Meng et al. [20] also prepared some lignin-based hydrogels from copolymerization of acrylic acid and spent sulfite cooking solution (or red liquor) directly obtained from the paper industry. The materials developed by Meng et al. [20] exhibited superswelling and slow-release behaviours in water. Song et al. [21] combined lignin, sodium alginate and konjaku flour for synthesis of hydrogels with excellent soil conditioning properties tested with tobacco plants.

Lignin has functional groups (phenolic hydroxyl, alcohol hydroxyl, methoxy and carboxyl groups) that can act as adsorption sites for dye molecules and heavy metals [22]. According to Meng et al. [12], these structures are therefore capable of attracting positive molecules through negatively charged functional groups and aromatic organics via $\pi-\pi$ reactions. For this reason, they have been used for absorption of both inorganic ions and organic compounds in soils and water [12]. Table 1 summarizes some works in this field.

Thus, according to Andrade Batista et al. [31], hydrogels would be an attractive alternative for their application in food packaging systems as absorbent pads. Apart from water absorption properties, these materials should increase stored food products' shelf life and avoid microbial growth on food surface [31]. Therefore, the antimicrobial activity of the polymers constituting the hydrogel network is crucial. In this context, lignin and its derivates and lignin-based hydrogel coatings have been shown to present antimicrobial behaviour [32–34]. For this reason, Yang et al. [35] proposed that their lignin-based hydrogels with antioxidant and antimicrobial properties could be used in food packaging.

Antimicrobial, antioxidant and low cytotoxicity features are also important for synthesis of biocompatible

Table 1

Literature review of hydrogels as pollutant removers.

Lignin type in hydrogels	Pollutant	Medium	Removal	Reference
Sodium lignosulfonate	Cadmium ions (Cd^{2+})	Soil	<61.77 ± 1.09 mg/g	[23]
Lignin	Methylene blue (MB) and lead ions (Pb^{2+})	Aqueous	201.7 mg/g MB and 753.5 mg/g Pb^{2+}	[24]
Alkali, kraft and organosolv lignins	Toluene	Aqueous	164–170 mg/g	[25]
Aminated alkali lignin	Heavy metal cations (Pb^{2+}, Hg^{2+} and Ni^{2+}) and dyes (MB, methyl orange and malachite green)	Aqueous	2.1–55 mg/g for heavy metal cations and 2–155 mg/g for dyes	[26]
Alkali, kraft and enzymatic hydrolysis lignin	Rhodamine 6G, crystal violet, MB and methyl orange	Aqueous	10–196 mg/g	[22]
Soda, kraft and organosolv lignins	MB	Aqueous	69–629 mg/g	[27]
Pine kraft lignin Indulin AT	Prednisolone drug and 3,4-dichloroaniline	Aqueous	1.35 mg/g for prednisolone and 4 mg/g for 3,4-dichloroaniline	[28]
Alkali lignin	Hexavalent chromium Cr(VI)	Aqueous	599.9 mg/g	[29]
Acid-pretreated alkali lignin	Pb^{2+}, Cu^{2+} and Cd^{2+} ions	Aqueous	1.076 mmol/g for Pb^{2+}, 0.3233 mmol/g for Cu^{2+} and 0.059 mmol/g for Cd^{2+}	[30]

materials. In this sense, hydrogels can provide effective removal of undesirable metabolites from wounds owing to their high absorption capacity, and the addition of lignin may help to protect the wound from future problems such as further injury or contamination, thanks to its good mechanical properties [16]. Hence, lignin has also gained interest in wound dressing [35] and tissue engineering [36].

Lignin-based hydrogels have also been shown to be useful in another important part of the biomedical field: the controlled release of both hydrophobic [33] and hydrophilic drugs. Stimulus-responsive hydrogels can be created by combining other (bio)polymers and lignin. These hydrogels are of great interest in drug delivery because they are able to alter their volume in response to environmental stimuli [37] such as pH, temperature or light [2]. Some authors, for instance, have studied the release kinetics of curcumin-loaded hydrogels at simulated human body conditions [33]. They concluded that as the lignin content was higher, the hydrogels were loaded with higher amounts of the drug, promoting a higher release of it [33].

Finally, the use of lignin-based materials applied to energy devices has proven to be promising [38]. Among other applications, these materials have gained attention as electrode materials for supercapacitors as a result of their high surface areas and chemical stability and superior electrical conductivity [38]. Liu et al. [39], for instance, created hybrid double-cross-linked lignin-based hydrogels by combining corncob lignin media with poly(ethylene glycol) diglycidyl ether in alkaline media and immersing them in sulfuric acid afterwards. These authors reported not only excellent electrochemical performance for their supercapacitors but also improved mechanical properties [39].

Conclusions

Taking all the aforementioned information into account, it can be concluded that, although lignin has been underused in the past, it presents multiple advantages not only from the economical (e.g. high availability and low cost) perspective but also from the environmental (i.e. renewable and biodegradable) and technological (i.e. excellent physicochemical features) points of view, making it greatly potential for many applications. Although lignin-based materials are still at early stages in the global market, many spin-offs, start-ups and companies have placed their bet on them, producing lignin aerogels (Aerogelex UG., Hamburg, Germany), for instance. A deeper understanding of the chemical structure and physicochemical properties of lignin would make it even more interesting and useful for the synthesis of globally used commodities in the near future. Thus, standardization of lignin manufacturing processes would lead to synthesis of bountiful sustainable products such as thermoplastic and elastomeric materials for automotive or building applications, for instance, as well as to production of materials for packaging and electronic applications. Therefore, it is important that research continues in this field to create green and sustainable materials for substitution of conventional ones.

Acknowledgements

AM would like to thank the University of the Basque Country (Training of Researcher Staff, PIF17/207). GA thanks the University of Vigo for his contract supported by 'Programa de retención de talento investigador da Universidade de Vigo para o 2018'.

Author contributions

Amaia Morales: Conceptualization, Writing- Original draft preparation. **Jalel Labidi, Patricia Gullón and Gonzalo Astray**: Supervision, Writing- Reviewing and Editing.

Declaration of competing interest

The authors declare that they have no known competing financial interests or personal relationships that could have appeared to influence the work reported in this paper.

References

Papers of particular interest, published within the period of review, have been highlighted as:

* of special interest

1. Kalinoski RM, Shi J: **Hydrogels derived from lignocellulosic compounds: evaluation of the compositional, structural, mechanical and antimicrobial properties**. *Ind Crop Prod* 2019, **128**:323–330.

2. * Rico-García D, Ruiz-Rubio L, Pérez-Álvarez L, Hernández-Olmos SL, Guerrero-Ramírez GL, Vilas-Vilela JL: **Lignin-based hydrogels: synthesis and applications**. *Polymers* 2020, **12**:81.
This work provides an interesting review about lignin-based hydrogels. For this aim, these authors explain the basic chemistry of lignin as well as its typical extraction methods. In addition, the main preparation routes of lignin-hydrogels reported in the last years are included and the current applications of lignin hydrogels as stimuli-responsive materials, flexible supercapacitors and wearable electronics for biomedical and water remediation applications are presented.

3. Singh V: *Hydrogels: applications and global markets to 2022*. Bccresearch.com; 2017. . [Accessed August 2020].

4. Nakajima H, Dijkstra P, Loos K: **The recent developments in biobased polymers toward general and engineering applications: polymers that are upgraded from biodegradable polymers, analogous to petroleum-derived polymers, and newly developed**. *Polymers* 2017, **9**:523.

5. RameshKumar S, Shaiju P, O'Connor KE, Babu R: **Bio-based and biodegradable polymers - state-of-the-art, challenges and emerging trends**. *Curr. Opin. Green Sustain. Chem.* 2020, **21**:75–81.

6. * Liao JJ, Latif NHA, Trache D, Brosse N, Hussin MH: **Current advancement on the isolation, characterization and application of lignin**. *Int J Biol Macromol* 2020, **162**:985–1024.

7. Bao Z, Xian C, Yuan Q, Liu G, Wu J: **Natural polymer-based hydrogels with enhanced mechanical performances: preparation, structure, and property**. *Adv Healthcare Mater* 2019, **8**: 1900670.

8. Dragone G, Kerssemakers AAJ, Driessen JLSP, Yamakawa CK, Brumano LP, Mussatto SI: **Innovation and strategic**

orientations for the development of advanced biorefineries. *Bioresour Technol* 2020, **302**:122847.

9. Tribot A, Amer G, Alio MA, de Baynast H, Delattre C, Pons A, *et al.*: **Wood-lignin: supply, extraction processes and use as bio-based material**. *Eur Polym J* 2019, **112**:228–240.

10. Morales A, Labidi J, Gullón P: **Assessment of green approaches for the synthesis of physically crosslinked lignin hydrogels**. *J Ind Eng Chem* 2020, **81**:475–487.

11. Thakur VK, Thakur MK: **Recent advances in green hydrogels from lignin: a review**. *Int J Biol Macromol* 2015, **72**:834–847.

12. Meng Y, Lu J, Cheng Y, Li Q, Wang H: **Lignin-based hydrogels: a review of preparation, properties, and application**. *Int J Biol Macromol* 2019, **135**:1006–1019.

13. Ilomuanya MO: **Hydrogels as biodegradable biopolymer formulations**. In *Biopolymer-based formulations – biomedical and food applications*. Edited by Pal K, Banerjee I, Sarkar P, Kim D, Deng WP, Dubey NK, *et al.*, Eds, Elsevier; 2020:561–585.

14. Iravani S, Varma RS: **Greener synthesis of lignin nanoparticles and their applications**. *Green Chem* 2020, **22**: 612–636.

15. Kun D, Pukánszky B: **Polymer/lignin blends: interactions, properties, applications**. *Eur Polym J* 2017, **93**:618–641.

16. * Yu O, Kim KH: **Lignin to materials: a focused review on recent novel lignin applications**. *Appl Sci* 2020, **10**:4626.
This publication reviews the recent research progress in lignin valorization, specifically focusing on medical, electrochemical, and 3D printing applications. The technoeconomic assessment of lignin application is also discussed

17. Mohammadinejad R, Malekib H, Larrañeta E, Fajardo AR, Nik AB, Shavandif A, *et al.*: **Review Status and future scope of plant-based green hydrogels in biomedical engineering**. *Appl. Mater. Today* 2019, **16**:213–246.

18. Mazloom N, Khorassani R, Zohuri GH, Emami H, Whalen J: *Development and characterization of lignin-based hydrogel for use in agricultural soils: preliminary evidence, clean- soil, air, water.* 2019:1900101.

19. Mazloom N, Khorassani R, Zohuri GH, Emami H, Whalen J: **Lignin-based hydrogel alleviates drought stress in maize**. *Environ Exp Bot* 2020, **175**:104055.

20. * Meng Y, Liu X, Li C, Liu H, Cheng Y, Lu J, Zhang K, Wang H: **Super-swelling lignin-based biopolymer hydrogels for soil water retention from paper industry waste**. *Int J Biol Macromol* 2019, **135**:815–820.
This interesting work proposes a novel method for the valorization of the waste generated by pulp and paper industry by fabricating super-swelling biopolymer hydrogels from it. This study reports the first time that hydrogels are prepared by combining non-purified red liquor with acrylic acid, obtaining materials with super-swelling capacities and slow release behaviors in water.

21. Song B, Liang H, Sun R, Peng P, Jiang Y, She D: **Hydrogel synthesis based on lignin/sodium alginate and application in agriculture**. *Int J Biol Macromol* 2020, **144**:219–230.

22. Wu L, Huang S, Zheng J, Qiu Z, Lin X, Qin Y: **Synthesis and characterization of biomass lignin-based PVA superabsorbent hydrogel**. *Int J Biol Macromol* 2019, **140**:538–545.

23. Liu Y, Huang Y, Zhang C, Li W, Chen C, Zhang Z, *et al.*: **Nano-FeS incorporated into stable lignin hydrogel: a novel strategy for cadmium removal from soil**. *Environ Pollut* 2020, **264**: 114739.

24. Qian H, Wang J, Yan L: **Synthesis of lignin-poly(N-methylaniline)-reduced graphene oxide hydrogel for organic dye and lead ions removal**. *J. Bioresour. Bioprod.* 2020, **5**: 204–210.

25. Tahari N, de Hoyos-Martinez PL, Abderrabba M, Ayadi S, Labidi J: **Lignin - montmorillonite hydrogels as toluene adsorbent**. *Colloids Surf. A Physicochem. Eng. Asp.* 2020, **602**: 125108.

26. Meng Y, Li C, Liu X, Lu J, Cheng Y, Xiao L-P, *et al.*: **Preparation of magnetic hydrogel microspheres of lignin derivate for application in water**. *Sci Total Environ* 2019, **685**:847–855.

27. Domínguez-Robles J, Peresin MS, Tamminen T, Rodríguez A, Larrañeta E, Jääskeläinen A-S: **Lignin-based hydrogels with "super-swelling" capacities for dye removal**. *Int J Biol Macromol* 2018, **115**:1249–1259.

28. Flores-Céspedes F, Villafranca-Sánchez M, Fernández-Pérez M: **Alginate-based hydrogels modified with olive pomace and lignin to removal organic pollutants from aqueous solutions**. *Int J Biol Macromol* 2020, **153**:883–891.

29. H. Yuan, J. Peng, T. Ren, Q. Luo, Y. Luo, N. Zhang, *et al.*, Novel fluorescent lignin-based hydrogel with cellulose nanofibers and carbon dots for highly efficient adsorption and detection of Cr(VI), Sci Total Environ https://doi.org/10.1016/j.scitotenv.2020.143395 (in press).

30. Liu M, Liu Y, Shen J, Zhang S, Liu X, Chen X, *et al.*: **Simultaneous removal of Pb^{2+}, Cu^{2+} and Cd^{2+} ions from wastewater using hierarchical porous polyacrylic acid grafted with lignin**. *J Hazard Mater* 2020, **392**:122208.

31. Andrade Batista R, Perez Espitia PJ, de Souza Siqueira Quintans J, Machado Freitas M, Cerqueira MÂ, Teixeira JA, *et al.*: **Hydrogel as an alternative structure for food packaging systems**. *Carbohydr Polym* 2019, **205**:106–116.

32. Spiridon I: **Biological and pharmaceutical applications of lignin and its derivatives: a mini-review**. *Cellul Chem Technol* 2018, **52**:543–550.

33. Larrañeta E, Imízcoz M, Toh JX, Irwin NJ, Ripolin A, Perminova A, *et al.*: **Synthesis and characterization of lignin hydrogels for potential applications as drug eluting antimicrobial coatings for medical materials**. *ACS Sustain Chem Eng* 2018, **6**: 9037–9046.

34. Yang W, Fortunati E, Bertoglio F, Owczarek JS, Bruni G, Kozanecki M, *et al.*: **Polyvinyl alcohol/chitosan hydrogels with enhanced antioxidant and antibacterial properties induced by lignin nanoparticles**. *Carbohydr Polym* 2018, **181**:275–284.

35. * Zhang Y, Yuan B, Zhang Y, Cao Q, Yang C, Li Y, *et al.*: **Biomimetic lignin/poly(ionic liquids) composite hydrogel dressing with excellent mechanical strength, self-healing properties, and reusability**. *Chem Eng J* 2020, **400**:125984.
This work provides the design and synthesis of novel lignin/poly(ionic liquids) composite hydrogels with excellent mechanical strength, self-healing properties, bactericidal activity and antioxidant activity. It is stated that the supramolecular interactions between the lignin/poly(-ionic liquids) compounds enhance the self-healing ability of the materials, and the introduction of lignin produces an improvement on their mechanical properties.of the hydrogel dressing.

36. Musilová L, Mráček A, Kovalcik A, Smolka P, Minařík A, Humpolíček P, *et al.*: **Hyaluronan hydrogels modified by glycinated Kraft lignin: morphology, swelling, viscoelastic properties and biocompatibility**. *Carbohydr Polym* 2018, **181**: 394–403.

37. Farhat W, Venditti R, Mignard N, Taha M, Becquart F, Ayoub A: **Polysaccharides and lignin based hydrogels with potential pharmaceutical use as a drug delivery system produced by a reactive extrusion process**. *Int J Biol Macromol* 2017, **104**: 564–575.

38. * Wang D, Lee SH, Kim J, Park CB: **"Waste to wealth": lignin as a renewable building block for energy harvesting/storage and environmental remediation**. *ChemSusChem* 2020, **13**: 2807–2827.
This work highlights the most recent advances in the development of lignin-based materials for energy and environmental applications, apart from reviewing its physic-chemical properties and possible modifications. The exposed applications include lithium-ion batteries, supercapacitors, solar cells, triboelectric nanogenerators and adsorbents.

39. Liu T, Ren X, Zhang J, Liu J, Ou R, Guo C, *et al.*: **Highly compressible lignin hydrogel electrolytes via double-crosslinked strategy for superior foldable supercapacitors**. *J Power Sources* 2020, **449**:227532.

II. Artikulua

Assessment of green approaches for the synthesis of physically crosslinked lignin hydrogels

II

A. Morales, J. Labidi, P. Gullón

http://10.1016/j.jiec.2019.09.037

J. Ind. Eng. Chem. 81 (2020) 475-487

Journal of Industrial and Engineering Chemistry 81 (2020) 475–487

Contents lists available at ScienceDirect

Journal of Industrial and Engineering Chemistry

journal homepage: www.elsevier.com/locate/jiec

Assessment of green approaches for the synthesis of physically crosslinked lignin hydrogels

Amaia Morales, Jalel Labidi*, Patricia Gullón

Chemical and Environmental Engineering Department, University of the Basque Country UPV/EHU, Plaza Europa 1, 20018 San Sebastián, Spain

ARTICLE INFO

Article history:
Received 2 August 2019
Received in revised form 25 August 2019
Accepted 21 September 2019
Available online 28 September 2019

Keywords:
Lignin
Poly(vinyl alcohol)
Physical crosslinking
Hydrogels
Swelling
Mechanical properties

ABSTRACT

Lignin is an excellent candidate to be used as a starting material for hydrogel synthesis due to its highly functional character. The exhaustible character of the fossil resources linked to the increase of plastic residues in the environment encourages an intensive research on biorenewable and biodegradable polymers to synthesize new materials. Taking into account this current scenario, this work searches for new green routes to elaborate physical hydrogels with excellent capacity of swelling and suitable consistency. To this end, lignin and poly(vinyl alcohol) were blended in different proportions following a three-level-two-factorial design and using six different routes of crosslinking and drying for each set of experiments. The hydrogels formed under the optimal conditions were characterized by FTIR, SEM, XRD, DSC and TGA and their mechanical properties were also evaluated by compression tests. The selected optimum synthesis routes enabled the obtaining of physically crosslinked hydrogels with up to 800% water retention ability. FTIR spectra confirmed the interactions between lignin and PVA showing shifts and modifications on the characteristic bands of the raw polymers. Compression tests showed that all the hydrogels kept complete integrity even compressing them up to an 80% of their initial thickness.

Introduction

Lignocellulosic biomass is mainly composed of carbohydrate polymers (cellulose and hemicellulose), and aromatic polymers (lignin and tannin) [1]. In recent years, these biorenewable polymers have attracted a greater attention of the research community due to the advantages such as eco-friendliness, low cost, biodegradability, etc.

Among these biorenewable polymers, lignin is the second most abundant and fascinating natural polymer next to cellulose. Lignin is primarily composed of three different phenylpropane units, namely, *p*-coumaryl, coniferyl and sinapyl alcohols. Different types of carbon–carbon/and carbon–oxygen bonds are formed between different monomer units in lignin [2]. Lignin can be obtained as a byproduct of the pulp and paper industry, bio-ethanol production and can be specifically generated in new biorefinery schemes [3], however, it is often burnt to generate energy for the process. Nevertheless, if added-value applications were searched for lignin, an integral valorisation of the lignocellulosic feedstock would be enabled and, hence, biorefineries would contribute to a circular economy.

The impressive properties of lignin, such as its high abundance, antioxidant, antimicrobial, and biodegradable nature, along with its CO_2 neutrality and reinforcing capability, make it an excellent candidate for chemical modifications and reactions as well as for the development of new biobased materials [4]. Lignin is, therefore, a low cost environmentally friendly feedstock with a great potential to be used as a starting material for hydrogel synthesis due to its highly functional character (i.e., rich in phenolic and aliphatic hydroxyl groups).

Hydrogels are three-dimensionally crosslinked polymeric networks with high water retention capacity which have significantly gained attention over the last 20 years [5]. They have been employed in many fields such as biomedicine or agriculture and they have become very interesting materials due to their adequate physic-chemical characteristics for many applications [6]. According to the type of crosslinking, they can be classified as physical (with physical entanglements or secondary forces) or chemical (with covalent bondages) hydrogels [5]. Chemical crosslinking is the highly resourceful method for the formation of hydrogels having an excellent mechanical strength but the crosslinkers used in hydrogel preparation should be extracted from the hydrogels before use due to their reported toxicity, which is a considerable inconvenience. Physical crosslinking methods for the preparation of hydrogels are the alternative solution to crosslinkers' toxicity and cost. They are usually formed by hydrogen bondages and

* Corresponding author.
E-mail address: jalel.labidi@ehu.es (J. Labidi).

https://doi.org/10.1016/j.jiec.2019.09.037
1226-086X/

electrostatic, hydrophobic and host-guest interactions [7]. However, due to the weak nature of these forces, these hydrogels are also known as reversible hydrogels and sometimes disintegrate and dissolve in water [8] and they can also be thermally reversible [9]. Nevertheless, the weakness problem can be solved by supramolecular chemistry [7,10] and the reversibility can be an advantage when talking about self-healable hydrogels, which have gained great interest in the last years [11,12]. Therefore, it is clear that physically crosslinked hydrogels present several benefits that chemically crosslinked ones do not, enabling at the same time a greener and a more economical synthesis process [13].

The increase of concern about the environmental and health impacts caused by the use of non-biodegradable polymers produced from fossil resources requires an urgent shift to renewable carbon-resource. This is why the possibility of synthesizing bio-based hydrogels has been investigated recently. The abundance and the cheapness of lignin, as well as the need to valorize it, have made lignin attractive to employ as a backbone polymer for hydrogel synthesis. Some authors have already incorporated lignin into hydrogels [14,15], but as it has a complex structure, it is difficult to design precise synthesis and obtain materials with the desired properties. Nevertheless, in spite of their brownish colour, the applicability of the lignin-based hydrogels is considerably wide (see Table 1). However, in most of the cases, chemical crosslinking has been performed and, hence, toxic reagents have been employed [2].

According to the aforementioned, the aim of this work was to find the optimum synthesis route to produce physical hybrid hydrogels based on biodegradable polymers via a greener synthesis route, avoiding the use of toxic chemical reagents. To this end, lignin was blended with poly(vinyl alcohol) (PVA), which is a biodegradable and non-toxic synthetic polymer [16]. In this way, the interactions between both components in the blend would enable the generation of highly hydrophilic three-dimensional networks. An experimental design was employed as the basis of the hydrogel synthesis, with lignin and PVA concentrations as input variables and lignin waste and swelling rate as output dependent variables. Three levels of the input variables were studied, which led to a factorial design of 3 levels, 3^2, with a triplicate central point. Eleven experiments were designed and they were subjected to six different synthesis pathways, varying the crosslinking method and curing method, in order to obtain the optimal lignin and PVA concentrations as well as the better synthesis routes to minimize the lignin waste and maximize the swelling rate. The accuracy of the six models was then evaluated by statistical analysis and, after selecting the best models, the hydrogels formed under the optimal conditions were characterized by Attenuated Total Reflection-Fourier Transformed Infrared Radiation (FTIR), Scanning Electron Microscopy (SEM), X-Ray Diffraction (XRD), Differential Scanning Calorimetry (DSC) and Thermogravimetric Analysis (TGA). Their mechanical properties were also evaluated by compression tests.

Materials and methods

Materials

Alkaline lignin and poly(vinyl alcohol) (PVA, M_w = 83,000–124,000 g/mol, 99+ % hydrolyzed) were supplied by Sigma Aldrich. Sodium hydroxide (NaOH, analytical grade, ≥98%, pellets) was purchased from PanReac Química SLU. All reagents were employed as supplied.

Hydrogel synthesis

Different hydrogels were synthesized according to the combinations designed by an experimental model (see Section "Model description"), in which the input variables were both the lignin and the PVA concentrations. All the hydrogels were prepared by adding the corresponding PVA amount (5, 8 or 11% (w/w)), i.e. 0.5, 0.8 or 1.1 g of PVA to 10 mL of a 2% NaOH aqueous solution, which was magnetically stirred and heated to 80–90 °C simultaneously. When the PVA pellets were dissolved, the corresponding amount of lignin (5, 15 or 25% (w/w), i.e. 0.5, 1.5 or 2.5 g) was incorporated under agitation until it was completely dissolved. Defined amounts of the blends were poured into silicon moulds and the bubbles on the surface were poked manually with a needle, while the ones trapped in the solution were eliminated by introducing the moulds into an ultrasound bath.

In order to study the influence of the synthesis paths, the blends were subjected to three different crosslinking (XL) methods: 3 and 5 cycles of freeze-thawing (16 h at −20 °C and 8 h at 28 °C) and inside a vacuum hood at 37 °C (−60 cm Hg) for a week. After the crosslinking stage, the hydrogels were separately washed in 50 mL of distilled water with orbital shaking several times. The washing was performed so as to eliminate the non-reacted lignin and the residual NaOH. Afterwards, the hydrogels were dried in two different ways: half of them were left to dry at room temperature while the other half dried under vacuum (−60 cm Hg) at 27 °C. These two drying or curing methods were employed in order to observe the influence of this stage (Fig. 1).

The hydrogels with the optimal compositions were prepared similarly employing the corresponding amounts of lignin and PVA into 15 mL of a 2% NaOH solution.

The six synthesis routes depicted in Fig. 2 represent the following used paths:

(1) Vacuum XL + Air Drying (Vac–Air)
(2) Vacuum XL + Vacuum Drying (Vac–Vac)
(3) 5 Cycles of Freeze–Thawing XL + Air Drying (F–T x5–Air)

Table 1
Literature overview about hydrogels with lignin and their applications.

Crosslinking type	Interactions	Type of hydrogel	Polymers	Applications	References
Chemical	Ester bondages	Synthetic polymer based	Poly(methyl vinyl ether *co*-maleic acid) and different technical lignins	Water purification	[15]
Chemical	Ester bondages	Synthetic polymer based	Lignin and poly(ethylene glycol)/ poly(methyl vinyl ether-*co*-maleic acid)	Drug delivery	[35]
Chemical	Chemical crosslinker	Polysaccharide-based	Glycinated Kraft lignin and Hyaluronan	Tissue engineering	[36]
Chemical	Chemical crosslinker	Synthetic polymer based	Poly(vinyl alcohol), cellulose nanofibrils and lignin	Pressure sensors	[37]
Chemical	Chemical crosslinker	Polysaccharide-based	Agarose and Kraft lignin	Non determined	[29]
Physical	Co-dissolution in 1-ethyl-3-methylimidazolium acetate	Polysaccharide- based beads	Cellulose and lignin	Lipase immobilizers	[14]
Physical	Electrostatic interactions	Polysaccharide-based	Chitosan and lignin	Scaffolds in tissue engineering	[38]

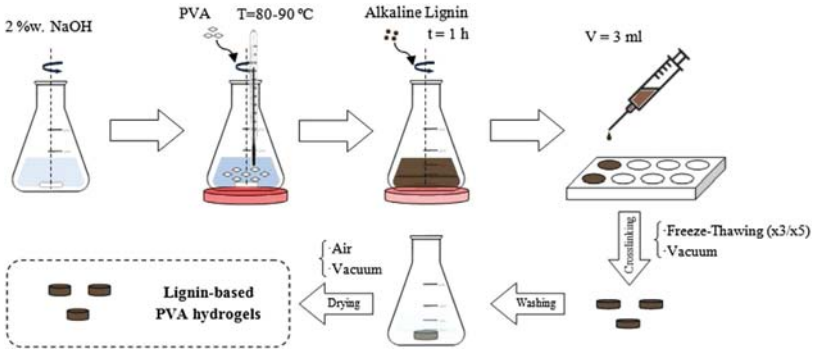

Fig. 1. Diagram of the experimental procedure of the hydrogel synthesis.

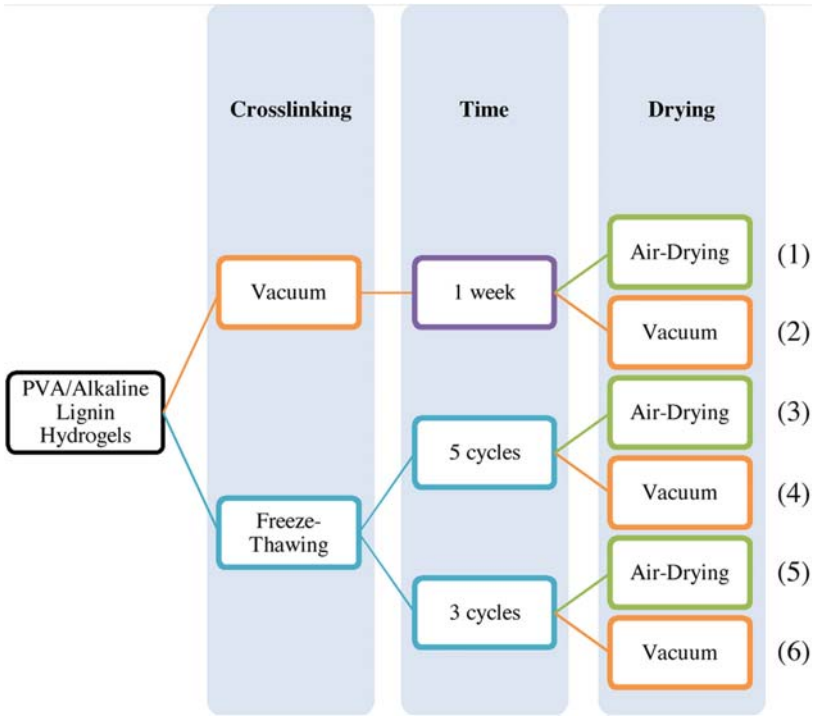

Fig. 2. Scheme of the six hydrogel synthesis pathways.

(4) 5 Cycles of Freeze–Thawing XL + Vacuum Drying (F–T x5–Vac)
(5) 3 Cycles of Freeze–Thawing XL + Air Drying (F–T x3–Air)
(6) 3 Cycles of Freeze–Thawing XL + Vacuum Drying (F–T x3–Vac)

Model description

Three-level-two-factorial design with three replicates in the central point and a Response Surface Methodology (RSM) were employed to perform the optimization of the conditions of the lignin-hydrogel synthesis. The selected independent variables were both the alkaline lignin (x_1) and the PVA concentrations (x_2), which ranged from 5 to 25% (w/w) and from 5 to 11% (w/w), respectively. These ranges were chosen on the basis of previous experiments (data not shown). The response variables were the swelling capacity of the hydrogels (%, y_1) and the lignin waste during the washing stage (%, y_2). Moreover, the accuracy of each of the models would also help to select the best synthesis route. Eleven experiments were designed for each pathway considering the selected parameter values and the triplicate central point (see Table 2), so sixty six experiments were carried out in total. Experimental data were fitted using a second-order polynomial described by Eq. (1):

$$y_j = \beta_0 + \beta_1 x_1 + \beta_2 x_2 + \beta_{11} x_1^2 + \beta_{22} x_2^2 + \beta_{12} x_1 x_2 \quad (1)$$

where y_j are the dependent variables (j = 1–2), β_0, β_1, β_2, β_{11}, β_{22} and β_{12} are the regression coefficients calculated from the experimental results by the least-squares method, and x_1 and x_2 are the

Table 2
Experimental design.

Experiment #	x_1	x_2	Alkaline lignin (%, w/w)	PVA (%, w/w)
1	−1	−1	5	5
2	−1	0	5	8
3	−1	1	5	11
4	0	−1	15	5
5	0	0	15	8
6	0	0	15	8
7	0	0	15	8
8	0	1	15	11
9	1	−1	25	5
10	1	0	25	8
11	1	1	25	11

dimensionless, normalized independent variables, with variation ranges from −1 to 1. Experimental data were fitted using the regression analysis function of Microsoft Excel's Data Analysis Add-In, USA. The adequacy of the model was determined by evaluating the lack of fit, the coefficient of determination (R^2) and the F-test value obtained from the analysis of variance.

To generate the experimental design, the statistical analysis and the regression model, Statgraphics Centurion version XVI (Statpoint Technologies Inc., Warrenton, VA, USA) software was employed. The figures were reproduced using OriginPro®9 (OriginLab Corp., Northampton, MA, USA). The models were validated by carrying out the experiments at the optimal points and comparing the results obtained experimentally with the predicted data.

Hydrogel characterization

Lignin waste

First, a calibration curve was performed by employing five lignin solutions (10 mL) prepared in 2% (w/w) NaOH with known concentrations (0.25, 0.5, 1.5, 2.5 and 5.0 mg lignin/mL solution) and a V-630 UV-Jasco spectrophotometer. In order to fix the correct wavelength to measure the absorbance of the samples, a preliminary scan was performed from 760 to 250 nm. Thus, the measurements were done at 515 nm and each absorbance was related to the concentration of the prepared dissolutions. In this way, a calibration curve was obtained, which corresponded to Eq. (2):

$$A_{515nm} = 0.7643 \cdot [Lignin] \quad (2)$$

The hydrogels were washed in 50 mL of distilled water until the water was clear, for 24–30 h approximately. During the washing stage, aliquots were taken each time and the washing water was changed every 2–3 h. The concentrations of the aliquots were calculated from the measured absorbance at 515 nm. Finally, taking the volume of each rinse into account, the total lignin loss was calculated.

Swelling

The hydrogels were weighted in dry state and immersed in 40 mL of distilled water for 48 h. For the swelling kinetics, the hydrogels were weighted at certain times, removing the water remaining on the surface with filter paper. The swelling degree was calculated from the following Eq. (3) [6]:

$$Swelling\,(\%) = \frac{m_{swollen} - m_{dry}}{m_{dry}} \cdot 100 \quad (3)$$

in which $m_{swollen}$ and m_{dry} are the masses of swollen and dry hydrogels, respectively.

Attenuated Total Reflection-Fourier Transformed Infrared Radiation (ATR-FTIR)

In order to study and verify the interactions between the polymers, a PerkinElmer Spectrum Two FT-IR Spectrometer equipped with a Universal Attenuated Total Reflectance accessory with internal reflection diamond crystal lens was used to collect Infrared spectra of the hydrogels. The studied range was from 600 to 4000 cm^{-1} and the resolution was 8 cm^{-1}. 20 scans were recorded for each grated dry sample.

Scanning Electron Microscopy (SEM)

SEM analyses were carried out in order to study the morphology of the hydrogels. The samples were swollen in water for 48 h at room temperature and then frozen at −20 °C. Afterwards, they were freeze-dried in an Alpha 1–4 LD freeze drier. The images of secondary electrons were taken with a MEB JEOL 7000-F. The working conditions were 5 kV and an intensity of 0.1 nA. The samples were covered with 20 nm of Cr by sputtering technique.

X-Ray Diffraction (XRD)

X-Ray Powder Diffraction tests were carried out using a Phillips X'Pert PRO automatic diffractometer operating at 40 kV and 40 mA, in theta-theta configuration. Monochromatic Cu-Kα (λ = 1.5418 Å) radiation and a PIXcel solid-state detector (active length in 2θ 3.347°) were employed. The collected data ranged from 5 to 80° 2θ at room temperature. The step size was 0.026 and the time per step was 80 s. 0.04 rad soller slit and fixed 1° divergence slit giving a constant volume of sample illumination were employed. The samples were subjected to XRD analysis grated and in dry state.

The approximate size (D) of crystallites was calculated using the Scherrer equation (Eq. (4)):

$$D = \frac{k \cdot \lambda}{\beta \cdot \cos\theta} \quad (4)$$

where D is the mean size of ordered domains (nm), k is the Scherrer constant (0.9), λ is the X-ray wavelength (0.154 nm) and β is the full-width at half-maximum of the reflection (FWHM) measured in 2θ of the corresponding Bragg angle [17,18].

Differential Scanning Calorimetry (DSC)

DSC analyses were done on a Mettler Toledo DSC 822 (Mettler Toledo, Spain). Between 3–5 mg of dry grated samples were subjected to a heating ramp from −25 °C to 225 °C at a rate of 10 °C/min under a nitrogen atmosphere to avoid oxidative reactions inside aluminium pans. After the first heating step, cooling and second heating stages were also performed. The glass transition temperature (T_g), was considered as the inflection point of the specific heat increment during the second heating scan. The calibration was performed with indium standard. The degree of crystallinity (χ_c) was obtained from the enthalpy evolved during crystallization using Eq. (5) [19]:

$$\chi_c = \frac{\Delta H}{\Delta H_0 \cdot (1 - m_{filler})} \cdot 100 \quad (5)$$

where ΔH, is the apparent enthalpy for melting or crystallization, ΔH_0 is the melting enthalpy of 100% crystalline PVA (average value: 161.6 J/g) and $(1 - m_{filler})$ is the weight percent of PVA in the hydrogels [19].

Thermogravimetric Analysis (TGA)

TGA analyses were done on a TGA/SDTA 851 Mettler Toledo (Mettler Toledo, Spain) instrument. Around 7 mg of dry grated sample were subjected to a heating ramp of 25 °C/min from room temperature up to 800 °C under a nitrogen atmosphere inside platinum pans.

Compression studies

Uniaxial compression tests were performed on the hydrogels in order to assess their mechanical strength. A compression gear was

set up on an Instron 5967 machine using a 500 N load cell with a crosshead speed of 2 mm/min. Square samples of around 5 × 5 mm were cut from the initial hydrogels, which were left to swell during 48 h at room temperature. Then, the samples were compressed up to the 80% of their initial thickness. This strain was selected according to other works and the limitations of the compression test equipment caused by the thicknesses of the samples. The swollen modulus, G_e, of each sample was calculated automatically by employing Eq. (6) [20,21]

$$\sigma = \frac{F}{A} = G_e \cdot \left(\lambda - \frac{1}{\lambda^2}\right) \quad (6)$$

where F is the force, A is the original cross sectional area of the swollen hydrogel, and $\lambda = L/L_0$ where L_0 and L are the thicknesses of the samples before and after compression, respectively.

Results and discussion

Modelling and optimization of hydrogel composition

In order to obtain the best hydrogel formulations and the best synthesis route, the optimization of the input variables was addressed using the three-level-two-factorial design combined with Response Surface Methodology for the six synthesis pathways. The results for the all the measured swelling capacities and lignin wastes are shown in Table 3. The six optimal concentrations for the maximum swelling and the minimum lignin waste calculated by the software, as well as the predicted values of the response variables, are shown in Table 4. The optimal conditions of the six paths were verified by the triplicate synthesis of the hydrogels.

Table 5 shows the regression coefficients obtained for each model according to a second-degree polynomial equation, their statistical significance (based on a Student's t-test), the parameters measuring the correlation (R^2) and statistical significance (Fisher's F test) of the models. The value determined for R^2 for most of the variables was higher than 0.86, which would indicate that the model was adequate to represent the real relationships among the selected variables [22], but in some other cases this value was lower than 0.82. Moreover, the estimated significance levels confirm the regular fit of the data. The values for each equation term were calculated in order to assess the contribution of their linear interaction, and quadratic effects of the independent variables. Employing the calculated significant regression coefficients at the 90% confidential level, two quadratic regression equations were set up, one for each output variable (y_1-Swelling and y_2-Lignin waste), for the six models. Hence, twelve equations were obtained in total Eqs. (7)–(18):

(1) Vacuum XL + Air Drying (Vac–Air):

$$y_{1(Swelling\ \%)} = 778.78 + 40.67x_1 - 64.45x_2 - 344.30x_1^2 + 42.65x_2^2 - 16.27x_1x_2 \quad (7)$$

$$y_{2(Lignin\ Waste\ \%)} = 80.99 - 0.93x_1 - 3.34x_2 - 10.18x_1^2 - 2.91x_2^2 + 6.19x_1x_2 \quad (8)$$

(2) Vacuum XL + Vacuum Drying (Vac–Vac)

$$y_{1(Swelling\ \%)} = 1144.76 + 46.89x_1 - 146.12x_2 - 686.08x_1^2 + 100.40x_2^2 - 26.17x_1x_2 \quad (9)$$

$$y_{2(Lignin\ Waste\ \%)} = 80.99 - 0.93x_1 - 3.34x_2 - 10.18x_1^2 - 2.91x_2^2 + 6.19x_1x_2 \quad (10)$$

Table 3
Values of the response variables for the six synthesis paths.

	(1) Vac–Air		(2) Vac–Vac		(3) F–T x5–Air		(4) F–T x5–Vac		(5) F–T x3–Air		(6) F–T x3–Vac	
	Swelling (%)	Ligning waste (%)	Swelling (%)	Ligning waste (%)	Swelling (%)	Ligning waste (%)	Swelling (%)	Ligning waste (%)	Swelling (%)	Ligning waste (%)	Swelling (%)	Ligning waste (%)
E1	454.52	77.90	467.93	77.90	732.94	77.90	411.06	77.90	968.07	68.90	910.01	68.90
E2	435.68	72.43	512.54	72.43	757.72	72.43	656.48	72.43	659.40	44.89	712.96	44.89
E3	376.51	59.03	455.68	59.03	562.00	59.03	553.42	59.03	397.16	44.49	463.58	44.49
E4	909.86	79.82	1647.59	79.82	970.53	79.82	314.48	79.82	779.88	68.08	380.05	68.08
E5	754.12	85.15	1172.55	85.15	905.98	85.15	434.21	85.15	584.94	66.49	674.16	66.49
E6	764.04	80.53	947.88	80.53	965.14	80.53	473.91	80.53	532.82	71.26	627.44	71.26
E7	806.91	80.81	1256.51	80.81	865.27	80.81	537.01	80.81	584.92	76.28	479.17	76.28
E8	744.23	72.79	900.06	72.79	704.59	72.79	372.25	72.79	367.62	65.20	521.91	65.20
E9	604.65	66.15	686.14	66.15	666.55	66.15	370.30	66.15	489.03	60.14	440.44	60.14
E10	444.50	65.63	462.15	65.63	534.15	65.63	432.10	65.63	512.94	48.40	505.00	48.40
E11	461.56	72.02	569.20	72.02	513.25	72.02	535.53	72.02	795.10	44.52	739.20	44.52

Table 4
Optimal conditions and predicted/experimental values for the response variables.

Synthesis route	Alkaline lignin (%, w/w)	PVA (%, w/w)	Predicted value		Experimental average value		Error (%)	
			Swelling (%)	Ligning waste (%)	Swelling (%)	Ligning waste (%)	Swelling (%)	Ligning waste (%)
(1)	23.02	5	710.29	69.17	345.30	81.16	51.39	−17.34
(2)	22.26	5	1083.59	70.88	199.26	82.75	81.61	−16.74
(3)	9.12	9.87	770.14	58.11	789.89	51.94	−2.57	10.63
(4)	5	10.39	587.82	49.09	567.06	41.06	3.53	16.35
(5)	25	11	719.77	46.71	659.67	45.77	8.35	2.02
(6)	25	11	729.51	46.71	547.93	44.12	24.90	5.55

Table 5
Regression coefficients and statistical parameters measuring the correlation and significance of the models.

	(1) Vac–Air		(2) Vac–Vac		(3) F–T x5–Air		(4) F–T x5–Vac		(5) F–T x3–Air		(6) F–T x3–Vac	
	y_1	y_2	y_1	y_2	y_1	y_2	y_1	y_2	y_1	y_2	y_1	y_2
β_0	778.78	80.99	1144.76	80.99	902.17	69.08	468.74	69.08	552.83	68.70	557.40	68.70
β_1	40.67[b]	−0.93	46.89	−0.93	−56.45	−1.83	−47.17	−1.83	−37.92	−0.87	−66.98	−0.87
β_2	−64.45[a]	−3.34	−146.12	−3.34	−98.37[b]	−10.58[a]	60.89[c]	−10.58[a]	−112.85[b]	−7.15[c]	−0.96	−7.15[c]
β_{11}	−344.30[a]	−10.18[a]	−686.08[a]	−10.18[a]	−241.29[a]	−14.26[a]	95.02[c]	−14.26[a]	55.44	−18.08[b]	105.88	−18.08[b]
β_{22}	42.65	−2.91	100.40	−2.91	−49.67	0.03	−105.90[c]	0.03	43.03	1.91	−52.12	1.91
β_{12}	−16.27	6.19[b]	−26.17	6.19[b]	4.41	1.49	5.72	1.49	219.24[a]	2.20	186.30[b]	2.20
R^2	0.98	0.92	0.86	0.92	0.93	0.90	0.76	0.90	0.89	0.82	0.77	0.82
F-exp	50.93	11.12	5.96	11.12	13.53	9.22	3.24	9.22	8.467	4.44	3.32	4.44
S.L.* (%)	99.97	99.03	96.39	99.03	99.37	98.54	88.87	98.54	98.24	93.61	89.29	93.61

* Significance level.
[a] Significant coefficients at the 99% confidence level.
[b] Significant coefficients at the 95% confidence level.
[c] Significant coefficients at the 90% confidence level.

(3) 5 cycles of Freeze–Thawing XL + Air Drying (F–T x5–Air)

$$y_{1(Swelling\ \%)} = 902.17 - 56.45x_1 - 98.37x_2 - 241.29x_1^2 - 49.67x_2^2 + 4.41x_1x_2 \quad (11)$$

$$y_{2(Lignin\ Waste\ \%)} = 69.08 - 1.83x_1 - 10.58x_2 - 14.26x_1^2 + 0.03x_2^2 + 1.49x_1x_2 \quad (12)$$

(4) 5 cycles of Freeze–Thawing XL + Vacuum Drying (F–T x5–Vac)

$$y_{1(Swelling\ \%)} = 468.74 - 47.17x_1 + 60.89x_2 + 95.02x_1^2 - 105.90x_2^2 + 5.72x_1x_2 \quad (13)$$

$$y_{2(Lignin\ Waste\ \%)} = 69.08 - 1.83x_1 - 10.58x_2 - 14.26x_1^2 + 0.03x_2^2 + 1.49x_1x_2 \quad (14)$$

(5) 3 cycles of Freeze–Thawing XL + Air Drying (F–T x3–Air)

$$y_{1(Swelling\ \%)} = 552.83 - 37.92x_1 - 112.85x_2 + 55.44x_1^2 + 43.03x_2^2 + 219.24x_1x_2 \quad (15)$$

$$y_{2(Lignin\ Waste\ \%)} = 68.70 - 0.87x_1 - 7.15x_2 - 18.08x_1^2 + 1.91x_2^2 + 2.20x_1x_2 \quad (16)$$

(6) 3 cycles of Freeze–Thawing XL + Vacuum Drying (F–T x3–Vac)

$$y_{1(Swelling\ \%)} = 557.40 - 66.98x_1 - 0.96x_2 + 105.88x_1^2 - 52.12x_2^2 + 186.30x_1x_2 \quad (17)$$

$$y_{2(Lignin\ Waste\ \%)} = 68.70 - 0.87x_1 - 7.15x_2 - 18.08x_1^2 + 1.91x_2^2 + 2.20x_1x_2 \quad (18)$$

Influence of the input variables on the swelling capacity

For the Vac–Air synthesis pathway, the minimum value (376%) was for experiment 3 while the maximum (909%) was registered for experiment 4 (see Table 3). For the Vac–Vac synthesis route, the minimum was also for experiment 3 (455%) whereas the maximum was for experiment 4 (1647%) too. Based on these results, it could be observed that despite being the minimum and maximum values for the same experiments, the type of drying has an effect on the swelling capacity, in fact, vacuum drying enhances it. It is worth to mention that experiment 4 had a film-like shape, so the contact surface with water was higher and this is why it was so swollen. However, for the other two vacuum dried routes, vacuum reduced the subsequent swelling rate of the hydrogels. In the case of F–T x5–Air synthesis, the minimum was found on experiment 11 (513%) and the maximum value was again for experiment 4 (970%). At the F–T x5–Vac synthesis, the minimum was observed for experiment 4 (314%) while the maximum value was for experiment 2 (656%). The swelling ability for the F–T x3–Air experiments ranged from 367 to 968%, being the minimum for the experiment 8 and the maximum for experiment 1. The values for F–T x3–Vac hydrogels were in the interval of 380–910 %, where the minimum value corresponded to experiment 4 whereas the maximum corresponded to experiment 1.

According to the regression coefficients (Table 5), it could be seen that the two input variables had an influence on the swelling capacity. Specifically, x_2 (PVA concentration) had a significant influence on this output variable, as well as the quadratic effect of x_1 (lignin concentration). The interaction between both input variables was also important in the case of the F–T x3–Air and F–T x3–Vac. The quadratic effect of x_2 presented a high influence on F–T x5–Vac synthesis. Ciolacu et al. (2017) and Yang et al. (2018) did also report that the swelling capacity depends on the composition of the hydrogels [18,23].

The surface plots for synthesis routes (1), (2) and (3) showed that for a fixed concentration of PVA, as lignin content was augmented, the swelling capacity of the hydrogel tended to increase (see Supplementary data). However, after a certain concentration of lignin, the swelling capacity decreased. So, it was found that the maximum point was in between the extreme concentrations of lignin. It is also worth to mention that the swelling ability was displayed to be higher for lower PVA concentrations, but the response variable was much more influenced by the lignin content than by PVA one. This behavior could be due to the high influence of the quadratic term of lignin on the swelling equations [22].The optimal conditions for routes (1),

(2) and (3) were 15.8% lignin and 5% PVA, 15.5% lignin and 5% PVA and 13.7% lignin and 5.3% PVA, subsequently.

The surface plots for synthesis routes (4), (5) and (6) showed that for a fixed concentration of PVA, as lignin content was augmented, the swelling capacity of the hydrogel tended to decrease (see Supplementary data). Nevertheless, after a certain concentration of lignin, the swelling capacity started to increase again. Therefore, the surfaces presented a minimum in between the extreme contents of lignin and, therefore, the highest swelling capacities were found on the upper and lower concentration limits. Thus, the optimal conditions for the achievement of the highest swelling capacities following the routes (4), (5) and (6) were 5% lignin and 8.8% PVA, 5% lignin and 5% PVA and 5% lignin and 5% PVA, subsequently. In these three surfaces, however, no clear dominant variable was observed, since the quadratic terms did not have such a high significance level.

It was clearly seen that the addition of lignin did, in all cases, have a positive effect on the swelling properties of the PVA hydrogels. This fact was confirmed by the synthesis and characterization of the blank hydrogels, i.e., neat PVA hydrogels with concentrations of 5, 8 and 11% PVA and the same crosslinking and drying pathways than the ones with lignin. In fact, the swelling ratio of these materials did not almost overpass the 350%. This behaviour may be attributed to the size of the attached lignin molecules, since they are high molecular weight chains and they can lead to the creation of bigger pores, which can permit the penetration of more water molecules [18,24]. This fact would justify the incorporation of lignin into water absorbent polymeric materials. Ciolacu et al. also reported the same behaviour for their PVA-lignin chemically crosslinked hydrogels [18]. Yang et al. also confirmed that lignin improved the swelling ability of chitosan-PVA hydrogels [25].

Influence of the input variables on the lignin waste

The lignin waste of the 11 experiments in Vac–Air and Vac–Vac synthesis pathways were in the interval of 59–85 %. The minimum value was found for experiment 3 while the maximum was registered for experiment 5 (see Table 3). For the F–T x3–Air and F–T x3–Vac synthesis routes, the minimum was for experiment 11 (42%) whereas the maximum was for experiment 7 (76%). In the case of F–T x5–Air synthesis, the minimum was found on experiment 3 (44%) and the maximum value was again experiment 7 (76%). It could be observed that the freeze–thawing method permits the retention of more lignin inside the matrix than the vacuum crosslinking. Moreover, the ranges in both freeze–thawing routes were very similar.

For the Vac–Air and Vac–Vac synthesis routes the most influencing regression coefficients on the lignin waste were the quadratic effect of x_1 and the interaction between both input variables x_1x_2. In the other four synthesis pathways, the most significant regression coefficients were the quadratic effect of x_1 and x_2 (PVA concentration) itself. Therefore, it can be concluded that the PVA content directly affects lignin waste. To the best of our knowledge, no data has been collected within the literature about the lignin waste during the washing stage into account when characterizing hydrogels. Hence, this statement cannot be contrasted with any other work.

The surface plots for all synthesis routes showed that for a fixed concentration of PVA, as lignin content was augmented (see Supplementary data), the lignin waste during the washing stage of the hydrogels tended to increase. This behaviour could be related to the addition of reactive sites and a higher crosslinking rate between both components. However, after a certain concentration of lignin, the lignin waste decreased. So, it could also be said here that the maximum points were found in between the extreme concentrations of lignin. It is also worth to mention that the swelling ability was tended to be higher for higher PVA concentrations; however, the response variable was much more influenced by the lignin content due to the significance level of its quadratic term. For the six routes, the optimal concentrations for the minimum lignin wastes were 5% lignin and 11% PVA (Vacuum XL, routes (1) and (2)), 25% lignin and 11% PVA (F–T x5 XL, routes (3) and (4)) and 5% lignin and 11% PVA (F–T x3 XL, routes (5) and (6)).

Optimization of the synthesis conditions and validation of the model

The objective of the optimization was to determine the formulations that would provide simultaneously the greatest swelling capacity and the lowest lignin waste during the washing stage via the six synthesis routes. Statgraphics Centurion XV software was used to carry out the optimization. For this aim, the values of the responses of each variable were converted using a desirability function. This function was considered to disclose the combination of the synthesis variables that maximize the swelling capacity and minimise the lignin waste at the same time. The optimum conditions for the independent variables as well as the predicted and experimental results for the response variables are displayed in Table 4.

The suitability of the response surface methodology model for quantitative predictions could only be verified by the agreement of the predicted and experimental values in two of the six synthesis routes. The errors in the output swelling variable were higher than a 4% in all the cases except for the two 5-times-freeze–thawed routes. However, the lowest errors in lignin waste were observed for the 3-times-freeze–thawed samples. The optimum formulations were repeated again in case the error was experimental, but similar results were obtained. Nevertheless, as the accuracy on swelling was considered more important than lignin waste and, as one of the aims of the optimization was to obtain the best synthesis route, the two via 5 freeze–thawing cycles were selected as the optimum pathways. Hence, the samples obtained via these two optimal routes were subjected to further characterization (namely 3 and 4 samples), together with their equivalent neat PVA hydrogels (namely 3.0 and 4.0). The swelling kinetics of these four samples are shown in Fig. 3.

Hydrogel characterization

Attenuated Total Reflection-Fourier Transformed Infrared Radiation (ATR-FTIR)

The two best optimal hydrogels (the ones obtained via the routes 3 and 4) were analyzed by FTIR technique. Fig. 4 represents the spectra of both of them (namely 3 and 4) along with the spectra of neat PVA hydrogels (namely 3.0 and 4.0), commercial PVA and alkaline lignin. As it can be seen, there was no significant difference between both hydrogels without lignin, since the employed PVA was the same and the only difference was the quantity used for their synthesis. These hydrogels showed the characteristic peaks of commercial PVA (see Table 6), and the peak around 2855 cm^{-1}, which was a small shoulder in the commercial PVA spectrum, got intensified. This band corresponds to the stretching C—H from alkyl groups, as reported by Mansur et al. [26]. A peak did also appear at around 1545 cm^{-1}, which was attributed to C—O bondages, probably created when dissolving it into water [27].

As for the hydrogels containing lignin, there was not any notable variation between their spectra due to the use of identical components for the blends. The lignin hydrogels presented similar peaks to these shown by the neat PVA hydrogels, but some bands appeared or were shifted due to the interactions with alkaline lignin (see Table 7). The band around 2920 cm^{-1}, for example, lost intensity, and was divided into two peaks at 2945 and 2916 cm^{-1}, probably due to the interactions with lignin, which presented two

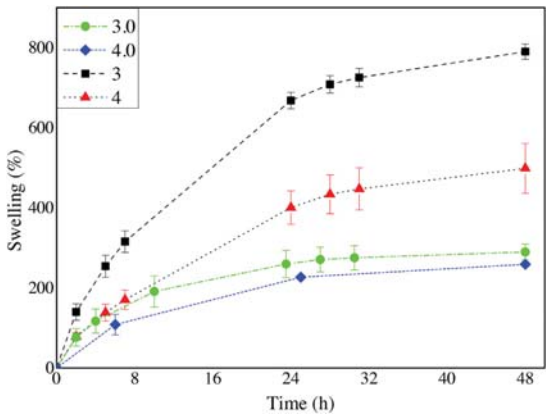

Fig. 3. Swelling performance of the hydrogels during the first 48 h.

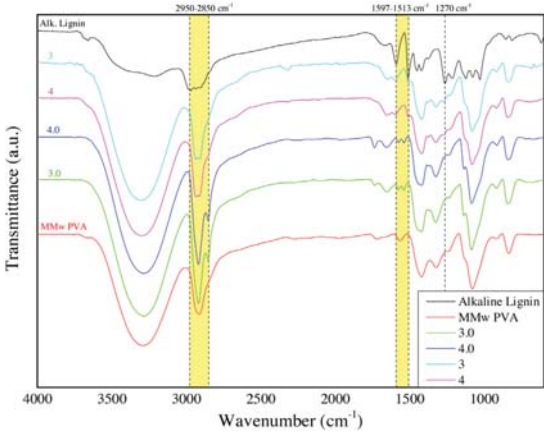

Fig. 4. FTIR of commercial PVA, commercial alkaline lignin and the selected hydrogels with (samples 3 and 4) and without lignin (samples 3.0 and 4.0).

bands at 2947 and 2913 cm^{-1}. These bands correspond to alkyl asymmetric and aromatic C—H stretch vibrations, and also to the intramolecular hydrogen bonds. Moreover, the peak corresponding to the ester C=O bonds (at 1720 cm^{-1}) lost intensity, and the one belonging to the C=C stretch vibration at around 1570 cm^{-1} shifted to higher wavenumbers due to the intense band presented by lignin at 1597 cm^{-1}. The band appearing around 1545 cm^{-1} shifted to lower wavenumbers, probably due to the interactions with

Table 6
Characteristic FTIR peaks of PVA.

Wavenumber (cm^{-1})	Assignment
3300	–OH stretch vibration
2920	Alkyl asymmetric C—H stretch vibration
2855	Symmetric C—H stretch vibration
1720	Ester C=O stretch vibration
1660	Residual C=O stretch vibration
1560	C=C stretch vibration
1425	CH_2 bending vibration
1325	O—H deformation vibration
1100	C—C stretching vibration
840	C—C and C—O stretching vibration

Table 7
Characteristic FTIR peaks of alkaline lignin.

Wavenumber (cm^{-1})	Assignment
3215	–OH stretch vibration
2947	Alkyl asymmetric vibration
2913	Aromatic C—H stretching vibration
1679	C=O ester bonds
1597	C=C stretch vibration
1513	C=C aromatic vibrations
1456	C—H bonds of the methyl groups
1429	C—H bonds of the methyl groups
1269	Guaiacyl units
1100	C—C bonds
1030	C—O stretching vibration
865	C—C stretching vibration
821	aromatic –CH out of plane vibration
618	C—S bonds

lignin, which presented a strong peak around 1513 cm^{-1} that corresponded to the C=C aromatic vibrations [28]. Around 1275 cm^{-1}, a shoulder did also appear, which could be related to the intense lignin peak at 1270 cm^{-1} and belonged to the guaiacyl units [29]. The band at 1100 cm^{-1} also got intensified, meaning that new C—C bonds might have been created and the peak at 840 cm^{-1} was enhanced too, which corresponded to C—O stretching vibrations.

The weak band at 618 cm^{-1} means that the commercial alkaline lignin contains carbon-sulphur bonds, which are characteristic of Kraft lignin [29].

Scanning Electron Microscopy (SEM)

SEM micrographs of the freeze-dried neat PVA and PVA-lignin hydrogels at two magnifications (250× and 2500×) are shown in Fig. 5. For all the analyzed samples highly porous structures and different pore size distributions could be observed. However, it seemed that for the neat PVA hydrogels (Fig. 5A–D) the morphology was more homogeneous than that for the lignin-PVA hydrogel (Fig. 5E and F). In addition, some macro-pores did also appear on the sample without lignin that was vacuum-dried (sample 4.0, Fig. 5C and D), indicating that apart from the crosslinking method [16], the curing method also affected the morphology. This behaviour was also reported by Dominguez-Robles et al. [15] for straw alkaline lignin solved in soda and crosslinked with poly(methyl vinyl ether co-maleic acid). Thombare et al. [24] explained that the macro-pores often allow a facile penetration of water into the polymeric network, which would be the cause of a rapid initial swelling ability. Once the macro-pores have been filled, water starts to diffuse gradually through micro-pores. This could have happened in the case of the blank hydrogels, since they presented considerably big pores. However, this observation was not done here; in fact, lignin hydrogels presented a higher water swelling capacity in all cases (see Fig. 3). Moreover, the walls that interconnect the micro voids amongst the sample with lignin are much smoother and more brittle than the ones presented by neat PVA in samples 3.0 and 4.0. This microstructure in PVA can be associated with its strong intra and inter- molecular hydrogen bonds [30]. Yang et al. also described a similar result on the SEM characterization of their PVA/Chitosan hydrogels [25].

As deduced from the micrographs, the majority of the pores presented by neat PVA hydrogels were smaller than 1 μm, while the ones presented by lignin-based hydrogels were larger. This fact would confirm the previous statement about the size of the pores created due to the high molecular weight of lignin and its repercussion on the swelling capacity (Section “Influence of the input variables on the swelling capacity”) [18]. Furthermore, unlike in the case of other authors [25], no lignin agglomerates were

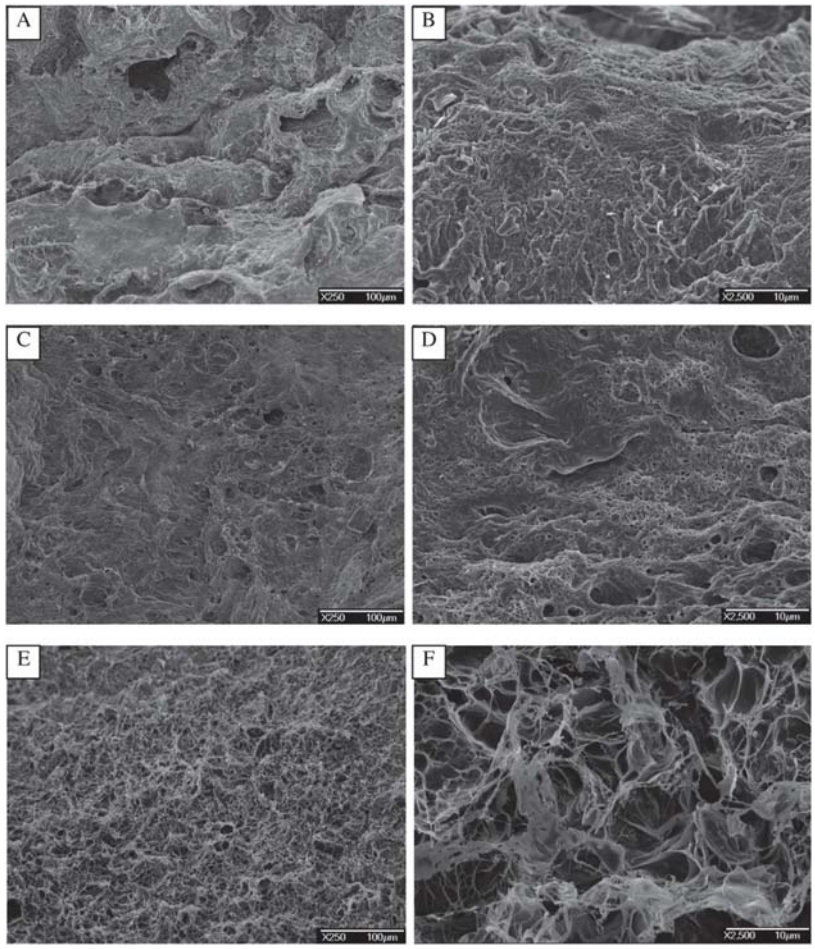

Fig. 5. SEM micrographs of the samples 3.0, 4.0 and 4 at 250× (A, C and E) and 2500× (B, D and F) magnifications.

found in the SEM images, which confirmed the good miscibility between the components [31].

X-Ray Diffraction (XRD)

The X-Ray Diffractograms for lignin, neat PVA hydrogels and lignin-PVA hydrogels are depicted in Fig. 6. Neat PVA hydrogels presented their characteristic crystalline peaks. As previously reported [18,32], a strong peak was observed at $2\theta = 19.77^{\circ}$, which corresponded to the (101) lattice plane, followed by a shoulder around 22.78°, corresponding to the (201) plane. Two weak peaks were also appreciated at 11.5 (attributed to the plane (100)) and 40.8°.

Lignin is an amorphous polymer and its diffractogram presented an intense broad peak at around 19° as shown in Fig. 6. Goudarzy et al. also reported a similar maximum diffraction angle for softwood Kraft lignin [17]. As lignin was incorporated to the hydrogels, the semicrystalline structure of PVA was slightly modified, although the main peaks did not disappear [18]. When lignin was added into the hydrogels, the strong signal at 19.77° was broadened, meaning that the crystalline regions of these hydrogels

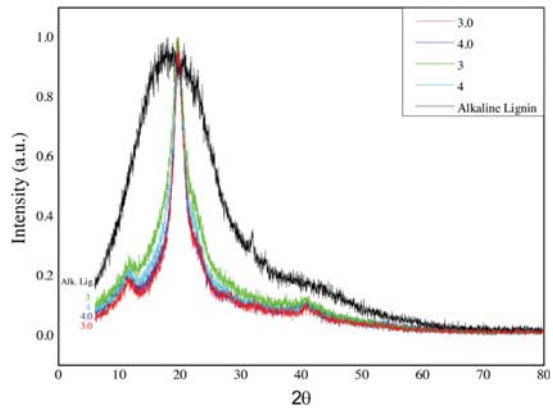

Fig. 6. XRD diffractograms of the hydrogels 3.0, 4.0, 3, 4 and commercial alkaline lignin.

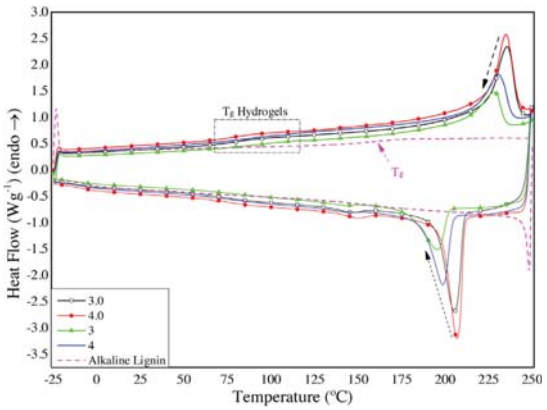

Fig. 7. DSC thermograms of the first cooling stage and second heating stage of hydrogels 3.0, 4.0, 3, 4 and commercial alkaline lignin.

were lessened and the degree of crystallinity was, therefore, decreased. This fact was also confirmed by DSC analyses.

In order to calculate the mean size of the crystallites, which are the ordered domains in a polymer, Scherrer's equation was employed (Eq. (4)). Measuring the width at half of the main crystalline peak, the estimated crystallite size for both blank and lignin-hydrogels was lower than 5 nm In addition, the notably wide peak of the lignin would mean that the crystallite size was significantly smaller than the ones in the hydrogels, since lignin is an amorphous biopolymer and usually has few ordered domains. Thus, the only conclusion we could get from these results was that all the crystallites were smaller than 5 nm and that the values calculated by any crystallinity equation would not be representative for the samples [33], although some authors have published these results [17,18].

Differential Scanning Calorimetry (DSC)

DSC analyses were performed in order to analyze the thermal properties of the synthesized hydrogels. The results for the analyzed parameters during the cooling and the second heating stages (T_c, ΔH_c, T_g, T_m, ΔH_m and χ_c) are summarized in Table 8, and the DSC curves for these stages are also shown in Fig. 7.

After removing the thermal history of the samples with the first heating scan, the appearance of a single T_g indicated a good blend miscibility [25], as previously observed in the SEM micrographs. This fact was noticed in all the analysed hydrogels. For neat PVA hydrogels (samples 3.0 and 4.0), the T_g values were similar (73.10 and 68.24 °C, successively). When lignin was incorporated into the samples, for hydrogels 3 and 4, the T_g values increased up to around 85 °C. This could be a consequence of the interactions such as hydrogen bonds between PVA and lignin, which could have restricted the chain mobility [19].

The T_m also got modified with the addition of lignin. Neat PVA hydrogels melted at around 236 °C, while the hydrogels containing lignin presented the fusion peak at around 230 °C. This behaviour is also an evidence of the good miscibility of the components [19]. As for the crystallization temperature (T_c), the addition of lignin also caused a decrease on it. In fact, the T_c of the neat PVA samples was placed around 205 °C and the one for the hydrogels with lignin at around 195 °C. Moreover, the crystallization enthalpy was also diminished from around 55 and 58 J/g (for samples 3.0 and 4.0, subsequently) to 27 and 41 J/g for samples 3 and 4, subsequently. This was attributed to the diminution of the crystalline regions as lignin was incorporated, which was also confirmed by the reduction on the melting enthalpy at the second heating scan. Thus, the degree of crystallinity (χ_c) was calculated from the latest data and Eq. (5). The results confirm that χ_c decreased with lignin the addition [19], since the values for neat PVA samples (21.63 and 23.04% for samples 3.0 and 4.0, subsequently) were around 1.5% higher than the ones for the lignin samples (20.10 and 21.56% for samples 3 and 4, subsequently). Moreover, the crystallinity degrees of the samples 3 and 3.0 were below the ones reported for 4 and 4.0, probably due to a lower PVA content and higher lignin content in the case of sample 3. However, it is important to bear in mind that these values derive from the second heating scan, so the initial crystallinity would be slightly higher. These results were in accordance with the ones obtained from XRD analysis. As previously reported [31], it is known that when an amorphous polymer is blended with a semicrystalline polymer, the degree of its crystallinity decreases, and this statement was also confirmed in this case.

Thermogravimetric Analysis (TGA)

TG and DTG curves of lignin, neat PVA hydrogels and lignin-PVA hydrogels are shown in Fig. 8A and 8B. The onset and maximum degradation temperatures, as well as the char residue at the end of the test are summarized in Table 9. Thermogravimetric studies were done in order to investigate the effect of lignin on the degradation of the blended hydrogels. For neat PVA hydrogels (3.0 and 4.0), four weight loss stages were observed. The first one appeared at around 150 °C and it was attributed to the evaporation of the adsorbed bound water [25]. A second stage was detected at around 250 °C, which still left an 85% of residue and belonged to the initial degradation of the polymer. The maximum weight loss and, hence, the major degradation was viewed at around 375 °C, corresponding to the depolymerization of the acetylated and deacetylated units of the polymer [25]. This stage was followed by another weight loss at 440 °C, achieved to the thermal degradation of some by-products generated by PVA, and a final residue of around 2.6% was accounted [25].

Commercial alkaline lignin presented a constant weight loss; however, the temperature of the maximum degradation was

Table 8
Summarized results for the analyzed parameters by DSC and calculations.

Cooling scan				2nd Heating scan					
Sample	T_c (ºC)	ΔH_c (W ºC/g)	ΔH_c (J/g)	T_g (ºC)	T_m (ºC)	ΔH_m (W ºC/g)	ΔH_m (J/g)	m_{filler} (%)	χ_c (%)
3.0	204.50	18.29	54.87	76.43	236.53	11.65	34.95	0	21.63
4.0	205.93	19.30	57.90	79.37	235.90	12.41	37.23	0	23.04
3	195.30	8.90	26.70	87.07	228.63	7.81	23.43	0.28	20.10
4	198.17	13.80	41.40	88.80	230.43	9.22	27.66	0.21	21.56

T_c: crystallization temperature; T_g: glass transition temperature; ΔH_m: melting enthalpy; χ_c: crystallinity degree; ΔH_c: crystallization enthalpy; T_m: melting temperature; m_{filler}: filler mass percentage.

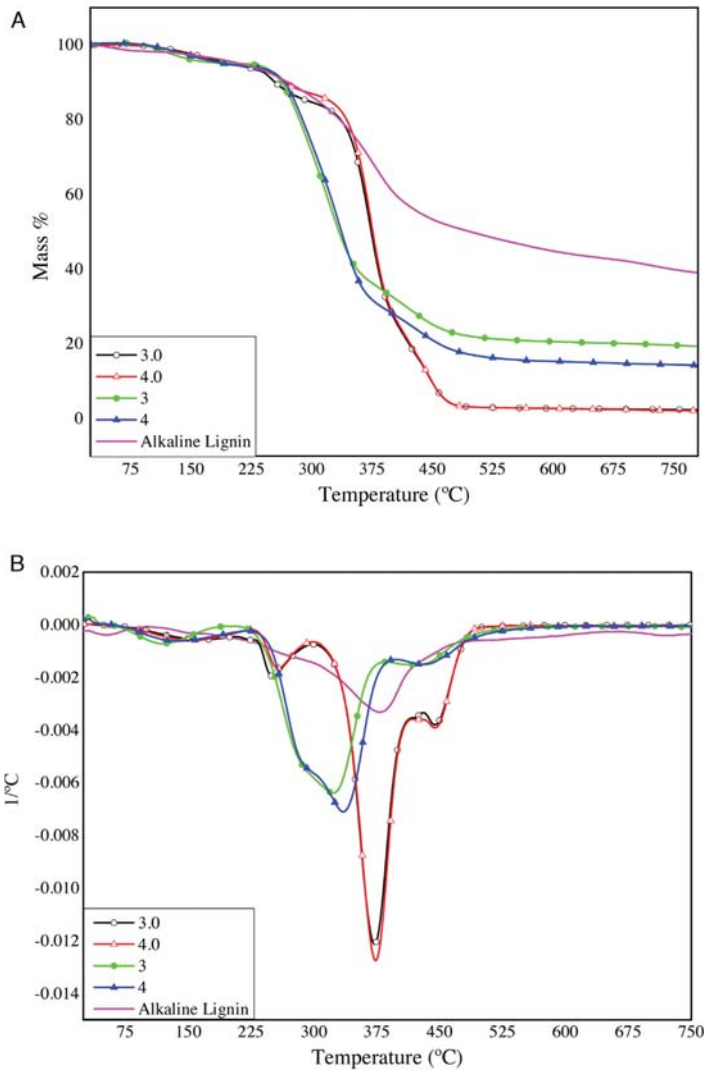

Fig. 8. (A) TG and (B) DTG curves of hydrogels 3.0, 4.0, 3, 4 and commercial alkaline lignin.

registered at 380 °C. No other significant degradation stages were detected and the final residue left was high, since it was almost of 40%. This implies that commercial alkaline lignin has many inorganic impurities, and would confirm the possibility of containing carbon-sulphur traces, as previously stated in Section "Attenuated Total Reflection-Fourier Transformed Infrared Radiation (ATR-FTIR)".

Table 9
Onset and maximum degradation temperatures and residue after TGA.

Sample ID	T_{onset} (ºC)	T_{max} (ºC)	Residue (%)
AL	172.0	380.0	39.0
3.0	225.0	372.5	2.7
4.0	230.5	374.0	2.6
3	217.0	323.0	19.5
4	223.0	334.5	14.7

When lignin was incorporated, the hydrogels presented three main weight loss stages, but there was a fourth stage which overlapped with the second one, as shown in Fig. 8B. The first stage was observed at around 120 °C and it was as well attributed to moisture evaporation. The main degradation stage appeared around 330 °C, but it was overlapped with the one at 280 °C. This loss might have been the one appearing at 250 °C in the case of neat PVA, but as lignin was incorporated, the thermal stability was enhanced and, hence, it could have shifted to higher temperatures. Hu et al. [34] explained this behaviour as the possible introduction of aromatic structures of lignin into PVA chains via strong hydrogen bonds. After the main degradation step, another loss was detected around 430 °C, which was shifted to a lower temperature than in the previous case. The residue left for both lignin hydrogels was between 14–20 %, which was directly related to lignin.

Table 10
Results for the compression tests of the samples.

Sample	Young's compression modulus (MPa)	Standard deviation (MPa)
3.0	77.57	8.40
4.0	41.64	3.42
3	18.75	0.53
4	29.21	6.18

Compression tests

The compression tests of the samples were studied and the calculated data from the stress–strain curves for compression to 80% of the initial thickness are shown in Table 10. At the maximum deformation, none of the samples were broken; in fact, all the samples had an excellent ability of integrity and recovery. This could be due to the accommodation of the stress by the rearrangement of the polymeric chains and the retractable elastic forces developed consequently [6]. Nevertheless, there were some variations in the estimated modulus. For the blank hydrogels (3.0 and 4.0) the reported moduli were of around 77.6 and 41.7 MPa, respectively. When lignin was added to the samples, the modulus decreased to around 18.8 and 29.2 MPa for samples 3 and 4, subsequently. Therefore, as lignin was incorporated, the moduli of the hydrogels were reduced despite the different drying method, making the samples less rigid. This could be related to the pore-size of the samples and would confirm what was concluded for the swelling capacity; in other words, when lignin was blended with PVA, greater pores were generated due to the reduction of interactions within PVA which, at the same time, enhanced the adsorption of water and made the hydrogel less compact and rigid [25]. Nonetheless, the obtained modulus for the PVA-lignin samples would be high enough to support the weight of soil layers if the final application was agricultural, for instance.

Conclusions

The optimization of the synthesis conditions of lignin-based PVA hydrogels was successfully carried out employing a three-level-two-factorial design. The statistical analysis showed that the PVA and lignin concentrations had great impact on the lignin waste during the washing stage and on the swelling capacity of the synthesized hydrogels. The selected optimum synthesis routes enabled the obtaining of physically crosslinked hydrogels with up to 800% water retention ability and a lignin waste between 40–50 %. The interactions between lignin and PVA were confirmed by the shifts and modifications on the FTIR bands. The SEM images permitted the observance of a different porous microstructure when lignin was added, which was responsible of the high swelling capacity. XRD analyses indicated the disappearance of some crystalline regions as amorphous lignin was incorporated, which was also confirmed by DSC and TGA techniques. Compression tests showed that, although Young's modulus was more than halved as lignin content increased, all the hydrogels kept complete integrity even compressing them up to an 80% of their initial thickness. In conclusion, physically crosslinked greener lignin hydrogels were synthesized via two methods, which had great water retention capacities as well as good thermal and mechanical properties, meaning they could be applied in many fields.

Acknowledgements

The authors would like to acknowledge the financial support of the Department of Education of the Basque Government (IT1008-16). A. Morales would like to thank the University of the Basque Country (Training of Researcher Staff, PIF17/207). P. Gullón would like to express her gratitude to MINECO for financial support (Grant reference IJCI-2015-25304). The authors thank for technical and human support provided by SGIker (UPV/EHU/ ERDF, EU).

Appendix A. Supplementary data

Supplementary material related to this article can be found, in the online version, at doi:https://doi.org/10.1016/j.jiec.2019.09.037.

References

[1] S. Laurichesse, L. Avérous, Prog. Polym. Sci. 39 (7) (2014) 1266, doi:http://dx.doi.org/10.1016/j.progpolymsci.2013.11.004.
[2] V.K. Thakur, M.K. Thakur, Int. J. Biol. Macromol. 72 (2015) 834, doi:http://dx.doi.org/10.1016/j.ijbiomac.2014.09.044.
[3] M.H. Sipponen, H. Lange, C. Crestini, A. Henn, M. Österberg, ChemSusChem 12 (10) (2019) 2038, doi:http://dx.doi.org/10.1002/cssc.201901218.
[4] V.K. Thakur, M.K. Thakur, P. Raghavan, M.R. Kessler, ACS Sustain. Chem. Eng. 2 (5) (2014) 1072, doi:http://dx.doi.org/10.1021/sc500087z.
[5] M. Mahinroosta, Z. Jomeh Farsangi, A. Allahverdi, Z. Shakoori, Mater. Today Chem. 8 (2018) 42, doi:http://dx.doi.org/10.1016/j.mtchem.2018.02.004.
[6] M.R. Guilherme, F.A. Aouada, A.R. Fajardo, A.F. Martins, A.T. Paulino, M.F.T. Davi, A.F. Rubira, E.C. Muniz, Eur. Polym. J. 72 (2015) 365, doi:http://dx.doi.org/10.1016/j.eurpolymj.2015.04.017.
[7] L. Voorhaar, R. Hoogenboom, Chem. Soc. Rev. 45 (14) (2016) 4013, doi:http://dx.doi.org/10.1039/c6cs00130k.
[8] P. Vashisth, V. Pruthi, Mater. Sci. Eng. C 67 (2016) 304, doi:http://dx.doi.org/10.1016/j.msec.2016.05.049.
[9] M. Li, X. Jiang, D. Wang, Z. Xu, M. Yang, Colloids Surf. B Biointerfaces 177 (September 2018) (2019) 370, doi:http://dx.doi.org/10.1016/j.colsurfb.2019.02.029.
[10] Y. Geng, X.Y. Lin, P. Pan, G. Shan, Y. Bao, Y. Song, Z.L. Wu, Q. Zheng, Polymer (Guildf) 100 (2016) 60, doi:http://dx.doi.org/10.1016/j.polymer.2016.08.022.
[11] B. Gyarmati, B.Á. Szilágyi, A. Szilágyi, Eur. Polym. J 93 (March) (2017) 642, doi:http://dx.doi.org/10.1016/j.eurpolymj.2017.05.020.
[12] Z. Gao, L. Duan, Y. Yang, W. Hu, G. Gao, Appl. Surf. Sci. 427 (2018) 74, doi:http://dx.doi.org/10.1016/j.apsusc.2017.08.157.
[13] A. Oryan, A. Kamali, A. Moshiri, H. Baharvand, H. Daemi, Int. J. Biol. Macromol. (2017), doi:http://dx.doi.org/10.1016/j.ijbiomac.2017.08.184.
[14] S. Park, S.H. Kim, J.H. Kim, H. Yu, H.J. Kim, Y.H. Yang, H. Kim, Y.H. Kim, S.H. Ha, S. H. Lee, J. Mol. Catal. B Enzym. 119 (2015) 33, doi:http://dx.doi.org/10.1016/j.molcatb.2015.05.014.
[15] J. Domínguez-Robles, M.S. Peresin, T. Tamminen, A. Rodríguez, E. Larrañeta, A. S. Jääskeläinen, Int. J. Biol. Macromol. 115 (2018) 1249, doi:http://dx.doi.org/10.1016/j.ijbiomac.2018.04.044.
[16] A. Kumar, S.S. Han, Int. J. Polym. Mater. Polym. Biomater. 66 (4) (2017) 159, doi:http://dx.doi.org/10.1080/00914037.2016.1190930.
[17] A. Goudarzi, L.-T. Lin, F.K. Ko, J. Nanotechnol. Eng. Med. 5 (2) (2014)021006, doi:http://dx.doi.org/10.1115/1.4028300.
[18] D. Ciolacu, G. Cazacu, J. Nanosci. Nanotechnol. 18 (4) (2018) 2811, doi:http://dx.doi.org/10.1166/jnn.2018.14290.
[19] X. He, F. Luzi, X. Hao, W. Yang, L. Torre, Z. Xiao, Y. Xie, D. Puglia, Int. J. Biol. Macromol. 127 (2019) 665, doi:http://dx.doi.org/10.1016/j.ijbiomac.2019.01.202.
[20] S.A. Bencherif, A. Srinivasan, F. Horkay, J.O. Hollinger, K. Matyjaszewski, N.R. Washburn, Biomaterials 29 (12) (2008) 1739, doi:http://dx.doi.org/10.1016/j.biomaterials.2007.11.047.
[21] M.N. Collins, C. Birkinshaw, J. Mater. Sci. Mater. Med. 19 (11) (2008) 3335, doi:http://dx.doi.org/10.1007/s10856-008-3476-4.
[22] B. Gullón, P. Gullón, T.A. Lú-Chau, M.T. Moreira, J.M. Lema, G. Eibes, Ind. Crops Prod 108 (April) (2017) 649, doi:http://dx.doi.org/10.1016/j.indcrop.2017.07.014.
[23] M. Yang, M.S.U. Rehman, T. Yan, A.U. Khan, P. Oleskowicz-Popiel, X. Xu, P. Cui, J. Xu, Bioresour. Technol. 249 (October 2017) (2018) 737, doi:http://dx.doi.org/10.1016/j.biortech.2017.10.055.
[24] N. Thombare, S. Mishra, M.Z. Siddiqui, U. Jha, D. Singh, G.R. Mahajan, Carbohydr. Polym. 185 (October 2017) (2018) 169, doi:http://dx.doi.org/10.1016/j.carbpol.2018.01.018.
[25] W. Yang, E. Fortunati, F. Bertoglio, J.S. Owczarek, G. Bruni, M. Kozanecki, J.M. Kenny, L. Torre, L. Visai, D. Puglia, Carbohydr. Polym. 181 (October 2017) (2018) 275, doi:http://dx.doi.org/10.1016/j.carbpol.2017.10.084.
[26] H.S. Mansur, C.M. Sadahira, A.N. Souza, A.A.P. Mansur, Mater. Sci. Eng. C 28 (4) (2008) 539–548, doi:http://dx.doi.org/10.1016/j.msec.2007.10.088.
[27] S. Karimi, J. Feizy, F. Mehrjo, M. Farrokhnia, RSC Adv. 6 (27) (2016) 23085–23093, doi:http://dx.doi.org/10.1039/c5ra25983e.
[28] A. Morales, B. Gullón, I. Dávila, G. Eibes, J. Labidi, P. Gullón, Ind. Crops Prod. 124 (2018), doi:http://dx.doi.org/10.1016/j.indcrop.2018.08.032.
[29] S. Sathawong, W. Sridach, K.A. Techato, J. Environ. Chem. Eng. 6 (5) (2018) 5879–5888, doi:http://dx.doi.org/10.1016/j.jece.2018.05.008.
[30] L.Y. Wang, M.J. Wang, ACS Sustain. Chem. Eng. 4 (5) (2016) 2830, doi:http://dx.doi.org/10.1021/acssuschemeng.6b00336.
[31] K.J. Lee, J. Lee, J.Y. Hong, J. Jang, Macromol. Res. 17 (7) (2009) 476, doi:http://dx.doi.org/10.1007/BF03218895.

[32] H. Dai, H. Zhang, L. Ma, H. Zhou, Y. Yu, T. Guo, Y. Zhang, H. Huang, Carbohydr. Polym. 209 (381) (2019) 51, doi:http://dx.doi.org/10.1016/j.carbpol.2019.01.014.
[33] A. Morales, M.Á. Andrés, J. Labidi, P. Gullón, Ind. Crops Prod. 131 (2019), doi:http://dx.doi.org/10.1016/j.indcrop.2019.01.071.
[34] X.-Q. Hu, D.-Z. Ye, J.-B. Tang, L.-J. Zhang, X. Zhang, RSC Adv. 6 (17) (2016) 13797, doi:http://dx.doi.org/10.1039/C5RA26385A.
[35] E. Larrañeta, M. Imízcoz, J.X. Toh, N.J. Irwin, A. Ripolin, A. Perminova, J. Domínguez-Robles, A. Rodríguez, R.F. Donnelly, ACS Sustain. Chem. Eng. 6 (7) (2018) 9037, doi:http://dx.doi.org/10.1021/acssuschemeng.8b01371.
[36] L. Musilová, A. Mráček, A. Kovalcik, P. Smolka, A. Minařík, P. Humpolíček, R. Vícha, P. Ponížil, Carbohydr. Polym. 181 (October 2017) (2018) 394, doi:http://dx.doi.org/10.1016/j.carbpol.2017.10.048.
[37] H. Bian, L. Jiao, R. Wang, X. Wang, W. Zhu, H. Dai, Eur. Polym. J. 107 (August) (2018) 267, doi:http://dx.doi.org/10.1016/j.eurpolymj.2018.08.028.
[38] K. Ravishankar, M. Venkatesan, R.P. Desingh, A. Mahalingam, B. Sadhasivam, R. Subramaniyam, R. Dhamodharan, Mater. Sci. Eng. C 102 (January) (2019) 447, doi:http://dx.doi.org/10.1016/j.msec.2019.04.038.

Assessment of green approaches for the synthesis of physically crosslinked lignin hydrogels

Amaia Morales, Jalel Labidi*, Patricia Gullón

Chemical and Environmental Engineering Department, University of the Basque Country UPV/EHU, Plaza Europa 1, 20018, San Sebastián, Spain

Supplementary Data

Figure S1: Response surfaces for the swelling capacity of paths 1, 2, 3, 4, 5 and 6 (A, B, C, D, E and F, subsequently).

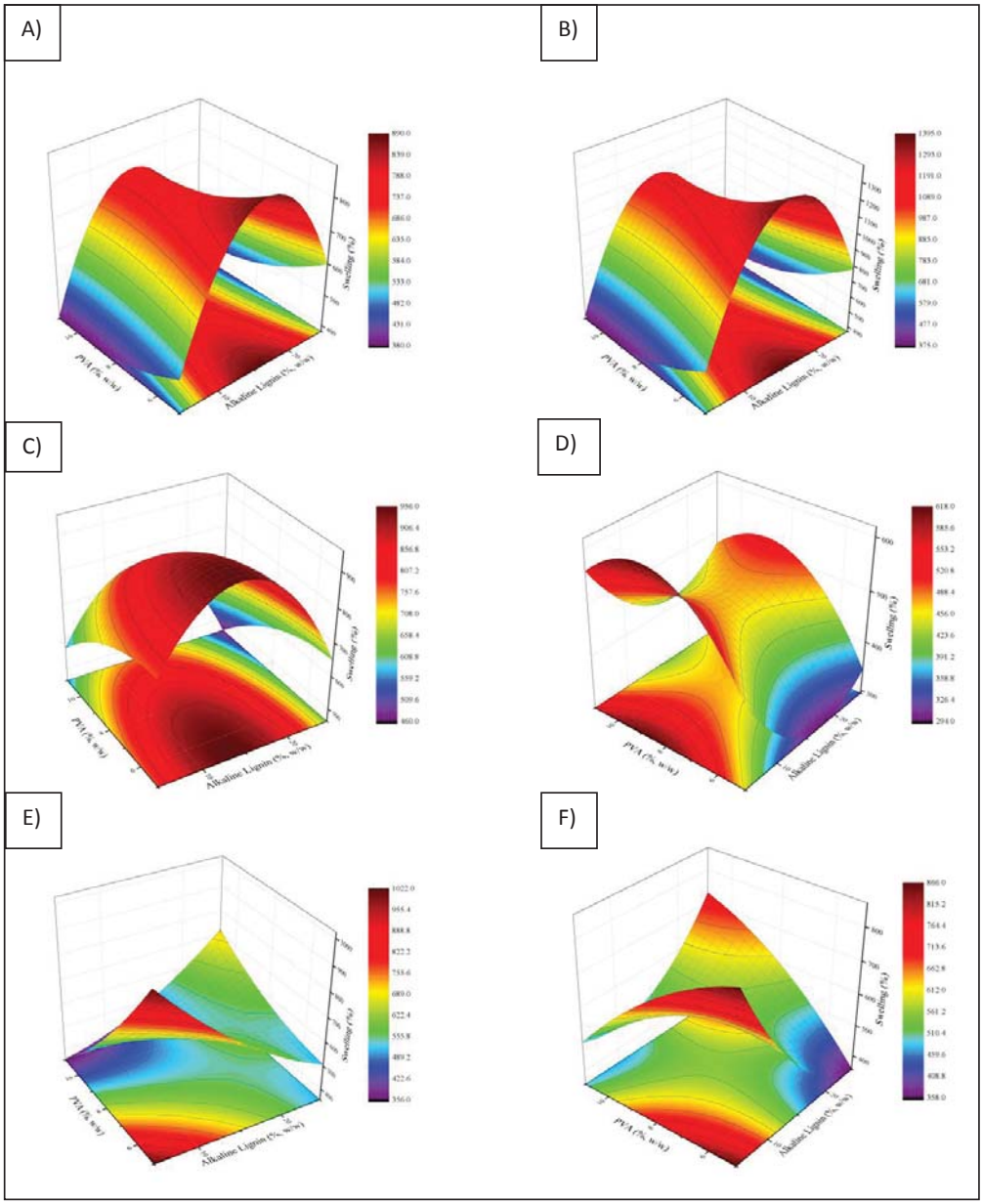

Figure S2: Response surfaces for the lignin waste of paths 1 and 2 (A), 3 and 4 (B) and 5 and 6 (C).

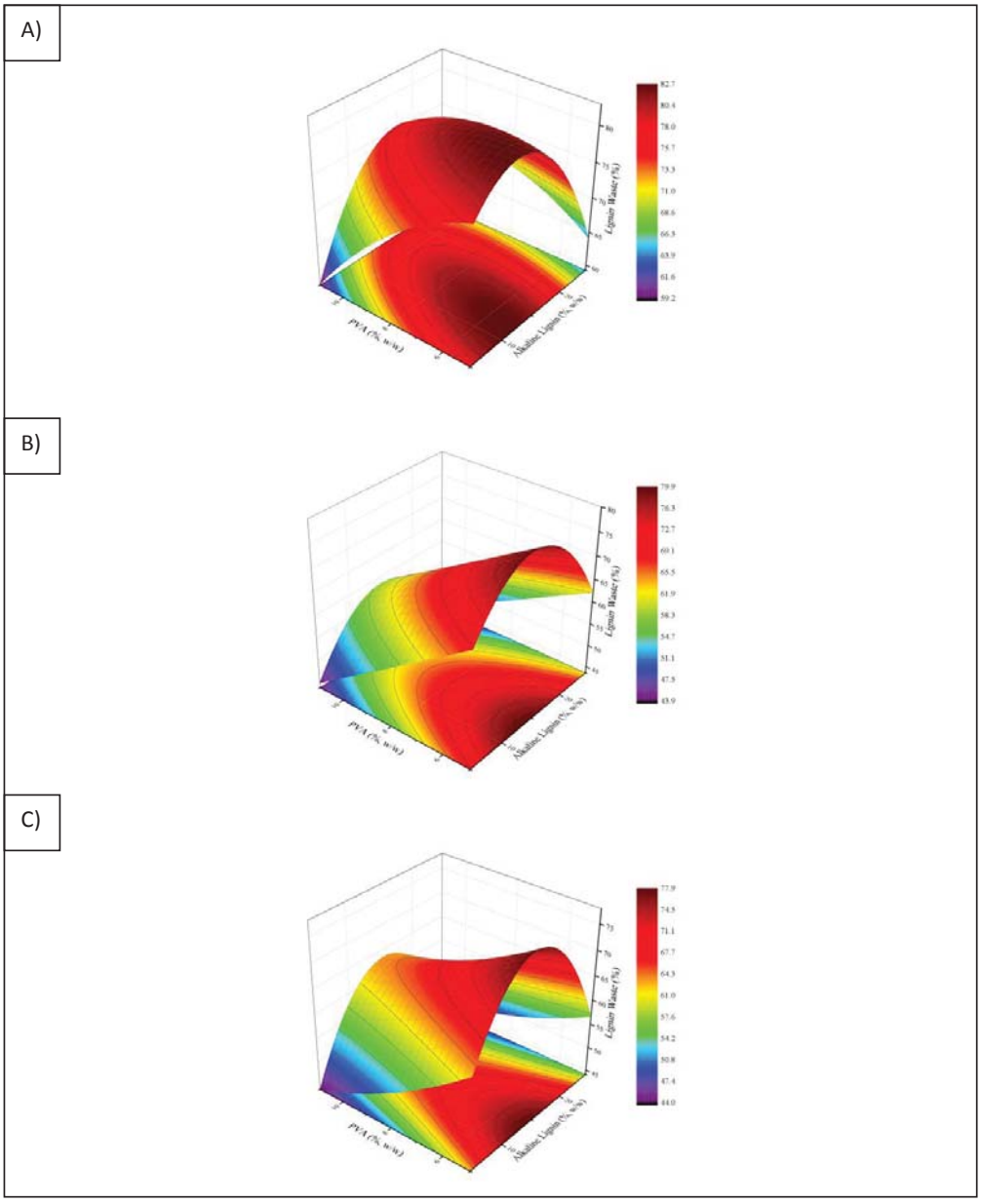

III. Artikulua

Effect of the formulation parameters on the absorption capacity of smart lignin-hydrogels

A. Morales, J. Labidi, P. Gullón

III

http://10.1016/j.eurpolymj.2020.109631
0014-3057/
Eur. Polym. J. 129 (2020) 109631

European Polymer Journal 129 (2020) 109631

Contents lists available at ScienceDirect

European Polymer Journal

journal homepage: www.elsevier.com/locate/europolj

Effect of the formulation parameters on the absorption capacity of smart lignin-hydrogels

Amaia Morales, Jalel Labidi*, Patricia Gullón

Chemical and Environmental Engineering Department, University of the Basque Country UPV/EHU, Plaza Europa 1, 20018 San Sebastian, Spain

ARTICLE INFO

Keywords:
Lignin
Poly (vinyl alcohol)
Molecular weight
Physical crosslinking
Hydrogels
Swelling

ABSTRACT

Hydrogels have become very popular in the last decades and they are widely employed in many application fields. Physically crosslinked hydrogels lack of toxic and expensive reagents and, thus, they enable a greener and a more economical synthesis process. Till date, many biopolymers have been explored for hydrogel synthesis, but lignin has promised to be a potential one for this aim. To this end, lignin and three different molecular weight PVA (Mw = 13,000–23,000 g/mol, 87–89% hydrolyzed; M_w = 83,000–124,000 g/mol, 99 + % hydrolyzed and Mw = 130,000 g/mol, 99 + % hydrolyzed) were blended in optimized concentrations via two routes of crosslinking. Only the two highest molecular weight PVAs enabled a successful crosslinking. The swelling capacity of the hydrogels in water as well as in four other mediums showed that lignin enhanced the water absorption capacity and the pH and temperature responsiveness. In addition, it was seen that the swelling rate and the lignin waste of the obtained hydrogels were directly influenced by the molecular weight of the employed PVA. Moreover, the re-swelling capacity of the hydrogels suggested that these materials could be re-used. The differences in pore size and morphology in SEM analyses were in accordance with the behaviour of the samples in compression tests. Additionally, lignin promoted dye adsorption capacity.

1. Introduction

The industrial development and the dizzying growth of the world population are provoking the depletion of fossil resources. This situation has led to the current environmental problems as consequence, among others, of the greenhouse gases derived from mankind activities and the presence of huge amounts of plastics in oceans with disastrous effects causing the deterioration of the different ecosystems of the planet. An attempt to change this current scenario is the transition from fossil fuels to the biorenewable biomass as a source of raw materials to obtaining chemical platforms, energy, and polymers as base of materials. For this, in the last decades, the efforts of researchers have been addressed towards the development of green and sustainable materials based on biorenewable polymers, what it is of prime interest from the environment, social, politician and economic point of view.

Among these polymers, lignin, one of the main components of lignocellulosic materials, is the most abundant aromatic biopolymer in the world. It is an amorphous copolymer [1], synthesized from random polymerization of trans-p-coumaryl, coniferyl and sinapyl alcohols, and it is obtained in huge amounts as a by-product in pulp and paper industry. Lignin is often burnt to produce energy or discarded as waste and, despite its abundance, only a minor proportion of the total volume produced in the forest industry is recovered for added value applications. Its recalcitrant character makes the development of adequate technologies for its use a great challenge for the researchers. Additionally, lignin presents several advantages facing other bio-polymers such as low cost and biodegradability. Therefore, the use of lignin for the synthesis of added-value compounds would mean a significant step forward, especially in the context of the biorefinery processes as it would contribute to a circular economy.

Recently, many authors have reported the use of lignin as starting material for the synthesis of hydrogels. It is well known that hydrogels are three-dimensionally crosslinked polymeric networks with high water retention capacity. Due to this property and other physic-chemical characteristics, they have significantly gained attention during the last decades [2] and they have already been employed in many fields such as biomedicine or agriculture [3].

Most of the lignin-based hydrogels described in the literature are synthesized through chemical crosslinking [4–7], which usually involves many disadvantages such as toxicity, need of removing the residual crosslinker and more expensive reagents than the ones used for physical crosslinking [8]. Hence, the production of greener hydrogels from the physical crosslinking of lignin would be interesting in order to revalorize this abundant by-product.

* Corresponding author.
E-mail address: jalel.labidi@ehu.es (J. Labidi).

https://doi.org/10.1016/j.eurpolymj.2020.109631
Received 18 February 2020; Received in revised form 17 March 2020; Accepted 18 March 2020
Available online 20 March 2020

Physically crosslinked hydrogels, compared to chemically crosslinked ones, lack of toxic and sometimes expensive crosslinking reagents, which is an advantageous fact. As a consequence, physical crosslinking enables a greener and a more economical synthesis process [8].

Due to the increasing concern about the environmental impact that synthetic plastics have caused, the possibility of producing bio-based and biodegradable materials such as hydrogels is currently being investigated. Bio-based hydrogels are environmentally friendly and biocompatible in comparison with the fossil-based hydrogels [9].

In this work, two of the previously studied synthesis routes [10] were employed combining commercial alkaline lignin with three different molecular weight poly (vinyl alcohol) via 3 and 5 cycles of freeze-thawing. This was done in order to study the influence of the molecular weight of the blending polymer and the time of the cycles on the properties of the final hydrogels, especially on the swelling capacity and the lignin waste.

The hydrogels that were successfully formed were characterized by FTIR, SEM, XRD, DSC and TGA. Their mechanical properties were also evaluated by compression tests and were compared with the results for the ones made via longer cycles. Their pH and temperature response was also studied. The swelling and re-swelling capacity of the hydrogels in water was assessed. Moreover, as the lignin waste during washing was rather meaningful, twin hydrogels were again synthesized using a reduced amount of lignin, subtracting the wasted one to the initially added lignin. Besides, organosolv lignin was also employed as substituent of the alkaline one in order to study the influence of the lignin type keeping the concentration of this component constant. Additionally, the adsorption capacity of the synthesized lignin-PVA hydrogels toward methylene blue was evaluated.

2. Materials and methods

2.1. Materials

Alkaline lignin and poly (vinyl alcohol) (PVA, Mw = 13,000–23,000 g/mol, 87–89% hydrolyzed; Mw = 83,000–124,000 g/mol, 99 + % hydrolyzed and Mw = 130,000 g/mol, 99 + % hydrolyzed) were supplied by Sigma Aldrich. Sodium hydroxide (NaOH, analysis grade, ≥98%, pellets), hydrochloric acid (HCl, 37% w/w) and methylene blue were purchased from PanReac Química SLU. Organosolv Lignin was supplied by Chemical Point. All reagents were employed as supplied.

2.2. Hydrogel synthesis

Hydrogels were synthesized according to two of the pathways studied previously (see Fig. 1) [10]. All the hydrogels were prepared in the same way, except for the difference on the number of cycles at the crosslinking stage: half of them were subjected to 3 freeze-thawing cycles while the others were subjected to 5. The concentrations of the blends were also determined according to a previous study [10]. All the hydrogels were prepared by adding a 9.87% (w/w) i.e. 5.92 g of the corresponding weight averaged molecular weight (Mw) PVA to 60 mL of a 2% (w/w) NaOH aqueous solution, which was magnetically stirred and heated to 80–90 °C simultaneously. Once the PVA pellets were dissolved, the lignin (9.12% (w/w), i.e. 5.47 g) was incorporated under agitation until it was completely dissolved. The blends were introduced into 6 mL syringes and then poured into silicon moulds, poking the visible air bubbles at the surface and eliminating any remaining internal bubbles introducing them in an ultrasound bath for 10 min.

On the previous work [10], the blends had been frozen for 16 h at −20 °C in a freezer and then thawed during 8 h at 28 °C in a heater, 3 and 5 times. In this work, the time of the cycles was optimized; in fact, when the blends were completely frozen (2.5 h approximately) they were taken out and put into the heater at 28 °C until they were totally thawed (1.5 h approximately). In this way, the crosslinking time was significantly reduced, since this stage used to take between 3 and 5 days and in this way, it lasted less than 2 days. After this stage, the washing was performed as done in the previous work [10] so as to eliminate the non-reacted lignin and the residual NaOH. Afterwards, the hydrogels were left to dry at room temperature.

In order to analyze the influence of the lignin type, complementary swelling tests were performed, for which organosolv-lignin-based hydrogels were similarly synthesized. Briefly, the same initial amounts of both MMw and HMw PVA and organosolv lignin were taken, and the same abovementioned experimental method was followed.

2.3. Hydrogel characterization

2.3.1. Lignin waste

During the washing stage, aliquots were taken each time the hydrogels were rinsed. A calibration curve was designed as described in the previous work [10]. Briefly, by employing several solutions of known concentrations of lignin and their absorbance measured at 515 nm by a V-630 UV-Jasco spectrophotometer the calibration curve was designed. Then, the absorbance of all aliquots was registered and, finally, their concentrations and the total lignin loss were calculated taking the volume of each rinse into account.

2.3.2. Swelling

The swelling of the synthesized hydrogels was estimated as in the previous work [10]. Briefly, they were weighted in dry state before being immersed into 50 mL of distilled water for 48 h. Then, they were

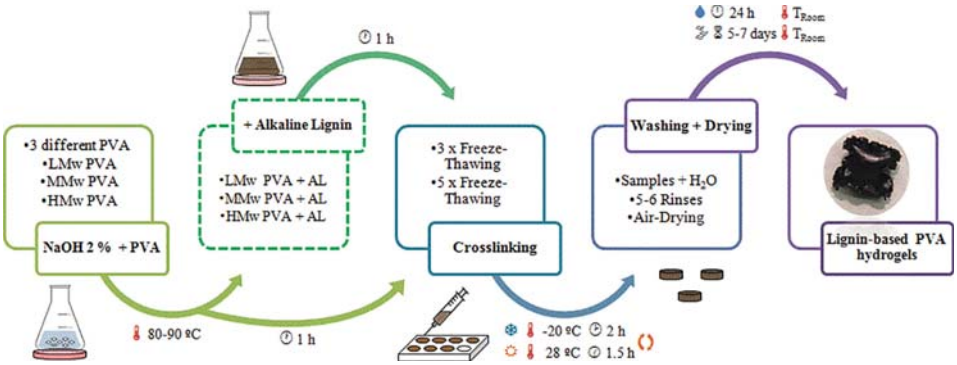

Fig. 1. Flow-diagram of the experimental procedure for hydrogel synthesis.

weighted at certain times, removing the water remaining on the surface with filter paper, for the swelling kinetics. The swelling degree was calculated from Eq. (1) [3]:

$$Swelling\ \ (\%) = (m_{swollen} - m_{dry})/m_{dry}\cdot 100 \quad (1)$$

in which $m_{swollen}$ and m_{dry} are the masses of swollen and dried hydrogels, successively.

Apart from distilled water, the swelling capacity of the synthesized hydrogels was also studied in a saline solution (1% NaCl) and two solutions of pH 2.5 and 12.20 prepared by adding dilute HCl or dilute NaOH. The influence of temperature was studied by keeping the samples in the corresponding solutions inside an incubator at 40 °C. The reswelling capacity was measured by introducing the hydrogels that were swollen and left to dry once again into water.

2.3.3. Attenuated Total Reflection – Fourier Transformed Infrared Radiation (ATR-FTIR)

In order to study and verify the interactions between the polymers, a PerkinElmer Spectrum Two FT-IR Spectrometer equipped with a Universal Attenuated Total Reflectance accessory with internal reflection diamond crystal lens was used to collect Infrared spectra of the hydrogels. The studied range was from 600 to 4000 cm^{-1} and the resolution was 8 cm^{-1}. 20 scans were recorded for each grated dry sample.

2.3.4. Scanning Electron Microscopy (SEM)

SEM analyses were carried out in order to study the morphology of the hydrogels. The samples were swollen in water for 48 h at room temperature and then frozen at −20 °C. Afterwards, they were freeze-dried in an Alpha 1–4 LD freeze drier. The images of secondary electrons were taken with a MEB JEOL 7000-F. The working conditions were 5 kV and an intensity of 0.1 nA. The samples were covered with 20 nm of Cr by sputtering technique.

2.3.5. X-Ray Diffraction (XRD)

The samples were subjected to XRD analysis grated and in dry state. X-Ray Powder diffraction tests were carried out using a Phillips X'Pert PRO automatic diffractometer operating at 40 kV and 40 mA, in theta-theta configuration. Monochromatic Cu-Kα (λ = 1.5418 Å) radiation and a PIXcel solid-state detector (active length in 2θ 3.347°) were employed. The collected data ranged from 5 to 80° 2θ at room temperature. The step size was 0.026 and the time per step was 80 s. 0.04 rad soller slit and fixed 1° divergence slit giving a constant volume of sample illumination were employed.

2.3.6. Differential Scanning Calorimetry (DSC)

DSC analyses were done on a Mettler Toledo DSC 822 (Mettler Toledo, Spain). Dry grated samples of between 3 and 5 mg were subjected to a heating ramp from −25 °C to 225 °C at a rate of 10 °C/min under nitrogen atmosphere to avoid oxidative reactions inside aluminium pans. After the first heating step, cooling and second heating stages were also performed. The glass transition temperature (T_g), was considered as the inflection point of the specific heat increment during the heating scans. The calibration was performed with indium standard. The degree of crystallinity (χ_c) was obtained from the enthalpy evolved during crystallization using Eq. (2) [11]:

$$\chi_c = \Delta H_m/[\Delta H_0\cdot(1 - m_{filler})]\cdot 100 \quad (2)$$

where ΔH_m, is the apparent enthalpy for melting, ΔH_0 is the melting enthalpy of 100% crystalline PVA (average value: 161.6 J/g) and $(1 - m_{filler})$ is the weight percentage of PVA in the hydrogels [11].

2.3.7. Thermogravimetric Analysis (TGA)

TGA analyses were done on a TGA/SDTA 851 Mettler Toledo (Mettler Toledo, Spain) instrument. Dry grated samples of around 7 mg were subjected to a heating ramp of 25 °C/min from room temperature up to 800 °C under a nitrogen atmosphere to avoid thermo-oxidative reactions.

2.3.8. Compression studies

Uniaxial compression tests were performed on the hydrogels in order to assess their mechanical strength. A compression gear was set up on an Instron 5967 machine using a 500 N load cell with a crosshead speed of 2 mm/min. Square samples of around 5 × 5 mm were cut from the initial hydrogels, which were left to swell during 48 h at room temperature. The swollen samples were compressed up to the 80% of their initial thickness. The swollen modulus, G_e, of each sample was calculated automatically by employing Eq. (3) [12,13].

$$\sigma = F/A = G_e\cdot(\lambda - 1/\lambda^2) \quad (3)$$

where F is the force, A is the original cross sectional area of the swollen hydrogel, and $\lambda = L/L_0$ where L_0 and L are the thicknesses of the samples before and after compression, respectively.

2.3.9. Methylene blue adsorption tests

The uptake of methylene blue (MB) was investigated as follows: a solution of MB was prepared at a concentration of 1 mg/L. All batch adsorption experiments were statically performed at room temperature for 24 h. The adsorption performance was calculated by Eq. (4) after the concentrations of the initial and final dissolutions were determined [14]. For this aim, a calibration curve was designed by employing several solutions of known concentrations (5–0.25 mg/L) of MB and their absorbance measured at 665 nm by a V-630 UV-Jasco spectrophotometer.

$$Q_e\ \ (mg_{MB}/g_{HG}) = (C_0 - C_{eq})/m\cdot V \quad (4)$$

where C_0 is the initial dye concentration, C_{eq} is the dye concentration at equilibrium, V is the total volume of dye employed for each sample and m is the dry weight of the hydrogel. The percentage of removal was also calculated by means of Eq. (5):

$$P\ \ (\%) = (C_0 - C_{eq})/C_0\cdot 100 \quad (5)$$

where P is the equilibrium adsorption rate of the hydrogel and the rest of variables are the same as the ones defined for Eq. (4) [14]. Desorption studies were also performed by immersing the dyed hydrogels into a 0.1 M HCl solution for 24 h. The dye release was quantified by spectrophotometry, as done for the adsorption study [14,15].

3. Results and discussion

3.1. Crosslinking

According to previous studies, the selected composition enabled the crosslinking between alkaline lignin and medium molecular weight PVA (MMw PVA) via both 3 and 5 cycles of freeze-thawing [10]. In this case, however, the cycles were shortened, but both MMw and high molecular weight PVA (HMw PVA) still leaded to a successful crosslinking with lignin. Nevertheless, the samples formed with low molecular weight PVA (LMw PVA) did not result in a proper crosslinking despite having a good visual aspect. A similar result was reported by Wu et al. [7], who tried to crosslink a solution of 10% alkaline lignin with different amounts of PVA (47,000 g/mol) adding epiclorohydrin. This might have happened due to the scarce reactive sites in PVA for such amount of lignin despite adding a crosslinker to favour the formation of the hydrogel. For this reason, LMw PVA samples were discarded for further studies. Nevertheless, LMw PVA could be used in the future for hydrogel formation but varying the PVA content and the lignin content. Wu et al. [7] did also relate the reagent concentration to the crosslinking degree. Moreover, the hydrolysis degree of the PVA might have had something to do with the crosslinking. The hydrolysis degree is related to the number of acetate groups in the PVA molecule, since PVA is synthesized from the hydrolysis of pre-polymerized

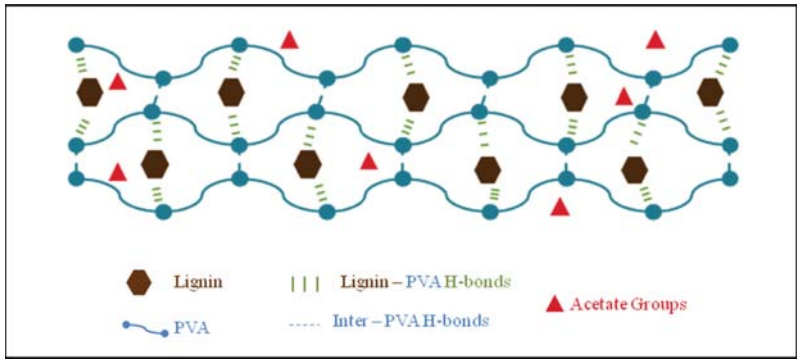

Fig. 2. Possible crosslinking scheme between PVA and lignin.

polyvinyl acetate [16,17]. Thus, a high hydrolysis degree means there will be a lower number of acetate groups in the PVA, and these groups can interfere on its chemical properties, solubility and the capacity of crystallization [17]. Moreover, the presence of acetate groups weakens both intra- and intermolecular hydrogen bonding interactions between nearby hydroxyl groups. In solution, as the degree of hydrolysis increases, the PVA interchain separation distance decreases [17]. Therefore, the non-successful crosslinking could be attributed to the lower degree of hydrolysis that LMw PVA had (87–89%) in comparison to MMw and HMw PVA (99+%), although a direct correlation is often difficult to determine [18] and might be more related to the molecular weight and concentration of PVA [7].

At first sight, comparing these hydrogels with the ones in the previous work [10], they seemed more brittle since it was more complicated to take them out of the moulds. Therefore, it can be concluded that the time as well as the number of the freeze-thawing cycles affects the consistence of the formed hydrogel [19], which would be associated to the crosslinking degree. A possible scheme of the interactions through the hydrogel matrix is proposed in Fig. 2.

3.2. Lignin waste

For the samples with HMw PVA (69.5 and 49.5% for samples 3HL and 5HL, subsequently) the lignin waste during the washing stage was lower than the one for MMw PVA samples (77.8 and 57% for the samples 3ML and 5ML, subsequently). The former could be related to the number of reactive sites in the PVA, i.e. longer polymer chains had more entanglements with lignin. According to Hennink et al. [19], the molecular weight of PVA affects the properties of the gel formed. In addition, the number of cycles also affected the lignin waste, since the hydrogels formed via 3 freeze-thawing cycles had a higher lignin waste than the ones formed via 5 cycles. This fact could mean that as the number of cycles was increased, more entanglements were formed between the elements in the blend [19,20].

3.3. Swelling capacity

As displayed in Fig. 3A, the swelling capacity was significantly higher for the hydrogels synthesized via 5 freeze-thawing cycles (890 and 790% for HMw and MMw PVA, subsequently) than for the ones made via 3 cycles (380 and 360% for HMw and MMw PVA, respectively). Moreover, for the hydrogels with the highest molecular weight PVA the swelling capacity was also the highest (≈900%). Other authors also reported this behavior for higher molecular weight lignin-PVA hydrogels [7]. This would again enhance the previous statement about the influence of parameters such as the molecular weight of the employed PVA and the number of cycles [19]. As cycles and the molecular weight of PVA are increased, the increment on the entanglements with lignin would permit the creation of more pores and, thus, higher water absorption ability. Wu et al. [7] also considered that an optimal amount of lignin would maintain the PVA network more relaxed, which would lead to higher water absorption. It is also worth to mention that the neat PVA hydrogels presented a very low swelling ability (200–300%), so this would confirm the fact that lignin enhances the pore size and, therefore, the water retention inside the network [4,7,21]. In addition, neat MMw PVA hydrogels presented a higher swelling rate than the ones synthesized from HMw PVA and this rate was kept higher for the ones with 5 cycles.

In comparison with the previously synthesized samples [10], which were synthesized from longer freeze-thawing periods, these hydrogels presented slightly lower swelling values (970% Vs. 890–790% for the previous and the current hydrogels, respectively). However, neat PVA samples were capable of swelling slightly more than in the previous work.

3.3.1. Influence of the pH on the swelling capacity

As smart materials are becoming of great interest, it is important to study the stimuli responsiveness (pH, temperature…) of the synthesized hydrogels [22]. Twin samples of the hydrogel 3HL were swollen into two solutions with different pH-s (2.5 and 12.20). In these experiments, it was seen that the basic medium improved the swelling capacity (see Fig. 3B). This behavior might have been observed due to the influence of soda in the expansion of crosslinked chains by electrostatic repulsions in the polymeric network [21]. On the other hand, the acidic medium hindered the swelling ability of the hydrogels. This could be attributed to protonation of the carboxylate anions, which convert −COO− groups to −COOH, eliminating the main anion-anion repulsive forces and decreasing at the same time the swelling values [23,24]. When pH is increased, H-bonding and the negative effect of H^+ on electrostatic repulsions are gradually weakened because many −COOH groups are converted to −COO−, contrary to what happened for low pH-s [24].

3.3.2. Influence of the temperature and NaCl on the swelling capacity

As aforementioned, temperature is also an external stimulus to which hydrogels are usually responsive. In addition, the swelling capacity of the hydrogels is significantly influenced by the charge valences and the salinity degree of the medium, and this capacity determines the suitability of the hydrogels to be used as water release systems in agriculture [24]. Therefore, in order to evaluate the effect of the temperature and the presence of a salt on the swelling capacity of the hydrogels, 3 samples cut into 4 of the series 3ML, 5ML and 5HL (12 samples in total, 4 per series) were submerged into different solutions. Half of them were put into 1% (w/w) NaCl solutions and the other half into distilled water. At the same time, two samples per series (one in saline media and another one in distilled water) were left to swell at

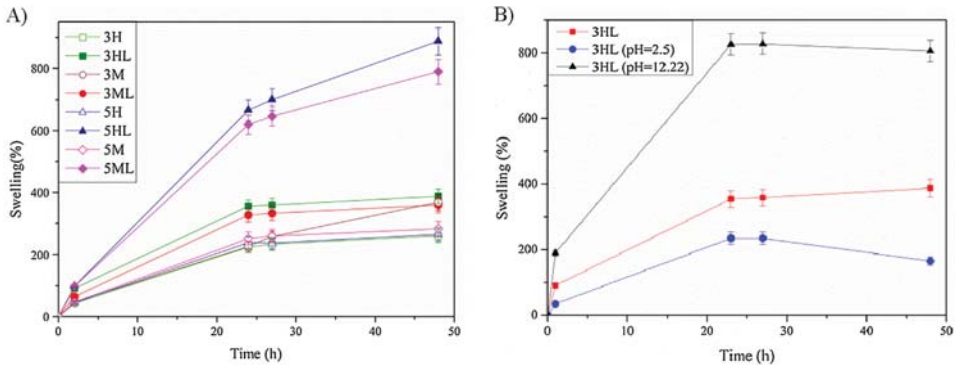

Fig. 3. Swelling performance of the hydrogels during the first 48 h (A) into distilled water (B) into solutions with different pHs.

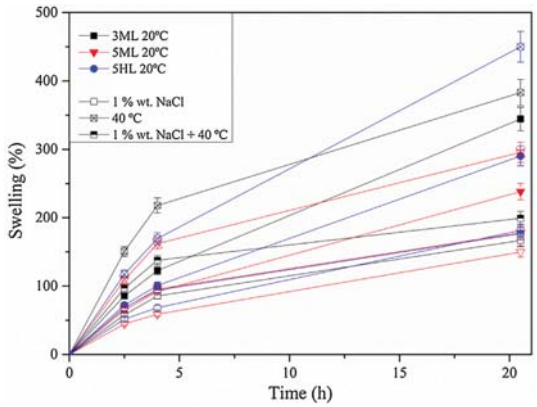

Fig. 4. Swelling performance of the hydrogels 3ML, 5ML and 5HL at 4 different mediums.

room temperature, and the other two were subjected to temperature (40 °C).

As shown in Fig. 4 temperature enhanced the swelling capacity in all cases whereas the saline medium hindered it. In fact, it could be observed that the saline medium at room temperature drastically affected the swelling abilities of all the samples since it decreased a 50, 40 and 40% for 3ML, 5ML and 5HL series, respectively. The warm saline medium also affected negatively the swelling capacity of the samples, since they swelled a 40, 25 and 40% for 3ML, 3HL and 5HL series, subsequently. At 40 °C the swelling was promoted and an increment of a 10, 25 and 55% was observed for 3ML, 5ML and 5HL series, respectively. The latest was also observed by Chang et al. [25], who saw that for the increasing salt concentration the swelling capacity kept decreasing due to the decline of anion-anion electrostatic repulsions caused by the charge screening effect of cations. The same was also reported by Tanan et al. [24], who stated that the type of salt has a strong influence on the swelling ratio due to the difference on the radiuses and charges of the cations. According to Batista et al. [26] an increase in temperature might improve the swelling ability because of environmental entropy and the improved separation of the polymeric chains. In this case, comparing to the control samples, the ones subjected to temperature were the only ones presenting an improvement on the swelling capacity. Even the samples with the combination of NaCl and temperature had swelling ratios below the ones for control samples. So, it could be said that the effect of the saline solution was greater than the one of temperature.

3.3.3. Re-swelling capacity

A re-swelling test was also performed in order to study the reusability of the hydrogels or, in other words, to see if subsequent swelling stages would be prejudicial to their initial swelling ability. The re-swelling of the samples is shown in Fig. 5. In general, a slight decline of around 7% was observed when comparing the swelling ability in the first and second tests. These results were in accordance with those reported by Tanan et al. [24], whose samples were subjected to five swelling and de-swelling cycles. These authors reported that the synthesized semi-IPN hydrogels, which also contained PVA, suffered a gradual loss in their swelling capacity when increasing the cycles. This behavior was attributed to the breakage of physical crosslinking points within the network during the repeating process of swelling-de-swelling, which could also have happened within the PVA-lignin hydrogels. These breakages could have damaged the polymeric structure, diminishing the ability to retain and absorb water at equilibrium [24]. However, the samples in this work were still capable of absorbing considerable amounts of water. Nevertheless, these hydrogels cannot be considered as reusable materials with the results of just one re-swelling test. Therefore, as reusability is an important feature nowadays, future work is needed and at least 5 re-swelling cycles should be performed.

3.4. Attenuated Total Reflection – Fourier Transformed Infrared Radiation (ATR-FTIR)

The hydrogels were analyzed by FTIR technique and their spectra are shown in Fig. S.1 (supplementary data). Both HMw and MMw PVA

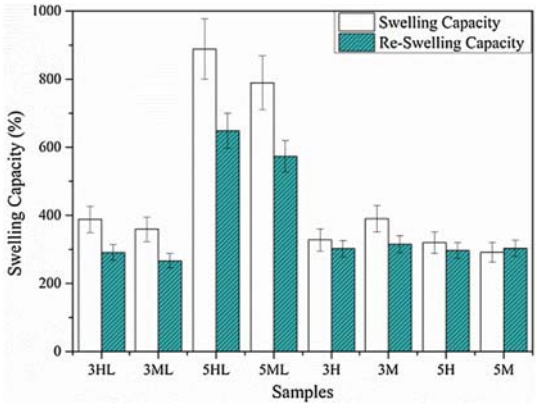

Fig. 5. Re-swelling capacity of the hydrogels.

presented almost identical spectra although HMw PVA displayed more noticeable peaks at 2920 and 2855 cm^{-1}, which could be related to the difference on their molecular weight. Nevertheless, the intensity of the bands between 1750 and 1735 cm^{-1} was very weak for both of them, meaning that few acetate groups were present in the polymer chain due to their high hydrolysis degree [17]. The samples of PVA with and without lignin presented similar spectra, except for the peaks at 1600, 1515 and 1270 cm^{-1} that PVA-lignin hydrogels showed. These three new bands confirmed the incorporation of lignin into the structure of PVA, and the shift of many other bands, such as the ones around 1720 and 1565 cm^{-1}, confirmed the interactions between the components [11]. The main spectra were similar to the one presented by commercial PVA, whose main peaks and their corresponding attributions are displayed in Table S.1 (supplementary data). The characteristic peaks of commercial alkaline lignin are shown in Table S.2 (supplementary data). It was seen that in spite of having different number of freeze-thawing cycles, the hydrogels did not present any difference on their functional groups. The FTIR results are similar to the ones reported in the previous work [10].

3.5. Scanning Electron Microscopy (SEM)

The SEM images of the samples at 2500× magnification are presented in Fig. 6, and 250× magnification in Fig. S.2 (supplementary data). The microstructures of the hydrogels exhibited three dimensionally interconnected porous networks. The freeze-thawing process is responsible for these porous structures as the ice crystals formed inside the hydrogels during the freezing stage melt during the thawing, leaving the porous structure in the samples [27].

The neat PVA samples presented a more homogeneously distributed porous structure, with bigger pores as the molecular weight of the polymer was higher and the number of cycles lower. As a result, MMw PVA hydrogels had a greater swelling capacity than the HMw ones due to the increase in the contact surface with water. Wang et al. [27] reported that neat PVA hydrogels presented high degrees of crosslinking, which were achieved due to the massive hydrogen bonding during the freeze-thawing process. This would explain the morphology of the PVA samples.

When lignin was added, the pore size distribution was more heterogeneous, leading to the creation of many macropores, since it is believed to act as a nucleation agent [16]. Bian et al. [28] reported that lignin nanoparticles acted as spacers and leaded, in their case, to a highly porous PVA/cellulose nanofibril structure. The behavior of the incorporated lignin as a spacer, could explain the formation of thinner walls between the micro voids, which were significantly helpful to the water-retention ability of the hydrogels due to the higher contact surface with it and, thus, its diffusion [21,28]. In this case, the hydrogel with 5 freeze-thawing cycles and HMw PVA was the one leading to the highest water retention (890%).

3.6. X-Ray Diffraction (XRD)

The XRD patterns of raw PVA, commercial alkaline lignin and the hydrogels are displayed in Fig. S.3 (supplementary data). PVA showed the typical semicrystalline structure since it presented an intense signal at around $2\theta = 19.77°$, which corresponded to the (1 0 1) lattice plane and a shoulder around 22.78°, corresponding to the (2 0 1) plane [29]. Two other weak peaks could also be detected at 11.5 and 40.8°. As reported by Ciolacu et al. [4], lignin usually displays an amorphous behaviour, which had a broad peak at 19°. As previously reported [10], the combination between the aforementioned polymers leaded to the formation of hydrogels still with a semicrystalline structure. The slight widening of the strong signal at 19.77° suggested that there was little change on the crystallinity degree of the samples, which was also supported by the results obtained by DSC analyses.

3.7. Differential Scanning Calorimetry (DSC)

In order to study the thermal properties of the synthesized hydrogels, DSC analyses were carried out. Temperatures of crystallization, melting and glass transitions are displayed in Table 1 (T_c, T_m and T_g), as well as melting and crystallization enthalpies (ΔH_m and ΔH_c). These parameters were recorded during the first heating, cooling and the second heating stages and the crystallization index χ_c was calculated from these data. The DSC curves for the cooling and second heating stages are presented in Fig. S.4 (supplementary data).

As seen in the previous work [10], after removing the thermal history of the samples with a first heating stage, a single T_g appeared in all the samples, which indicated the good blend miscibility [16]. This could also be intuited from the SEM micrographs, in which no lignin agglomerations were observed.

For all the samples, the T_g values were significantly higher during the first heating scan than in the second one. This usually happens due to the reduction of crystalline regions formed during the cooling stage, which at the same time enables the chain mobility at lower temperatures. The hydroxyl groups in neat PVA hydrogels tend to be highly

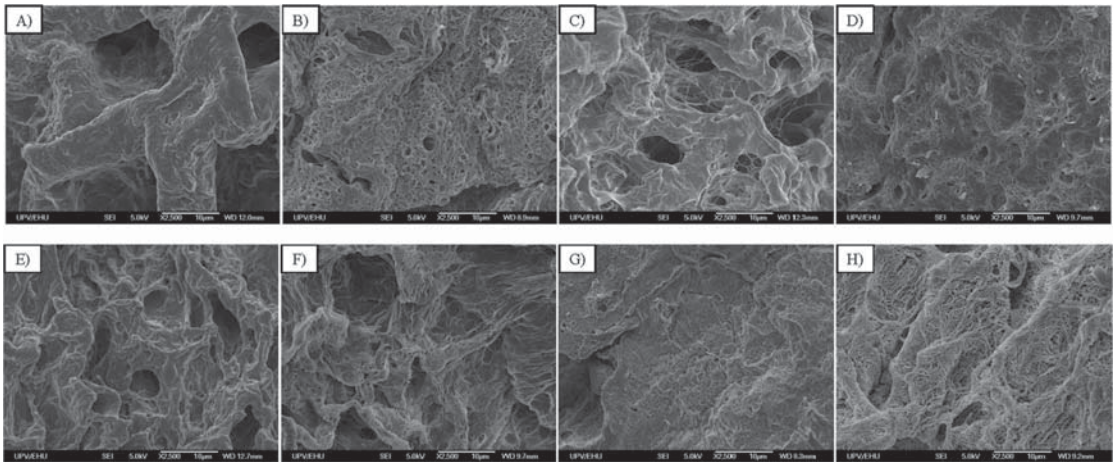

Fig. 6. SEM micrographs of the samples 3H, 3HL, 3 M, 3ML, 5H, 5HL, 5 M and 5ML at x2500 (A–H) magnification.

Table 1
Summarized results for the analyzed parameters by DSC and calculations.

Sample	1st Heating Scan						Cooling Scan			2nd Heating Scan					
	T_g (°C)	T_m (°C)	ΔH_m (W·°C/g)	ΔH_m (J/g)	m_{filler} (%)	χ_c (%)	T_c (°C)	ΔH_c (W·°C/g)	ΔH_c (J/g)	T_g (°C)	T_m (°C)	ΔH_m (W·°C/g)	ΔH_m (J/g)	m_{filler} (%)	χ_c (%)
3H	106	236	17	51	0	31	204	17	52	78	236	14	43	0	27
3HL	107	232	13	38	0.30	34	199	13	39	79	2312	9	27	0.30	24
3M	97	237	16	48	0	30	207	18	53	88	235	15	44	0	27
3ML	116	233	12	35	0.20	27	201	14	42	83	233	10	30	0.20	23
5H	111	236	18	54	0	33	204	17	52	78	234	14	41	0	25
5HL	119	232	12	36	0.38	37	197	12	35	93	230	10	29	0.38	29
5M	112	235	15	45	0	28	207	18	55	80	236	13	38	0	24
5ML	101	232	13	38	0.36	37	199	12	38	83	232	10	30	0.36	30

T_c: Crystallization temperature; T_g: Glass transition temperature; ΔH_m: Melting enthalpy; χ_c: Crystallinity degree; ΔH_c: Crystallization enthalpy; T_m: Melting temperature; m_{filler}: filler mass percentage.

interconnected by hydrogen bonding, leading to high glass transition temperatures (T_g) [30]. During the first heating scan, the T_g values for neat PVA samples with 5 freeze-thawing cycles (111 and 112 °C, for 5H and 5 M samples, subsequently) was slightly higher than for the ones with 3 cycles (106 and 97 °C, for 3H and 3 M, subsequently). However, during the second scan, the T_g values were similar. Therefore, it was concluded that the number of cycles could influence the glass transition temperature although once it had been melted the cycles did not affect. Nevertheless, the molecular weight of PVA influenced the T_g value, despite the difference being of around 3 °C.

When lignin was added, the registered T_g were, in general, higher than those for neat PVA samples since the introduction of other functional groups may support the bonding and enhance T_g values [30].The same behaviour was observed previously, and it was attributed to the restriction on the chain mobility that lignin could have provoked due to the hydrogen bonds between the components [10,11]. The most notable difference was observed in 3ML sample, in which the temperature raised around 19 °C. The highest T_g was registered for the sample 5HL. In this case, the cycles and the molecular weight of PVA chains could have leaded to a higher packaging and, therefore, to this increase in T_g.

Regarding the melting temperature, no significant change was observed between both heating scans. In addition, the molecular weight of PVA did not affect the T_m. However, a decrease on the melting enthalpy was noticed when lignin was incorporated. As reported by He et al. [11], this could be due to the disruption that lignin causes on the crystalline regions that PVA chains form, breaking existing intra- and intermolecular hydrogen bondages in the matrix and creating new ones between both polymers. The melting enthalpies were slightly lower on the second heating stage as less crystalline regions were formed. This was also confirmed by the crystallization temperatures and enthalpies, which were as well reduced with the addition of lignin (see Table 1). Once again, the molecular weight of PVA did not alter the T_c.

The crystallization indexes calculated from the reported enthalpies suggested that there was no significant difference on the crystalline regions of the samples. Besides, according to the calculations, the crystallinity degree of the lignin-PVA hydrogels seemed to be higher. This behaviour was also reported by He et al. [11], who clarified that large contents (> 5% wt.) of lignin nano-particles formed crystalline regions due to an increased interface interaction via hydrogen bonding between the abundant hydroxyl groups on LNP and PVA. This would support the results for χ_c in Table 1, which decreased during the second heating stage due to the short time for crystallization.

3.8. Thermogravimetric Analysis (TGA)

TGA was performed for a rapid evaluation of the thermal stability of the samples and in order to obtain the degradation temperatures of their forming polymers. TG and DTG curves of neat PVA hydrogels and lignin-PVA hydrogels are shown in Fig. 7A and B. As expected, all the neat PVA samples presented similar degradation profiles, also alike the ones in the previous work [10]. Four main weight loss stages were observed: the first one at around 150 °C, the second one close to 250 °C, the third and maximum degradation stage at 375 °C and the fourth around 440 °C. The first step was related to physically weak and chemically strong bound water evaporation [24], and despite the difference on the molecular weight, no variance was observed in the temperature. The second step was attributed to the initial degradation of PVA, which for the samples with lower molecular weight started some degrees earlier. The maximum degradation stage happened at the same temperature for all the samples, but a higher weight loss was observed for the MMw PVA hydrogels. This was related to the depolymerization of the acetylated and deacetylated units of the polymer, and finally, the last stage, corresponding to the thermal degradation of some by-products generated by PVA, was common for all. However, the loss was slightly more notable for the samples with HMw PVA. The registered final residue in all samples was lower than 3% of the initial weight.

When lignin was added, four main degradation steps were also observed. The first one, which was detected around 150 °C, was attributed to moisture evaporation and, as in the case of neat PVA hydrogels, no difference was noticed as the molecular weight of the polymer matrix was varied. Then, an overlapping of the second and third stages was seen. The second one was detected at around 280 °C for the samples with MMw PVA and close to 290 °C for the samples with HMw PVA, which was higher than that reported for neat PVA hydrogels. The shift of the onset temperature to higher values could be attributed to the thermal stability of lignin [31]. It was seen that having a higher molecular weight PVA had greater influence on the onset temperature than having different freeze-thawing cycles. The third and main degradation step was found at 330 °C for every sample, which was lower than the one reported by other authors for lignin-containing hydrogels [31,32]. Even though, this fact could be related to the lack of additional components in the hydrogels such as crosslinkers or reinforcing fibres, which could have leaded to the formation of weaker lignin-PVA linkages and permitted a more facile degradation. After this stage, there was still around a 30% of the initial samples left. The fourth weight loss was observed at 425 °C and no clear variation was detected as the molecular weight of the samples changed. However, there was a significant increase on the residue with the addition of lignin, being the sample with highest molecular weight and greater number of cycles (5HL) the one leaving the highest residual content (17%). The sample with the least residual weight (12.5%) was the one with the lowest molecular weight and fewer cycles (3ML). Thus, the addition of lignin leaded to a higher final residue, as well as the increase on the number of cycles and on the molecular weight of the employed matrix polymer. In general, it can be said that the variation on the molecular weight PVA and the freeze-thawing cycles do not affect the thermal stability of the samples as strongly as the addition of lignin does.

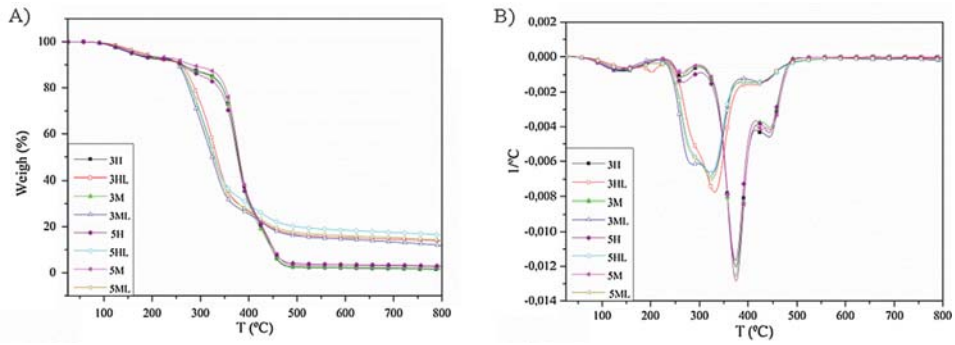

Fig. 7. (A) TG and (B) DTG curves of the hydrogels.

3.9. Compression studies

The compression behaviour of the samples was analyzed up to the 80% of their initial thickness and the compression modulus for each sample was calculated from their stress-strain curves. The calculated data is displayed in Table 2. At the maximum deformation, all the samples presented good ability of recovery, since none of them was broken and kept a total integrity. However, as expected, there were some differences among the calculated modulus.

For the samples without lignin, Young's modulus ranged from 18 to 28 MPa. The samples with MMw PVA presented the lowest values (18.13 and 19.85 MPa for 3 and 5 cycles, successively) compared to the ones for HMw PVA hydrogels (28.13 and 22.06 MPa for 3 and 5 cycles, respectively). It was surprising to observe such a fall in the modulus for HMw PVA hydrogels from 3 to 5 cycles, but as 5H sample also presented higher water retention (265%), it might also be possible to have a less compact structure. In the case of MMw PVA, an opposite behaviour was seen; in fact, the modulus was increased as the number of cycles increased.

When lignin was added, the 3HL sample did not present an adequate form for compress tests, so the rest of the series were studied. A clear decrease of the modulus was observed in all cases (> 50%). For instance, 5HL sample presented a modulus of 10.32 MPa, while the one for the same sample without lignin (5H) was of 22.06 MPa. This is a direct consequence of the reported great swelling capacity for 5HL (890%) comparing to the one presented by 5H (265%), which had a highly crosslinked and compact structure. As for 3ML and 5ML samples, there was also a clear drop on their modulus with respect to their twin blank hydrogels. In addition, there was a slight increase on the modulus when the number of cycles was augmented (8.77 MPa for 3ML and 9.64 MPa for 5ML), which would be in agreement with the reported trend for neat MMw PVA hydrogels. However, no clear correlation could be done between the swelling ability and the modulus, since 5ML presented higher water retention ability and modulus than the ones shown by 3ML sample. Nevertheless, it was clearly seen that lignin provoked a significant drop on the compression modulus of all the samples, regardless of which the molecular weight of PVA was. This behaviour was also seen by Chen et al. [33] on their PAM hydrogels with high lignin contents. Wu et al. [7] also reported a dominant elastic behaviour on their lignin-PVA-epichlorohydrin samples.

Comparing the synthesized hydrogels with the ones in the previous work [10], it can be confirmed that, as the modulus decreases up to 50%, the time of the cycles also has a great impact on the compression behaviour of the final hydrogels.

Table 2
Results for the compression tests of the samples.

Sample	Compression Modulus (MPa)	Standard Deviation (MPa)
3M	18.13	4.23
3ML	8.77	2.27
3H	28.13	4.4
5M	19.85	2.53
5ML	9.64	4.56
5H	22.06	3.29
5HL	10.32	3.05

3.10. Methylene blue adsorption tests

Many authors have previously reported the success of lignin-hydrogels in dye removal [5,7]. Lignin-based hydrogels present large negative charges on their surface due to the numerous carboxylic acid groups and thanks to the π–π hydrophobic interactions, these hydrogels can trap positively charged dyes, i.e. cationic dyes [7]. For this reason, the adsorption of MB was evaluated. This substance is commonly used for cotton, wood and silk dying and it has been proven to be very harmful for human and animals [5].

The uptake of MB on the first 24 h was evaluated by spectrophotometry. Although the yield values were not as high as the ones reported by other authors [5,7], the removal values were even higher than the ones reported by them. Fig. 8A shows the removal and yield values for the samples 5HL, 5H and 3ML. It was observed that 5HL (0.012 mg MB/g hydrogel) had a lower yield than that calculated for 3ML (0.014 mg MB/g hydrogel) but the percentage of removal was greater (71.6% for 5HL and 69.1% for 3ML). For the hydrogel without lignin (5H), the yield was 0.002 mg MB/g hydrogel) and the removal was of 34.8%. These values demonstrate that lignin enhances the

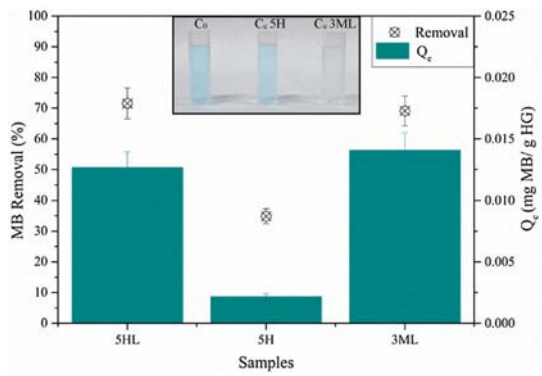

Fig. 8. (A) MB adsorption performance and removal of 5HL, 5H and 3ML samples (B) real appearance of the initial MB solution and equilibrium concentrations of 5H and 3ML samples after 24 h.

potential of these hydrogels as cationic dye adsorbents, which can also be appreciated in Fig. 8B, where the visual appearance of the initial concentration and equilibrium concentration for the samples 5H and 3ML are shown.

3.11. Complementary swelling studies

3.11.1. Influence of the Lignin Content

As shown in Section 3.2, the lignin waste during the washing stage was quite significant in all cases. In order to optimize the lignin content of the hydrogels to save lignin, an estimation of the composition of the hydrogels after washing was done, taking into account the lost lignin. In this way, no excessive lignin amount would be added, just the necessary to obtain the "same" hydrogels.

After the corresponding calculations had been done, the estimated "reduced" amount of lignin was added for each hydrogel formulation (3HL.R, 3ML.R, 5HL.R and 5ML.R). The procedure was exactly as the one for the previous hydrogels.

It was observed, that for all the synthesized hydrogels, the lignin waste was still notable. In fact, the accounted minimum lignin waste was of 37.5%, in the case of 3ML.R sample. It is true that this percentage was significantly reduced since the initial lignin waste of the same sample was of 77.8%. Nevertheless, for the three other samples (3HL.R, 5HL.R and 5ML.R) the lost lignin was of around 50%, which was still a high amount.

With regard to the swelling ability, for the samples synthesized from 5 freeze-thawing cycles, a great drop was noticed (over a 50% of their initial ability), while for the 3-times-freeze-thawed samples, just a slight variation of their swelling capacities was seen. However, these samples did not show as high swelling rates as at the beginning. This might be related to the amount of reactive sites of lignin that are initially introduced in the blend, which promote the crosslinking reactions between the PVA chains and lignin. In other words, if less reactive sites are introduced, there is a lower possibility for them to interact with the PVA chains, since no additional reagent is enhancing the reaction. Thus, the non-reacted lignin molecules get removed from the hydrogel together with NaOH as the washing stage is performed. Therefore, it can be concluded, that the initial lignin amount, the washing stage and the loss of lignin have an important effect on the subsequent swelling capacity of the hydrogel. Wu et al. [7] studied the effect of the lignin concentration on the swelling capacity of their hydrogels. These authors observed that, for the same concentration of PVA, as the concentration of lignin increased, the swelling ratio was enhanced until a maximum value, from which an increase in the lignin concentration had a negative influence on the swelling ratio [7]. In addition, they concluded that as lignin has good compatibility with PVA through hydrogen bonding, more lignin could be used to fabricate hydrogels with higher swelling ratios [7]. This might mean that for the hydrogels in this work, a reduction of the amount of PVA could have a higher impact on the swelling capacity rather than the lignin concentration. Nevertheless, it is important to bear in mind that these authors did also incorporate epichlorohydrin as a crosslinker [7].

3.11.2. Influence of the lignin type

After studying several influent factors on the swelling behaviour of the hydrogels, another variable was decided to explore. As the structure of the lignin depends on its source and extraction method, the synthesis of organosolv-lignin-based hydrogels was considered. Organosolv lignin is usually more environmentally friendly than alkaline lignin, which in this case was confirmed to be sulphur-containing kraft lignin. Therefore, the same initial amount of reagents was taken, this time with commercial organosolv lignin and also both MMw and HMw PVA, and the same experimental method was followed. The synthesized samples were then named 3MO, 3HO, 5MO and 5HO. The molecular weight distributions of both alkaline and organosolv lignins are shown in Table S.3 (supplementary data).

During the washing stage of these hydrogels, the waste of large amounts of lignin was also observed. None of the samples lost less than 70% of the organosolv lignin added initially, which was almost in all cases higher than that for the alkaline lignin. This could be directly related to the variation on total reactive sites that the lignins could have, as well as with their molecular weight. In fact, organosolv lignin presented an apparent weight average molar mass of 33,000 g/mol, with a polydispersity index of 29, while for the alkaline lignin it was of around 9300 g/mol, with a polydispersity index lower than 7.

As for the swelling ability, all the samples presented a lower water retention capacity than that shown with alkaline lignin. The maximum swelling rate was observed for the 5MO sample (352%), followed by the one for 5HO sample (350%). 3MO and 3HO samples presented a swelling capacity of 284 and 260%, respectively. This high drop on the swelling capacity demonstrates that the lignin type, apart from the molecular weight of PVA, has a strong influence on the final properties of the hydrogel, especially on the water retention rate. This could be related to the heterogeneity of the employed organosolv lignin, whose heaviest molecules might not have been able to interact with PVA, letting the smallest molecules attach to the PVA chains and, thus, leading to a lower swelling ability.

This fact was also confirmed by Wu et al. [7], who reported very different swelling capacities for the hydrogels synthesized employing three types of lignin.

4. Conclusions

Several hydrogels were successfully synthesized from medium and high molecular weight PVA and alkali lignin. It was observed that LMw PVA did not enable a good crosslinking with lignin, so it was concluded that the Mw of PVA is a key factor when synthesizing hydrogels. Apart from increasing the Mw of PVA, as the number of cycles was increased, the crosslinking of the hydrogels was also promoted and the swelling capacity of the obtained hydrogels was higher. When lignin was incorporated, the water absorption ability was greatly improved (up to 890%), and by increasing the number of cycles, the lignin waste was reduced probably due to the increment on the formed interactions and the generated porous microstructure. The hydrogels were pH and temperature responsive since they presented higher swelling capacities at high pH values and higher temperatures. Moreover, although further studies are needed, the samples could be reusable materials since they were able to swell and de-swell more than once. The thermal properties were gently influenced by the molecular weight of the polymer. The compression modulus was greater for the highest molecular weight samples; however, when lignin was incorporated it was drastically lowered. In spite of this drop, the hydrogels presented complete integrity after compressing them to the 80% of their initial thickness. Moreover, the lignin hydrogels presented improved MB adsorption capacity, making them interesting to be employed in this field.

It was observed that the twin hydrogels with reduced amounts of lignin had considerably lower swelling capacities. Therefore, the initial lignin content and the washing stage could be vital for ensuring high swelling abilities. The lignin type did also affect the swelling capacity since organosolv lignin did not enable such high water absorption rates.

In conclusion, this study shows that the molecular weight of the matrix polymer, as well as the crosslinking method and the lignin type directly affect the final properties of the hydrogels.

CRediT authorship contribution statement

Amaia Morales: Investigation, Validation, Data curation, Formal analysis, Writing - original draft. **Jalel Labidi:** Funding acquisition, Methodology, Supervision, Writing - review & editing. **Patricia Gullón:** Visualization, Formal analysis, Writing - review & editing.

Declaration of Competing Interest

The authors declare that they have no known competing financial interests or personal relationships that could have appeared to influence the work reported in this paper.

Acknowledgements

The authors would like to acknowledge the financial support of the Department of Education of the Basque Government (IT1008-16). A. Morales would like to thank the University of the Basque Country (Training of Researcher Staff, PIF17/207). P. Gullón would like to express her gratitude to MINECO for financial support (Grant reference IJCI-2015-25304). The authors thank for technical and human support provided by SGIker (UPV/EHU/ERDF, EU).

Appendix A. Supplementary material

Supplementary data to this article can be found online at https://doi.org/10.1016/j.eurpolymj.2020.109631.

References

[1] P. Azadi, O.R. Inderwildi, R. Farnood, D.A. King, Liquid fuels, hydrogen and chemicals from lignin: a critical review, Renew. Sustain. Energy Rev. 21 (2013) 506–523, https://doi.org/10.1016/j.rser.2012.12.022.
[2] M. Mahinroosta, Z. Jomeh Farsangi, A. Allahverdi, Z. Shakoori, Hydrogels as intelligent materials: A brief review of synthesis, properties and applications, Mater. Today Chem. 8 (2018) 42–55, https://doi.org/10.1016/j.mtchem.2018.02.004.
[3] M.R. Guilherme, F.A. Aouada, A.R. Fajardo, A.F. Martins, A.T. Paulino, M.F.T. Davi, A.F. Rubira, E.C. Muniz, Superabsorbent hydrogels based on polysaccharides for application in agriculture as soil conditioner and nutrient carrier: A review, Eur. Polym. J. 72 (2015) 365–385, https://doi.org/10.1016/j.eurpolymj.2015.04.017.
[4] D. Ciolacu, G. Cazacu, New Green Hydrogels Based on Lignin, J. Nanosci. Nanotechnol. 18 (2018) 2811–2822, https://doi.org/10.1166/jnn.2018.14290.
[5] J. Domínguez-Robles, M.S. Peresin, T. Tamminen, A. Rodríguez, E. Larrañeta, A.S. Jääskeläinen, Lignin-based hydrogels with “super-swelling” capacities for dye removal, Int. J. Biol. Macromol. 115 (2018) 1249–1259, https://doi.org/10.1016/j.ijbiomac.2018.04.044.
[6] S. Park, S.H. Kim, J.H. Kim, H. Yu, H.J. Kim, Y.H. Yang, H. Kim, Y.H. Kim, S.H. Ha, S.H. Lee, Application of cellulose/lignin hydrogel beads as novel supports for immobilizing lipase, J. Mol. Catal. B Enzym. 119 (2015) 33–39, https://doi.org/10.1016/j.molcatb.2015.05.014.
[7] L. Wu, S. Huang, J. Zheng, Z. Qiu, X. Lin, Y. Qin, Synthesis and characterization of biomass lignin-based PVA super-absorbent hydrogel, Int. J. Biol. Macromol. 140 (2019) 538–545, https://doi.org/10.1016/j.ijbiomac.2019.08.142.
[8] A. Oryan, A. Kamali, A. Moshiri, H. Baharvand, H. Daemi, Chemical crosslinking of biopolymeric scaffolds: Current knowledge and future directions of crosslinked engineered bone scaffolds, Int. J. Biol. Macromol. 107 (2018) 678–688, https://doi.org/10.1016/j.ijbiomac.2017.08.184.
[9] S. Huang, S. Shuyi, H. Gan, W. Linjun, C. Lin, X. Danyuan, H. Zhou, X. Lin, Y. Qin, Facile fabrication and characterization of highly stretchable lignin-based hydroxyethyl cellulose self-healing hydrogel, Carbohydr. Polym. 223 (2019), https://doi.org/10.1016/j.carbpol.2019.115080.
[10] A. Morales, J. Labidi, P. Gullón, Assessment of green approaches for the synthesis of physically crosslinked lignin hydrogels, J. Ind. Eng. Chem. 81 (2020) 475–487, https://doi.org/10.1016/j.jiec.2019.09.037.
[11] X. He, F. Luzi, X. Hao, W. Yang, L. Torre, Z. Xiao, Y. Xie, D. Puglia, Thermal, antioxidant and swelling behaviour of transparent polyvinyl (alcohol) films in presence of hydrophobic citric acid-modified lignin nanoparticles, Int. J. Biol. Macromol. 127 (2019) 665–676, https://doi.org/10.1016/j.ijbiomac.2019.01.202.
[12] M.N. Collins, C. Birkinshaw, Physical properties of crosslinked hyaluronic acid hydrogels, J. Mater. Sci. Mater. Med. 19 (2008) 3335–3343, https://doi.org/10.1007/s10856-008-3476-4.
[13] S.A. Bencherif, A. Srinivasan, F. Horkay, J.O. Hollinger, K. Matyjaszewski, N.R. Washburn, Influence of the degree of methacrylation on hyaluronic acid hydrogels properties, Biomaterials 29 (2008) 1739–1749, https://doi.org/10.1016/j.biomaterials.2007.11.047.
[14] L. Zeng, M. Xie, Q. Zhang, Y. Kang, X. Guo, H. Xiao, Y. Peng, J. Luo, Chitosan/organic rectorite composite for the magnetic uptake of methylene blue and methyl orange, Carbohydr. Polym. 123 (2015) 89–98, https://doi.org/10.1016/j.carbpol.2015.01.021.
[15] A. Labidi, A.M. Salaberria, S.C.M. Fernandes, J. Labidi, M. Abderrabba, Functional chitosan derivative and chitin as decolorization materials for methylene blue and methyl orange from aqueous solution, Materials (Basel) 12 (2019), https://doi.org/10.3390/ma12030361.
[16] W. Yang, E. Fortunati, F. Bertoglio, J.S. Owczarek, G. Bruni, M. Kozanecki, J.M. Kenny, L. Torre, L. Visai, D. Puglia, Polyvinyl alcohol/chitosan hydrogels with enhanced antioxidant and antibacterial properties induced by lignin nanoparticles, Carbohydr. Polym. 181 (2018) 275–284, https://doi.org/10.1016/j.carbpol.2017.10.084.
[17] H.S. Mansur, C.M. Sadahira, A.N. Souza, A.A.P. Mansur, FTIR spectroscopy characterization of poly (vinyl alcohol) hydrogel with different hydrolysis degree and chemically crosslinked with glutaraldehyde, Mater. Sci. Eng. C 28 (2008) 539–548, https://doi.org/10.1016/j.msec.2007.10.088.
[18] T.M.C. Maria, R.A. de Carvalho, P.J.A. Sobral, A.M.B.Q. Habitante, J. Solorza-Feria, The effect of the degree of hydrolysis of the PVA and the plasticizer concentration on the color, opacity, and thermal and mechanical properties of films based on PVA and gelatin blends, J. Food Eng. 87 (2008) 191–199, https://doi.org/10.1016/j.jfoodeng.2007.11.026.
[19] W.E. Hennink, C.F. van Nostrum, Novel crosslinking methods to design hydrogels, Adv. Drug Deliv. Rev. 64 (2012) 223–236, https://doi.org/10.1016/j.addr.2012.09.009.
[20] K. Varaprasad, G.M. Raghavendra, T. Jayaramudu, M.M. Yallapu, R. Sadiku, A mini review on hydrogels classification and recent developments in miscellaneous applications, Mater. Sci. Eng. C 79 (2017) 958–971, https://doi.org/10.1016/j.msec.2017.05.096.
[21] N. Thombare, S. Mishra, M.Z. Siddiqui, U. Jha, D. Singh, G.R. Mahajan, Design and development of guar gum based novel, superabsorbent and moisture retaining hydrogels for agricultural applications, Carbohydr. Polym. 185 (2018) 169–178, https://doi.org/10.1016/j.carbpol.2018.01.018.
[22] Y. Meng, J. Lu, Y. Cheng, Q. Li, H. Wang, Lignin-based hydrogels: A review of preparation, properties, and application, Int. J. Biol. Macromol. 135 (2019) 1006–1019, https://doi.org/10.1016/j.ijbiomac.2019.05.198.
[23] W. Farhat, R. Venditti, N. Mignard, M. Taha, F. Becquart, A. Ayoub, Polysaccharides and lignin based hydrogels with potential pharmaceutical use as a drug delivery system produced by a reactive extrusion process, Int. J. Biol. Macromol. 104 (2017) 564–575, https://doi.org/10.1016/j.ijbiomac.2017.06.037.
[24] W. Tanan, J. Panichpakdee, S. Saengsuwan, Novel biodegradable hydrogel based on natural polymers: Synthesis, characterization, swelling/reswelling and biodegradability, Eur. Polym. J. 112 (2018) 678–687, https://doi.org/10.1016/j.eurpolymj.2018.10.033.
[25] C. Chang, B. Duan, J. Cai, L. Zhang, Superabsorbent hydrogels based on cellulose for smart swelling and controllable delivery, Eur. Polym. J. 46 (2010) 92–100, https://doi.org/10.1016/j.eurpolymj.2009.04.033.
[26] R.A. Batista, P.J.P. Espitia, J. de S.S. Quintans, M.M. Freitas, M.Â. Cerqueira, J.A. Teixeira, J.C. Cardoso, Hydrogel as an alternative structure for food packaging systems, Carbohydr. Polym. 205 (2019) 106–116, https://doi.org/10.1016/j.carbpol.2018.10.006.
[27] L.Y. Wang, M.J. Wang, Removal of heavy metal ions by poly(vinyl alcohol) and carboxymethyl cellulose composite hydrogels prepared by a freeze-thaw method, ACS Sustain. Chem. Eng. 4 (2016) 2830–2837, https://doi.org/10.1021/acssuschemeng.6b00336.
[28] H. Bian, L. Wei, C. Lin, Q. Ma, H. Dai, J.Y. Zhu, Lignin-containing cellulose nanofibril-reinforced polyvinyl alcohol hydrogels, ACS Sustain. Chem. Eng. 6 (2018) 4821–4828, https://doi.org/10.1021/acssuschemeng.7b04172.
[29] X.-Q. Hu, D.-Z. Ye, J.-B. Tang, L.-J. Zhang, X. Zhang, From waste to functional additives: thermal stabilization and toughening of PVA with lignin, RSC Adv. 6 (2016) 13797–13802, https://doi.org/10.1039/C5RA26385A.
[30] O.W. Guirguis, M.T.H. Moselhey, Thermal and structural studies of poly (vinyl alcohol) and hydroxypropyl cellulose blends, Nat. Sci. 04 (2012) 57–67, https://doi.org/10.4236/ns.2012.41009.
[31] H. Bian, L. Jiao, R. Wang, X. Wang, W. Zhu, H. Dai, Lignin nanoparticles as nanospacers for tuning the viscoelasticity of cellulose nanofibril reinforced polyvinyl alcohol-borax hydrogel, Eur. Polym. J. 107 (2018) 267–274, https://doi.org/10.1016/j.eurpolymj.2018.08.028.
[32] I.E. Raschip, G.E. Hitruc, C. Vasile, M.C. Popescu, Effect of the lignin type on the morphology and thermal properties of the xanthan/lignin hydrogels, Int. J. Biol. Macromol. 54 (2013) 230–237, https://doi.org/10.1016/j.ijbiomac.2012.12.036.
[33] Y. Chen, K. Zheng, L. Niu, Y. Zhang, Y. Liu, C. Wang, F. Chu, Highly mechanical properties nanocomposite hydrogels with biorenewable lignin nanoparticles, Int. J. Biol. Macromol. 128 (2019) 414–420, https://doi.org/10.1016/j.ijbiomac.2019.01.099.

Effect of the formulation parameters on the absorption capacity of smart lignin-hydrogels

Amaia Morales, Jalel Labidi*, Patricia Gullón

Chemical and Environmental Engineering Department, University of the Basque Country UPV/EHU, Plaza Europa 1, 20018, San Sebastián, Spain

Supplementary data

Figure S.1: FTIR spectra of the hydrogels, commercial alkaline lignin and MMw/HMw PVA.

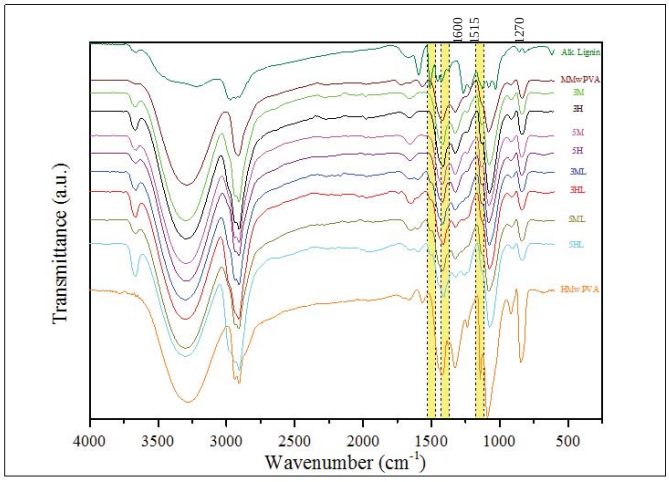

Figure S.2: SEM micrographs of the samples 3H, 3HL, 3M, 3ML, 5H, 5HL, 5M and 5ML at x250 (A–H) magnification.

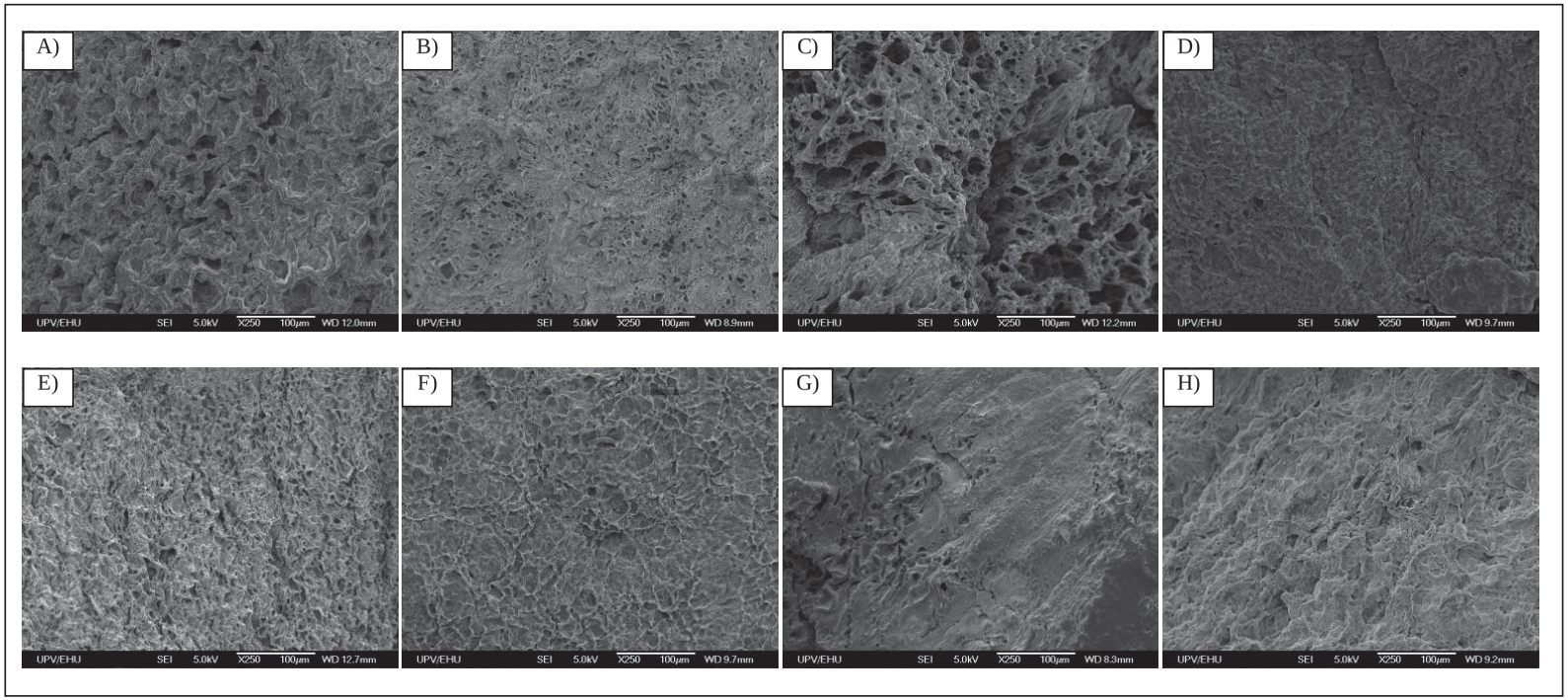

Figure S.3: XRD diffractograms of the hydrogels.

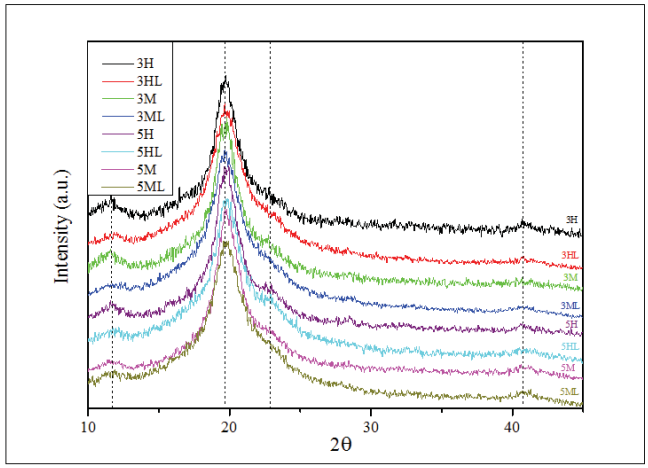

Figure S.4: DSC thermograms of the first cooling stage and second heating stage of the hydrogels.

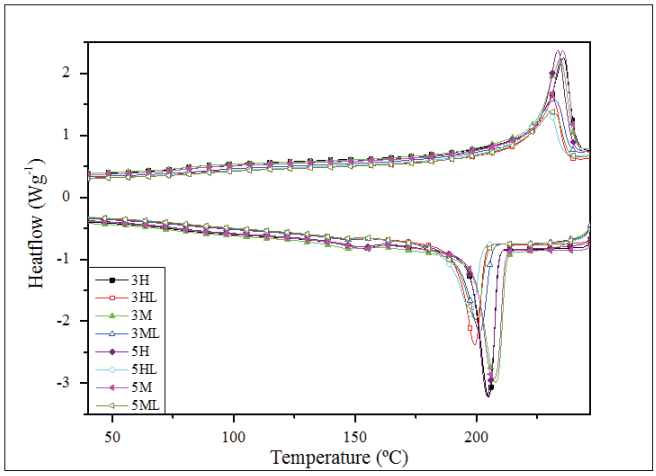

Table S.1: Characteristic FTIR peaks of PVA.

Wavenumber (cm^{-1})	Assignment
3300	-OH stretch vibration
2920	Alkyl asymmetric C-H stretch vibration
2855	Symmetric C-H stretch vibration
1720	Ester C=O stretch vibration
1660	Residual C=O stretch vibration
1560	C=C stretch vibration
1425	CH_2 bending vibration
1325	O–H deformation vibration
1100	C-C stretching vibration
840	C-C and C-O stretching vibration

Table S.2: Characteristic FTIR peaks of alkaline lignin.

Wavenumber (cm^{-1})	Assignment
3215	-OH stretch vibration
2947	Alkyl asymmetric vibration
2913	Aromatic C-H stretching vibration
1679	C=O ester bonds
1597	C=C stretch vibration
1513	C=C aromatic vibrations
1456	C-H bonds of the methyl groups
1429	C-H bonds of the methyl groups
1269	Guaiacyl units
1100	C–C bonds
1030	C-O stretching vibration
865	C-C stretching vibration
821	aromatic -CH out of plane vibration
618	C-S bonds

Table S.3: Molecular weight distribution of alkaline and organosolv lignins.

Type of Lignin	Mw (Da)	Percentage (%)	Average Mw (Da)	Mw/Mn
Alkaline	10,424	89.2	9,333	6.8
	345	10.0		
	155	0.8		
Organosolv	82,538	37.9	32,933	29.3
	9,393	7.9		
	3,731	18.4		
	1,004	18.8		
	353	14.9		
	152	2.1		

IV. Artikulua

Impact of the lignin type and source on the characteristics of physical lignin hydrogels

A. Morales, J. Labidi, P. Gullón

IV

http://10.1016/j.susmat.2021.e00369
2214-9937/
Sustain. Mater. Technol. 31 (2021) e00369

Sustainable Materials and Technologies 31 (2022) e00369

Contents lists available at ScienceDirect

Sustainable Materials and Technologies

journal homepage: www.elsevier.com/locate/susmat

Impact of the lignin type and source on the characteristics of physical lignin hydrogels

Amaia Morales [a], Jalel Labidi [a,*], Patricia Gullón [b]

[a] Chemical and Environmental Engineering Department, University of the Basque Country UPV/EHU, Plaza Europa 1, 20018 San Sebastián, Spain
[b] Centro de Apoio Científico e Tecnolóxico á Investigación, Universidade de Vigo, Technology Park of Galicia- Tecnopole, CTC Building, 32901, San Cibrao das Viñas, Ourense, Spain

ARTICLE INFO

Keywords:
Lignin
Poly (vinyl alcohol)
Almond shells
Walnut shells
Physical hydrogels

ABSTRACT

Multiple natural polymers have been investigated for the synthesis of hydrogels to the present date, but lignin has demonstrated to be a promising one for this purpose for the multiple advantages it offers. Lignin can be isolated from lignocellulosic material such as nut shells, which are usually undervalued wastes, and would be a great step forward on circular economy. Thus, in the present work, lignin was extracted from almond and walnut shells following a single-step (delignification) and double-step (autohydrolysis and delignification) biorefinery scheme. After the chemical composition and structures of these lignins were determined, hydrogels were synthesized combining them with poly (vinyl alcohol) by the means of freeze-thawing cycles so as to study the influence of the different lignins on their final properties. Additionally, the last thawing cycle of the synthesis process was lengthened in order to confirm previous assumptions about its effect on the characteristics of the synthesized materials. The obtained results showed significant variation between the 8 lignin samples, especially in their purity, molecular weights and total phenolic contents. The variation on the lignins leaded to several hydrogel morphologies, which directly affected their properties, primarily their swelling capacity, glass transition temperatures and compression strengths. It was also demonstrated the great effect that the duration of the last thawing had on the morphology and, hence, on the characteristics of the obtained materials. The synthesized samples were successfully employed as dye adsorbents and the evaluation of their antifungal activity showed positive results in some of the samples, which could be applied for food packaging.

1. Introduction

Synthetic polymer-based items like hydrogels have completely stirred up our everyday lives. These materials are comprised by tridimensionally entangled polymeric chains that exhibit high water retention capacity due to the multiple hydrophilic groups they contain [1]. In addition to their great swelling properties, their internal structure together with their mechanical properties have made them gain considerable attention in the last years [2]. Hydrogels can be arranged according to the types of crosslinks that their polymeric chains present, which can be physical or chemical [2]. The chemical ones often demand the presence of toxic and costly crosslinking reagents whereas the physical ones do not. Thus, physical crosslinking makes the synthesis process greener and more economical [3]. Hydrogels can be presented in many substrates and forms, which, together with the aforementioned features, make them useful in a wide range of applications such as agriculture and environment, personal hygiene or biomedicine, among others [1].

The beginning of the 21st century has been marked by a significant economic boost coupled with high plastic pollution which have leaded to several irrecoverable environmental concerns. In this context, the possibility of introducing biodegradable and renewable polymers to produce new materials such as hydrogels is nowadays one of the principal goals of research. Biopolymers, which are polymers coming from plants, animals and microorganisms, seem to be the solution to the stated problem since, apart from helping to face ecological problems [4], they would also contribute to sustainability and circular economy [5].

Biopolymers and other co-products (e.g. biofuels and biochemicals) can be extracted from biomass through biorefinery processes [6]. Lignocellulosic biomass, for instance, has emerged as a potential, renewable and available source of biopolymers and biochemicals. This type of biomass involves forestry, urban and alimentary residues [7].

* Corresponding author.
E-mail address: jalel.labidi@ehu.eus (J. Labidi).

https://doi.org/10.1016/j.susmat.2021.e00369
Received 5 July 2021; Received in revised form 14 September 2021; Accepted 26 November 2021
Available online 29 November 2021

The main constituents of lignocellulosic biomass are cellulose, hemicelluloses and lignin, which can be employed as backbones on the formulation of hydrogels and other materials.

Among these natural polymers, lignin is the most bountiful aromatic one on Earth [8]. Its amorphous and complex structure is principally constituted by a random combination of three kinds of phenyl propane monomers (coniferyl, *p*-coumaryl and sinapyl alcohols) connected through several stable linkages [8]. The isolation method influences the properties of the extracted lignin such as its reactivity. The typical lignin extraction methods include Kraft, sulphite, alkaline and organosolv delignifications [9]. Lignin is commonly obtained as a by-product of pulp and paper industries; nevertheless, a small percentage of the entire quantity (<2%) of lignin generated every year has an added-value [8]. Hence, employing it for the synthesis of hydrogels, for instance, would contribute to cover the urgent need of safe and greener alternative materials.

Almond and walnut shells are an abundant waste all over the world. The low percentage of edible kernel in both nuts leads to an enormous production of shells with no recognized industrial or commercial application [7,10]. However, these shells belong to the lignocellulosic biomass and are very rich in lignin and other biopolymers. Therefore, these residues could be further valorised though a biorefinery strategy so as to use them as input feedstocks for the production of added-value materials [7,10].

In the last years, several researchers have described the synthesis of hydrogels with lignin from different sources and with different extraction methods [11,12]. Nonetheless, a great part of the published works reports the production of chemically crosslinked hydrogels, generally involving the use of toxic crosslinkers as well as the need of removing the residual part of it [3].

In this light, the objective of the present study was to analyse the influence of the type of lignin and its features on the final characteristics of physically crosslinked lignin-hydrogels. For this aim, lignin was extracted through alkaline and organosolv delignifications from walnut and almond shells (with and without prior hydrothermal pretreatment) [7,10] and hydrogels were formulated combining lignin and poly (vinyl alcohol) following the synthesis route reported previously [13]. In addition, hydrogels were also synthesized through a variation of the initial synthesis route, which consisted in lengthening the last thawing stage. In this way, the properties of these hydrogels were compared to the other ones, highlighting the most significant differences. The isolated lignins were characterised via purity, Py-GC/MS, HPSEC, FTIR, XRD, TGA and TPC analysis. The lignin waste and swelling capacity of all the synthesized hydrogels were measured and they were further characterised by FTIR, SEM, DSC and compression tests. Finally, the adsorption capacity of the hydrogels was evaluated by employing methylene blue as water pollutant, and their antifungal capacity against *Aspergillus niger* was also studied so as to explore their applicability in food packaging, for example.

2. Materials and methods

2.1. Materials

Almond shells (AS) were supplied by local farmers (Marcona variety) and walnut shells (WNS) were kindly supplied by Olagi cider house (Altzaga, Gipuzkoa). The shells were milled and sieved (particle size between 2 and 1 mm) and stored in a dark and dry place at room temperature until use.

Poly (vinyl alcohol) (M_w = 83,000–124,000 g/mol, 99 + % hydrolyzed), phosphate buffer saline (PBS) tablets, trypan blue solution and methylene blue powder were purchased from Sigma Aldrich. Sodium hydroxide (NaOH, analysis grade, ≥98%, pellets) was supplied by PanReac Química SLU. Potato dextrose agar (PDA) was acquired from Scharlab S.L. and DMSO from Fisher Scientific S.L. All reagents were employed as supplied.

2.2. Lignin extraction

The operational conditions were chosen in accordance to prior knowledge [7,10]. The alkaline and organosolv delignification stages were carried out twice for each type of shells: the first one without a prior hydrothermal treatment and the second one with a prior hydrothermal treatment (autohydrolysis). Table 1 summarizes the conditions employed for each lignin extraction.

2.3. Hydrogel synthesis

Lignin-hydrogels were synthesized according to a previous work [13]. The concentrations of the blends (9.87 w.% PVA and 9.12 w.% lignin) were also determined on the basis of previous studies. Briefly, the corresponding amount of PVA (5.92 g) was added to 60 mL of a 2% (*w*/w) NaOH aqueous solution and it was magnetically stirred and heated to 90 °C. Once the PVA was dissolved, lignin (5.47 g) was added while stirring until completel dissolution. The blends were poured into silicon moulds. The internal bubbles were eliminated by ultrasounds and the remaining superficial air bubbles were then poked manually.

The blends were frozen for 2.5 h at −20 °C and they were then thawed at 28 °C for 1.5 h. This cycle was repeated five times, leaving the samples freezing overnight during the second and fifth cycles. Afterwards, the hydrogels were washed as it was done previously [13] in order to remove the residual lignin and NaOH. Finally, the hydrogels were dried at room temperature.

Based on prior experiments (data not shown), it was thought that the duration of the last thawing step could alter the features of the synthesized hydrogels. For this reason, hydrogels with a longer 5th thawing stage (24 h inside the heater) were also prepared. These samples were tagged as LC samples (long cycle) and the previous ones as SC (short cycle).

2.4. Characterization methods

The characterization methods and equipments used in this work both for the extracted lignins and the synthesized hydrogels are described in Table 2.

2.5. Methylene blue adsorption tests

The removal of methylene blue (MB) was investigated according to a

Table 1
Operational conditions for each of the extracted lignins.

Abbreviation	Description	Autohydrolysis	Delignification
AAL	AS alkaline lignin	–	121 °C, 90 min, 7.5 w.% NaOH, LSR 6:1
AOL	AS organosolv lignin	–	200 °C, 90 min, 70/30 (v/v) EtOH/H_2O, LSR 6:1
WAL	WNS alkaline lignin	–	121 °C, 90 min, 7.5 w.% NaOH, LSR 6:1
WOL	WNS organosolv lignin	–	200 °C, 90 min, 70/30 (v/v) EtOH/H_2O, LSR 6:1
AAAL	Autohydrolysed AS alkaline lignin	179 °C (isothermal), 23 min, LSR 8:1	121 °C, 90 min, 7.5 w.% NaOH, LSR 6:1
AAOL	Autohydrolysed AS organosolv lignin	179 °C (isothermal), 23 min, LSR 8:1	200 °C, 90 min, 70/30 (v/v) EtOH/H_2O, LSR 6:1
AWAL	Autohydrolysed WNS alkaline lignin	200 °C (non-isothermal), LSR 8:1	121 °C, 90 min, 7.5 w.% NaOH, LSR 6:1
AWOL	Autohydrolysed WNS organosolv lignin	200 °C (non-isothermal), LSR 8:1	200 °C, 90 min, 70/30 (v/v) EtOH/H_2O, LSR 6:1

Table 2
Characterization methods and equipments for the extracted lignins and synthesized hydrogels.

Analysis	Sample	Equipment	Reference
Purity	Lignin	HPLC-RI/PDA (Jasco LC-Net II/ ADC, 300 × 7.8 mm Aminex HPX-87H column)	[21]
Acid soluble lignin	Lignin	UV–Vis spectrophotometer (Jasco V-630, JASCO)	[18]
Composition	Lignin	Py-GC/MS (Py: 5150 Pyroprobe, GC: Agilent 6890, MS: Agilent 5973)	[21]
Average molecular weight	Lignin	GPC (JASCO LC-Netll/ADC, detector: RI-2031Plus,Two Polar Gel-M columns: 300 mm × 7.5 mm)	[18]
Total phenolic content (TPC)	Lignin	UV–Vis spectrophotometer (Jasco V-630, JASCO)	[18]
Thermal degradation	Lignin	TGA/DTG (TGA/SDTA RSI analyser 851 Mettler Toledo)	[13]
Crystallinity	Lignin	XRD (Phillips X'Pert Pro Automatic multipurpose diffractometer)	[13]
Chemical structure	Lignin	ATR-FTIR (PerkinElmer Spectrum Two FTIR Spectrometer)	[22]
Lignin Waste	Hydrogels	UV–Vis spectrophotometer (Jasco V-630, JASCO)	[13]
Swelling	Hydrogels	$Swelling\ (\%) = \frac{m_{swollen} - m_{dry}}{m_{dry}} x\ 100$	[13]
Morphology	Hydrogels	SEM (Hitachi S-4800, 5 kV, 20 nm Au covering)	[56]
Glass transition temperature	Hydrogels	DSC (Mettler Toledo DSC 822)	[13]
Compression tests	Hydrogels	Mechanical test machine (Instron 5967, 500 N load cell)	[13]

previous study [13]. In brief, first, multiple solutions of certain concentrations (5–0.25 mg/L) of MB were prepared. Then, their absorbance was measured at 665 nm by a V-730 UV-Jasco spectrophotometer, and relating each concentration with its corresponding absorbance a calibration curve was designed. For the adsorption experiments, a solution containing 1 mg/L of MB was prepared, and around 0.5 g of dry samples were introduced in 15 mL of this solution, keeping them at room temperature and static regimen for 24 h. The percentage of MB removal was also calculated by means of Eq. (1) after the concentrations of the initial and final dissolutions were determined by the calibration curve:

$$P(\%) = \frac{C_0 - C_{eq}}{C_0} \cdot 100 \quad (1)$$

where P is the equilibrium adsorption rate of the hydrogel, C_0 is the initial dye concentration, C_{eq} is the dye concentration at equilibrium.

The adsorption performance was similarly calculated by Eq. (2).

$$Q_e\left(\frac{mg_{MB}}{g_{HG}}\right) = \frac{C_0 - C_{eq}}{m} \cdot V \quad (2)$$

where V is the total volume of dye employed for each sample and m is the dry weight of the hydrogel and the rest of the variables are the same as the ones defined for Eq. (1) [13].

2.6. Antifungal studies

The antifungal activity of the extracted lignins and hydrogels was measured according to the methods previously reported by Salaberria et al. (2017) and Da Silva et al. (2018) with slight modifications [14,15]. Briefly, after culturing the mould fungus *Aspergillus niger* (CBS 554.65) on Petri dishes covered with PDA for 7 days at 25 °C ± 1.5 °C in a climatic chamber, some spores were diluted in a PBS dissolution and its concentration was adjusted to around 1.21 × 10^6 spores/ml using an automatic cell counter for the measurements (Cellometer® Mini, Nexcelom Bioscience LLC). Then, the procedure was varied according to the type of sample.

The lignins were firstly dissolved in DMSO (around 75–100 mg/mL) and then, 40 μL of the sample dissolution was poured on a Petri dish covered with PDA and the fungal strain was sprayed around. The blank was performed with DMSO [15].

In the case of the hydrogels, square portions (approximately 1 cm × 1 cm) of each sample were introduced into the PDA covered Petri dishes after having inoculated them with fungal strain. The blank was performed using neat PVA hydrogel portions.

All the tests were done by duplicate. After 7 days of incubation at 25 °C ± 1.5 °C, the lignins were evaluated visually using a numerical scale reported by da Silva et al. (2018) in accordance with ISO 846, whereas the hydrogels were extracted from the agar and washed with 1 mL of PBS in order to collect the spore solution into an Eppendorf. Afterwards, these solutions were tinged blue with 5 μL trypan blue solution and after shaking them, their spore concentration was determined with the abovementioned cell counter [14]. The fungal growth inhibition (FGI) of the samples were calculated through the equation given by Salaberria et al. (2017) [14].

3. Results and discussion

3.1. Lignin characterization

3.1.1. Purity

So as to analyse the selectivity of the lignin extraction processes, the purity of the lignin samples together with the amount of impurities that had precipitated with them was determined by quantitative acid hydrolysis. The measured purities for the obtained lignins were calculated taking the Klason lignin and acid soluble lignin (ASL) into account.

As shown in Table 3, the purity results were, in general, higher for organosolv lignins than for alkaline ones. These results are related to the selectivity of organosolv extractions [16]. It was also observed that the organosolv lignins without autohydrolysis (AOL and WOL) had purities over 90%, whereas the ones for alkaline lignins were lower than 59%. However, after autohydrolysis, the purities for the latest increased up to 88–95% while for the organosolv ones this increment was just of a 3–5%. Therefore, it can be said that autohydrolysis greatly improves the purity of the extracted lignins, especially in alkaline processes, because of the effective prior elimination of hemicelluloses, which are the main impurities after lignin extraction as demonstrated by Dávila et al. (2017). The obtained results are consistent with those reported previously [7,10].

3.1.2. Composition of the lignins

Pyrolysis-Gas Chromatography/Mass Spectrometry (Py-GC/MS) analyses were performed in order to study the composition of the eight different lignins. The resulting pyrograms are shown in Fig. 1. The numbered peaks correspond to lignin-derived phenolic compounds with

Table 3
Summary of the purity, GPC, TPC and TGA results for the isolated lignins.

Lignin sample	Purity (%)	M_w[a] (g/mol)	M_n[b] (g/mol)	M_w/M_n[c]	TPC (% GAE[d])	T_{max}[e] (°C)
AAL	58.2	4770	1109	4.3	13.8	307
AOL	90.4	8301	1072	7.8	15.6	389
WAL	49.4	4761	1054	4.5	10.6	295
WOL	92.7	6371	1246	5.1	16.5	388
AAAL	88.2	12,793	1528	8.4	33.1	355
AAOL	95.2	9020	1520	5.9	26.2	357
AWAL	95.7	16,670	1604	10.4	33.8	354
AWOL	95.2	7644	1359	5.6	27.2	365

[a] M_w: weight average molecular weight.
[b] M_n: number average molecular weight.
[c] M_w/M_n: polydispersity index.
[d] % GAE: percentage of gallic acid equivalents.
[e] T_{max}: maximum degradation temperature from TG/DTGA curves.

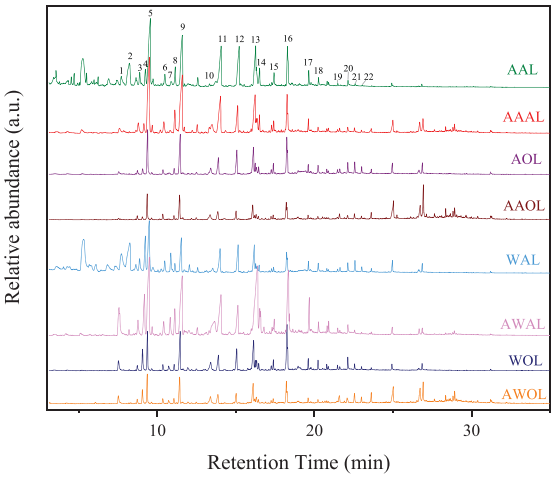

Fig. 1. Pyrograms of the extracted lignins.

larger area than 1% in at least one of the lignin samples, and their identification is displayed in Supplementary data. The untagged peaks at early times (3–7 min) mainly corresponded to degradation compounds from impurities. Furfural, for instance, was one of these compounds coming from carbohydrates and it appeared at minute 5 [10]. These impurities were especially visible in AAL and WAL samples, which also presented the lowest purity values in Table 3. From minute 23 on, the majority of the compounds with large areas were fatty acids, which are characteristic of nuts [17]. Thus, the identified compounds were detected in the range of 7–23 min and they were grouped based on the origin of their aromatic structure (*p*-hydroxyphenyl (H), guaiacol (G) and syringol (S)) [7,10].

Among the identified compounds, guaiacol (peak #5), 4-methylguaiacol (peak #9), syringol (peak #13) and 4-methylsyringol (peak #16) were the most abundant ones in all the lignin samples, constituting the 15%, 13.7%, 11.8% and 10.8% of the tagged compounds, subsequently. 4-ethylguaiacol and 4-vinylguaiacol (peaks #11 and #12, respectively) were also present in large amounts in all the samples. The compounds coming from the *p*-hydroxyphenyl unit such as phenol, *p*-cresol and *p*-ethylphenol seemed to be more abundant in WNS lignins (peaks #1, #3 and #4).

Regarding the estimated S/G ratios, all the samples presented more G units except for WOL and AWOL samples. This means that almost all the S/G ratios were below 1. However, an increase of this ratio was observed for the samples from the double-step process, which will be further studied so as to find a consistent explanation However, these values are quite different to the ones reported previously for AS and WNS lignins [7,10], which could be related to any possible modification on the composition of the feedstock or in the extraction process.

3.1.3. Average molecular weight analysis

From the GPC analyses, based on the molecular weight distributions of the lignin samples, their number-average (M_n) and weigh average (M_w) molecular weights were determined and their polydispersity indexes (M_w/M_n) were estimated. These values are displayed in Table 3.

The lignins after autohydrolysis presented higher weight and number average molecular weights in all cases. In addition, the organosolv lignins without autohydrolysis presented higher M_w than the alkaline ones, whereas for the lignins with autohydrolysis, the opposite behaviour was observed. A similar trend was perceived for the polydispersity indexes. It should also be noticed that the M_w for all the organosolv lignins was very alike, whereas for the alkaline lignins this difference was huge. However, and looking at the purity percentages and previous works [18], these results make us believe that the analysed lignin fractions for AAL and WAL were not representative of the whole lignin samples; in other words, there were probably bigger chains than 0.40 μm (which is the pore size of the used filter) that were excluded from the analysis. These would explain such enormous difference in M_w reported for alkaline lignins with and without autohydrolysis.

Some authors also reported small variations on the molecular weights of organosolv lignins from solids with and without an autohydrolysis process [19,20]. In addition, they reported that autohydrolysis permitted the obtaining of lower polydispersity indexes for organosolv lignins [19,20], as happened in the present work.

Although it is hard to find previous research on the comparison of alkaline delignification treatments with and without a prior hydrothermal treatment, the results for alkaline lignins in Table 3 are aligned with those reported in literature [10,16,21].

3.1.4. Total phenolic content (TPC)

The phenolic hydroxyl groups in the structure of lignins are usually related to its antioxidant capacity as well as to its suitability for the synthesis of new materials [22]. Therefore, it is important to study the TPC of the lignin samples. Looking at the results, it was observed that the values for the lignin samples coming from the direct delignification of the raw material (AAL, AOL, WAL and WOL) were considerably lower than those reported for the ones coming from the two-step process (AAAL, AAOL, AWAL and AWOL), which could be related to their purities [22]. It was also appreciated that AAL and WAL presented slightly lower TPC values than AOL and WOL, and they were aligned with the results obtained by García et al. (2012, 2017) and Sequeiros et al. (2014) for soda lignin [23–25]. Nevertheless, the TPC of organosolv lignins (AOL and WOL) were significantly lower than those reported by other authors [23,24,26]. As commented, the lignin samples obtained after a prior autohydrolysis process, presented significantly greater percentages of GAE (26.2–33.8% GAE). A comparable behaviour was reported by Dávila et al. (2019) for alkaline lignin extracted from pre-treated and non-treated vine shoots [22], suggesting that a prior hydrothermal treatment can be crucial to obtain high total phenolic contents in lignin. In this case, alkaline lignin samples (AAAL and AWAL) presented higher TPC values than the ones obtained for organosolv lignins. These results are in agreement with the ones reported previously for almond shells [10]. Other authors purified lignins coming from the direct delignification of the feedstock with an acid hydrolysis; nonetheless, they reported much lower GAE percentages in the purified samples than in the original ones [23,24,27]. This fact also supports the idea of subjecting the raw material to a hydrothermal pre-treatment if high TPC values want to be achieved.

3.1.5. Thermal degradation analysis (TGA)

The thermal stability of lignins is also an important characteristic to take into account, especially for their use in the production of composite materials. Thus, the thermal degradation of the extracted lignins was studied. The TGA curves are shown in Supplementary data. The maximum degradation temperatures of the samples are displayed in Table 3. All the samples had a common initial degradation step below 100 °C, corresponding to moisture evaporation. The second degradation step was the maximum degradation stage for all the samples. However, the temperatures differed depending on the lignin extraction. In fact, for the alkaline lignins obtained though a single-step process (AAL and WAL), the maximum degradation happened around 300 °C, whereas for the organosolv lignins this temperature was significantly higher (≈390 °C). This could be ascribed to their high amount of impurities as well as to the fractions with low molecular weight [21,28], as reported in Section 3.1.3. The lignins coming from the double-step processes presented similar maximum degradation temperatures (354–365 °C), which were within the ones reported for single-step process lignins and were in accordance with previous results [10]. In this temperature

range, the scission of β–O–4 ether bondages tend to occur, followed by the division of C—C linkages and aromatic rings [28].

A third degradation stage was observed around 420 °C, although this temperature was again lower for AAL and WAL (≈390 °C) samples and higher for AOL and WOL samples (≈ 470 °C). The latest then presented a constant weight loss until 37% of their initial weight. The rest of the samples presented a fourth degradation step around 700 °C, leading to a final residue between 20 and 29% of their initial weight. This last stage could be related to the demethoxylation or condensation reactions of the volatile products of lignin [28], and the amounts of residue were aligned with those reported previously [10].

3.1.6. Crystallinity

The XRD patterns of the lignin samples are depicted in Fig. 2. As shown, all the organosolv lignins and the alkaline ones coming from the double-step processes (AAAL and AWAL), presented the typical broad signal around 2θ = 22°, representing its amorphous structure [29]. AAL and WAL samples presented narrower peaks at the same diffraction angle. Moreover, they also presented sharp signals at 11, 12, 19, 25 and 31°, which are more characteristic of the crystalline domains of cellulose [30,31] and hemicelluloses [32]. Therefore, an important presence of impurities in these lignins was again confirmed by XRD analysis, leading to a modification on the ordered domains.

3.1.7. Chemical structure

The main functional groups of the isolated lignins were determined by FTIR technique (Figure 3). Although all the recorded spectra presented the typical lignin bands [7,22,26], the intensities of some of them changed from sample to sample. Some of these variations were observed in the range 2827–2998 cm^{-1}, which corresponded to the C—H (CH_3, CH_2 and CH) stretching vibration of lignin and polysaccharides [19], and were more notable for alkaline lignin samples, probably due to the lower elimination of sugars during the autohydrolysis step. Before the footprint range, at 1650 cm^{-1}, a peak corresponding to conjugated C═O stretching vibration [19] was detected for the single-step lignins, but it disappeared after the autohydrolysis step. Although some authors have previously related this band to alkaline processes [33], it may be attributed to the presence of impurities in AAL, WAL, AOL and WOL lignins. On the footprint range (1500–600 cm^{-1}) the main changes were seen on the intensity of the bands. AAL and WAL samples, for instance, presented a clear decrease on the intensity of the bands ascribed to the condensed syringil or guaiacyl unit breathing (1325 cm^{-1}) [34,35] and aromatic methyl ethers of lignin (1215 cm^{-1}) [19]. Conversely, the peaks at 1157, 1080, 975 and 896 cm^{-1}, corresponding to C—O stretching vibration in ester groups [34,35], C—O deformation in secondary alcohol and aliphatic ethers, —HC═CH out-of-plane and C—H deformation vibrations [35], subsequently, got intensified in the aforementioned samples. The remaining bands were similar for all the lignin samples, confirming the existence of syringyl and guaiacyl units in all the lignins, although their ratios were different, as demonstrated in Section 3.1.2.

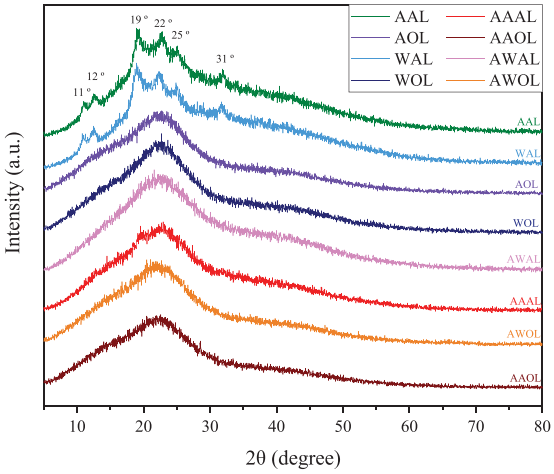

Fig. 2. XRD patterns of the extracted lignins.

3.2. Hydrogel characterization

3.2.1. Lignin waste

The lignin waste of the samples was analysed so as to determine their final lignin content. The results are shown in Table 4. For the samples made from alkaline lignin, the ones containing lignins from the single-step processes (AA and WA) presented higher lignin wastes than the ones containing lignins coming from double-step processes (AAA and AWA). A similar trend was observed for organosolv lignins from WNS (WO and AWO), whereas for the ones coming from AS (AO and AAO) the reported behaviour was the opposite. This might be related to the polidispersity of the lignins, since except for AOL and AAOL, the polydispersity of the rest of the lignins increased from single to double-step lignins. This fact suggests that highest molecular weight lignin chains might have been able to interact with the PVA matrix, whereas lowest molecular weight fractions were eliminated. However, further studies should be done in order to verify this statement. Moreover, lower waste percentages were accounted for AS lignins than for WNS lignins in the case of the single-step lignins (56.2–66.5% vs. 60.0–68.5%), while for the double-step lignins the contrary was appreciated (44.2–59.9% vs. 59.6–71.1%). These values are in great accordance with those reported previously [13]. It should also be noted that among the single-step lignin containing samples the ones with alkaline lignin showed greater lignin wastes that the ones containing organosolv lignin, whereas the samples with double-step lignins exhibited the inverse trend.

In addition, the samples with a long last thawing step, in general, presented lower lignin waste values, suggesting that the lengthening of the last cycle may have enhanced the interactions between the PVA and the lignin. Furthermore, the samples with single-step alkaline WNS lignin (WA) showed a significant reduction on their lignin waste. On the contrary, the samples with double-step alkaline WNS lignin (AWA) presented much greater lignin waste values than those reported before. It can also be said that, except for AWA sample, all the alkaline lignin containing hydrogels lost less lignin than the ones containing organosolv lignin.

3.2.2. Swelling

As the swelling capacity of the hydrogels is determining for assessing their applications, this property was measured for all the samples and it is displayed in Fig. 4.

The samples with short last thawing cycle presented swelling values between 336 and 505%, which corresponded to AWO and WA samples, respectively. Moreover, the samples containing alkaline lignin showed in all cases higher swelling capacities, which is in accordance with the data reported previously [13], which could be related to the attachment of the fractions with highest molecular weights to the matrix. Comparing the aforementioned samples with the ones with a long last thawing stage, a huge enhancement of this property was clearly seen. The most significant improvement (80% more regarding its prior swelling ability) was seen on AWO sample, which was the one that had previously presented the lowest swelling capacity. On the contrary, the sample that exhibited the slightest enhancement was AWA, whose swelling ability was just improved about 22%. Agudelo et al. (2018) studied the influence of various synthesis parameters such as the time of the freeze-thawing cycles on the swelling capacity of neat PVA hydrogels [36]. According to their work, the excessive lengthening of the thawing cycles

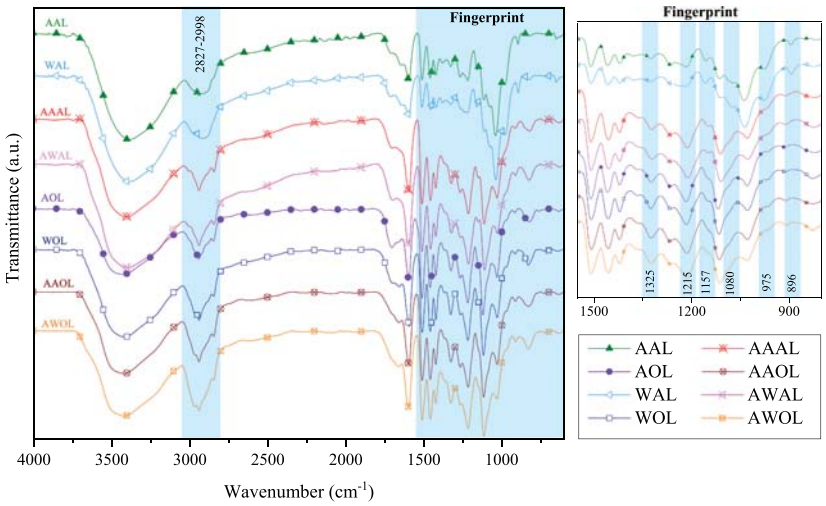

Fig. 3. FTIR spectra of the extracted lignins.

Table 4
Lignin waste (%) of the analysed short (SC) and long (LC) last thawing step samples.

Sample	SC (%)	LC (%)
AA	66.5 ± 2.9	48.5 ± 3.0
AO	56.2 ± 2.4	53.9 ± 3.4
WA	68.5 ± 0.7	26.0 ± 6.4
WO	60.0 ± 1.8	53.9 ± 2.1
AAA	59.6 ± 2.8	36.3 ± 2.0
AAO	71.1 ± 3.0	48.1 ± 3.3
AWA	44.2 ± 1.6	74.3 ± 3.7
AWO	59.9 ± 4.0	51.7 ± 2.2

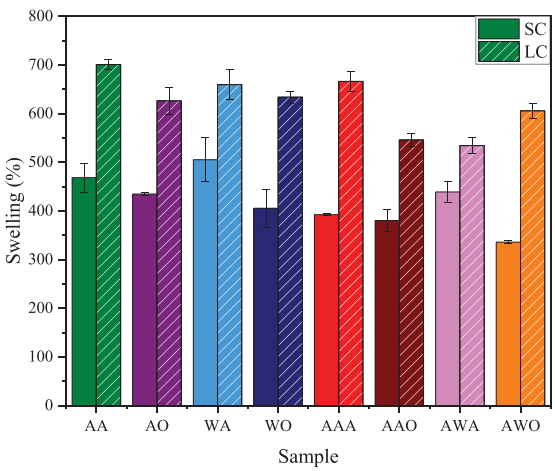

Fig. 4. Swelling capacity of the synthesized hydrogels with short (SC) and long (LC) last thawing steps.

leads to the dissolution of the formed crystallites, which reduces of their quantity and size and, hence, also the crosslinking density and the swelling capacity of the hydrogel [36]. Thus, as in the present work the lengthened thawing step was the last one, the molten crystallites might have evaporated, reducing the crosslinking density of the samples and resulting in a notable enhancement of their swelling capacity. Nevertheless, this phenomenon should be further investigated in order to find a more reliable explanation.

It should also be mentioned that the samples containing lignins coming from single-step processes, presented higher swelling capacities than the ones coming from the double-step processes, probably due to the interactions of their impurities with the polymeric matrix. Although Wu et al. (2019) related the swelling properties to the content of phenolic hydroxyl groups and to the molecular weight of the employed lignins, their hypothesis would not explain the behaviour of the hydrogels in this work [12]. In fact, the samples containing lignin with the lowest total phenolic contents and lowest average molecular weights (AA and WA) presented the highest swelling capacities. However, this might support the previous statement about the non-representative average molecular weights determined for these lignins (Section 3.1.3) and also the one about the interactions with non-lignin components (Section 3.2.1), since these samples presented high lignin wastes.

3.2.3. Morphology

The morphology of the synthesized hydrogels was studied by Scanning Electron Microscopy (SEM). The corresponding micrographs for the samples containing AS lignins at 500× and 5000× magnifications are shown in Fig. 5 and the ones for WNS lignin samples in Supplementary data.

At first sight, it was seen that all the hydrogels presented different appearances. Although all the samples presented porous structures at different levels, their distribution, size and density was distinct. In fact, all the samples that corresponded to hydrogels containing lignins from single-step processes were quite similar and presented a highly porous honeycomb structure, as expected for lignin containing PVA hydrogels [13,37–39]. Their pore sizes and distributions were quite homogeneous, but the walls between the micro voids were smoother and more brittle in the case of AA and WA samples than in AO and WO samples, which presented thicker walls. These structures were responsible for their high water absorption capacities [40] and could have been created due to the interactions of PVA with the highest molecular weight lignin fractions.

When lignins from the double-step processes were employed, the synthesized hydrogels displayed much denser and continuous structures with hardly recognizable pores, which may be related to a higher

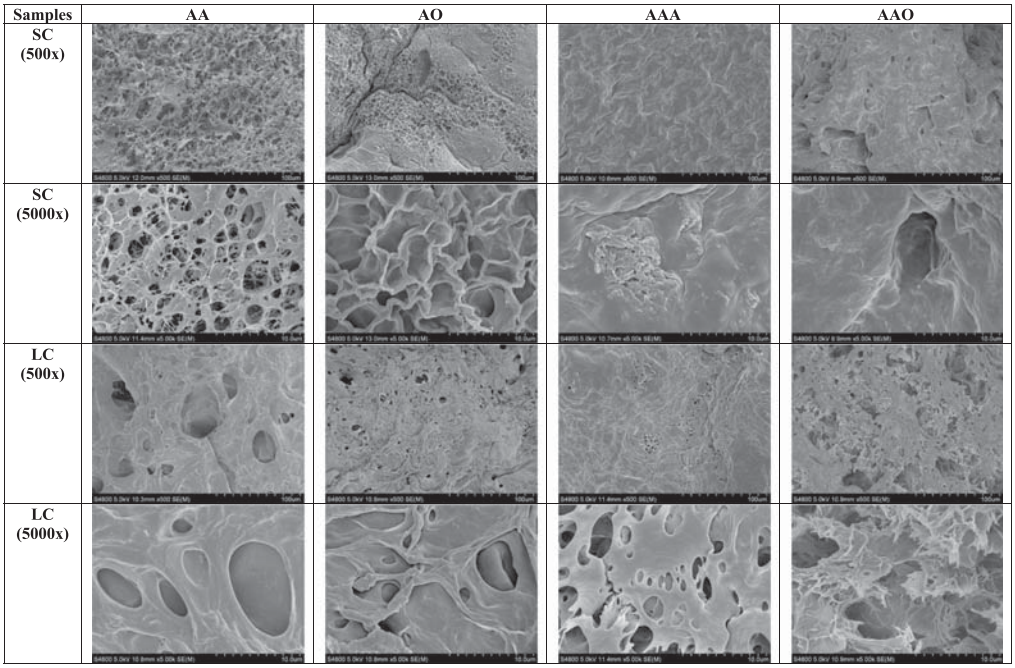

Fig. 5. SEM micrographs of the hydrogels containing AS lignins at 500× and 5000× magnifications.

crosslinking density with these lignins due to their higher contents in phenolic hydroxyl groups [12]. Rachip et al. (2013) also reported variable hydrogel morphologies according to the —OH and —COOH groups in lignin [41]. These microstructures would explain the drop on the swelling ability of the present samples compared to the aforementioned ones.

It was also appreciated that when the last thawing step was lengthened, there was an evident creation of macro pores in all cases. As aforementioned, this might be ascribed to the evaporation of molten crystallites during the last step of the synthesis, which permitted the formation of these structures and improved the swelling performance of all the hydrogels, regardless of their origin or extraction type.

Although the influence of the number of cycles has been previously studied by many authors for freeze-thawed PVA hydrogels [13,36,40,42,43], the duration of last thawing step has not been investigated. So, the present study could pave the way to new synthesis routes since it offers a simple way of enhancing the swelling capacity of the samples.

3.2.4. Glass transition temperature

The glass transition temperature (T_g) is an important characteristic of polymeric materials since it determines their applicability. Thus, the synthesized hydrogels were subjected to Differential Scanning Calorimetry (DSC) analyses and the results are presented in Table 5.

The samples containing alkaline lignins presented higher T_g values ranging from 72 to 91 °C whereas the ones containing organosolv lignins showed lower T_g values (69–86 °C). The highest T_g values were found for AA and AAA samples (≈91 °C), which might be because the impurities could have acted as bridges between the PVA and the lignin chains, enhancing their interactions and hindering the relaxation and arrangement of the chains [41,44]. On the contrary, although WA sample contained lignin with a higher amount of impurities, part of the latest might have dissolved in the aqueous phase, being washed out during the washing step and, hence, being unable to enhance the interactions between PVA and lignin. Therefore, in this case, the T_g value was lower.

Table 5
Glass transition temperatures (T_g) and compression modules of the synthesized hydrogels after short (SC) and long (LC) last thawing steps.

Sample	T_g (°C)		Compression module (MPa)		MB removal (%)	
	SC	LC	SC	LC	SC	LC
AA	91.0	77.3	16.3 ± 1.8	10.8 ± 3.2	79.5 ± 3.6	81.3 ± 1.8
AO	73.0	66.6	5.0 ± 1.9	2.1 ± 0.7	90.3 ± 0.6	83.4 ± 2.8
WA	79.0	64.0	14.9 ± 1.9	13.6 ± 0.8	75.3 ± 3.7	82.3 ± 3.0
WO	69.7	77.7	6.0 ± 1.0	2.0 ± 0.8	89.6 ± 1.0	86.9 ± 4.4
AAA	91.1	66.6	13.1 ± 0.8	7.5 ± 2.7	86.6 ± 3.2	93.3 ± 1.1
AAO	85.8	82.8	2.1 ± 1.0	2.0 ± 0.8	90.1 ± 2.2	87.1 ± 6.7
AWA	72.1	66.4	6.6 ± 2.9	6.4 ± 1.3	87.9 ± 3.6	86.9 ± 5.5
AWO	70.8	92.2	5.4 ± 2.8	2.88 ± 1.2	93.0 ± 0.6	88.6 ± 1.9

Except for AWA sample, the hydrogels containing double-step lignins presented higher T_g values than the ones with single-step lignins, which also matched with the previously reported drop on their swelling capacity due to a higher crosslinking degree between lignin and PVA. However, this could also be attributed to the increment on the average molecular weights of the lignins as well as to their total phenolic content. These two factors affect the total —OH groups of lignin, which although according to Raschip et al. (2013) seemed to decrease the T_g of pure lignin, they could have enhanced the hydrogen bonding with the matrix polymer, making its chains flow at higher temperatures [41].

When the last thawing step was lengthened, all the T_g values dropped except for WO and AWO samples. This might have occurred due to an increment on the interactions between lignin and PVA after water evaporation due to the rearrangement of WO and AWO chains, which presented low average molecular weights and the lowest polydispersities. Thus, the resulting hydrogels were more thermally stable. Nevertheless, to the best of our knowledge there is no literature that supports and explains this fact.

3.2.5. Compression tests

The mechanical performance of the hydrogels was studied compressing them up to the 80% of their initial thickness. From the obtained stress-strain diagrams, the compression modules were calculated, as displayed in Table 5. As in the previous work, at the end of the tests none of the tested hydrogels was fractured and showed excellent recoverability. Nevertheless, the samples containing alkaline lignin from the single-step processes were slightly damaged due to their heterogeneous appearance.

The aforementioned samples (AA and WA) were the ones presenting the highest compression modules (14.8 and 16.3 MPa, respectively) although they were also the ones with the highest swelling ability, which might be related to the formed honeycomb structures due to the interactions of the matrix with lignin and its impurities, as shown in Section 3.2.3. In spite of their analogous morphology, the samples containing single-step organosolv lignins (AO and WO) presented much lower compression modules (4.95 and 6.01 MPa, respectively). A similar behaviour was observed for the samples composed of double-step lignins: the ones with alkaline lignin presented higher compression modules (6.63–13.07 MPa) than the organosolv ones (2.05–5.4 MPa).

The modules of all the samples presented a slight drop when increasing the duration of the last thawing step, probably due to the creation of the macro pores, as aforementioned. This trend was also aligned to the one observed for T_g values. All the estimated modules were in great accordance with previous results [13], and were higher than those reported by other authors for lignin-based hydrogels [1,45].

3.3. Methylene blue adsorption studies

So as to study the applicability of the designed hydrogels as dye adsorbents, methylene blue (MB) adsorption tests were performed following the procedure described before [13]. It is known that thanks to interactions of the multiple negative charges on the surface of ligninhydrogels, these materials are able to capture positively charged compounds such as cationic dyes [12,13], which are also employed in many medical applications [46].

As displayed in Table 5, it was demonstrated that the synthesized samples presented great potential for MB adsorption for the tested solution, being the lowest removal value 75% and the highest 93% of the pollutant, which exceeded in both cases previous results [13]. In general, the samples containing double-step lignins were able to trap larger quantities of dye, and the alkaline lignin-based hydrogels removed slightly lower values of MB than the organosolv-based ones, which is also in line with the trend reported for the TPC of the lignins. Dominguez-Robles et al. (2018) also reported lower MB adsorption values for their samples containing soda lignin than for the ones with organosolv lignin, which could be related with the values they reported for the phenolic hydroxyl groups in these lignins [11]. In contrast, when the last thawing cycle was lengthened, the MB adsorption capacity of the samples containing alkaline lignins was enhanced whereas the MB removal of organosolv lignin-based hydrogels got slightly reduced. This fact suggested that although the last thawing cycle intensified the porosity of the samples, the availability of the negative charges on the surface was altered; nevertheless, this statement cannot be demonstrated.

In spite of the removal values being very high, it is true that the yield of the adsorption tests was much lower than in other studies. Whereas values from 2 to 200 mg dye/g hydrogel have been previously reported for lignin hydrogels [11,47–49], in this work none of the synthesized hydrogels surpassed 0.1 mg dye/g hydrogel. Furthermore, in recent years biochars have been used for the removal of these dyes, which far exceed the yields reported in this work [11,50]. Thus, the present hydrogels could be used for diluted MB environments, and modifications could be studied together with the combination with other compounds in order to enhance the adsorption yields.

3.4. Antifungal tests

The urgent need of searching for alternative eco-friendly materials has also swayed the food-packaging sector. In this context, bio-based hydrogels have emerged as potential absorbents for these systems [51]. However, these materials should extend the shelf-life of the packaged products, which involves hindering the growth of microorganisms and fungi on them [51,52]. Thus, the antifungal properties against *Aspergillus niger* (brown-rot fungi), one of the most common fungi in food spoilage, were studied for all the synthesized hydrogels.

First of all, a visual evaluation of lignin's antifungal capacity was performed (see Supplementary data). Although mainly white-rot fungi are able to depolymerise lignin [53], some authors have also seen that brown-rot fungi are also capable to be lignin degraders. Nevertheless, in this case the tested fungi did not seem to have such ability. In spite of the growth of fungi the agar surface of all the samples, the deposited lignin drops could be clearly observed after the period of the test. This showed the antifungal ability of lignin, as also demonstrated by other authors before. Among the studied samples, the alkaline ones seemed to be able to inhibit more effectively the fungal growth than the organosolv ones, leading to a growth intensity of 3 (GI = 3), whereas most of the rest of the samples presented greater intensities (GI ≈ 4), according to ISO 846 [15].

On the other hand, the same test was performed to the hydrogels. In all cases, the whole hydrogel portion was visible after the test (see Supplementary data). At first sight, the samples with alkaline WNS lignins (WA and AWA) as well as the samples containing organosolv AS lignins (AO and AWO) seemed to hinder the fungal development more than the samples containing other lignins. Moreover, there was almost no appreciable fungal growth on the top surface of the samples. In this case, the growth intensity would be between 3 and 4 for every sample [15].

The samples were washed with PBS and the surrounding spores were quantified as aforementioned. From the estimated FGI values (Fig. 6), it was seen that among the studied samples, the ones presenting the lowest fungal activity were WO and AAO (58 and 56.5% FGI, respectively), and the one presenting the highest growth was surprisingly AWA (almost 40% more than the control sample). It was observed that the samples containing single-step AS lignins presented lower FGI values than the ones with double-step AS lignins. Conversely, the samples containing double-step WNS lignins presented worse antifungal activity than the ones with single-step WNS lignins. Although the estimated values were approximate, these results helped making an idea of the antifungal properties that the synthesized samples presented. It is also worth to mention that none of the studied samples lost weight during the

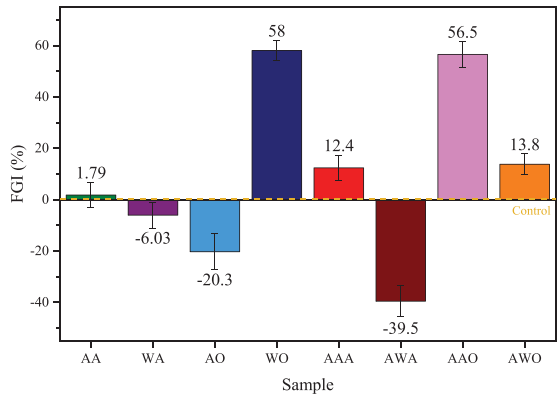

Fig. 6. Fungal growth inhibition (FGI, %) of the samples with respect to the control hydrogels (y = 0).

antifungal test, which supports their effectiveness against *A. niger*.

Several authors have reported similar FGI values for other materials for food packaging applications. For instance, Salaberria et al. (2017) reported 52–62% of inhibition for PLA films containing functionalized chitin nanocrystals [14]. In the study of Fernandez-Marin et al. (2021), these values were between 72 and 86% for their chitosan/β-chitin nanofibers nanocomposites due to the incorporation of deterpenated *Origanum majorana* L. essential oil [54]. Conversely, Dey et al. (2021) reported values between 51 and 56% for neat PVA films, which were negatively affected by the addition of cellulose nanocrystals and chitosan nanoparticles [55]. Thus, taking these data into account, it can be concluded that the results reported for WO and AAO hydrogels were in total agreement with the ones reported by other authors and could be employed in food packaging.

4. Conclusions

In this study, alkaline and organosolv lignins were extracted from almond and walnut shells through two different biorefinery strategies and successfully employed for the synthesis of lignin-based physical hydrogels. The characterization of the extracted lignins showed significant differences between the lignin samples, especially on their composition, average molecular weights and total phenolic contents. As expected, the autohydrolysis enhanced the purity of the lignins, especially in the case of alkaline ones, and it also promoted the extraction of lignins with higher average molecular weights. These changes altered the morphology of the produced hydrogels and, hence, their properties such as their swelling capacity, glass transition temperatures and compression modules. In fact, hydrogels containing lignins from the single-step process resulted into a more honeycomb porous structure and, thus, a higher water absorption capacity. In addition, when the last thawing step was lengthened, larger pores were created, which also leaded to a notable enhancement of the swelling percentage of the hydrogels. The synthesized materials showed good methylene blue removal (75–93%) and, in some cases, antifungal properties (up to 58% of FGI), demonstrating their versatility on various application fields.

Declaration of Competing Interest

The authors declare that they have no known competing financial interests or personal relationships that could have appeared to influence the work reported in this paper.

Acknowledgements

The authors would like to acknowledge the financial support of the Department of Education of the Basque Government (IT1008-16). A. Morales would like to thank the University of the Basque Country (Training of Researcher Staff, PIF17/207). P. Gullón would like to acknowledge the Grants for the recruitment of technical support staff (PTA2019-017850-I) under the State Plan for Scientific and Technical Research and Innovation 2017–2020. The authors thank SGIker (UPV/EHU/ERDF, EU) for their technical and human support.

Appendix A. Supplementary data

Supplementary data to this article can be found online at https://doi.org/10.1016/j.susmat.2021.e00369.

References

[1] R.M. Kalinoski, J. Shi, Hydrogels derived from lignocellulosic compounds: evaluation of the compositional, structural, mechanical and antimicrobial properties, Ind. Crop. Prod. 128 (2019) 323–330, https://doi.org/10.1016/j.indcrop.2018.11.002.

[2] D. Rico-García, L. Ruiz-Rubio, L. Pérez-Álvarez, S.L. Hernández-Olmos, G. L. Guerrero-Ramírez, J.L. Vilas-Vilela, Lignin-based hydrogels : synthesis and applications, Polymers (Basel). 12 (2020) 1–23.

[3] A. Oryan, A. Kamali, A. Moshiri, H. Baharvand, H. Daemi, Chemical crosslinking of biopolymeric scaffolds: current knowledge and future directions of crosslinked engineered bone scaffolds, Int. J. Biol. Macromol. 107 (2018) 678–688, https://doi.org/10.1016/j.ijbiomac.2017.08.184.

[4] H. Nakajima, P. Dijkstra, K. Loos, The recent developments in biobased polymers toward general and engineering applications: polymers that are upgraded from biodegradable polymers, analogous to petroleum-derived polymers, and newly developed, Polymers (Basel). 9 (2017) 1–26, https://doi.org/10.3390/polym9100523.

[5] S. RameshKumar, P. Shaiju, K.E. O'Connor, P. Ramesh Babu, Bio-based and biodegradable polymers - state-of-the-art, challenges and emerging trends, Curr. Opin. Green Sustain. Chem. 21 (2020) 75–81, https://doi.org/10.1016/j.cogsc.2019.12.005.

[6] A.T. Ubando, C.B. Felix, W.H. Chen, Biorefineries in circular bioeconomy: a comprehensive review, Bioresour. Technol. 299 (2020), https://doi.org/10.1016/j.biortech.2019.122585.

[7] A. Morales, J. Labidi, P. Gullón, Hydrothermal treatments of walnut shells: a potential pretreatment for subsequent product obtaining, Sci. Total Environ. 764 (2021), 142800, https://doi.org/10.1016/j.scitotenv.2020.142800.

[8] G. Dragone, A.A.J. Kerssemakers, J.L.S.P. Driessen, C.K. Yamakawa, L.P. Brumano, S.I. Mussatto, Innovation and strategic orientations for the development of advanced biorefineries, Bioresour. Technol. 302 (2020), 122847, https://doi.org/10.1016/j.biortech.2020.122847.

[9] J.J. Liao, N.H.A. Latif, D. Trache, N. Brosse, M.H. Hussin, Current advancement on the isolation, characterization and application of lignin, Int. J. Biol. Macromol. 162 (2020) 985–1024, https://doi.org/10.1016/j.ijbiomac.2020.06.168.

[10] A. Morales, F. Hernández-Ramos, L. Sillero, R. Fernández-Marín, I. Dávila, P. Gullón, X. Erdocia, J. Labidi, Multiproduct biorefinery based on almond shells: impact of the delignification stage on the manufacture of valuable products, Bioresour. Technol. 315 (2020), https://doi.org/10.1016/j.biortech.2020.123896.

[11] J. Domínguez-Robles, M.S. Peresin, T. Tamminen, A. Rodríguez, E. Larrañeta, A. S. Jääskeläinen, Lignin-based hydrogels with "super-swelling" capacities for dye removal, Int. J. Biol. Macromol. 115 (2018) 1249–1259, https://doi.org/10.1016/j.ijbiomac.2018.04.044.

[12] L. Wu, S. Huang, J. Zheng, Z. Qiu, X. Lin, Y. Qin, Synthesis and characterization of biomass lignin-based PVA super-absorbent hydrogel, Int. J. Biol. Macromol. 140 (2019) 538–545, https://doi.org/10.1016/j.ijbiomac.2019.08.142.

[13] A. Morales, J. Labidi, P. Gullón, Effect of the formulation parameters on the absorption capacity of smart lignin-hydrogels, Eur. Polym. J. 129 (2020), 109631, https://doi.org/10.1016/j.eurpolymj.2020.109631.

[14] A.M. Salaberria, R.H. Diaz, M.A. Andrés, S.C.M. Fernandes, J. Labidi, The antifungal activity of functionalized chitin nanocrystals in poly (Lactid acid) films, Materials (Basel). 10 (2017) 1–16, https://doi.org/10.3390/ma10050546.

[15] D.T. Da Silva, R. Herrera, B.M. Heinzmann, J. Calvo, J. Labidi, Nectandra grandiflora by-products obtained by alternative extraction methods as a source of phytochemicals with antioxidant and antifungal properties, Molecules. 23 (2018) 1–16, https://doi.org/10.3390/molecules23020372.

[16] J. Fernández-Rodríguez, X. Erdocia, C. Sánchez, M. González Alriols, J. Labidi, Lignin depolymerization for phenolic monomers production by sustainable processes, J. Energy Chem. 26 (2017) 622–631, https://doi.org/10.1016/j.jechem.2017.02.007.

[17] C.S.G.P. Queirós, S. Cardoso, A. Lourenço, J. Ferreira, I. Miranda, M.J.V. Lourenço, H. Pereira, Characterization of walnut, almond, and pine nut shells regarding chemical composition and extract composition, Biomass Convers. Biorefin. 10 (2020) 175–188, https://doi.org/10.1007/s13399-019-00424-2.

[18] A. Morales, B. Gullón, I. Dávila, G. Eibes, J. Labidi, P. Gullón, Optimization of alkaline pretreatment for the co-production of biopolymer lignin and bioethanol from chestnut shells following a biorefinery approach, Ind. Crop. Prod. 124 (2018), https://doi.org/10.1016/j.indcrop.2018.08.032.

[19] J. Li, P. Feng, H. Xiu, J. Li, X. Yang, F. Ma, X. Li, X. Zhang, E. Kozliak, Y. Ji, Morphological changes of lignin during separation of wheat straw components by the hydrothermal-ethanol method, Bioresour. Technol. 294 (2019), https://doi.org/10.1016/j.biortech.2019.122157.

[20] M.Q. Zhu, J.L. Wen, Y.Q. Su, Q. Wei, R.C. Sun, Effect of structural changes of lignin during the autohydrolysis and organosolv pretreatment on Eucommia ulmoides Oliver for an effective enzymatic hydrolysis, Bioresour. Technol. 185 (2015) 378–385, https://doi.org/10.1016/j.biortech.2015.02.061.

[21] I. Dávila, P. Gullón, M.A. Andrés, J. Labidi, Coproduction of lignin and glucose from vine shoots by eco-friendly strategies: toward the development of an integrated biorefinery, Bioresour. Technol. 244 (2017) 328–337, https://doi.org/10.1016/j.biortech.2017.07.104.

[22] I. Dávila, B. Gullón, J. Labidi, P. Gullón, Multiproduct biorefinery from vine shoots: bio-ethanol and lignin production, Renew. Energy 142 (2019) 612–623.

[23] A. García, M. González Alriols, G. Spigno, J. Labidi, Lignin as natural radical scavenger. Effect of the obtaining and purification processes on the antioxidant behaviour of lignin, Biochem. Eng. J. 67 (2012) 173–185, https://doi.org/10.1016/j.bej.2012.06.013.

[24] A. García, G. Spigno, J. Labidi, Antioxidant and biocide behaviour of lignin fractions from apple tree pruning residues, Ind. Crop. Prod. 104 (2017) 242–252, https://doi.org/10.1016/j.indcrop.2017.04.063.

[25] A. Sequeiros, D.A. Gatto, J. Labidi, L. Serrano, Different extraction methods to obtain lignin from almond shell, J. Biobased Mater. Bioenergy. 8 (2014) 370–376, https://doi.org/10.1166/jbmb.2014.1443.

[26] S. De, S. Mishra, E. Poonguzhali, M. Rajesh, K. Tamilarasan, Fractionation and characterization of lignin from waste rice straw: biomass surface chemical composition analysis, Int. J. Biol. Macromol. 145 (2020) 795–803, https://doi.org/10.1016/j.ijbiomac.2019.10.068.
[27] I. Gómez-Cruz, M. del Mar Contreras, I. Romero, E. Castro, A biorefinery approach to obtain antioxidants, lignin and sugars from exhausted olive pomace, J. Ind. Eng. Chem. 96 (2021) 356–363, https://doi.org/10.1016/j.jiec.2021.01.042.
[28] C. Xu, F. Liu, M.A. Alam, H. Chen, Y. Zhang, C. Liang, H. Xu, S. Huang, J. Xu, Z. Wang, Comparative study on the properties of lignin isolated from different pretreated sugarcane bagasse and its inhibitory effects on enzymatic hydrolysis, Int. J. Biol. Macromol. 146 (2020) 132–140, https://doi.org/10.1016/j.ijbiomac.2019.12.270.
[29] A. Goudarzi, L.-T. Lin, F.K. Ko, X-ray diffraction analysis of Kraft Lignins and lignin-derived carbon nanofibers, J. Nanotechnol. Eng. Med. 5 (2014), 021006, https://doi.org/10.1115/1.4028300.
[30] S. Kumar, Y.S. Negi, J.S. Upadhyaya, Studies on characterization of corn cob based nanoparticles, Adv. Mater. Lett. 1 (2010) 246–253, https://doi.org/10.5185/amlett.2010.9164.
[31] A.C.F. Louis, S. Venkatachalam, Energy efficient process for valorization of corn cob as a source for nanocrystalline cellulose and hemicellulose production, Int. J. Biol. Macromol. 163 (2020) 260–269, https://doi.org/10.1016/j.ijbiomac.2020.06.276.
[32] M.K. Haider, A. Ullah, M.N. Sarwar, Y. Saito, L. Sun, S. Park, I.S. Kim, Lignin-mediated in-situ synthesis of CuO nanoparticles on cellulose nanofibers: a potential wound dressing material, Int. J. Biol. Macromol. 173 (2021) 315–326, https://doi.org/10.1016/j.ijbiomac.2021.01.050.
[33] M. Brahim, N. Boussetta, N. Grimi, E. Vorobiev, I. Zieger-Devin, N. Brosse, Pretreatment optimization from rapeseed straw and lignin characterization, Ind. Crop. Prod. 95 (2017) 643–650, https://doi.org/10.1016/j.indcrop.2016.11.033.
[34] X. Yang, Y. Zhao, H. Mussana, M. Tessema, L. Liu, Characteristics of cotton fabric modified with chitosan (CS)/cellulose nanocrystal (CNC) nanocomposites, Mater. Lett. 211 (2018) 300–303, https://doi.org/10.1016/j.matlet.2017.09.075.
[35] L. Chen, X. Wang, H. Yang, Q. Lu, D. Li, Q. Yang, H. Chen, Study on pyrolysis behaviors of non-woody lignins with TG-FTIR and Py-GC/MS, J. Anal. Appl. Pyrolysis 113 (2015) 499–507, https://doi.org/10.1016/j.jaap.2015.03.018.
[36] J.I. Daza Agudelo, J.M. Badano, I. Rintoul, Kinetics and thermodynamics of swelling and dissolution of PVA gels obtained by freeze-thaw technique, Mater. Chem. Phys. 216 (2018) 14–21, https://doi.org/10.1016/j.matchemphys.2018.05.038.
[37] X. Han, Z. Lv, F. Ran, L. Dai, C. Li, C. Si, Green and stable piezoresistive pressure sensor based on lignin-silver hybrid nanoparticles/polyvinyl alcohol hydrogel, Int. J. Biol. Macromol. 176 (2021) 78–86, https://doi.org/10.1016/j.ijbiomac.2021.02.055.
[38] Q. Wang, J. Guo, X. Lu, X. Ma, S. Cao, X. Pan, Y. Ni, Wearable lignin-based hydrogel electronics: a mini-review, Int. J. Biol. Macromol. (2021), https://doi.org/10.1016/j.ijbiomac.2021.03.079.
[39] L. Sun, Z. Mo, Q. Li, D. Zheng, X. Qiu, X. Pan, Facile synthesis and performance of pH/temperature dual-response hydrogel containing lignin-based carbon dots, Int. J. Biol. Macromol. 175 (2021) 516–525, https://doi.org/10.1016/j.ijbiomac.2021.02.049.
[40] A. Morales, J. Labidi, P. Gullón, Assessment of green approaches for the synthesis of physically crosslinked lignin hydrogels, J. Ind. Eng. Chem. 81 (2020) 475–487, https://doi.org/10.1016/j.jiec.2019.09.037.
[41] I.E. Raschip, G.E. Hitruc, C. Vasile, M.C. Popescu, Effect of the lignin type on the morphology and thermal properties of the xanthan/lignin hydrogels, Int. J. Biol. Macromol. 54 (2013) 230–237, https://doi.org/10.1016/j.ijbiomac.2012.12.036.
[42] A.H.A. Wahab, A.P.M. Saad, M.N. Harun, A. Syahrom, M.H. Ramlee, M.A. Sulong, M.R.A. Kadir, Developing functionally graded PVA hydrogel using simple freeze-thaw method for artificial glenoid labrum, J. Mech. Behav. Biomed. Mater. 91 (2019) 406–415, https://doi.org/10.1016/j.jmbbm.2018.12.033.
[43] S. Butylina, S. Geng, K. Oksman, Properties of as-prepared and freeze-dried hydrogels made from poly(vinyl alcohol) and cellulose nanocrystals using freeze-thaw technique, Eur. Polym. J. 81 (2016) 386–396, https://doi.org/10.1016/j.eurpolymj.2016.06.028.
[44] X.-Q. Hu, D.-Z. Ye, J.-B. Tang, L.-J. Zhang, X. Zhang, From waste to functional additives: thermal stabilization and toughening of PVA with lignin, RSC Adv. 6 (2016) 13797–13802, https://doi.org/10.1039/C5RA26385A.
[45] Y. Chen, K. Zheng, L. Niu, Y. Zhang, Y. Liu, C. Wang, F. Chu, Highly mechanical properties nanocomposite hydrogels with biorenewable lignin nanoparticles, Int. J. Biol. Macromol. 128 (2019) 414–420, https://doi.org/10.1016/j.ijbiomac.2019.01.099.
[46] A.B. Albadarin, M.N. Collins, M. Naushad, S. Shirazian, G. Walker, C. Mangwandi, Activated lignin-chitosan extruded blends for efficient adsorption of methylene blue, Chem. Eng. J. 307 (2017) 264–272, https://doi.org/10.1016/j.cej.2016.08.089.
[47] H. Qian, J. Wang, L. Yan, Synthesis of lignin-poly(N-methylaniline)-reduced graphene oxide hydrogel for organic dye and lead ions removal, J. Bioresour. Bioprod. 5 (2020) 204–210, https://doi.org/10.1016/j.jobab.2020.07.006.
[48] L. Wu, S. Huang, J. Zheng, Z. Qiu, X. Lin, Y. Qin, Synthesis and characterization of biomass lignin-based PVA super-absorbent hydrogel, Int. J. Biol. Macromol. 140 (2019) 538–545, https://doi.org/10.1016/j.ijbiomac.2019.08.142.
[49] Y. Meng, C. Li, X. Liu, J. Lu, Y. Cheng, L.-P. Xiao, H. Wang, Preparation of magnetic hydrogel microspheres of lignin derivate for application in water, Sci. Total Environ. (2019), https://doi.org/10.1016/j.scitotenv.2019.06.278.
[50] X.J. Liu, M.F. Li, S.K. Singh, Manganese-modified lignin biochar as adsorbent for removal of methylene blue, J. Mater. Res. Technol. 12 (2021) 1434–1445, https://doi.org/10.1016/j.jmrt.2021.03.076.
[51] R.A. Batista, P.J.P. Espitia, J.S.S. de Quintans, M.M. Freitas, M.Á. Cerqueira, J. A. Teixeira, J.C. Cardoso, Hydrogel as an alternative structure for food packaging systems, Carbohydr. Polym. 205 (2019) 106–116, https://doi.org/10.1016/j.carbpol.2018.10.006.
[52] N. Nguyen Van Long, C. Joly, P. Dantigny, Active packaging with antifungal activities, Int. J. Food Microbiol. 220 (2016) 73–90, https://doi.org/10.1016/j.ijfoodmicro.2016.01.001.
[53] O.Y. Abdelaziz, D.P. Brink, J. Prothmann, K. Ravi, M. Sun, J. García-Hidalgo, M. Sandahl, C.P. Hulteberg, C. Turner, G. Lidén, M.F. Gorwa-Grauslund, Biological valorization of low molecular weight lignin, Biotechnol. Adv. 34 (2016) 1318–1346, https://doi.org/10.1016/j.biotechadv.2016.10.001.
[54] R. Fernández-Marín, M. Mujtaba, D. Cansaran-Duman, G. Ben Salha, M.Á. A. Sánchez, J. Labidi, S.C.M. Fernandes, Effect of deterpenated origanum majorana l. Essential oil on the physicochemical and biological properties of chitosan/β-chitin nanofibers nanocomposite films, Polymers (Basel). 13 (2021), https://doi.org/10.3390/polym13091507.
[55] D. Dey, V. Dharini, S.P. Selvam, E.R. Sadiku, M.M. Kumar, J. Jayaramudu, U. N. Gupta, Physical, antifungal, and biodegradable properties of cellulose nanocrystals and chitosan nanoparticles for food packaging application, Mater. Today Proc. 38 (2021) 860–869, https://doi.org/10.1016/j.matpr.2020.04.885.
[56] I. Zarandona, A.I. Puertas, M.T. Dueñas, P. Guerrero, K. de la Caba, Assessment of active chitosan films incorporated with gallic acid, Food Hydrocoll. 101 (2020), https://doi.org/10.1016/j.foodhyd.2019.105486.

Impact of the lignin type and source on the characteristics of physical lignin hydrogels

Amaia Morales[a], Jalel Labidi[a,*], Patricia Gullón[b]

[a]Chemical and Environmental Engineering Department, University of the Basque Country UPV/EHU, Plaza Europa 1, 20018, San Sebastián, Spain

[b]C.A.C.T.I. Laboratory, Technology Park of Galicia- Tecnopole, CTC Building, 32901, San Cibrao das Viñas, Ourense, Spain

[*]Corresponding author: jalel.labidi@ehu.eus

Supplementary data

Table S1. Identification of the compounds detected by Py-GC/MS for the extracted lignins.

Peak #	RT (min)	Compound	Origin	AA	AO	WA	WO	AAA	AAO	AWA	AWO
1	7.5-7.7	Phenol	H	1.62	0.98	6.56	3.29	1.16		4.26	2.95
2	8.2	2-Methyliminoperhydro-1,3-oxazine	-	5.77		9.95					
3	8.7-8.9	o-cresol	H	1.53	1.04	2.42	1.22	1.80	1.14	1.66	1.21
4	9.0-9.2	p-cresol	H	1.82	1.62	5.22	5.31	1.39	0.92	4.58	4.12
5	9.3-9.5	Guaiacol	G	13.62	11.80	9.30	8.91	17.14	7.40	11.72	7.56
6	10.4	Phenol, 2,6-dimethyl-	H	1.68	1.38	1.45	1.53	1.95	1.77	1.44	1.52
7	10.7-10.8	p-Ethylphenol	H	0.74		2.40	1.66	0.54		1.71	1.43
8	11.0-11.1	3-Methylguaiacol	G	2.08	1.35	0.94	1.29	3.90	1.17	2.28	1.24
9	11.4-11.6	4-Methylguaiacol	G	9.75	12.74	5.23	10.86	15.19	8.08	10.07	7.73
10	13.3-13.5	3-Methoxycatechol	S	0.19	3.29	0.95	4.22	2.56	3.67	4.39	4.33
11	13.8-14.0	4-Ethylguaiacol	G	7.78	5.67	3.80	5.15	8.82	3.63	7.09	3.79
12	15.0-15.2	4-Vinylguaiacol	G	6.94	7.16	3.76	5.77	4.52	3.00	3.51	3.10
13	16.1-16.2	Syringol	S	7.45	9.69	3.96	10.57	8.13	5.42	16.52	7.18
14	16.3	3,4-Dimethoxyphenol	S	1.69	1.87	0.64	2.55	1.82	0.88		2.13
15	17.4	cis-Isoeugenol	G	1.12	1.70	0.34	1.60	1.19	0.85	1.35	0.84
16	18.3	4-Methylsyringol	S	4.75	12.03	2.69	13.66	5.94	6.80	9.23	7.54
17	19.6	4-Ethylsyringol	S	1.02	1.28	0.78	1.95	1.16	0.82	2.47	0.90
18	20.2-20.8	4-Vinylsyringol	S	0.23	1.92	0.24	1.72	0.62	0.73	0.87	0.96
19	21.6	Syringaldehyde	S		1.20	0.47	0.62	0.40	1.65	0.16	2.56
20	22.1	4-Allylsyringol	S	0.51	2.09	0.83	2.11	0.50	0.40	0.51	1.56
21	22.5	Acetosyringone	S	0.13	2.03	0.87	0.86	0.34	1.45	0.17	2.44
22	23.0	Homosyringic acid	S		1.07		0.42	0.15	0.64		1.30
			Total S	15.96	36.48	11.43	38.67	21.62	22.47	34.31	30.90
			Total G	41.29	40.44	23.37	33.57	50.78	24.14	36.02	24.26
			Total H	7.39	5.02	18.05	13.00	6.84	3.84	13.65	11.23
			S/G ratio	0.39	0.90	0.49	1.15	0.43	0.93	0.95	1.27

Figure S1. TGA curves of the synthesized hydrogels.

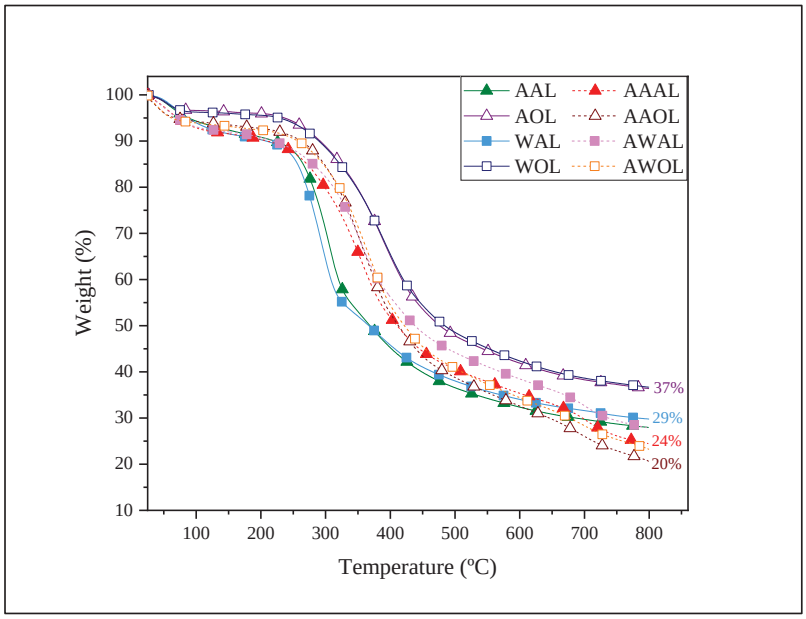

Figure S2. SEM micrographs of the hydrogels containing WNS lignins at 500x and 5000x magnifications.

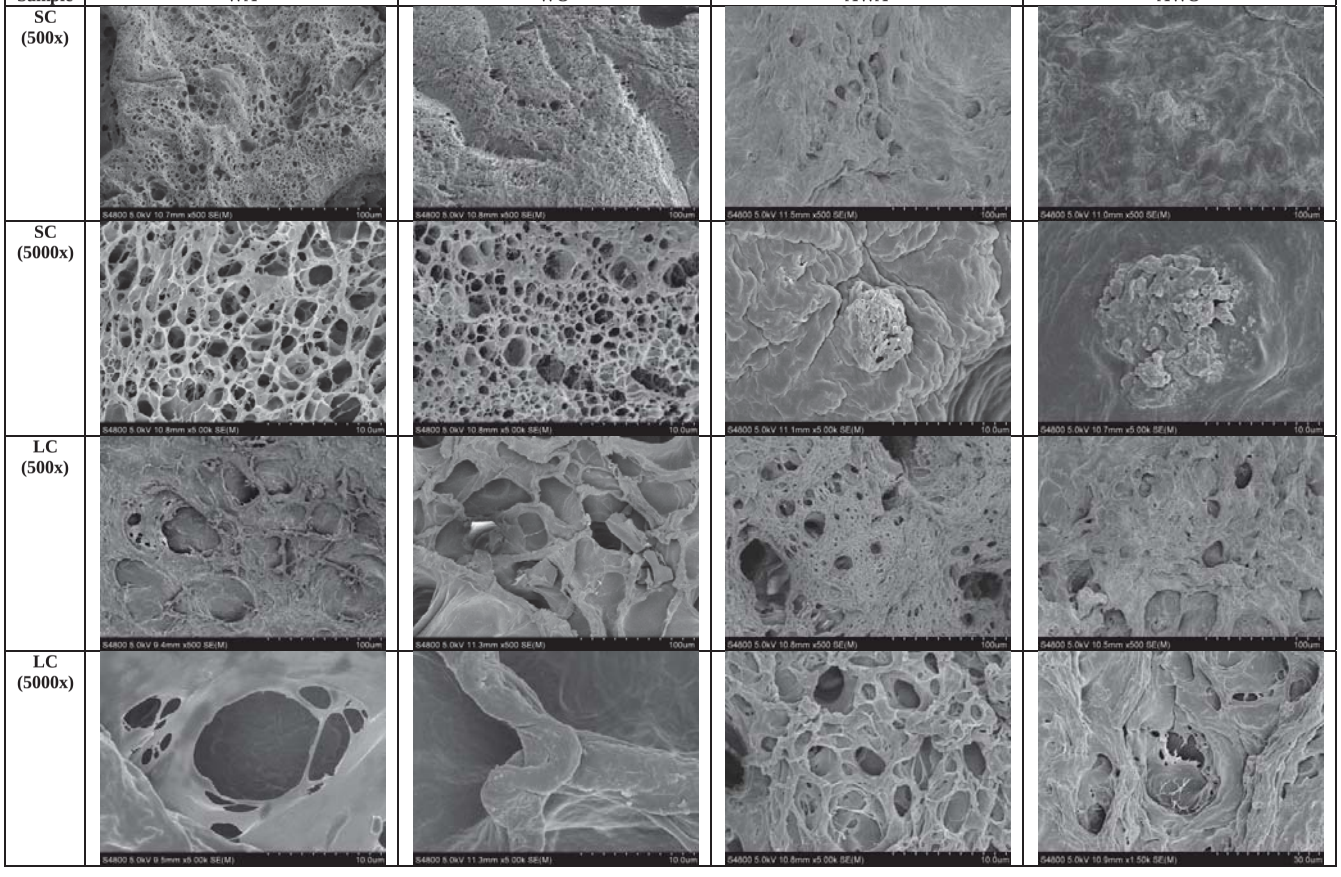

Figure S3. Images of the antifungal tests of lignins (a) and hydrogels (b).

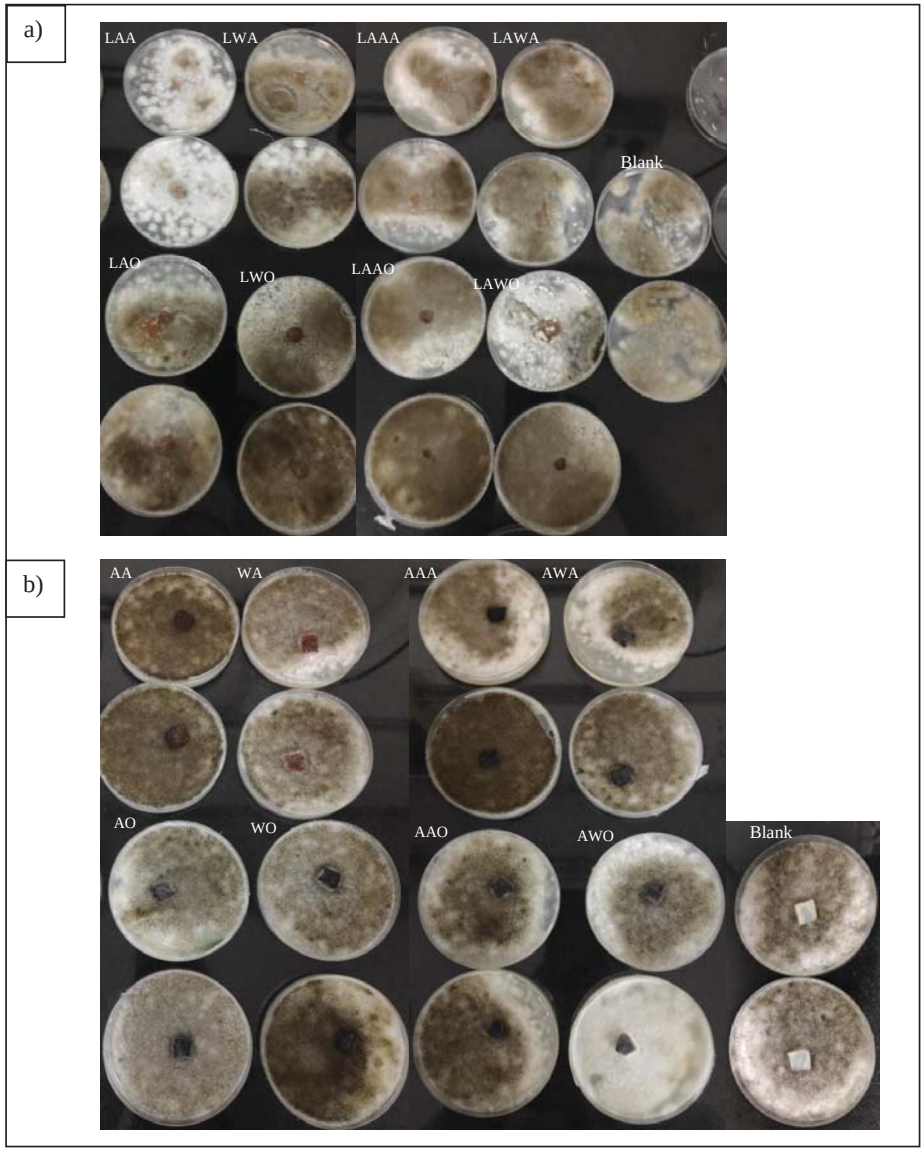

V. Artikulua

Influence of lignin modifications on physically crosslinked lignin hydrogels for drug delivery applications

A. Morales, J. Labidi, P. Gullón

V

Ind. Crops. Prod. aldizkarira bidalia.
2021eko abendua

Influence of lignin modifications on physically crosslinked lignin hydrogels for drug delivery applications

Amaia Morales[a], Jalel Labidi[a,*], Patricia Gullón[b]

[a]Chemical and Environmental Engineering Department, University of the Basque Country UPV/EHU, Plaza Europa 1, 20018, San Sebastián, Spain
[b]C.A.C.T.I. Laboratory, Technology Park of Galicia- Tecnopole, CTC Building, 32901, San Cibrao das Viñas, Ourense, Spain
[*]Corresponding author: jalel.labidi@ehu.eus

A**bstract:** So far, the possibility of synthesising hydrogels based on multiple biopolymers has been investigated, and among them lignin has proven to be one of the potentials for this purpose due to the multiple advantages it offers. However, because of its high molecular weight, steric hindrance and few reactive sites on its structure, it is sometimes necessary to improve its reactivity though chemical modifications. On the basis of previous results, two chemical modifications were selected in order to enhance almond, walnut and commercial alkaline and organosolv lignins' reactivity: a peroxidation reaction for alkaline ones and a hydroxymethylation for organosolv ones. Both reactions were confirmed by multiple techniques (i.e. FTIR, GPC and TGA). Hydrogels were synthesized from these lignins according to previous works. The high lignin waste of the synthesized hydrogels suggested that despite the modification of the lignins, just the highest molecular weight fractions reacted with the matrix polymer. Moreover, the swelling capacity of modified alkaline lignin-based hydrogels was negatively affected, whereas the one for organosolv lignin-based samples improved. The SEM micrographs explained the aforementioned, and the results from the DSC and compression tests were in accordance with them. Self-extracted quercetin loading and release studies suggested that these samples could be used for controlled drug delivery.

Keywords: modified lignin, peroxidation, hydroxymethylation, hydrogels, drug delivery

1. Introduction

The insatiable demand for energy and fossil resources has driven the current society to many global environmental and social concerns. In this context, lignocellulosic biomass has opened an alternative door to the production of chemicals, materials and fuels (Yoo et al., 2020). This biomass is constituted by lignin, hemicelluloses and cellulose. Although biorefineries, the sustainable combination of processes able to transform biomass into a great variety of commercial products (Dragone et al., 2020), have mostly been focused on cellulose and hemicelluloses for the production of paper and bioethanol (Kumar et al., 2020), for instance, the conversion of lignin into value-added compounds is vital for the cost-competitiveness of biorefineries (Wang et al., 2019). In fact, lignin can constitute up to 40% of woody biomass and 15% of herbal one (Tribot et al., 2019) and it has demonstrated to possess interesting properties not just in energetic terms but also for the synthesis of new bio-based materials (Iravani and Varma, 2020).

Lignins' structure is an intricate and random combination of phenylpropanoid units (i.e. coniferyl, coumaril and sinapyl alcohols), which varies according to the source and kind of plant, its culture conditions and the used lignin isolation method (Zevallos Torres et al., 2020). In addition, the lignin structure is highly branched and has multiple functional groups including carbonyl (C=O), hydroxyl (–OH), carboxyl (–COOH) and methoxy (–CH_3O) groups (Tribot et al., 2019), which have a direct effect on its reactivity (X. Meng et al., 2019). Moreover, the reactivity of this biopolymer is usually not high enough owing to its high molecular weight, steric hindrance and few reactive sites (Chen et al., 2020; Dragone et al., 2020). Therefore, in order to overcome this drawback it is sometimes necessary to perform a chemical modification of its structure (Goliszek et al., 2021). For this aim, there are four main ways: the first one involves its depolymerization or fragmentation, the second one focuses on the creation of chemically active sites, the third one is related to the modification of the hydroxyl groups in its structure; and the last one would be through the production of graft copolymers (Figueiredo et al., 2018).

According to various studies, lignin can confer interesting properties to lignin-based composite materials such as antioxidant or antibacterial capacity (Musilová et al., 2018). This fact makes lignin attractive for the formulation of materials to be used in the biomedical field. A clear example of this is the rising trend of lignin addition into hydrogels (Rico-García et al., 2020), which are very useful materials for drug delivery

(Larrañeta et al., 2018), wound dressing (Zhang et al., 2020) and tissue engineering and regenerative medicine (Barros et al., 2016), for instance.

Recently, modified lignins have been used for the formulation of hydrogels in order to overcome some drawbacks such as agglomeration or water insolubility (Musilová et al., 2018), although many of them have been applied for pollutant adsorption (Goliszek et al., 2021; Y. Meng et al., 2019). Moreover, lignin modifications can be crucial to avoid the use of chemical crosslinking agents, promoting the synthesis of physically-crosslinked hydrogels, which are usually more environmentally friendly and economical (Oryan et al., 2018).

Previously, the influence of the source and characteristics of alkaline and organosolv nut-shell (almond and walnut) lignins was studied (Morales et al., 2021) as well as the impact of commercial ones (Morales et al., 2020a) on the characteristics of the hydrogels. Nevertheless, a great lignin waste was generally observed in all the systems as well as a lower swelling degree in organosolv lignin-containing hydrogels. Thus, the objective of this work was to modify previously employed lignins in order to enhance the aforementioned weaknesses and to observe their impact on the properties of the synthesized physical hydrogels. For this aim, alkaline lignins were fragmented via an oxidation reaction and the organosolv ones were hydroxymethylated so as to introduce new reactive sites into them. The modified lignins were characterised and the modifications were confirmed via various techniques (FTIR, GPC and ^{31}P NMR). Then, hydrogels were synthesized from modified lignins and their lignin wastes, swelling capacities, morphology, glass transition temperatures and mechanical properties were studied. In addition, the possibility of using these hydrogels as drug deliverers was studied by analysing their release kinetics of self-extracted quercetin.

2. Materials and Methods

2.1. Materials

Organosolv lignin was purchased from Chemical Point. Poly (vinyl alcohol) (Mw = 83,000-124,000 g/mol, 99+ % hydrolyzed), alkaline lignin and phosphate buffer saline (PBS) tablets were supplied by Sigma Aldrich. Sodium hydroxide (NaOH, analysis grade, ≥ 98%, pellets), hydrogen peroxide (30% w/v, for analysis), formaldehyde (37-38% w/w, stabilized with methanol, for analysis) and hydrochloric acid (37%, for analysis) were purchased from PanReac Química SLU. All reagents were employed as supplied.

Almond (AS) and walnut shell (WNS) alkaline and organosolv lignins extracted in a previous work via subsequent autohydrolysis and delignification processes were used in this work (Morales et al., 2021).

2.2. Lignin modification

Alkaline lignins from AS and WNS as well as the commercial one were subjected to a microwave assisted peroxidation reaction with hydrogen peroxide as described by Infante et al. (2007)(Infante et al., 2007). Briefly, lignin and hydrogen peroxide were introduced into a high-pressure vessel keeping a LSR of 10:1 (mL:g). After sealing the vessel, it was subjected to three irradiation cycles of 10 seconds at 1100 W with a 30 second suspension period between them. Afterwards, the vessel was cleaned with distilled water and the collected mixture was left to dry over an oven.

Organosolv lignins (from AS, WNS and the commercial one) were exposed to a hydroxymethylation reaction with formaldehyde following the procedure reported by Chen et al. (2020)(Chen et al., 2020) with slight modifications. Concisely, 0.6 g of lignin were dissolved in an aqueous NaOH solution (140 mL). Then, 0.495 mL of formaldehyde were added and the solution was heated up to 80 ºC under magnetic stirring and refrigeration. The reaction was left for 3.5 hours. Afterwards, the modified lignin was precipitated with 2% hydrochloric acid, filtered, neutralized and dried.

2.3. Lignin characterisation

All the lignins were characterised employing the methods described in previous works. Their purity and composition (Dávila et al., 2017), average molecular weights and total phenolic contents (Morales et al., 2018), thermal degradation, crystallinity and chemical structure (Morales et al., 2020a) were determined. In addition, in order to confirm the chemical modification of organosolv lignins, ^{31}P-NMR was employed following the protocol described by Meng et al. (2019) (X. Meng et al., 2019).

2.4. Hydrogel synthesis

The synthesis of the hydrogels was performed based on a previously detailed method (Morales et al., 2021, 2020a). In brief, 60 mL of a 2% (w/w) NaOH aqueous solution containing 9.87 w. % PVA was prepared and heated up to 90 ºC until complete dissolution of PVA. Then, 9.12 w. % of lignin was added. After the lignin was dissolved, the blends were poured into silicon moulds, eliminating the remaining internal bubbles via ultrasound and the superficial air bubbles manually.

Five freeze-thawing cycles were then performed: firstly, the blends were completely frozen (2.5 hours) at -20 ºC and, then, they were thawed at 28ºC (1.5 hours). During the second and last cycles, the samples were left at the freezer overnight. Finally, the hydrogels were washed into distilled water and dried at room temperature.

2.5. Hydrogel characterisation

The characterisation of the hydrogels was also done based on previous works (Morales et al., 2021, 2020a, 2020b). Their lignin waste, swelling capacity, morphology, thermal behaviours and compression modules were studied.

2.6. Drug extraction and loading-release tests

Quercetin was extracted as a drug combining the methods reported by George et al. (2019) and Jin et al. (2011) (George et al., 2019; Jin et al., 2011). Firstly, onion peels were cleaned and dried at 50 ºC before being powdered. Quercetin, together with other compounds, was then extracted by microwave assisted extraction (MAE), which was based on previous experiments (data not shown) modifying the microwave power reported by Jin et al. (2011) (Jin et al., 2011). The extraction was done with a 70% ethanol/water (v/v) solution, keeping a LSR of 40:1 (v/w). Since the used equipment was not a commercial microwave oven, the employed power for intermittent 10 second irradiations was fixed at 375 W. The total reaction time was 2 minutes, leaving a 20 second interval between the irradiations. After the reaction, the solid was filtered and the liquid phase was rotary evaporated for the complete elimination of ethanol. The remaining aqueous solution was considered as quercetin extract (QE).

The concentration of the quercetin extract was determined by UV spectrophotometry. For this purpose, a calibration curve was constructed using some solutions of certain concentrations of commercial quercetin (CQE) and measuring their absorbances at 375 nm (Jin et al., 2011). The total phenolic and flavonoid contents (TPC and TFC, respectively) of QE were estimated as described by Sillero et al. (2019) (Sillero et al., 2019), although in the case of TFC the standard was done with CQE. QE was freeze-dried and analysed by FTIR and compared with the spectrum of CQE.

The loading tests were performed by introducing dry hydrogel samples into diluted QE (1 mL QE into 250 mL distilled water) solutions for 24 hours. The absorbed QE amount was calculated by the difference on the concentrations of the initial and final solutions (George et al., 2019). After the loaded hydrogels were dried, they were weighted and again immersed into PBS at 37 ºC, simulating *in vitro* conditions, for 24 hours. The release kinetics was performed by measuring the concentration of QE in PBS at certain times. All release tests were done in triplicates. The obtained results were introduced into various kinetic models including zero order, first order, Korsmeyer–Peppas and Higuchi (see Equations 1-4) so as to understand the release mechanism for QE (George et al., 2020, 2019; Saidi et al., 2020).

$$F = k_0 t \quad (1)$$

$$\ln(1 - F) = -k_1 t \quad (2)$$

$$\frac{M_t}{M_\infty} = k_{kp} t^n \quad (3)$$

$$F = k_h t^{1/2} \quad (4)$$

Being F the percentage of quercetin released at time t, n the diffusion exponent and k_0, k_1, k_{kp} and k_h the rate constants of zero order, first order, Korsmeyer-Peppas and Higuchi kinetic models, subsequently.

3. Results and Discussion

3.1. Lignin Characterisation

As shown in Table 1 the purity of the lignins was altered after the modification reaction, especially in self-extracted lignins. This might be due to the employed reagents. As for their molecular weight, their weight average molecular weights augmented in all cases, especially in alkaline lignins. Their number average molecular weights got decreased for modified self-extracted alkaline lignins and for commercial organosolv lignin, leading to a more meaningful rise in their polidispersity index. Surprisingly, commercial organosolv lignin (COL) and its modified version (MCOL) were the most heterogeneous lignins, whereas the self-extracted native and modified organosolv lignins (AAOL, AWOL, MAAOL and MAWOL) were the most homogeneous ones. Although the peroxidation reaction was supposed to fractionate lignin, a high percentage of the chains seemed to undergo re-condensation reactions, which made the total weight average molecular weights increase. However, no certain evidence of this has been found in literature. The change on the total phenolic content suggested the degradation of aromatic rings in lignin (Infante et al., 2007; Ouyang et al., 2010). However, CAL presented the opposite trend, which could be related to the differences on the pH of the solutions. According to the results reported by Xinping et al. (Ouyang et al., 2010), the reaction might have yielded more degradation compounds under alkaline conditions (Figueiredo et al., 2018), but as Infante et al. (2007) had demonstrated that this could also be achieved with the non-presence of a catalyst, the present

Table 1. Summary of the purity, GPC, TPC and TGA results for the modified lignins.

Lignin Sample	Purity (%)	M_w[a] (g/mol)	M_n[b] (g/mol)	M_w/M_n[c]	TPC (% GAE[d])	T_{max}[e] (ºC)
AAAL	88.2	12793	1528	8.4	33.1	355
AAOL	95.2	9020	1520	5.9	26.2	357
AWAL	95.7	16670	1604	10.4	33.8	354
AWOL	95.2	7644	1359	5.6	27.2	365
CAL	91.5	9333	1365	6.8	20.3	379
COL	92.5	32933	1123	29.3	19.3	343
MAAAL	85.2	17675	1348	13.1	25.3	384
MAAOL	92.3	9557	1636	5.8	20.4	383
MAWAL	84.0	19939	1369	14.6	27.6	384
MAWOL	83.6	8187	1420	5.8	23.6	383
MCAL	91.9	12141	1718	7.1	25.8	396
MCOL	96.5	32997	968	34.07	21.5	390

[a] M_w: weight average molecular weight; [b] M_n: number average molecular weight; [c] M_w/M_n: polydispersity index; [d] % GAE: percentage of gallic acid equivalents; [e] T_{max}: maximum degradation temperature from TG/DTGA curves.

work was done according to the latter (Infante et al., 2007). In addition, the differences on the range 1600-1730 cm^{-1} on their FTIR spectra confirmed the reaction (see Figure 1a). In fact, the band around 1710 cm^{-1} moved to higher wavenumbers in all cases, which was attributed to the –OH oxidation of side chains, together with the weakening of the peak at 1599 cm^{-1} corresponding to aromatic C=C streching vibration. In addition, as reported by Infante et al., the appearance of the band around 1640 cm^{-1} was also representative of the degradation of aromatic rings (Infante et al., 2007).

As for the hydroxymethylated lignins, it is known that formaldehyde may react with lignin in alkaline medium in two ways: the first one, by substituting the free ortho positions in the aromatic rings, and the second one, by reacting with the side chains containing carbonyl groups (Aini et al., 2019; Chen et al., 2020; Gilca et al., 2014). Nevertheless, if reactivity of the lignin is wanted to increase, the latter reaction should be avoided (Gilca et al., 2014). Moreover, hydroxymethyl groups can also react at free positions of other lignin units forming methylene bonds and leading to the condensation of the structure (Aini et al., 2019; Gilca et al., 2014). The variation on the distributions and average molecular weights suggested that the modification occurred (Gilca et al., 2014). Despite de fact that the change on the polydispersity of the lignins was not representative of having obtained more homogeneous modified lignins, their molecular weight distributions (Supplementary data) evoked a trend of homogenization of the highest molecular weight fractions towards the ones with lower molecular weights. This behaviour was also observed by other authors (Căpraru et al., 2012). Moreover, the increase on the number and weight average molecular weights was observed for MAAOL and MAWOL samples, which was also reported by Capraru et al. (2012) for grass lignins.

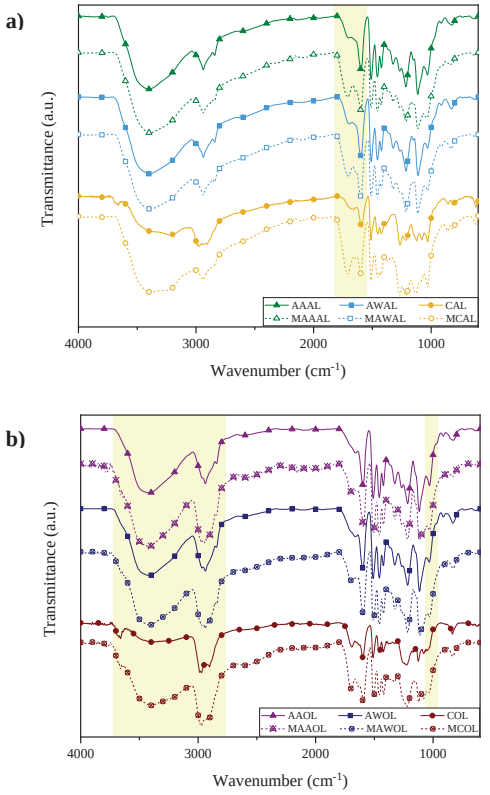

Figure 1. FTIR spectra of modified and native alkaline (a) and organosolv (b) lignins.

The FTIR spectra of native and modified organosolv lignins also indicated the success of the reaction (Figure 1b)(Căpraru et al., 2012). In fact, the intensification of the –OH band (at 3400 cm^{-1}), the one corresponding to C–H (around 2930 cm^{-1}), the one

attributed to methoxyl and hydroxymethyl groups (around 2850 cm^{-1}) and the one related to the C–O stretching vibration of aliphatic C–OH and hydroxymethyl C–OH (around 1030 cm^{-1}) were a clear evidence of the introduction of hydroxymethyl groups via the modification reaction (Chen et al., 2020; Gilca et al., 2014). The appearance of a shoulder at 3660 cm^{-1} suggested the presence of free –OH groups within the modified lignin structures (Zang et al., 2015). These results were in agreement with those obtained from ^{31}P NMR analyses, in which an increase on the aliphatic hydroxyl signal between 150 and 145.4 ppm was observed for all the samples after the hydroxymethylation reaction (X. Meng et al., 2019) (Supplementary data).

The thermal stability of all the samples was altered through the modification reactions. In fact, the maximum degradation step was shifted to higher temperatures in all cases. However, in the case of alkaline lignins, another degradation step appeared between the stage corresponding to moisture evaporation (< 100 ºC) and the maximum degradation stage. This peak was detected around 300 ºC, and was attributed to the lower molecular weight fractions of lignin generated during the modification step (Dávila et al., 2017; Xu et al., 2020). It was also observed that organosolv lignins were more thermally stable and started to lose weight at higher temperatures than alkaline lignins, although their maximum degradation temperatures were slightly lower. Compared to native lignins, modified organosolv lignins presented higher thermal stability and final residue, which was also observed by Chen et al. (2020) (Chen et al., 2020). In addition, despite all the left residues being of around the 40% of the initial sample weight, modified organosolv lignins left higher residues than alkaline ones, conversely to what happened for native lignins, which may be attributed to the modification and lignin precipitation stages.

The crystallinity of the samples was almost unaltered by the modification reactions (Supplementary data). All the samples presented a wide peak around 22º, which is related to the amorphous structure of lignin (Ciolacu and Cazacu, 2018; Goudarzi et al., 2014).

3.2. Hydrogel characterization

3.2.1. Lignin waste

As in previous works, the lignin waste of the synthesized hydrogels was determined through UV spectroscopy (Table 2) (Morales et al., 2021, 2020a, 2020b). It was expected to have lower lignin wastes than in the previous works due to the higher reactivity of the modified lignins. Nevertheless, the results proved that the hypothesis was incorrect, since the lignin waste determined for all the samples resulted to be higher than those reported previously. This change was significantly greater for the samples containing MCAL and MCOL, which presented a loss of almost 89 and 97% of their initial amount of lignin, respectively. The samples containing MAWA did also show a huge increase. The rest of the samples exhibited lower lignin waste raises, ranging from 12–14%.

Table 2. Lignin waste (%) of native and modified lignin-containing hydrogels.

Sample	Native (%)	Modified (%)
AAA	59.6 ± 2.8	73.5 ± 0.5
AAO	71.1 ± 3.0	83.4 ± 4.6
AWA	44.2 ± 1.6	71.6 ± 0.5
AWO	59.9 ± 4.0	74.0 ± 4.8
CA	67.8 ± 2.0	88.7 ± 3.4
CO	77.4 ± 1.7	96.5 ± 0.3

As the observed lignin wastes were so unexpected and so as to study the reusability of lignins in the washing solutions, it was decided to precipitate these lignins and study their molecular weights. These results are shown in Table 3. It was observed that in all cases the lost lignins had a lower weight average molecular weight than the native ones, and they were also more homogeneous, since their polydispersity indexes were lower. These results suggested that the polymeric matrix could have reacted with the highest molecular weight fractions, leading to a big elimination of the lowest molecular weight fractions.

Table 3. Average molecular weights and polydispersity indexes of the lignins recovered from the washing solutions.

Lignin Sample	M_w[a] (g/mol)	M_n[b] (g/mol)	M_w/M_n[c]
MAAAL	10134	1317	7.7
MAAOL	7250	1592	4.5
MAWAL	10350	1643	6.3
MAWOL	6804	1569	4.5
MCAL	9710	1985	4.9
MCOL	3685	636	5.8

[a] M_w: weight average molecular weight; [b] M_n: number average molecular weight; [c] M_w/M_n: polydispersity index

3.2.2. Swelling capacity

In order to determine the effect that the lignin modifications had on the properties of the synthesized hydrogels, their swelling capacity was studied. The results are depicted in Figure 2.

Comparing to previous results (Morales et al., 2021), it was observed that in the case of the alkaline lignin-containing

samples, the swelling capacity got significantly reduced when modified lignins were employed for their synthesis. These results suggest that the peroxidation of lignin performed in the present work was not an appropriate modification to obtain hydrogels with a high swelling capacity. On the other hand, when modified organosolv lignins were used, their swelling capacity was enhanced, especially in the case of the samples with MCOL (450%), which had also presented the highest lignin waste. Moreover, MAAO samples were the second ones with improved swelling capacity (410%), which also coincided with the second highest lignin waste. Similarly, MAWO samples exhibited the lightest enhancement on their swelling degree and had displayed the lowest lignin waste among the samples containing modified organosolv lignins. Thus, it could be concluded that hydroxymethylation could be a good method to enhance the swelling ability of organosolv lignin-based hydrogels.

Looking at the present results and comparing them with previous ones, it should be mentioned that although hydroxymethylation demonstrated to be effective for improving the swelling capacity of lignin-hydrogels, other variations during the synthesis process (lengthening the last thawing step, for instance) leaded to higher improvements on this property, without needing to modify the native lignins.

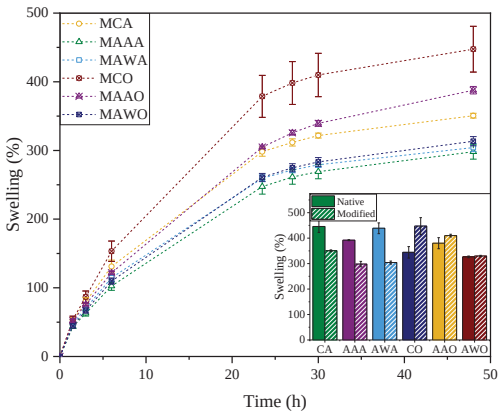

Figure 2. Swelling performance of modified lignin-based hydrogels during the first 48 h.

3.2.3. Morphology

Scanning Electron Microscopy (SEM) permitted studying the morphology of the samples. The obtained micrographs at 500x and 1500x magnifications are shown in Figure 3.

The images, in general, did not reveal highly porous structures; indeed they showed quite dense and continuous morphologies with scarcely detectable voids. This fact was more evident in the samples containing alkaline lignins, which may be attributed to a greater crosslinking density, which would also clarify the decline on their swelling ability. For the samples containing organosolv lignins, especially for MAAO samples, the created voids were more obvious, which were probably responsible for the augment on their water absorption capacity. Hence, it is clear that the lignin modifications had direct impact on the microstructures of the synthesized hydrogels, which also clearly affected their swelling capacity.

2.1.1. Thermal behaviour

For some applications, the glass transition (T_g) and melting temperatures (T_m) of polymeric materials are determining features. Hence, these parameters together with the melting enthalpy (ΔH_m) and the crystallinity indexes (χ_c) for each sample were defined by Differential Scanning Calorimetry (DSC) and the results are displayed in Table 4. The T_g was found on the inflection point of the specific heat increment during the second heating scan, after removing the thermal memory of the samples, but the rest of the parameters were identified from the first heating scan. All the determined T_g values were in the range of 77–103 ºC. These values were higher than those reported previously (Morales et al., 2021), suggesting that lignin modifications leaded to more compact structures in which the movement of the amorphous polymeric chains was hindered, which was also related to the obtained SEM micrographs. In addition, it was observed that the hydrogels containing modified organosolv lignins presented lower T_g values than the ones containing alkaline ones. Moreover, these results were aligned with the ones reported for the swelling capacity of the samples, being the aforementioned higher for the samples with lower T_g. Despite all the melting temperatures being similar (≈ 235 ºC), they were quite close to pure the T_m of PVA hydrogels (Morales et al., 2020a, 2020b), and their melting enthalpies were also high, suggesting the existence of many crystalline regions (Yang et al., 2018). The crystallization indexes were calculated based on a well-known equation (He et al., 2019; Morales et al., 2020a), and the results suggested that a great part of the hydrogels was crystalline. In addition, the samples with higher filler contents seemed to have higher crystallinity degrees, which would be in accordance with previous results (Morales et al., 2020a) and could be due to an enhancement of interfacial interactions via hydrogen bonding between the multiple hydroxyl groups on the matrix polymer and lignin (He et al., 2019).

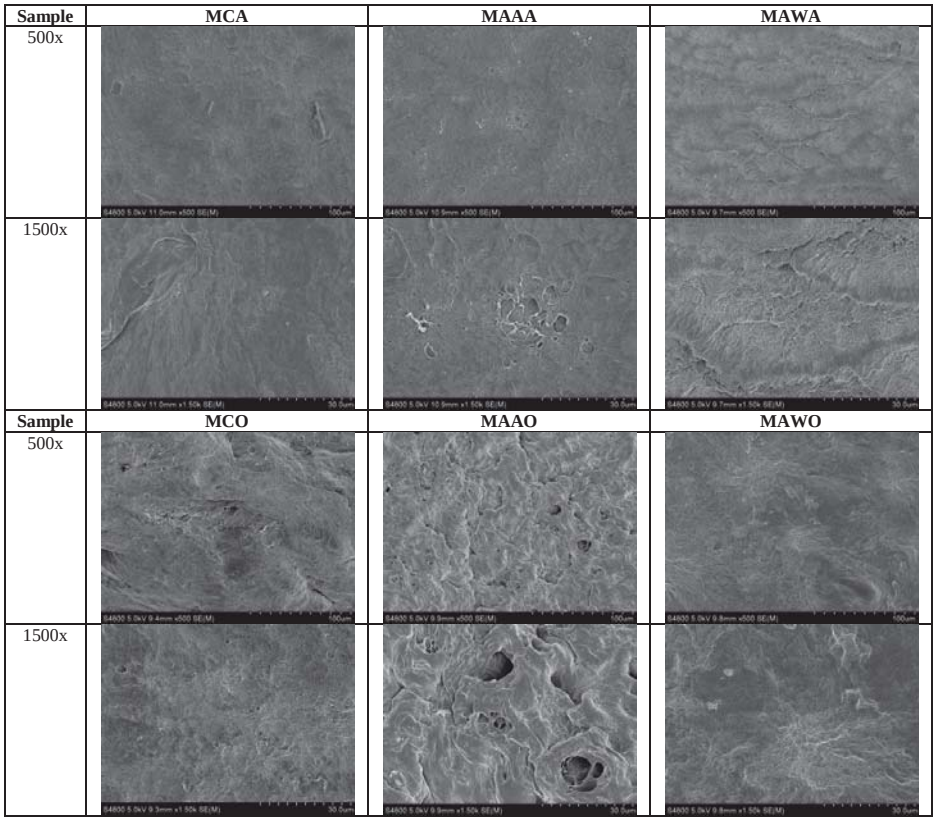

Figure 3. SEM micrographs for modified lignin-based hydrogels at 500x and 1500x magnifications.

Table 4. Summarized results for the analyzed parameters by DSC and calculations.

Sample	1st heating scan				2nd heating scan
	T_m (ºC)	ΔH_m (J/g)	m_{filler} (%)	χ_c (%)	T_g (ºC)
MAAA	235	64	25	53	103
MAAO	235	59	15	43	92
MAWA	236	62	27	52	81
MAWO	234	61	25	50	77
MCA	235	60	11	42	91
MCO	234	59	4	38	88

It was also observed that the samples containing alkaline lignin presented higher crystallinity indexes, which would explain their lower swelling abilities and higher T_g values.

2.1.2. Compression tests

The compression tests of the samples were performed in order to determine the impact that lignin modification had on their compression modulus at 80% of strain. Once again, all the tested hydrogels were able to keep total integrity and good recoverability thanks to their elastic behaviour.

From the results in Figure 4 it was concluded that hydrogels containing alkaline lignins had greater compression modulus than those containing organosolv lignins. The latter is consistent with the results obtained for their crystallinity, since the more crystalline and compact the sample is the higher its compression modulus should be (Holloway et al., 2013). Nevertheless, this improvement of the compression modulus could also be attributed to the higher solid content (m_{filler}) on alkaline hydrogels, as explained by Queiroz et al. (2021) (Queiroz et al., 2021). Moreover, all the modules values for the samples with alkaline lignin were in the range of 10-12 MPa, whereas the ones for hydrogels with organosolv lignin were between 4.5 and 6 MPa. Comparing to the previous work (Morales et al., 2021), an enhancement of its compression modulus was especially observed for MAWA samples, although MAAO also got slightly higher. All these values were aligned with the results reported for lignin-hydrogels by some authors (Cai et al., 2020) but they

were also higher than those obtained by others (Chen et al., 2019; Kalinoski and Shi, 2019; Queiroz et al., 2021).

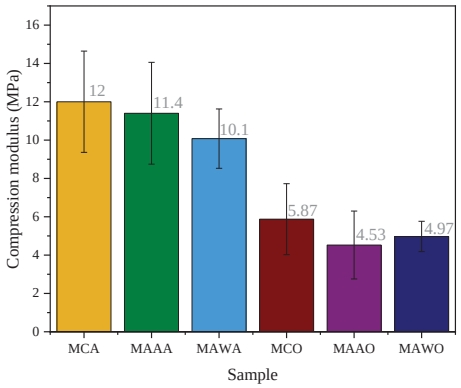

Figure 4. Compression behaviours of modified lignin-based hydrogels.

2.1.3. Drug loading and delivery tests

Quercetin (QE) is a bioflavonoid present in fruits and vegetables with interesting anti-inflammatory, antioxidant, anti-carcinogenic and anti-obesity properties (George et al., 2019; Jin et al., 2011; Lee et al., 2017). Due to the aforementioned characteristics and the current trend of preferring natural compounds rather than synthesized drugs, quercetin has recently gained great attention. This compound can be found in onion peels, which are an abundant waste all over the world. Thus, the obtaining of a flavonoid-rich extract from this waste would give an added-value to it, contributing to circular economy.

Among the extraction strategies that have been studied for QE, microwave assisted extraction (MAE) has proven to be a promising sustainable and green process (Jin et al., 2011). Therefore, QE was extracted though MAE.

2.1.3.1. Characterisation of QE extract

The solid content on the extract was determined through gravimetric analyses, drying 1 ml of the extract at 105 ºC for 24 h. This measurement revealed a solid content of 18.3 ± 0.2 mg of solid/g of liquid extract. TPC and TFC analyses showed high phenolic and flavonoid contents for the extract (576.4 ± 75.4 mg GAE/g dry extract and 470.1 ± 22.5 mg CQE/g dry extract). These values for TPC were higher than those reported by other authors and the ones for TFC were similar (George et al., 2019). In addition, the characteristic peaks of CQE reported by George et al. (2019) were also present on the FTIR spectra of QE, confirming the existence of this compound in the extract (see Figure 5a)(George et al., 2019).

2.1.3.2. Drug loading tests

The drug loading tests were performed by immersing dry hydrogels into diluted QE solutions (68.4 mg quercetin/L). The objective of these tests was to analyse the capacity of these samples of absorbing and releasing this drug, not to optimize the loading-release kinetic.

According to the absorbance difference between the initial and final solutions, all the samples were capable of trapping between 26 and 34% of the drug in the initial solution (see Table 5), being this percentage higher for the hydrogels containing organosolv lignins, which had also presented the highest swelling capacities.

2.1.3.3. Drug release tests

After the loaded hydrogels had dried, they were immersed in PBS at 37 ºC for drug release, simulating *in vitro* conditions. The absorbance of the release medium was performed at several times during the first 6.5 h. As the hydrogels contained lignin, and this lignin presented an absorbance peak at 330 nm, at high concentrations this peak sagged the results of the peak corresponding to QE at 375 nm. Thus, the release kinetics was performed during the first 6.5 h, while the released lignin was negligible.

From the release profiles shown in Figure 5b it was concluded that although all the samples were able to be loaded with similar drug amounts, the release capacity was completely different for each sample. In fact, with respect to the loaded amounts of drug, the released drug percentages ranged from 12 to 30%. The samples displaying the highest release drug percentage were MAWA, followed by MAAO and MAAA. The lowest release was observed for MCO samples, suggesting that despite having higher drug loading abilities, the interactions with the drug made its release difficult. Nevertheless, it should be noted that these profiles were just for the first 6.5 h, and cannot be extrapolated to longer times.

So as to determine the release kinetics, several models were applied (i.e. zero order, first order, Korsmeyer–Peppas and Higuchi) (George et al., 2020, 2019; Saidi et al., 2020). The estimated kinetic parameters for each of these models are displayed in Table 5 and the graphic representations of the four kinetic models in the Supplementary data. From the original release profile, it was inferred that the release kinetics would not fit correctly to a zero order model, which was confirmed by the determination coefficients (R^2). Among the rest of the models, Korsmeyer–Peppas model was the one fitting the best, except

for MCA sample, whose fitting did not improve either with Higuchi model.

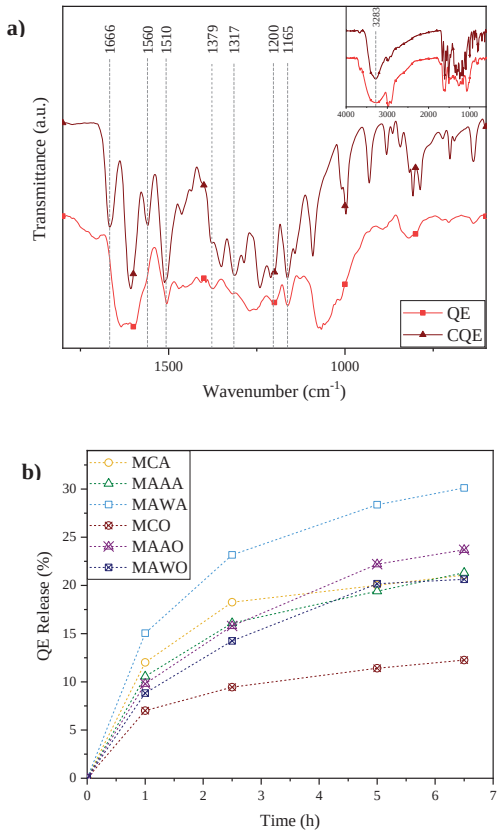

Figure 5. (a) FTIR spectra of self-extracted (QE) and commercial (CQE) quercetin extract and (b) QE release profiles of modified lignin-based hydrogels.

As indicated by Saidi et al. (2020) (Saidi et al., 2020), the release exponents (n) and the rate constants (k_{kp}) were determined from the slopes and intercepts of the plots (ln (QE %) versus ln t) of the experimental data. As shown in Table 5, all the estimated values for n were below 0.5. Although Fickian diffusion is usually considered when n=0.5 (George et al., 2020, 2019), in this case it could also be said that the QE release followed a Fickian diffusion (George et al., 2019). Thus, it could be said that the synthesized hydrogels could be used as controlled drug delivery systems.

3. Conclusions

On the basis of the results obtained for the properties of previously synthesized alkaline and organosolv lignin-based hydrogels, two chemical modifications were performed to these lignins in order to enhance their reactivity.The peroxidation of alkaline lignin was confirmed by FTIR, but the molecular weight studies suggested that condensation reactions had also happened during the reaction, leading to fractions with higher average molecular weights. The hydroxymethylation of organosolv lignin was also confirmed by FTIR, ^{31}P NMR and GPC. Moreover, this reaction leaded to more thermally stable lignins, which supported the success of the reaction. The lignin waste of the synthesized hydrogels was higher than the one reported for previously synthesized samples, suggesting that despite the modification of lignins, just the highest molecular weight fractions reacted with the matrix polymer. Moreover, the swelling capacity of modified alkaline lignin-based hydrogels was negatively affected, whereas the one for organosolv lignin-based samples improved. The continuous and compact structures seen on SEM micrographs explained the aforementioned, and the results from the DSC and compression tests were in accordance with them. The drug loading and release studies suggested that these samples allowed a Fickian diffusion of QE and they could be employed as controlled drug delivery systems.

Table 5. Kinetic parameters estimated from models for QE release from hydrogels.

Sample	Loading (%)	Zero order R^2	First order R^2	Korsmeyer–Peppas R^2	Korsmeyer–Peppas n	Korsmeyer–Peppas k_{kp}	Higuchi R^2
MAAA	29.0	0.82	0.84	0.99	0.37	10.9	0.98
MAAO	31.8	0.90	0.92	0.99	0.48	9.9	0.99
MAWA	30.4	0.81	0.85	0.98	0.37	15.5	0.97
MAWO	32.0	0.88	0.90	0.99	0.47	9.0	0.99
MCA	26.0	0.73	0.75	0.93	0.29	12.6	0.93
MCO	34.5	0.77	0.79	0.99	0.30	7.1	0.96

Acknowledgements

The authors would like to acknowledge the financial support of the Department of Education of the Basque Government (IT1008-16). A. Morales would like to thank the University of the Basque Country (Training of Researcher Staff, PIF17/207). P. Gullón would like to acknowledge the Grants for the recruitment of technical support staff (PTA2019-017850-I) under the State Plan for Scientific and Technical Research and Innovation 2017-2020. The authors thank SGIker (UPV/EHU/ERDF, EU) for their technical and human support.

References

Aini, N.A.M., Othman, N., Hussin, M.H., Sahakaro, K., 2019.

Hydroxymethylation-Modified Lignin and Its Effectiveness as a Filler in Rubber Composites. Processes 7, 315. https://doi.org/10.3390/pr7050315

Barros, A., Quraishi, S., Martins, M., Gurikov, P., Subrahmanyam, R., Smirnova, I., Duarte, A.R.C., Reis, R.L., 2016. Hybrid Alginate-Based Cryogels for Life Science Applications. Chemie-Ingenieur-Technik 88, 1770–1778. https://doi.org/10.1002/cite.201600096

Cai, J., Zhang, X., Liu, W., Huang, J., Qiu, X., 2020. Synthesis of highly conductive hydrogel with high strength and super toughness. Polymer (Guildf). 202, 122643. https://doi.org/10.1016/j.polymer.2020.122643

Căpraru, A.M., Ungureanu, E., Trincă, L.C., Mălutan, Ț., Popa, V.I., 2012. Chemical and spectral characteristics of annual plant lignins modified by hydroxymethylation reaction. Cellul. Chem. Technol. 46, 589–597.

Chen, Y., Zhang, H., Zhu, Z., Fu, S., 2020. High-value utilization of hydroxymethylated lignin in polyurethane adhesives. Int. J. Biol. Macromol. 152, 775–785. https://doi.org/10.1016/j.ijbiomac.2020.02.321

Chen, Y., Zheng, K., Niu, L., Zhang, Y., Liu, Y., Wang, C., Chu, F., 2019. Highly mechanical properties nanocomposite hydrogels with biorenewable lignin nanoparticles. Int. J. Biol. Macromol. 128, 414–420. https://doi.org/10.1016/j.ijbiomac.2019.01.099

Ciolacu, D., Cazacu, G., 2018. New Green Hydrogels Based on Lignin. J. Nanosci. Nanotechnol. 18, 2811–2822. https://doi.org/10.1166/jnn.2018.14290

Dávila, I., Gullón, P., Andrés, M.A., Labidi, J., 2017. Coproduction of lignin and glucose from vine shoots by eco-friendly strategies: Toward the development of an integrated biorefinery. Bioresour. Technol. 244, 328–337. https://doi.org/10.1016/j.biortech.2017.07.104

Dragone, G., Kerssemakers, A.A.J., Driessen, J.L.S.P., Yamakawa, C.K., Brumano, L.P., Mussatto, S.I., 2020. Innovation and strategic orientations for the development of advanced biorefineries. Bioresour. Technol. 302, 122847. https://doi.org/10.1016/j.biortech.2020.122847

Figueiredo, P., Lintinen, K., Hirvonen, J.T., Kostiainen, M.A., Santos, H.A., 2018. Properties and chemical modifications of lignin: Towards lignin-based nanomaterials for biomedical applications. Prog. Mater. Sci. 93, 233–269. https://doi.org/10.1016/j.pmatsci.2017.12.001

George, D., Begum, K.M.M.S., Maheswari, P.U., 2020. Sugarcane Bagasse (SCB) Based Pristine Cellulose Hydrogel for Delivery of Grape Pomace Polyphenol Drug. Waste and Biomass Valorization 11, 851–860. https://doi.org/10.1007/s12649-018-0487-3

George, D., Maheswari, P.U., Begum, K.M.M.S., 2019. Synergic formulation of onion peel quercetin loaded chitosan-cellulose hydrogel with green zinc oxide nanoparticles towards controlled release, biocompatibility, antimicrobial and anticancer activity. Int. J. Biol. Macromol. 132, 784–794. https://doi.org/10.1016/j.ijbiomac.2019.04.008

Gilca, I.A., Ghitescu, R.E., Puitel, A.C., Popa, V.I., 2014. Preparation of lignin nanoparticles by chemical modification. Iran. Polym. J. (English Ed. 23, 355–363. https://doi.org/10.1007/s13726-014-0232-0

Goliszek, M., Kołodyńska, D., Pylypchuk, I. V., Sevastyanova, O., Podkościelna, B., 2021. Synthesis of lignin-containing polymer hydrogels with tunable properties and their application in sorption of nickel(II) ions. Ind. Crops Prod. 164, 20–31. https://doi.org/10.1016/j.indcrop.2021.113354

Goudarzi, A., Lin, L.-T., Ko, F.K., 2014. X-Ray Diffraction Analysis of Kraft Lignins and Lignin-Derived Carbon Nanofibers. J. Nanotechnol. Eng. Med. 5, 021006. https://doi.org/10.1115/1.4028300

He, X., Luzi, F., Hao, X., Yang, W., Torre, L., Xiao, Z., Xie, Y., Puglia, D., 2019. Thermal, antioxidant and swelling behaviour of transparent polyvinyl (alcohol) films in presence of hydrophobic citric acid-modified lignin nanoparticles. Int. J. Biol. Macromol. 127, 665–676. https://doi.org/10.1016/j.ijbiomac.2019.01.202

Holloway, J.L., Lowman, A.M., Palmese, G.R., 2013. The role of crystallization and phase separation in the formation of physically cross-linked PVA hydrogels. Soft Matter 9, 826–833. https://doi.org/10.1039/c2sm26763b

Infante, M., Ysambertt, F., Hernández, M., Martínez, B., Delgado, N., Bravo, B., Cáceres, A., Chávez, G., Bullón, J., 2007. Microwave assisted oxidative degradation of lignin with hydrogen peroxide and its tensoactive properties. Rev. Tec. la Fac. Ing. Univ. del Zulia 30, 108–117.

Iravani, S., Varma, R.S., 2020. Greener synthesis of lignin nanoparticles and their applications. Green Chem. 22, 612–636. https://doi.org/10.1039/c9gc02835h

Jin, E.Y., Lim, S., Kim, S. oh, Park, Y.S., Jang, J.K., Chung, M.S., Park, H., Shim, K.S., Choi, Y.J., 2011. Optimization of various extraction methods for quercetin from onion skin using response surface methodology. Food Sci. Biotechnol. 20, 1727–1733. https://doi.org/10.1007/s10068-011-0238-8

Kalinoski, R.M., Shi, J., 2019. Hydrogels derived from lignocellulosic compounds: Evaluation of the compositional, structural, mechanical and antimicrobial properties. Ind. Crops Prod. 128, 323–330. https://doi.org/10.1016/j.indcrop.2018.11.002

Kumar, A., Anushree, Kumar, J., Bhaskar, T., 2020. Utilization of lignin: A sustainable and eco-friendly approach. J. Energy Inst. 93, 235–271. https://doi.org/10.1016/j.joei.2019.03.005

Larrañeta, E., Imízcoz, M., Toh, J.X., Irwin, N.J., Ripolin, A., Perminova, A., Domínguez-Robles, J., Rodríguez, A., Donnelly, R.F., 2018. Synthesis and Characterization of Lignin Hydrogels for Potential Applications as Drug Eluting Antimicrobial Coatings for Medical Materials. ACS Sustain. Chem. Eng. 6, 9037–9046. https://doi.org/10.1021/acssuschemeng.8b01371

Lee, S.G., Parks, J.S., Kang, H.W., 2017. Quercetin, a functional

compound of onion peel, remodels white adipocytes to brown-like adipocytes. J. Nutr. Biochem. 42, 62–71. https://doi.org/10.1016/j.jnutbio.2016.12.018

Meng, X., Crestini, C., Ben, H., Hao, N., Pu, Y., Ragauskas, A.J., Argyropoulos, D.S., 2019. Determination of hydroxyl groups in biorefinery resources via quantitative 31P NMR spectroscopy. Nat. Protoc. 14, 2627–2647. https://doi.org/10.1038/s41596-019-0191-1

Meng, Y., Li, C., Liu, X., Lu, J., Cheng, Y., Xiao, L.-P., Wang, H., 2019. Preparation of magnetic hydrogel microspheres of lignin derivate for application in water. Sci. Total Environ. https://doi.org/10.1016/j.scitotenv.2019.06.278

Morales, A., Gullón, B., Dávila, I., Eibes, G., Labidi, J., Gullón, P., 2018. Optimization of alkaline pretreatment for the co-production of biopolymer lignin and bioethanol from chestnut shells following a biorefinery approach. Ind. Crops Prod. 124. https://doi.org/10.1016/j.indcrop.2018.08.032

Morales, A., Labidi, J., Gullón, P., 2021. Impact of the lignin type and source on the characteristics of physical lignin hydrogels. Sustain. Mater. Technol. e00369. https://doi.org/10.1016/j.susmat.2021.e00369

Morales, A., Labidi, J., Gullón, P., 2020a. Effect of the formulation parameters on the absorption capacity of smart lignin-hydrogels. Eur. Polym. J. 129, 109631. https://doi.org/10.1016/j.eurpolymj.2020.109631

Morales, A., Labidi, J., Gullón, P., 2020b. Assessment of green approaches for the synthesis of physically crosslinked lignin hydrogels. J. Ind. Eng. Chem. 81, 475–487. https://doi.org/10.1016/j.jiec.2019.09.037

Musilová, L., Mráček, A., Kovalcik, A., Smolka, P., Minařík, A., Humpolíček, P., Vícha, R., Ponížil, P., 2018. Hyaluronan hydrogels modified by glycinated Kraft lignin: Morphology, swelling, viscoelastic properties and biocompatibility. Carbohydr. Polym. 181, 394–403. https://doi.org/10.1016/j.carbpol.2017.10.048

Oryan, A., Kamali, A., Moshiri, A., Baharvand, H., Daemi, H., 2018. Chemical crosslinking of biopolymeric scaffolds: Current knowledge and future directions of crosslinked engineered bone scaffolds. Int. J. Biol. Macromol. 107, 678–688. https://doi.org/10.1016/j.ijbiomac.2017.08.184

Ouyang, X., Lin, Z., Deng, Y., Yang, D., Qiu, X., 2010. Oxidative Degradation of Soda Lignin Assisted by Microwave Irradiation. Chinese J. Chem. Eng. 18, 695–702. https://doi.org/10.1016/S1004-9541(10)60277-7

Queiroz, B.G., Ciol, H., Inada, N.M., Frollini, E., 2021. Hydrogel from all in all lignocellulosic sisal fibers macromolecular components. Int. J. Biol. Macromol. 181, 978–989. https://doi.org/10.1016/j.ijbiomac.2021.04.088

Rico-García, D., Ruiz-Rubio, L., Pérez-Álvarez, L., Hernández-Olmos, S.L., Guerrero-Ramírez, G.L., Vilas-Vilela, J.L., 2020. Lignin-Based Hydrogels : Synthesis and Applications. Polymers (Basel). 12, 1–23.

Saidi, M., Dabbaghi, A., Rahmani, S., 2020. Swelling and drug delivery kinetics of click-synthesized hydrogels based on various combinations of PEG and star-shaped PCL: influence of network parameters on swelling and release behavior. Polym. Bull. 77, 3989–4010. https://doi.org/10.1007/s00289-019-02948-z

Sillero, L., Prado, R., Andrés, M.A., Labidi, J., 2019. Characterisation of bark of six species from mixed Atlantic forest. Ind. Crops Prod. 137, 276–284. https://doi.org/10.1016/j.indcrop.2019.05.033

Tribot, A., Amer, G., Abdou Alio, M., de Baynast, H., Delattre, C., Pons, A., Mathias, J.D., Callois, J.M., Vial, C., Michaud, P., Dussap, C.G., 2019. Wood-lignin: Supply, extraction processes and use as bio-based material. Eur. Polym. J. 112, 228–240. https://doi.org/10.1016/j.eurpolymj.2019.01.007

Wang, H., Pu, Y., Ragauskas, A., Yang, B., 2019. From lignin to valuable products–strategies, challenges, and prospects. Bioresour. Technol. 271, 449–461. https://doi.org/10.1016/j.biortech.2018.09.072

Xu, C., Liu, F., Alam, M.A., Chen, H., Zhang, Y., Liang, C., Xu, H., Huang, S., Xu, J., Wang, Z., 2020. Comparative study on the properties of lignin isolated from different pretreated sugarcane bagasse and its inhibitory effects on enzymatic hydrolysis. Int. J. Biol. Macromol. 146, 132–140. https://doi.org/10.1016/j.ijbiomac.2019.12.270

Yang, W., Fortunati, E., Bertoglio, F., Owczarek, J.S., Bruni, G., Kozanecki, M., Kenny, J.M., Torre, L., Visai, L., Puglia, D., 2018. Polyvinyl alcohol/chitosan hydrogels with enhanced antioxidant and antibacterial properties induced by lignin nanoparticles. Carbohydr. Polym. 181, 275–284. https://doi.org/10.1016/j.carbpol.2017.10.084

Yoo, C.G., Meng, X., Pu, Y., Ragauskas, A.J., 2020. The critical role of lignin in lignocellulosic biomass conversion and recent pretreatment strategies: A comprehensive review. Bioresour. Technol. 301. https://doi.org/10.1016/j.biortech.2020.122784

Zang, D., Liu, F., Zhang, M., Gao, Z., Wang, C., 2015. Novel superhydrophobic and superoleophilic sawdust as a selective oil sorbent for oil spill cleanup. Chem. Eng. Res. Des. 102, 34–41. https://doi.org/10.1016/j.cherd.2015.06.014

Zevallos Torres, L.A., Lorenci Woiciechowski, A., de Andrade Tanobe, V.O., Karp, S.G., Guimarães Lorenci, L.C., Faulds, C., Soccol, C.R., 2020. Lignin as a potential source of high-added value compounds: A review. J. Clean. Prod. 263. https://doi.org/10.1016/j.jclepro.2020.121499

Zhang, Yiwen, Yuan, B., Zhang, Yuqing, Cao, Q., Yang, C., Li, Y., Zhou, J., 2020. Biomimetic lignin/poly(ionic liquids) composite hydrogel dressing with excellent mechanical strength, self-healing properties, and reusability. Chem. Eng. J. 400, 125984. https://doi.org/10.1016/j.cej.2020.125984

Influence of lignin modifications on physically crosslinked lignin hydrogels for drug delivery applications

Amaia Morales[a], Jalel Labidi[a,*], Patricia Gullón[b]

[a]Chemical and Environmental Engineering Department, University of the Basque Country UPV/EHU, Plaza Europa 1, 20018, San Sebastián, Spain

[b]C.A.C.T.I. Laboratory, Technology Park of Galicia- Tecnopole, CTC Building, 32901, San Cibrao das Viñas, Ourense, Spain

[*]Corresponding author: jalel.labidi@ehu.eus

Supplementary data

Figure S1. Molecular weight distributions of modified and native alkaline (a) and organosolv (b) lignins.

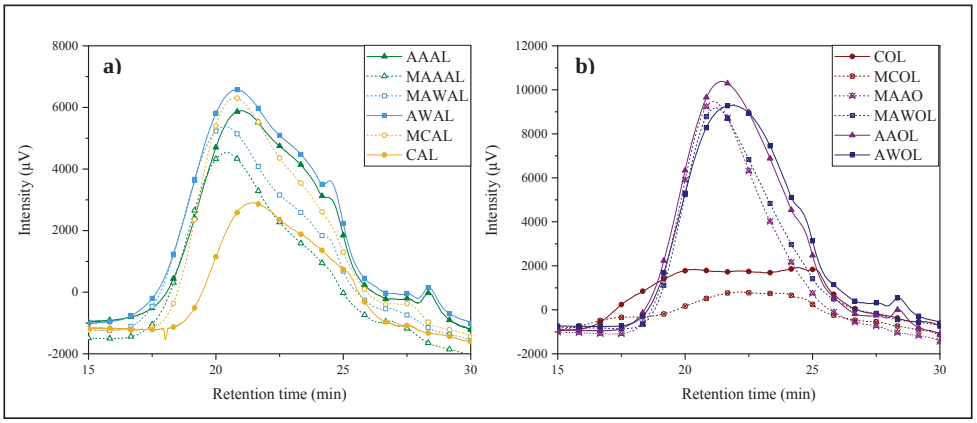

Figure S2: ^{31}P NMR spectra of COL and MCOL samples.

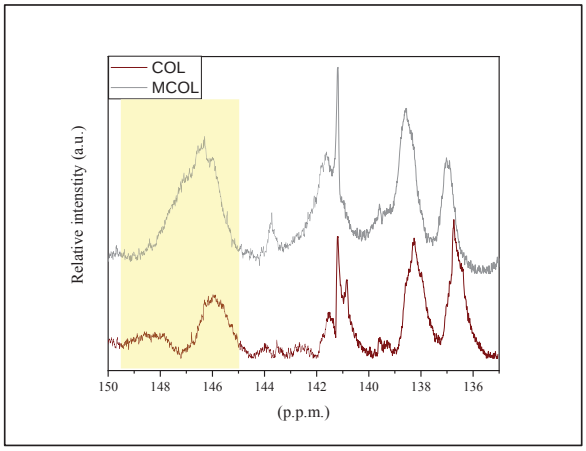

Figure S3. XRD patterns of modified and native alkaline (a) and organosolv (b) lignins.

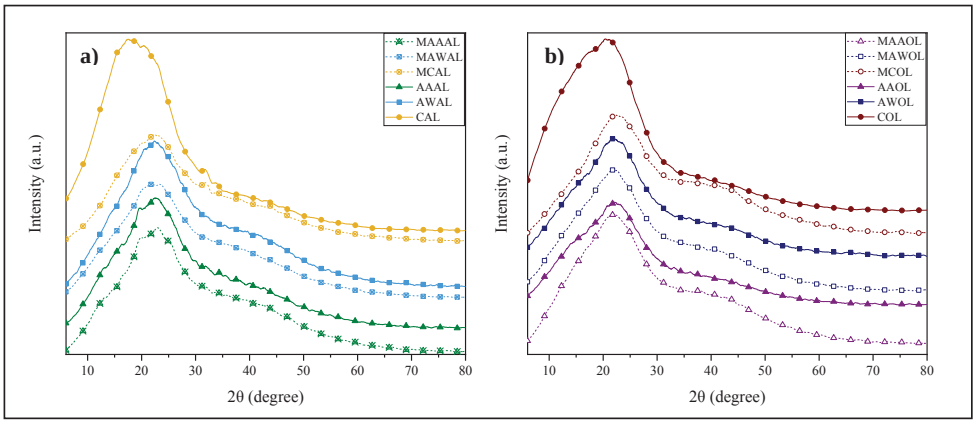

Figure S4. QE release kinetic models of zero order (a), First order (b), Korsmeyer–Peppas (c) and Higuchi models (d).

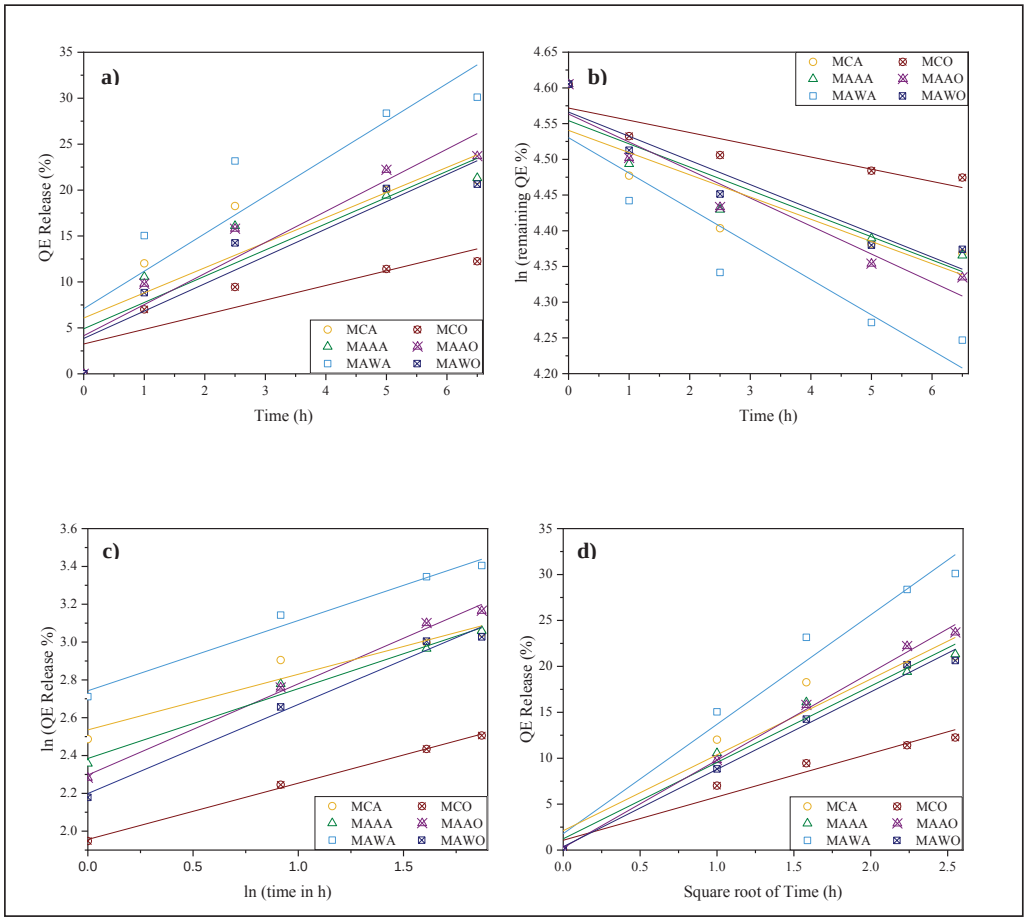

Baliabide fosilen agortzeak eta polimero sintetikoen biodegradagarritasun ezak eragindako ingurumen-inpaktu handiak biopolimeroak bezalako baliabide jasangarri eta ekologikoagoak ustiatzeko premia sustatu dute. Biopolimero hauen artean, biomasa lignozelulosikotik erraz isola daitekeen lignina karbonoan oinarritutako konposatuak fabrikatzeko, hala nola produktu kimiko eta materialetarako, etorkizun handiko hautagaia da. Hala ere, biopolimero hau gutxi ustiatuta dago oraindik, ziurrenik oso egitura egonkor eta konplexua duelako, baina honi balioa ematea funtsezkoa da biofindegiak lehiakorrak izan daitezen.

Testuinguru horretan, tesi hau ligninaren balorizazioan oinarritzen da, biopolimero hau hidrogelak bezalako balio erantsi altuko produktuak sortzeko erabiliz, hain zuzen ere. Emaitzek agerian utzi zuten osagaiak eta sintesi-prozedura arretaz hautatzearen garrantzia, eta baita lignina gehitzearen onurak nabarmendu ere. Gainera, material horiek tindagaien adsortzioan eta botiken administrazioan emaitza oparoak erakutsi zituzten, eta horietako batzuek propietate antifungikoak ere izan zituzten, sektore askotarako erabilgarriak egiten dituena.

Universidad del País Vasco
Euskal Herriko Unibertsitatea

Tesi hau Euskal Herriko Unibertsitateak emandako laguntza ekonomikoari esker burutu da